Charpy Impact Test

Factors and Variables

John M. Holt, editor

ASTM

STP 1072

STP 1072

Charpy Impact Test: Factors and Variables

John M. Holt, editor

ASTM
1916 Race Street
Philadelphia, PA 19103

ASTM Publication Code Number (PCN): 04-010720-23
ISBN: 0-8031-1295-5
Library of Congress No: 90-085687

NOTE

The Society is not responsible, as a body,
for the statements and opinions
advanced in this publication

Peer Review Policy

Each paper published in this volume was evaluated by three peer reviewers. The authors addressed all of the reviewers' comments to the satisfaction of both the technical editor(s) and the ASTM Committee on Publications.

The quality of the papers in this publication reflects not only the obvious efforts of the authors and the technical editor(s), but also the work of these peer reviewers. The ASTM Committee on Publications acknowledges with appreciation their dedication and contribution of time and effort on behalf of ASTM.

Printed in Chelsea, Mich.
December 1990

Foreword

The Symposium on Charpy Impact Test: Factors and Variables, sponsored by ASTM Committee E-28 on Mechanical Testing, was held in Lake Buena Vista, Florida, on 8-9 November 1989. John M. Holt, Alpha Consultants & Engineering, served as chairman and has also edited this publication.

Contents

THE SPECIMEN: SIZE

THE TEST TECHNIQUE

Introduction

INTRODUCTORY REMARKS

The Symposium on Charpy Impact Test--Factors and Variables had its genesis at the second meeting of Subcommittee 4--Fracture of ISO Technical Committee 164--Mechanical Testing. Subcommittee 4 had the assignment of reviewing ISO Recommended Practice for Verification of Pendulum Impact Testing Machines for Testing Steel, ISO Designation R442, and of revising where necessary. Although ISO, as does ASTM, requires that documents be reviewed at intervals not exceeding five years, this document had not been reviewed since it was first published in 1965 under the jurisdiction of ISO Technical Committee 17--Steel. There were 15 representatives from seven member countries and a representative from the European Community Bureau of Reference (BCR) at that meeting. The members of ISO technical committees are the national standard writing bodies--not individuals; national-standards writing bodies are organizations such as BSI, AFNOR, SIS, etc. Because there is no national-standards writing body in the United States, Congress has designated the American National Standards Institute (ANSI), as the de-facto body and therefore, the member from the United States.

At the subcommittee meeting, agreement was reached that numerous changes needed to be made--some tolerances were too restrictive, some were not restrictive enough, but there were problems in agreeing to the "correct" values. Agreement was reached for some values because various delegates informally presented work that they had personally performed, or reported on work that had been done in their country. However, other values could not be agreed upon because of divergent requirements in various national standards and the supporting data for the various proposals was not currently available. It was suggested that an international symposium be held to discuss the factors and variables that effect the Charpy impact test so that researchers around the world would have a forum at which to present data that would answer some of the questions that had been raised. The USA representative, on behalf of ASTM Committee E28-Mechanical Testing, agreed to sponsor such a symposium as part of the E28 meetings in November 1989. This STP is the result of that symposium.

The original goal of having world-wide research presented on the factors and variables of the Charpy test was achieved. There were three sessions containing 16 papers presented by authors from five different countries. Because attendance exceeded expectations, it appears as if more than just those writing specifications are interested in the topic.

SPECIFIC REMARKS

Twelve of the papers presented are being published in this STP, and one will be published in the ASTM Journal of Testing and Evaluation (Reference 1). The twelve papers fall into three categories, (1) those discussing the pendulum-impact machine, (2) those discussing the specimen, and (3) those discussing the testing techniques; several papers discuss more than one category. In summary, the papers present information on:

* the effect of many of the dimensional parameters of an impact machine, including metrological techniques to evaluate these parameters and a compliance technique for verifying machine acceptability;
* the effect of the geometry of the striker, that is, the 2-mm radius striker specified by ISO and much of the rest of the world, and the 8-mm striker specified by the ASTM;
* the effect of the method of fabricating the notch of a CVN test piece including fatigue precracking;
* the effect of specimen sizes in Charpy impact testing;
* the effect of strain rate including slow-bend tests.

Because the dimensional parameters of the machines are so very important to obtain "proper" impact values, the papers by Porro, et.al., by Schmieder, by Revise, by Lowe, and by Naniwa all discuss how the test machine can influence the results obtained. These papers discuss the effects ranging from the attachment of the machine to its foundation to the metrological methods used to determine angles and linear dimensions. Several of the papers discuss several potential sources for variation in test results due to machine variations. Attention is drawn to the paper by Porro, et.al. presenting the results of a study on the compliance of a machine as a means of assessing its physical condition. Naniwa presents the results of an in-depth study of the differences in the behavior and the deformation of the specimen when struck by an 8-mm striker (the "ASTM striker") and when struck by a 2-mm striker (the "ISO striker").

The specimen was investigated from two points of view: (1) the method of preparing the notch, and (2) the size of the specimen. The papers by Koester and by Fink studied the effects of grinding versus single-point machining; the papers by Fields, et.al., by Mikalac, et.al., and by Interrante, et.al. studied the effect of notch acuity and the method(s) of obtaining a sharp notch. Alexander, et.al. investigated specimen size.

The influence of the temperature conditioning media on test results was reported by Nanstad, et.al. Their paper, and Reference 1, indicate that the temperature of the specimen in the vicinity of the notch at the instant of impact is not necessarily the same as the temperature of the conditioning media.

As a result of the various studies presented, ASTM Committee E28 has initiated ballots changing some of the requirements of ASTM Method E23. ISO Subcommittee 4 has begun to study the results to see how they apply to the revision of their Method R442.

Prior to the Symposium, one attendee was overheard saying, "I see that there is a symposium on the Charpy test; what can be new there?" I believe that the symposium and this STP are definite statements that much is happening in the field of Charpy testing to further the understanding of what is required to obtain acceptable Charpy test results and the proper interpretation of those results.

ACKNOWLEDGEMENTS

I wish to thank the many people that helped to arrange the symposium -- in particular, Dorothy Savini, and the many other members of the ASTM staff, the session co-chairmen, R.D. Koester, and R.J. Goode, and the many people who reviewed manuscripts.

Thanks are also in order to the people who have been instrumental in seeing that this STP was published. These include Monica Armata, Rita Harhut, and the editors of the ASTM Staff and Jim Perrin of the ASTM Publication Committee. In addition, the original reviewers again reviewed the revised papers to insure their quality.

John M. Holt
Alpha Consultants & Engineering
1504 Williamsburg Place
Pittsburgh, PA 15235-4924

Reference 1: Tobler, R.L., R.P.Reed, I.S. Hwang, M. Morra, R.G. Ballinger, H. Nakajima, and S. Shimamoto; Journal of Testing and Evaluation, Vol 19, January 1991, pp.34-40.

The Pendulum-Impact Machine

Francesco Porro, Rodolfo Trippodo, Roberto Bertozzi and Gianluca Garagnani

IMPACT TESTER COMPLIANCE: SIGNIFICANCE, SENSITIVITY AND EVALUATION

REFERENCE: Porro,F.,Trippodo,R.,Bertozzi,R.,Garagnani,G.,"Impact Tester Compliance: Significance, Sensitivity and Evaluation", Charpy Impact Test: Factors and Variables. ASTM STP 1072 , John M. Holt, editer, American Society for Testing and Materials, Philadelphia 1990.

ABSTRACT: The compliance is very sensitive to internal mechanical factors concerning the load system, as the hammer, the tup, the anvils and the base to foundation attachement.
In order to verify the sensitivity of compliance measurements, a series of experimental tests has been performed, with artificial and real defect located at the most critical parts.
In order to overcame the need of an instrumented impact tester an instrumented specimen has been prepared, together with its electronic system for impact tester compliance measurement.
The compliance measurement, after verification of the impact tester with direct and indirect methods, as per ASTM E 23 or ISO R 442, can be helpful for verification of the good working condition of the pendulum and for the detection of onset of anomalies.

KEYWORDS: compliance, impact testers, pendulum, Charpy specimens,

INTRODUCTION

As pointed out by Bluhm [1] the flexibilties and the softness of the impact machine play a primary role in the determination of the correct value of the energy spent to break the specimen.

Dr.Porro is Quality engineering supervisor at Ansaldo ABB Componenti, via Lorenzi 8, 16152 Genova, Italy;
Ing. Trippodo is the director of CERMET (Regional Research Center for Materials), via Moro 26, 40068 San Lazzaro di Savena, Bologna, Italy;
Mr.Bertozzi is research scientist at CERMET; Dott. Garagnani is research scientist at Department of Metallurgy, University of Bologna, Italy.

The record of the strain of an instrumented tup actually made on an instrumented impact machine, Fig.1, definitely supports the hypothesis of the presence of vibrations during specimen rupture, resulting in loss of energy by elastic deformations, in the case of brittle fracture.

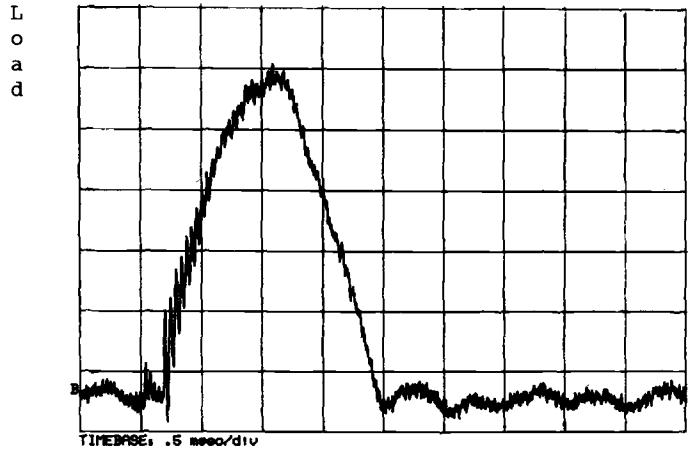

Fig.N.1: load signal from an instrumented impact tester tup showing typical vibrations during specimen rupture

In order to minimize the influence of this vibrational energy on the adsorbed energy reading, it is necessary to have an impact tester with low compliance.

This important conclusion motivated the authors to take into consideration verification of the impact tester compliance to assure homogeneity of behaviour from one tester to another.

It is well known that the reliability of the impact tester measurements is a matter of discussion when two impact testers (typically customer or inspection agency and manufacturer impact testers) measure different energy values from specimens of the same material.

This work is oriented to analyze the possibility to use the compliance, together with other characteristic impact tester parameters, for the detection of existing or impending anomalies.

BACKGROUND

The rule that governs the energy transformation during an impact test is as follows:

$$Ep = Ea + Ek + Ee + Ef \qquad (1)$$

where Ep = potential energy of the hammer (weight * height) to be converted into kinetic energy after the hammer release;
Ea = energy absorbed by the specimen during its rupture;

Ek = kinetic energy remaining after impact;
Ee = energy stored by the system hammer/specimen/anvils by elastic deformation;
Ef = energy lost by friction and windage during the blow;

The quantity Ee represents the energy stored and lost by the loading system of the specimen and therefore unavailable for breaking the specimen.

The energy dissipated as elastic deformation of the loading system, for a given load P, introducing the definition of stiffness that is the ratio load/deflection, is:

$$Ee = \frac{P^2}{2 * Sm} \qquad (2)$$

where Ee = energy stored by the system hammer/specimen/anvils by elastic deformation (J);
P = load (N)
Sm = system stiffness (N/m)

The compliance, or displacement under a given load, can be expressed in terms of stiffness of the system as follow:

$$Co = \frac{1}{2 * Sm} \qquad (3)$$

where
Sm = stiffness of the loading system (N/m)
Co = impact tester compliance (m/N)

After substitution, the formula (2) can be written:

$$Ee = Co * P^2 \qquad (4)$$

After the original idealized model suggested by Bluhm [1] for the determination of the stiffness, two methods are currently available.

The first, described by Venzi [2], has only experimental difficulties; this approach has been followed by the authors and the results obtained will be discussed in the following.

The second, used by Ireland [3], requires an instrumented impact tester, presents sufficient mathematical difficulties to require a computer for integration and shows lack of precision due to the interpretation limits of the computer during the determination of the characteristic points on load-time curve (yielding load and yielding

time).

Following the Venzi approach [2], the pendulum-specimen system can be sketched as follows, during a blow in the elastic field :

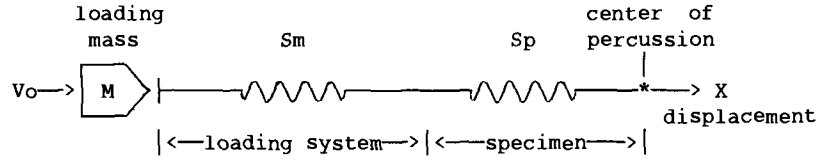

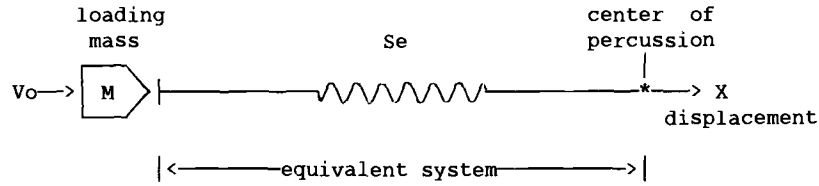

where:

M = pendulum mass (specimen mass is neglected, as Bluhm [1])
Vo= impact velocity (just before impact)
X = displacement of the centre of mass M,coincident with the centre of percussion (one degree of freedom assumed as Bluhm [1])
Sm= loading system stiffness, inverse of loading system compliance Cm
Sp= specimen stiffness, inverse to specimen compliance Cp
Se= equivalent stiffness (ratio load/deflection), inverse of equivalent compliance Ce

The displacement "x" is the sum of the displacements of the specimen and the loading system:

$$X = X_{\text{loading system}} + X_{\text{specimen}} \qquad (5)$$

and the following law relates the three stiffnesses:

$$\frac{P}{Se} = \frac{P}{Sm} + \frac{P}{Sp} \qquad (6)$$

where P is the load on the system (action and reaction at the interface tup-specimen)

Then the relation between the stiffness and the compliance is:

$$\frac{1}{Se} = \frac{1}{Sm} + \frac{1}{Sp} \qquad (7)$$

$$Ce = Cm + Cp \tag{8}$$

In order to solve the equation, i.e to obtain the value of Sm, it is necessary to have the values of Sp and Se.

The value of Sp can be calculated theoretically. The formula for a unnotched specimen with square cross section is :

$$Sp = \frac{(4 * E * L)^4}{W^3} \tag{9}$$

where Sp = specimen stiffness (N/m)
E = elastic modulus of the material
L = specimen width (typ. 10 * 10 mm)
W = span between anvils (typ. 40 mm)

The value of Sp for a standard unnotched specimen made in AISI 4340 hardened steel (55 HRC) is:

$$Sp = 133.4 * 10^6 \quad N/m \tag{10}$$

The value of Se can be obtained experimentally with the following considerations.

The law that describes the equilibrium of the hammer translation for a blow in an elastic field is (drop angle $\alpha < 10°$):

$$M * \frac{d^2 X}{d t^2} + Se * X = 0 \tag{11}$$

the solution of this equation is:

$$X = Xo * \sin(\Omega * t) \tag{12}$$

where $$\Omega = \left(\frac{Se}{M}\right)^{\frac{1}{2}} = \frac{2 * \pi}{T} \tag{13}$$

T = oscillation period of the system pendulum-specimen for elastic blow

The value of Se is determined by the equation:

$$Se = \left(\frac{2 \pi}{T}\right)^2 * M \tag{14}$$

By the knowledge of Sp and Se it is now possible to solve the equation (7) to obtain the value of Sm.

MEASUREMENT OF THE COMPLIANCE

The previous common approach for the measurement of the compliance, following the Venzi approach, was to use an instrumented tup in order to obtain the value of T by detecting the load signal, as indicated in Fig. N.2.

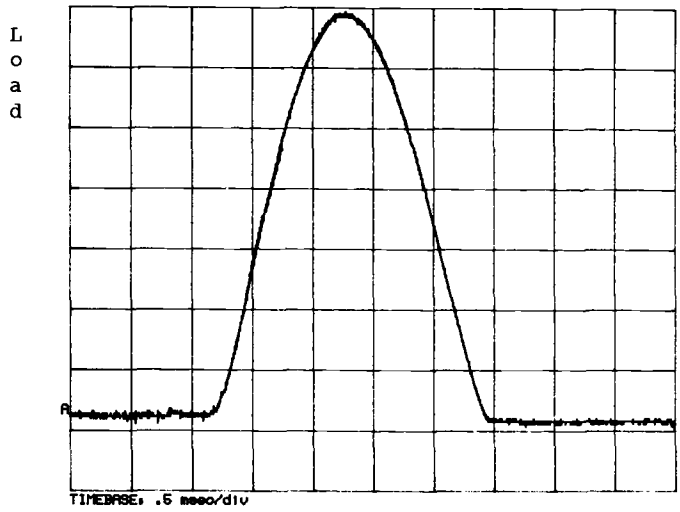

Fig.N.2: load signal from an instrumented impact tester tup under low blow (deformation in elastic field) for determination of typical oscillation period [T].

The requirement of having an instrumented impact tester, and the scarcity of this type of machine, resulted in generally low interest in using the compliance paramenter because of the difficulty in determining it.

To overcome the need for an instrumented impact tester, and to allow a low-cost determination of the compliance on impact testers, an instrumented specimen was prepared together with an electronic system for detection of the tup-specimen contact time, i.e., the half period T/2.

The system consists of the following:

An unnotched specimen 10 mm wide,10 mm heigh and 55 mm long, made of AISI 4340 steel, hardened to 55 HRC, with a surface roughness of 32 rms. The specimen is provided with two threaded holes at its ends to allow the insertion of two screw that are utilized as hooks for a thin rubber band for fastening the specimen against the anvils during repeated blows.

A longitudinal strain gage is cemented at mid length and mid height on the specimen side opposite the hammer.

This strain gage is connected in bridge configuration to a strain signal conditioner located near the specimen itself. This strain signal conditioner is equipped with gain and balance (zero) adjustment trimmers.

The strain gage conditioner detects the strain signal due to the displacement of the specimen during the impact of the hammer, i.e the load. The output of the strain conditioner during absence of load could be zero or a pre-set value.

The output of the strain signal conditioner is sent to an electronic trigger that detects the strain signal as it changes from the pre-set value.

The output of the trigger starts time counting (on a timer) when the trigger detects strain signal and stops the counting when the trigger detect the end of the strain imposed by the load

The output of the trigger is also sent to a counter that can count the number of subsequent repeated blows while the timer measures the total time of contact of each blow.

T/2, the oscillation half period , is the value that is experimentally determined, as sketched in Fig.3.

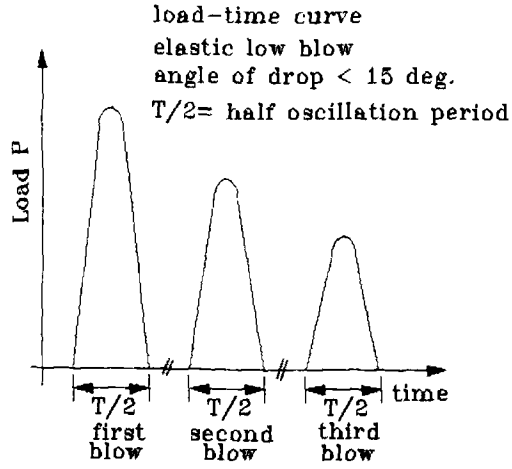

Fig.N.3: load signal as detected during a low blow and for two subsequent rebound.

The accumulated time intervals (T/2 or its multiples), the number of blows and the pre-set balance value are displayed on the instrument.

The system is also provided with an output for an oscilloscope for directly viewing the strain signal or for recording it.

The system arrangement for the measurement is presented in fig.4.

The interesting features of the system are the following:

1) portability: it is completly hand-portable;
2) simplicity : its electronic circuitry is very simple and very common, made with standard industrial components;
3) flexibility: it is not fixed or made for a specific impact tester, but can work on different machines, allowing intercomparison between pendulums, labs, etc;
4) low cost : it is much less expensive than an instrumented impact tester.

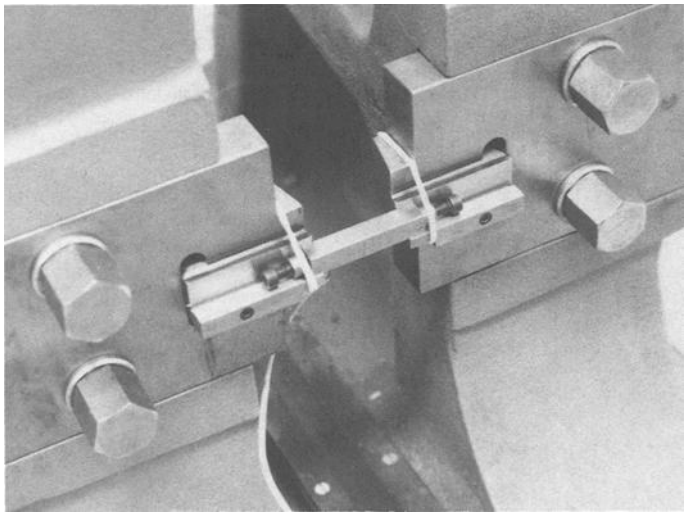

Fig.N.4: Typical instrumented Charpy specimen arrangement for time of contact measurement under low blow.
The rubber bands prevent movement of the specimen under repetitive low blows

SIGNIFICANCE OF THE COMPLIANCE

The value of the compliance in an impact tester is related to the geometry and the material properties of the loading system.

At least the following components of the loading system should be considered:

-the hammer and its fixtures to the supporting bar,

-the tup and its fixtures to the hammer,

-the anvils and their fixtures to the pendulum base,

-the pendulum base and its attachements to the floor.

The geometry of the loading system is defined by the manufacterer of the impact machine and normally it is not possible to vary or modify it.

Becouse the compliance is affected by variation of the working condition of the impact tester, i.e. change in the fastening condition or wear of the mechanical components, it is therefore important to periodically check the value of compliance in order to detect the onset of anomalous conditions.

The following point out the significance of the compliance and its power in the determination of change in the working condition of an impact tester.

-First test:

After a measurement of the compliance of a low range instrumented impact tester (20 J capacity) , several artificial defects were introduced in order to verify the capability of the compliance measurement to detect such defects or anomalous working conditions [5].

The choice of a low range impact tester was because, at the time of this test, work in progress using the standard 360 J impact tester did not permit the risk of loss of the Watertown Certification due to the introduction of the artificial defects. Moreover it was not possible to risk the possibility of irreversible damaging.

The instrumented impact tester was a Tinius Olsen model 74, with a maximun impact energy of 25 J, "U" type hammer, with the tup fastened to the hammer by four screws. The tup is presented in Fig.5.

The instrumentation, ETI 300 System, was manufactured by Effect Technology Inc.

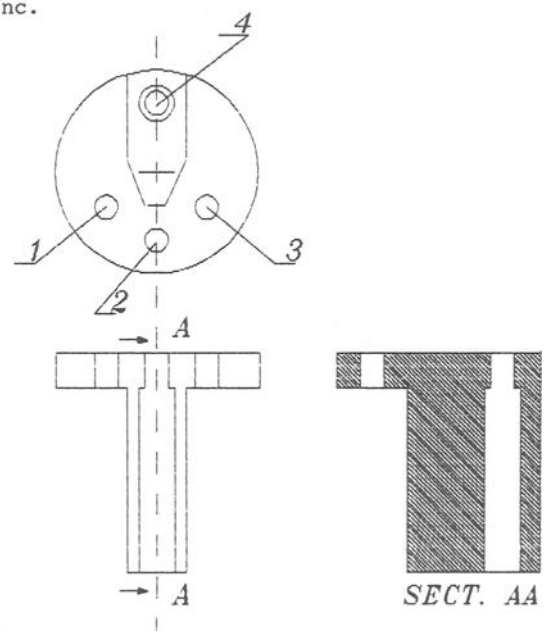

Fig.N.5: Tinius Olsen mod.74 (25 J) impact tester tup sketch showing the four fastening screws.

The defects introduced in the system were as follows:

A = referred as normal operating conditions
B = loosened central bolt (bolt No.4)
C = two loosened bolts (bolts No. 2 & 4)
D = three loosened bolts (bolts No. 1,2 & 4)
E = elastic deformation of fixing points the bolts 1, 2 & 3 are each loading two cup springs with a force of 50 Kgf.
F = elastic deformation of fixing points the bolts 1, 2 & 3 are each loading two cup springs with a force of 58 Kgf.
G = loosened attachement to the base

The results in terms of compliance measurements, taken by the pendulum instrumentation, are presented below:

defect status	brief description of defect	T/2 msec	Sp $N/m \cdot 10^6$	Se $N/m \cdot 10^6$	Sm $N/m \cdot 10^6$	Co $m/N \cdot 10^{-9}$
A	normal cond.	1.47	133.4	16.87	19.32	24.5
B	1 loose bolt	1.57	133.4	14.91	16.77	28.5
C	2 loose bolts	1.65	133.4	13.83	15.40	31.8
D	3 loose bolts	1.75	133.4	11.96	13.14	36.3
E	50 kgf spring	1.80	133.4	10.63	11.57	38.6
F	58 kgf spring	1.96	133.4	8.82	9.41	46.5
G	loose base	1.41	133.4	18.44	21.38	22.2

-Second test:

Compliance measurements were used to verify the working condition of a standard (non instrumented) impact tester (360 J capacity) manufactured by Metrocom Italy, during its initial installation [6].

The impact tester was then moved and re-installed in another laboratory, and new compliance measurements were taken.

All the measurements were taken utilizing the instrumented specimen and the electronic equipment.

The results show the capability of the compliance measurements to detect several anomalous situations during the installation, ranging from the loosening of the foundation bolts, the presence of a thick paint layer under the nuts (acting as an elastic medium), the difference in anvil spacing, and the presence of an out of level condition.

It is difficult to predict which is the correct compliance value of an installed impact tester, because the value seems to be affected by the system of fastening of the base to the floor.

Nevertheless after the istallation and the calibration of the impact tester performed under the relevant specification (E 23, UNI 6882, ISO R442, etc.) the test of the compliance can detect the onset of anomalous conditions.

The compliance values at the final fixing, for both the first and second installations were determined after both direct (metrological) and indirect (by standardized Charpy specimens) verification had been completed.

The results of tests of the first installation, taken by the use of the instrumented specimen and related electronics are the following:

first installation:

defect status	brief description of the situation	T/2 msec	Se $N/m \cdot 10^6$	Sm $N/m \cdot 10^6$	Co $m/N \cdot 10^{-9}$
1	anvil spacing 40.1	2.410	33.9	45.4	10.90
2	anvil spacing 40.6	2.340	35.9	49.2	10.10
3	loose base	1.775	62.5	117.0	4.25
4	looser base	1.846	57.8	101.0	4.90
5	1 loose anvil bolt	1.885	55.4	94.7	5.27
6	2 loose anvils bolts	2.25	38.9	54.9	9.10
7	all loose anvil bolts	2.350	35.6	48.6	10.20
8	first final fixing	1.911	53.9	90.4	5.52

The results of tests of the second installation, taken by the use of the instrumented specimen are the following:

second installation:

defect status	brief description of the situation	T/2 msec	Se $N/m \cdot 10^6$	Sm $N/m \cdot 10^6$	Co $m/N \cdot 10^{-9}$
9	paint under base fastening nuts	1.884 1.998	55.5 49.3	94.9 78.2	5.26 6.38
10	cleaned base surfaces under fastening nuts	1.852 1.933	57.4 52.7	100.0 87.0	4.95 5.74
11	after pre-work	1.960	51.2	83.2	6.00
12	after base tigtening	2.000	49.2	78.0	6.40
13	after base levelling	1.940	52.3	86.0	5.80
14	after 2nd levelling	1.910	53.9	90.6	5.51
15	final fixing	1.860	56.9	99.2	5.03

As previously stated, the parameters which affect the compliance also affect the energy reading; the correlation between compliance variation and energy variation is presented in the following table:

defect status	brief description of the situation	Co -9 m/N *10	Delta Compl. %	Delta Energy %
1	anvil spacing 40.1	10.90	+116.6	-4.7
2	anvil spacing 40.6	10.10	+100.7	-3.8
3	loose base	4.25	-15.5	+1.1
8	first final fixing	5.52	+9.7	+0.3
14	after 2nd levelling	5.51	+9.5	-0.58
15	final fixing (ref.val)	5.03	0.0	0.0

It was important to measure the value of the compliance for impact testers manufactered by different manufacturers, after the completetion of both direct and indirect verification tests, in order to have a table of the value of the compliance of each type of machine in the "verified condition".

The measured values of the compliance, measured by the use of the instrumented specimen and the electronic equipment, referred to the impact tester are the following:

manufacterer	capacity J	pendulum type	-9 Co*10 m/N
Tinius Olsen	365	U	5.87
Metrocom	300	C	5.03
Galdabini	300	C	4.48
WPM (Ceast)	300	C	5.71

CONCLUSIONS

Tests performed in this study demonstrate that impact tester compliance can be very helpful with other characteristic measurements, in the verification of good working condition of impact testers and in the detection of onset of anomalies.

A mandatory condition for the consistency of compliance measurements is that the impact tester shall comply with standard verification rules, both direct, as, for example ASTM E23 or ISO R442, and indirect, with verification Charpy specimens.

Many of the parameters taken into account by these rules, as shown with the tests performed during impact tester installation, will greatly affect the time of contact, destroying the consistency of the compliance measurements.

REFERENCES

[1] Bluhm, J.I, "The Influence of Pendulum Flexibilities on Impact Energy Measurements", Symposium on Impact Testing, Atlantic City, june 27 1955, ASTM STP N.176

[2] Venzi, S, "La Resilienza Strumentata per la Misura del KIC Dinamico",C.S.M (Centro Sperim. Metallurgico) Report 1087R, June 1978

[3] Ireland, D, "Effect Technology Inc. Technical Report TR 974-29R" November 1974

[4] ASTM E-23 "Notched Bar Impact Testing of Metallic Materials." Annual book of ASTM standards, Section 3, Vol 03.01

[5] Porro, F, Trippodo, R, Wagner, V, "Theoretical and Experimental Evaluation of Compliance of Impact Testing Machines" AMTT Report, Januari 1982, BCR contract 861/1/4/143/80/12-BCR-I-10

[6] Trippodo, R, Bertozzi, R, "Programma di Messa a Punto e Realizzazione di un Sistema per la Resilienza Strumentata" CERMET Report, July 1987 N.50-e101

Albert K. Schmieder

COMPARISON OF METROLOGICAL TECHNIQUES FOR CHARPY IMPACT MACHINE VERIFICATION

REFERENCE: Schmieder, A. K., "Comparison of Metrological Techniques for Charpy Impact Machine Verification," Charpy Impact Test - Factors and Variables: ASTM STP 1072, J. M. Holt, Ed., American Society for Testing and Materials, Philadelphia, 1990.

ABSTRACT: Different measuring techniques were used to determine some of the specified characteristics of nine Charpy impact machines. In general, the techniques used were specified or recommended by one or more national standards. For example, the elevation of a raised pendulum was determined by direct measurement with a ruler and also by calculation from the measured angle of the pendulum rod. Both methods gave equal values with about the same reproducibility. On the other hand, significant differences were found when the friction loss in the pendulum was measured by a single swing and by multiple, successive swings. Significant differences in the period of oscillation were also found when the maximum angle of swing was 15 degrees as compared with 5 degrees. Both values were specified as permitted maximums in some national standards.

KEYWORDS: impact machines, Charpy machines, friction loss, period of oscillation, clinometer

The increase in international trade has stimulated efforts to reduce the differences between national standards for materials specifications and the methods of testing used to obtain the specified values. This paper is part of that effort. The objective is to present information which will be helpful in reducing the differences between various standards which specify the characteristics of pendulum impact machines.

In most cases, when the indicated value varies with the choice of instrument or technique, the measuring technique is specified by the national standards. In a few cases, different standards require or at least recommend different techniques. These different techniques were compared by using two or more to measure selected characteristics of one or more testing machines. The characteristics chosen for evaluation are:

Mr. Schmieder is a consultant on mechanical testing residing at R.D.7, Box 330, Closson Road, Scotia, NY 12302.

(a) pendulum elevation
(b) friction and windage losses during a full swing
(c) period of oscillation of the pendulum
(d) variation of friction loss with angle of swing
(e) location of center of gravity
(f) affect of stem bending on elevation measurement

To simplify the presentation and reduce the need to refer to previous sections while reading, each of the six programs listed above are reported and discussed under a separate major heading. An exception is that the conclusions drawn from each are gathered under one heading. Elements common to several programs are reported in the following section.

INFORMATION APPLICABLE TO ALL TESTS

Nomenclature

In most cases, the names of machine parts and quantities to be measured will follow ISO-R442 [1] [1]. Most of these are defined pictorially on Figures 1 and 6 which are in that document. Uncommon terms or specialized uses of common terms are defined below.

cg line - the straight line from the axis of rotation through the center of gravity.

cg point - a point on the cg line at the same distance from the axis of rotation as the center of strike. Note that the term center of gravity has its usual definition.

specified accuracy - accuracy of a measurement required by a standard method of verification.

permitted inaccuracy - one tenth of the specified tolerance.

Machines Whose Characteristics Were Measured

During the study of some of the variables listed above, nine machines were measured; during others, only one. In each section, the machines measured will be identified by the symbol shown in Table 1. The letter in the symbol indicates the form of pendulum hammer. The letter C refers to the disk shape in which the striking edge can be observed during a test. The letter U refers to the hammer form having the striker projecting from an upper plate and hidden by side pieces. It is not the intent of this report to identify and compare individual machines, so the dimensions are nominal.

TABLE 1 -- Description of Machines

Identifying Symbol	C1	C2	C3	C4	U1	U2	U3	U4	U5
Rating, J	3	20	350	2500	100	350	350	350	400
(ft·lbf)	(2)	(15)	(250)	(1900)	(75)	(250)	(250)	(250)	(300)
Angle of fall, degrees	150	150	110	130	135	135	135	120	135
Pendulum length, m	0.3	0.3	1	2	1	1	1	1	1
(ft)	(1)	(1)	(3)	(6)	(3)	(3)	(3)	(3)	(3)

[1] Figures in square brackets identify references listed on the last page.

Methods of Calculation

Unless stated otherwise, the methods of calculation were those shown in the reference previously cited [1] .

Measurement of Angular Position of the Pendulum

A clinometer was clamped to the pendulum shaft and read while the pendulum was held in a stationary position. The instrument consists of a frame in which is mounted a protractor carrying a sensitive spirit level. The protractor is rotated by a micrometer screw graduated each minute of arc. Angles were read to 0.5 minutes. The angles at the end of the swing were retained by the position of the friction pointer. This position was recorded by attaching a thin strip of polished metal over the scale and marking this strip with a fine scribe line at the tip of the pointer. A prop with a jack screw was used to hold the pendulum at the marked position while the clinometer was read. The prop was positioned so that the line of action of the supporting force passed near the center of gravity of the pendulum.

A 4X magnifier was used while reading or marking the pointer position. The estimated accuracy of determing the pointer position was 1/4 millimeter (0.01 inches). For a friction pointer of average length, this corresponds to a maximum estimated error of 4 minutes of arc.

If the pendulum is assumed to be rigid, the clinometer may be mounted in any position without affecting the accuracy of the readings relative to the reading at a known pendulum angle, in this case, the vertical position of the pendulum. The only limitation on mounting position is that the plane of the protractor be parallel to the plane of swing of the pendulum. However, it is essential that the clinometer does not move relative to the pendulum during all readings.

During these tests, the only situation in which the lack of rigidity of the pendulum introduced a significant error was while the pendulum was latched. The reported readings were corrected for this error by a method explained in a later section.

COMPARISON OF METHODS OF DETERMINING PENDULUM ELEVATION

Method of Test

Elevation of the pendulum of machine U4 was measured using two methods: the first by direct measurement, the second by calculation from measurement of the angular positions of the pendulum stem. For the direct measurement, a beam with machined flange surfaces supported by jack screws was leveled using a precision level graduated in intervals of 1.5 minutes of arc. The distance of a cg point above the beam was measured using an engraved steel scale and a 4X magnifier. The method of locating the cg point is described in a separate section. Scale measurements were made at three positions of the pendulum: latched, hanging, and supported on an adjustable prop at its static position at the end of a free swing from the latched position.

For the second method, the angular position of the stem was measured using a clinometer at three positions of the pendulum. These were (1) while the striker was latched, (2) while the striker was held in contact with a specimen in the testing position, and (3) while the striker was propped at the position of the end of a free swing. The first reading was corrected for stem deflection as discussed in a later section. The second reading was corrected to the free-hanging position.

Tests by each method were repeated five times to measure the reproducibility under a variety of instrument orientations. Between tests, both the reference beam and the clinometer were turned in the sequence listed below.

Test Number	1	2	3	4	5
Orientation change	Original	End-for-End	Upside Down	End-for-End	Original

Results

For the direct method, the elevation of any position is by definition the difference between the ruler reading at the position and the reading at the free-hanging position. The non-dimensional friction loss per swing is the elevation at the latch position minus that at the end of the upswing, that difference then divided by the latched elevation.

The calculation of elevation using angular measurements was more involved. The observed angle at the latched position was corrected for stem deflection by the method described in the section on that subject. The observed angle when the striker was in contact with a specimen was corrected by the movement necessary to reach that position from the freely hanging position.

The average friction loss for the five tests is 0.55 percent by both methods. The standard deviations are 0.03 percent for the direct measurement and 0.04 percent for the values calculated from angle measurements, excluding the error in establishing the cg point.

Discussion

The values shown above indicate that direct measurement by a scale resting on a level reference surface is equal in accuracy to elevation values calculated from measurements of pendulum angle by a clinometer.

The direct measurement has the advantages of requiring less expensive equipment which is available in many laboratories and of requiring less knowledge of mathmatics to calculate the final result.

The major disadvantage of the direct method for an inspection service is the difficulty of moving the reference surface and scale, both being about two meters (six feet) in length. The clinometer and associated equipment can be carried in a tool box that will fit under an airplane seat.

The additional time required to set the level reference for the direct method is about equal to that needed for the correction for stem deflection when required. On average, the direct method requires

about 10 percent more time for a typical six-point scale calibration and a single swing friction measurement.

FRICTION AND WINDAGE LOSSES DURING FULL SWINGS

Method of Test

Each machine was tested by the following series of free swings from the latched position. The series was repeated at least once.

(1) single swing with the pointer set at full scale before release,
(2) with pointer set as in (1) swinging was allowed to continue until the pendulum is near the latched position for the fifth time, then the pointer is reset to ten percent of full scale,
(3) with pointer set as in (1), repeatedly latched and released without pointer reset until the pointer shows no further motion,
(4) repeat (1),
(5) repeat (2) but with the addition of a pointer reset to full scale each time the pendulum is near the latched position.

The angle of the pendulum was marked at the following positions: while latched, while hanging freely, and after each of the series above. If the difference in marked position was greater than the amount discernible by using a 4X magnifier, the series was repeated twice more and the average reported.

Results

The percentage values per swing are shown in Table 2 . The values shown are calculated from the series of tests previously listed. Test 3 of the series measures the loss in the pendulum during one swing. It is shown on the first line[1] of the table. Test 1 measures the loss in the pendulum due to one swing plus the loss in the pointer due to one upswing. The difference between the losses measured in Tests 1 and 3 is the loss in the pointer. It is shown on the second line.

Test No. 2 of the series measures the loss due to one upswing of the pointer plus ten swings of the pendulum. This value minus the pointer loss is divided by 11 and shown on the third line.

The fifth line shows the loss due to the pointer during one upswing. It is one fifth of the difference in loss during Tests No. 5 and 2.

The fourth line shows the average loss in the pendulum only. It is equal to one tenth of the loss during Test 2 minus the single upswing loss in the pointer shown on the fifth line.

The last line is the ratio of the single swing loss in the pendulum(determined by a single, isolated swing)to the corresponding average loss from a series of ten successive swings. That ratio is

[1]The line numbers in this section all refer to Table 2 .

TABLE 2 -- Friction and windage loss, percent per swing.

Machine identification	C1	C2	C3	C4	U1	U2	U3	U4	U5
For single swing									
Pendulum only	0.44	0.73	0.10	....	0.59	0.30	0.25	0.25	0.33
Pointer only	3.90	0.31	0.00	0.00	0.00	0.00	0.00	0.26	0.00
For multiple swings									
E 23 procedure [2]	0.49	0.72	0.11	0.38	0.72	0.35	0.29	0.27	0.33
Pendulum only	0.54	0.79	0.12	0.42	0.79	0.38	0.32	0.32	0.36
Pointer only	3.78	0.30	0.01	0.02	0.01	0.03	0.00	0.26	0.03
Ratio, Single:Multiple[a]	0.81	0.92	0.83	....	0.75	0.86	0.78	0.78	0.92

TABLE 3 -- Percentage decrease in period for 15, 10, 5 degree swings.

Machine identification	C1	C2	C3	C4	U1	U2	U3	U4	U5
For largest swing									
Start, deg.	7.5	7.5	7.4	7.8	7.3	8.4	7.0	7.5	7.4
Cycle count	20	10	100	100	50	100	100	100	50
Loss, deg. per cycle	0.091	0.197	0.004	0.017	0.049	0.025	0.001	0.013	0.044
Period, sec.	1.150	1.150	1.9002	2.7795	1.7778	1.7959	1.7956	1.9070	1.8986
Decrease, largest to medium percent	0.09	0.26	0.09	0.06	0.10	0.11	0.02	0.05	0.08
Decrease, largest to smallest percent	0.13	1.48	0.14	0.09	....	0.24	0.08	0.08	0.28
Ellip. Integ. Correction									
Largest angle, percent	0.08	0.08	0.10	0.09	0.05	0.10	0.08	0.09	0.08
Medium angle, percent	0.12	0.29	0.13	0.10	0.11	0.15	0.06	0.09	0.12
Smallest angle, percent	0.13	1.48	0.15	0.09	....	0.26	0.08	0.09	0.29
For smallest swing									
Start, degrees	2.5	2.5	2.5	2.4	2.4	3.0	1.9	2.5	2.4
Finish, degrees	0.8	1.0	2.2	1.6	0.4	1.7	1.4	1.6	0.6
Ratio: Finish to Start	0.32	0.40	0.88	0.67	0.17	0.57	0.77	0.64	0.25

[a]For pendulum only

obtained by dividing the value in the first line by that in the fourth line. The average and standard deviations are 0.83 and 0.06.

Discussion

Typical standard values for maximum friction loss in the pendulum and pointer combined are 0.5 percent (1) and 0.75 percent (3) . The sum of the first and second lines[1] of the tabulated results show all except machines C1, C2, and U1 meet the requirement of both standards. These machines differ from the others in design. The first two are small machines designed for testing nonmetallic materials. Machines listed as U1 and U2 are actually the same machine frame and bearings supporting different pendulums. The bearings are adequate for the rating of U2, which is four times that of U1. Presumably, the bearings are larger than necessary for the rating of U1 and, therefore, have excessive friction losses.

A standard value (3) for maximum friction in the pointer alone is 0.25 percent. This requirement is easily met by the machines used for testing metals with the exception of U4, which slightly exceeds the requirement.

The third line shows an arbitrary measure of the condition of the bearings. The standard value (3) not to be exceeded is 0.40. This criterion of the friction losses is in agreement with the one above in the evaluation of the condition of the machines.

The bottom line shows that the friction losses per swing by the multiple swing tests are somewhat greater than those for a single swing. This is consistent with the concept of the following air flow of one swing being an opposing air flow for the return swing. If values from the multiple swing tests were compared to the maximum permitted values shown in the standards, machines C1, C2, and U1 would again be found to have excessive friction. As would be expected due to the measuring of a larger quantity with the same instrument, the precision of the value per swing by the multiple swing method is greater than that for the single swing method. Other advantages of the latter test are that it is less time consuming and that it can be made without additional instruments if the accuracy of the energy scale is assured by a previous calibration.

PERIOD OF OSCILLATION OF THE PENDULUM

Method of Test

The pendulum was displaced from the free-hanging position and held manually against an adjustable, non-magnetized stop. At the instant of release, a stopwatch reading in 0.01 second intervals was started. The number of times the pendulum approached the stop was counted. When a preselected number was reached, the watch was stopped. The timed interval was 100 cycles unless prevented by the rate of decay of the oscillation. Then, the count chosen was the maximum that would be completed while the oscillation was still large enough to be easily counted.

[1] Line number in this section refers to Table 2 .

Tests were made with the adjustable stop set to allow the pendulum to be deflected from the vertical by approximately 7.5, 5.0, or 2.5 degrees. The adjustable stop was left in each position while the test was repeated a minimum of three times. If the range of the observed times was less than 0.1 seconds, the average was divided by the count and reported as the period of the pendulum. If the range exceeded 0.1 seconds, the tests were repeated until the last test changed the average by less than 0.02 seconds. Then, the last average was divided by the count and reported as the period.

Results

Table 3 shows the change in the average period of oscillation due to changes in the initial amplitude. In order to compare directly machines of widely different sizes, the values of period of oscillation are shown as percentage decreases from the period with the largest initial oscillation.

Discussion

Test methods for impact machine verification commonly require that the center of strike be located within one percent of the distance from the axis of rotation to the center of percussion. Since this distance varies as the square of the pendulum period, the permitted inaccuracy of the period measurement is 0.05 percent. The sixth line[1] shows that only about half of the machines tested achieved this degree of agreement between the periods measured with the maximum specified angle of swing, 15 degrees, and the minimum, 5 degrees. This indicates that it would be desirable to have closer agreement between the various standards on the magnitude of this angle. Factors pertinent to the choice of this angle are considered next.

The derivation of the formula used to calculate the distance from the axis of rotation to the center of percussion uses the fact that for sufficiently small angles of swing, the sine of the angle and its radian measure are equal. In this region, the period of the pendulum is independent of the angle. The fifth and sixth lines show that the period of the pendulum decreases progressively as the angle of swing is decreased. This indicates that the range in which the assumption above holds has been exceeded by the permitted angles of swing. Reducing the maximum specified angle of swing to less than 5 degrees is undesirable for two reasons. First, even at 5 degrees, some machines with friction losses less than those specified elsewhere in the standard will not continue swinging for the specified 100 cycles. Second, the reproducibility of the period during successive counts decreases noticeably as the angle of swing decreases and also as the number of cycles during the timed interval decreases.

Elliptic integrals [3] provide solutions for the period of the pendulum which are not limited to small angles. If this calculation would result in the corrected period being the same for all the angles tested, use of the correction could be specified instead of further restricting the angle of swing to be used during verification. The seventh, eighth, and ninth lines show the results comparable to those in the preceding two lines but corrected by elliptic integral

[1] Line numbers in this section all refer to Table 3.

solutions. For four of the machines, this correction reduced the variation due to angle of swing to less than the permitted inaccuracy. The other machines showed a variation greater than twice the permitted inaccuracy. Comparing the seventh, eighth, and ninth lines to the third line shows that when the change in period is 0.05 percent or less, the rate of decay of the oscillation amplitude from 7.5 degrees is 0.17 degrees per cycle or less. With more rapid decay, the range of the corrected values for the period increases progressively. Apparently, the effect of friction on the observed period is not negligible. Similarly, comparing the change in period to the twelfth line shows that the corrected periods for three angles of swing vary by less than 0.05 percent only if the angle after 100 cycles is greater than 60 percent of the intial value. An exception is machine C1 which is not normally used to test metals.

VARIATION OF FRICTION LOSS WITH ANGLE OF SWING

Method of Test

Machine U4 is equipped with a device for changing the latch position by five degree increments. Using this device, single swing tests were made using the same test method described in the preceding section on full swing tests; that is, by measuring the elevation at the latched position and then at the end of the upswing. Since the difference is less than one half of one percent of the measured quantities, the results showed scatter large enough to leave the trend line poorly defined. To reduce this scatter, tests were made by the multiple-swing method described in the preceding section on measurement of the pendulum period by low angle swings. By this method, the change in elevation is determined from the difference in position of the friction pointer at the top of the first upswing compared to the last counted upswing of an uninterrupted series.

Two tests with successive swings were made for each latch position. During the first test, the friction pointer was reset only enough to contact the driving arm during the last 10 percent of the first and the last upswings. During the second test, the pointer was reset to sweep from the maximum energy graduation to the end of the upswing during each upswing.

Each type of test was repeated at each latch position at least twice. If the results differed by more than twice the estimated reading error of the scale at that level, the tests were repeated until the change in the average due to additional tests was equal to or less than the reading error.

Results

The scale of machine U4 reads absorbed energy. For a given number of cycles without full pointer reset, the change in reading is the friction of the pendulum for a number of swings equal to two less than double the number of cycles. The loss per swing was calculated for each latch position. Table 4 shows the ratio of other values to the loss from the highest latch position. The amplitude of swing was determined by two different measures: (1) the angle of swing and (2) the residual energy. By definition, the residual energy is the machine

rating minus the scale reading. For each measure of amplitude, the average of the value at first and last swings was taken as the point at which the average loss per cycle occurred. The test conditions and the ratios of these average values are also shown in Table 4. Table 5 shows the results of a linear regression analysis of the friction loss and amplitude as measured by each method.

A similar series of tests were made with the friction pointer reset to the maximum energy graduation as each cycle was completed. The energy loss with the reset minus that without the reset was divided by the number of pointer resets to obtain the energy loss due to the pointer. These values were converted in the same way as the values of pendulum loss and reported in the same tables.

TABLE 4 -- Friction loss, amplitude of swing and residual energy for various latch positions.

Latch position, degrees	Cycle count	Ratios for pendulum			Ratios for pointer		
		Loss	Angle	Energy	Loss	Angle	Energy
120	20	1.000	1.000	1.000	1.000	1.000	1.000
110	20	0.828	0.965	0.908	0.91	0.965	0.908
100	20	0.684	0.882	0.792	0.83	0.882	0.792
90	40	0.530	0.774	0.647	0.74	0.774	0.647
80	40	0.407	0.691	0.521	0.59	0.691	0.521
70	40	0.297	0.608	0.429	0.51	0.608	0.429
60	60	0.190	0.516	0.319	0.41	0.516	0.319
50	80	0.120	0.426	0.224	0.32	0.426	0.224

TABLE 5 -- Linear correlation of (a) angle of swing with friction loss and (b) residual energy with friction loss.

	For pendulum only		For pointer only	
Coefficient of correlation	(a) 0.985	(b) 0.995	(a) 0.996	(b) 0.997
Slope of best fit line	0.662	0.893	0.85	1.14
Loss intercept	-0.600	-0.170	-0.19	+0.13

Discussion

Most test methods that require or suggest a correction of the absorbed energy for friction loss assume that loss to be proportional to the angle of swing. This is equivalent to assuming Coulomb friction in which the friction force is independent of velocity. A different reasonable assumption is that the loss is mostly due to windage. Then, for blunt shapes such as the pendulums, the loss varies as the square of the velocity, which in turn varies as the elevation of the pendulum at the top of its down swing or upswing. This elevation is proportional to the residual energy; that is, the energy at the latched position minus the absorbed energy. The purpose of these tests is to compare the results from these two assumptions with the measured values of friction work during swings from various elevations. To quantify this comparison, a linear regression analysis was made of the friction work with each of these measures of the amplitude of swing. The pendulum loss and the pointer loss were considered separately.

If the two variables were perfectly proportional, the coefficient of correlation would be 1.000. Due to the ratio form in which the data were analyzed, a perfectly proportional relationship would result in a slope of 1.000 and an intercept at 0.000 loss. The values in Table 5 show that for the pendulum loss, the assumption of loss proportional to residual energy is significantly more accurate than the angle-of-swing assumption. For the pointer loss, the two assumptions seem to be equally applicable.

LOCATION OF A LINE FROM THE AXIS OF ROTATION TO THE CENTER OF GRAVITY

Method of Test

Several methods were used to mark or measure the position of the cg line and cg point on machine U4. Only one of these methods was used when testing the other machines. Before any of the tests, the pendulum was started in a small oscillation in a room without perceptible air currents. Measurements were made after the pendulum came to rest. To redistribute the lubricant in the bearings, the pendulum was swung from the latched position between each small-swing measurement.

The methods used consist of two steps. The first step is to locate the striking edge relative to the specimen supports. The second step is to determine the distance at which a vertical line through the axis of rotation passes a specimen or pin resting on the supports.

The first step was accomplished by either of the two following devices and procedures. The first device was a proximity detector mounted on a micrometer calibrating stand. The oscillation decay to rest was recorded on a chart. Then the pendulum was moved to contact a pin resting on the specimen support. The micrometer was advanced until the record again showed the rest position. The second procedure was similar except that the proximity detector was replaced by a dial indicator supported on a magnetic stand. The stand was advanced toward the latch until the spindle tip was separated from the hammer by the smallest visable gap. The bezel was set to zero, then the pendulum moved to contact the pin and the indicator read.

The second step used one of two different devices, either a plumb bob and scale or a clinometer. The plumb bob string was held above the shaft so as to barely touch a machined portion while the bob tip was just above a scale held horizontally against the anvil portion of the specimen support. The clinometer was clamped to the pendulum stem and read while the striking edge was pressed against a specimen or pin on the supports. The reading was adjusted by an angle equal to the motion measured in the first step divided by the pendulum length.

For U-type pendulums, a depth micrometer was used to transfer to the outside surface the distance from the leading face to the striking edge and also the distance from the plane of the bottom to the center of strike. From the point so established, the distance determined from the measurements in the two steps above was laid off horizontally to establish the cg point.

Results

It was noted that when the striker was brought into contact with the pin on the anvils and released, the pin rolled or slid to maintain the contact. This caused an obvious increase in the rate of decay of the oscillation. This effect was eliminated by avoiding contact between the pin and the striker during oscillation. In testing machine U4, a standard Charpy specimen was used in place of the pin. The specimen was dragged when the pendulum was released from contact to start the oscillation. When the oscillation was started with a gap, the presence of the specimen still had an effect readily measurable on the proximity detector record. The position at rest was 0.05 mm (0.002 in) closer to the anvils when the specimen was located there.

Proximity detector records of repeated tests on machine U4 showed no discernable shift of the rest position after oscillation even though the record was readable to 0.01 mm (0.0004 in).

From the reproducibility, it was estimated that the error in measuring the distance between the striking edge and the specimen supports by the two detection devices is 0.1 and 0.3 minutes of arc for the proximity detector and the dial indicator, respectively.

The error in establishing the cg line was similarly estimated at 0.5 minutes of arc by the clinometer and 1.5 minutes by the plumb bob and scale.

Discussion

Standard values of accuracy for determination of the elevation of the pendulum are 4 minutes of arc (1) or 0.1 percent of the elevation (3). These limits are equivalent for a typical machine having an angle of swing of 240 degrees. Comparing these values to the estimated accuracies above shows that the plumb bob method of determining the cg point contributes to the error about one third of the specified maximum, which seems acceptable.

If an error of the maximum amount specified occurred in locating the cg point, this amount would be added to the down swing and subtracted from the upswing such that the loss in determining pendulum friction would be 0.2 percent of the elevation. Since the pendulum friction loss is specified as 0.5 percent (1), the effect of the error is 40 percent of the quantity. This is four times the permitted inaccuracy of 10 percent of the quantity being measured.

It is known that repeated blows to hardened steel, properly oriented to the earth's magnetic field, will cause the steel to become magnetized. Such magnetization of the striking edge and anvils is thought to be the cause of the specimen movement noted above. It might cause a significant error if the free-hanging pendulum is very close to a specimen of magnetic material.

The principal objective of the early section on comparisons of methods of measuring elevation was to compare the clinometer method to the scale method. Therefore, the cg line and cg point were established once and used for all five tests. The results above indicate that if these references had been re-established each time, the

standard deviation for the percent friction would have been 0.06 and 0.05 for the scale and the clinometer methods, respectively.

CORRECTION OF CLINOMETER READINGS FOR PENDULUM ROD BENDING

Method of Test

The clinometer was attached at six equally-spaced positions along the pendulum rod of machine U2 and read both while the pendulum was supported by the latch and while the pendulum was supported on an adjustable vertical prop whose axis, extended, passed close to the center of gravity of the pendulum. Machine U2 was selected for these tests because the latch is located at the shaft hub where it did not limit positioning of the extensometer.

The prop was adjusted to return the center of gravity of the unlatched pendulum to the same position it had while latched. The motion of the center of gravity was measured by means of a dial indicator supported on a rod resting on the machine foundation and having the spindle touching the hammer at a point under the center of gravity.

To calculate the location of the center of gravity, the dimensions of the hammer and pendulum rod were recorded, except for the wall thickness of the cylindrical rod, which was not accessible.

Results

The correction values tabulated below are equal to the angle of the cg line minus the clinometer reading. The tabulated position of the clinometer is the distance from the axis of rotation to its mid length as a percentage of the distance from the axis of rotation to the center of gravity.

TABLE 6 -- Variation of clinometer correction with position.

Distance, percent	20	30	40	50	60	70	80
Correction, minutes of arc	-4.5	-2.5	-1	+1	+2	+3	+3

The position of the center of gravity was calculated by the moments of the calculated weights of the individual portions of the pendulum about the axis of rotation and dividing by the total weight. The value obtained by assuming the rod to be standard weight pipe differed by 1.3 percent from that obtained by assuming extra heavy pipe. Both positions were within 1.5 percent of the mid point between the top plane of the hammer and the center of strike. For these calculations this mid point was assumed to be the center of gravity.

Discussion

The central portion of the pendulum rod is elastically deformed upward by the bending moment due to the force from the latch and the component of the weight of the hammer perpendicular to the rod axis. Thus, when a clinometer is attached near the axis of rotation, it will read an angle larger than the angle of rise of the center of gravity. Conversely, if the clinometer is attached on or near the hammer, the observed angle will be smaller than the angle of rise. The theory

for deflection of simple beams shows that at the maximum deflection, the tangent to the beam has the same slope as a line between the points of support. Therefore, when the clinometer is located there, the correction is zero. Furthermore, the theory shows that for an approximately straight beam of uniform cross section, the point of maximum deflection is

$$x = \sqrt{\frac{a\,(a + 2b)}{3}}, \quad \text{when a is greater than b,} \quad (1)$$

where:

a = the distance from an outer loaded point to the intermediate point;
b = the distance from the other outer loaded point to the intermediate point; and
x = the distance to the point of maximum deflection measured from the same loaded point as distance a.

For machine U2, distance x converted to be comparable to the positions in Table 6 is 42 percent. Thus, the theoretical value of the point of zero correction agrees with the experimental value interpolated from Table 6 within the estimated experimental error.

For machines with a pendulum rod of variable cross section, the formula above should not be used. It is usually simpler and faster to measure the correction than to derive a comparable formula for that specific shape. An example of this case is machine C3 which has a tapered pendulum rod of I-beam cross section. Using position measurements comparable to those in Table 6, the latch is at 40 percent. With the clinometer at 63 percent, the measured correction was +1.8 minutes of arc.

CONCLUSIONS AND RECOMMENDATIONS

The direct method of measuring elevation and the calculation of elevation from measurements of pendulum angle are about equal in accuracy and time required. It is recommended that both be permitted by standard test methods.

The relationship between the loss per swing by the multiple swing method compared to that of the single swing method is consistent enough to allow the use of either in evaluating the machine condition. However, the accuracy of the single swing method is not adequate for measuring the specified friction losses. It is recommended that a multiple swing method be specified. The multiple swing method takes less time and requires no auxiliary equipment, which further recommends its use.

The center of percussion can be determined with useful accuracy if the period of the pendulum is measured while the friction losses are limited to an amount which will permit 100 cycles of oscillation after release from a 2.5 degree displacement from the vertical position, with the added limitation that the amplitude at the 100th swing be at least one half of that at the first swing. For some machines it may be necessary to suspend the pendulum and shaft from well lubricated centers to meet this requirement.

For the eight machines tested, the friction loss in the pendulum during an upswing was found to be more nearly proportional to the change in the residual energy than to the change in angle. It is recommended that standards requiring or allowing a friction correction use that assumption.

For machines with pendulum rods of uniform cross section, the error in the clinometer reading while the pendulum is latched can be eliminated by attaching the clinometer at the point of maximum bending deflection of the rod. The location of that point can be easily calculated. If the pendulum rod has a non-uniform cross section or the clinometer is attached at other locations, significant errors in the angle of fall may result unless the observed angle is corrected for the deflection of the pendulum rod.

ACKNOLEDGMENTS

The scope of this investigation would have been more limited if the author did not have permission to visit several laboratories and make measurements on machines located there. The assistance of the following people in arranging such visits is gratefully acknowledged.

N.V. Gjaja, Schenectady Materials and Processes Laboratory
G.J. Leclerc, General Electric Co., Corporate Research and Development
R.E. Pasternak, Army Materials and Technology Laboratory

REFERENCES

[1] Recommendation R424 Verification of Pendulum Impact Testing Machines for Testing Steels, 1st ed., July 1965, International Organization for Standardization.

[2] Designation E 23-86 "Standard Method for Notched Impact Testing of Metallic Materials," 1989 Annual Book of ASTM Standards, Volume 03.01, American Society for Testing and Materials, Philadelphia, Section 5.2.6.2, p. 196.

[3] von Karman, T., and Biot, M.A., "Elementary Problems in Dynamics - Motion of a pendulum," in Mathematical Methods in Engineering, McGraw Hill Book Co., New York and London, 1940, pp. 115-119.

G. Revise

INFLUENCE OF DIMENSIONAL PARAMETER OF AN IMPACT TEST MACHINE ON THE RESULTS OF A TEST

REFERENCE: Revise, G., "Influence of Dimensional Parameter of an Impact Test Machine on the Results of a Test," Charpy Impact Test: Factors and Variables, ASTM STP 1072, John M. Holt, Ed., American Society for Testing and Materials, Philadelphia, 1990.

ABSTRACT: The calibration of impact test machines is done by two methods. A direct method which consists to verify and control the dimensions of the machines; an indirect method which consists to compare the results of a test done with reference test pieces, between a reference machine and a machine which is to verify. The values of the geometrical parameters of the machines, have an influence on the results of a test. The present work quantifies the parameters variations and compares the results obtained with bending specimens and with charpy specimens. As a matter of fact, the influence of the dimensional parameters of machines can be finally expressed in different values of energy obtained with the test pieces, and allow the comparison of different types of specimens. The choice of reference specimen is now done by ISO and by ECISS. This present work has brought some constructive element before the choice.

KEYWORDS: impact test, charpy machine, resilience, bending, anvils

Gilbert Revise
Chief of Department
Laboratoire National D'Essais
5, rue Enrico Fermi
ZA Trappes Elancourt
Trappes FRANCE

1 - Introduction

The impact test machine often known as Charpy machine, is used for the characterisation of resilience which is a relevant characteristic of a material and specially for steel. The test is very simple in its principle and in its procedure, but it gives highly dispersed results even when the homogenity is very good.

This high dispersion is not acceptable today and, if it is due to the machine, it can be improved.

Some years ago, the "Bureau Communautaire de Référence" from European Community undertook a research to make a resilience standard sample to calibrate the impact test machines in the same conditions of an ordinary test. This study had two parts :

- study of the manufacture of reference test piece which should reduce the dispersion of the results.
- study of the influence of the mechanical and dimensional parameters of the impact test machine on the results.

This part should have been done after the first one, using the reference sample. Because some difficulties have appeared in the manufacture of the sample, we performed the work with bending specimens which were used in the ISO recommendation, and in the French standard, for the calibration of the test machines.

At the same time, we found in literature other works which were done with Charpy specimens showing the influence of an impact test on the results of a test.

A part of these works is presented here.

2 - The impact test machine is constituted of a pendulum oscillating around a horizontal axis which is supported by a rigid fixed frame. The different active and reactive parts of an impact test machine are showed on figure 1.

The French and ISO standards allow a certain tolerance for the geometrical parameters of the machine.

We have made some variations of those parameters, and we made bending as indicated by the French Standard tests in the different configurations obtained.

The tests have been performed on metallic samples of 3, 5 and 7 mm thickness, as per the French standard, on a 300 J Wolpert impact test machine.

The different parameters for the active part, were :

- the position of the center of percussion
- the radius of the knife
- the speed of impact

And for the reactive part of the machine :

- the distance between the anvils
- the radius of the anvils
- the position of the plan of the anvils
- the position of the plan of the support
- the position of the sample between the anvils

Figure 1

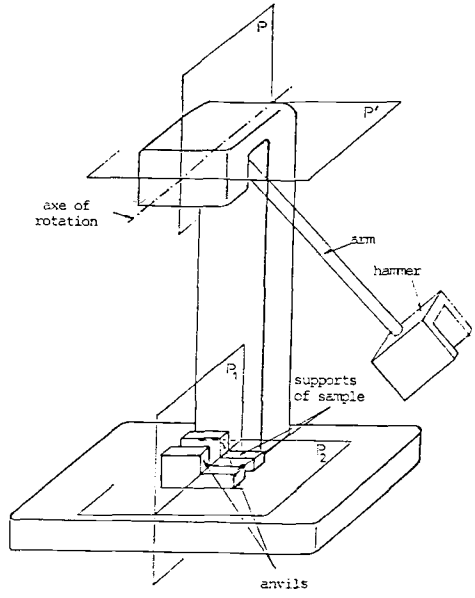

A - Influence of the position of the center percussion

If the center of percussion and the impact point are not similar, occurs a torque which gives elastic deformations to the arm of the pendulum, during the test.

This phenomena was shown with two arms of the pendulum which were of the same lenght but with different cross sections. The characteristics of the two arms, are shown in the table I.

Table I

Arm mark	Length (mm)	Type and radius (mm)	Moment of inertia (mm^4)	Equivalent of length pendulum	
				Without additional mass	With additional mass
A	635	Rod R = 14	$36,2 \cdot 10^6$	788,8	800,1
B		Tube r = 27	$280 \cdot 10^6$	773,3	800,4

In theory it is necessary to place an additional mass on the two pendulums to bring the center of percussion on the impact point. The distance between the rotation axis and the impact point is fixed at 800 mm on the impact test machine.

The deformations of the arm of the pendulum measured during a bending test of 5 mm thick samples, shows that, with the arms A and B, the vibrations have a larger amplitude if the pendulum has an additional mass. This phenomena is reproduced on the records shown on figure 2.

Figure 2

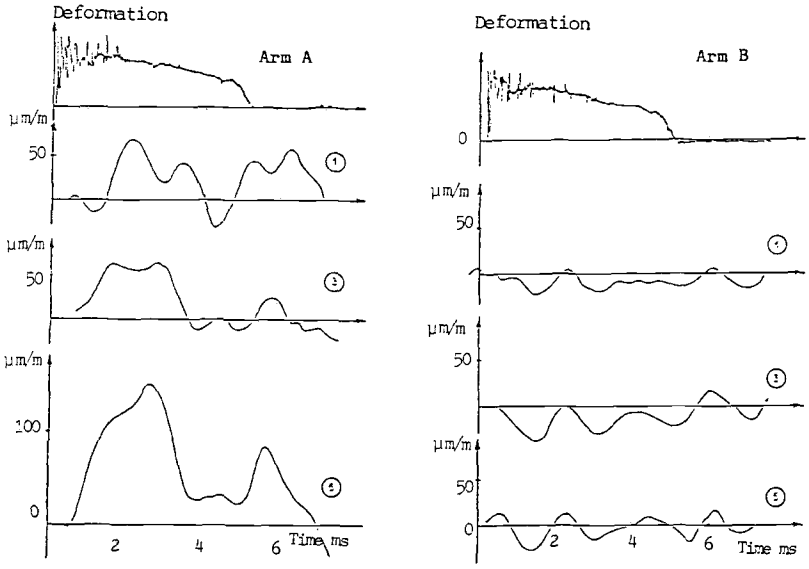

If we simulate the arm of the pendulum as a beam on two anvils which is submitted at a concentrated charge, after calibration of the measured deformations, a very simple calculation permits the evaluation of the energy which is stored in the arm. In this case, the energy is approximatively equal to 0.1 Joule, which is negligeable in the evaluation of the energy absorbed by the bending of sample.

As shown in table II, the influence of the rigidity of the arm appears as negligeable in the case of a bending test. However, the dispersion is greater when an additional mass is mounted on the hammer of the pendulum with the aim of changing the center of percussion.

Table II

Arm mark		Average Energy (J)	Maxi Distance (J)	Standard deviation
A	Without additional mass	69,7	0,5	0,2
	With additional mass	68,8	1,2	0,5
B	Without additional mass	69,3	0,3	0,15
	With additional mass	69,2	1,3	0,7

B - Influence of the radius of the knife

At the ISO meeting held in Washington in September 1988, the Japanese delegation presented a report on the comparison between the ISO and ASTM knives. What we show here, is only the effect on energy value with both knives, during a bending test.

Table III

Bending sample thickness (mm)	ISO Knife		ASTM Knife		Absolute difference (J)	Relative difference to ISO
	Average Value (J)	Maximum difference (J)	Average Value (J)	Maximum difference (J)		
3	21,7	0,5	22,0	0,5	+0,3	+1,4
5	65,8	0,9	66,7	0,3	+0,9	+1,4
7	156,8	0,9	161,8	4,6	+5,0	+3,2

The values given in table III are the averages of 5 tests. The absolute difference between the measured values exist whatever the energy level, and its value increases with the energy level.

The examination of the tested sample showed that the mark of the knife is clearly visible ; with a profile projector, it is possible to verify the radius of the knife.

For exemple, on figure 3, are given the marks obtained with three types of knives (ASTM, ISO, and a mark with a damage knife).

Figure 3

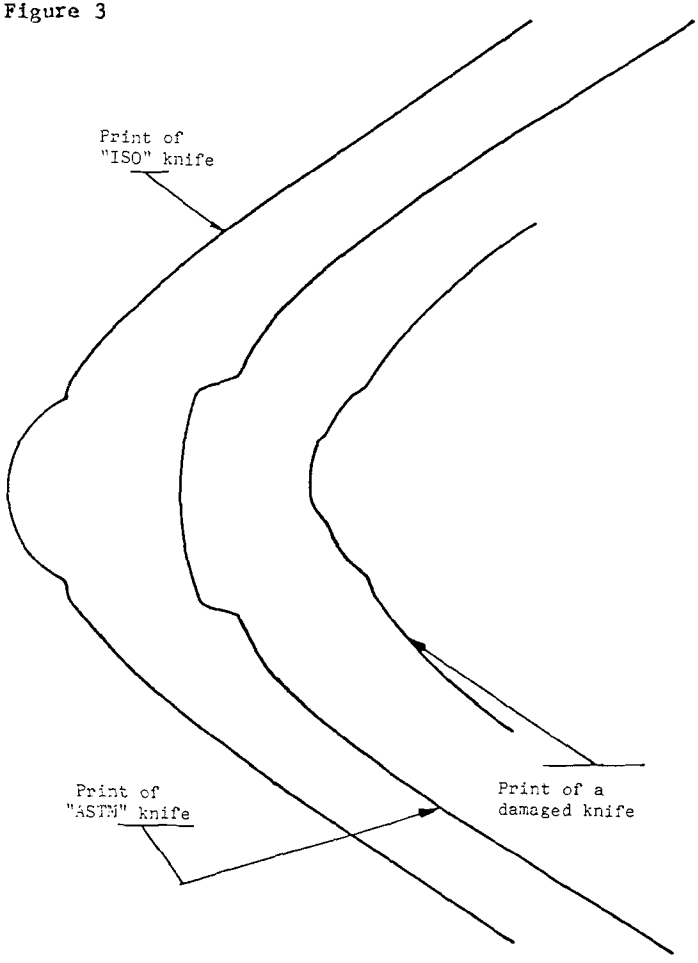

C - Influence of the impact speed

The potential energy and the impact speed are both related to the fall height of the pendulum. Some tests have been done with 3 mm thick sample and with impact speeds equal to 5.3 and 3.2 m/s. The results are in table IV.

Table IV

Impact Speed (m/s)	Measured Energy (J)
5,3	21,7
3,2	21,4

This difference which appears is not significant. The tolerance of the standard appears as very good (for bending specimen).

D - Influence of the distance between anvils

The French standard states 0.5 mm tolerance for industrial machines and 0.2 mm tolerance for reference machines. The distances which has been selected for the test are 40 mm, 40.2, 40.5 with a tolerance of .02 mm. The distances and the position of the knife between the anvils has been verified with a casted print.

The measured energy decreases with increasing distance between anvils. The relative difference in percent is more important when the energy is low.

Table V

Thickness of the bending sample	d = 40,02 Energy (J)	DISTANCE BETWEEN ANVILS					
		d = 40,2			d = 40,5		
		Energy (J)	Difference (J)	Difference (%)	Energy (J)	Difference (J)	Difference (%)
3	24,4	23,0	-1,4	-5,7	22,9	-1,5	-6,1
5	69,0	67,6	-1,4	-2,0	66,9	-2,1	-3,0
7	156,8	154,1	-2,7	-1,7	150,3	-6,5	-4,1

Figure 4 - Influence of the distance between anvils

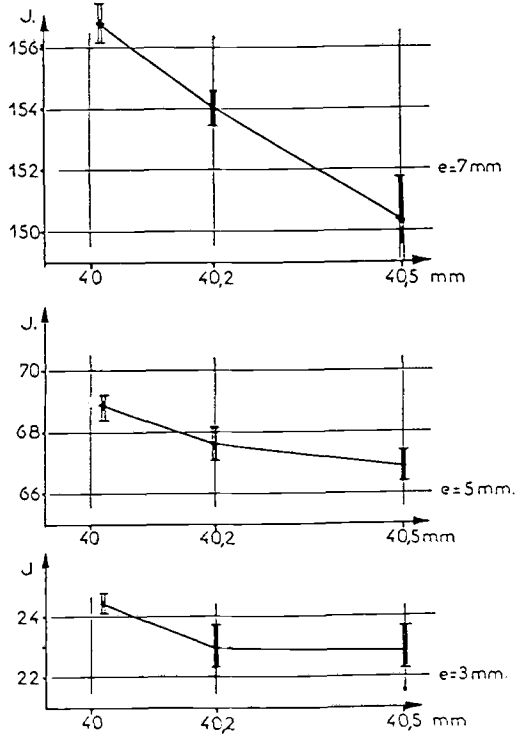

Figure 5

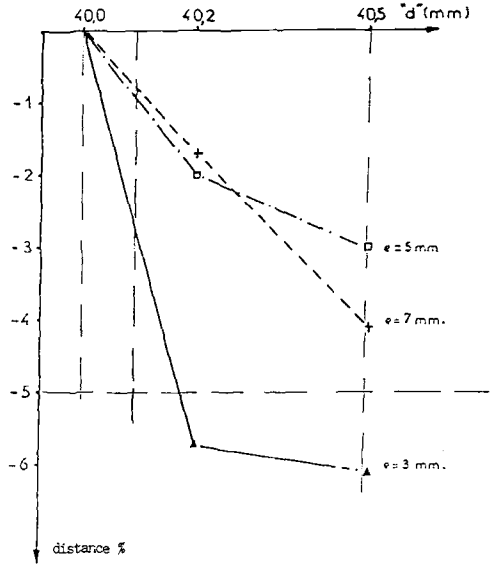

E - Influence of the radius of the anvils

The French standard states a radius of anvils between 1 and 1.25 mm. We manufactured anvils with the same dimensions, rigidity, fastening system, but with following radius 0.9, 1.0 and 1.1 mm. These anvils have been set up on the impact test machine.

Table VI

Thickness of the bending sample (mm)	Radius=10 mm Mean Value (J)	Radius R = 0,9 mm			Radius R = 1,1 mm		
		Average Value (J)	Absolute difference (J)	Distance % $\frac{R_1 - R_{0,9}}{R_1}$	Average Value (J)	Absolute difference (J)	Distance % $\frac{R_1 - R_{1,1}}{R_1}$
3	21,7	21,4	-0,3	-1,4	20,6	-1,1	-5,1
5	65,5	64,9	-0,6	-0,9	64,1	-1,1	-1,7
7	148,6	148,9	+0,3	+0,2	146,1	-2,5	-1,7

Figure 6 Influence of anvils radius

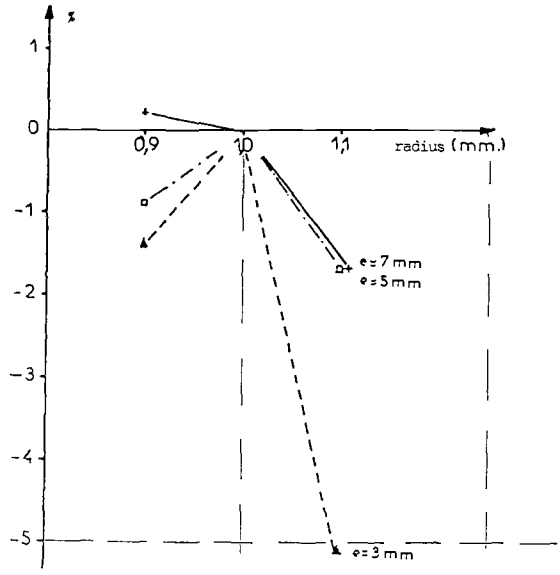

Figure 7 Values obtained

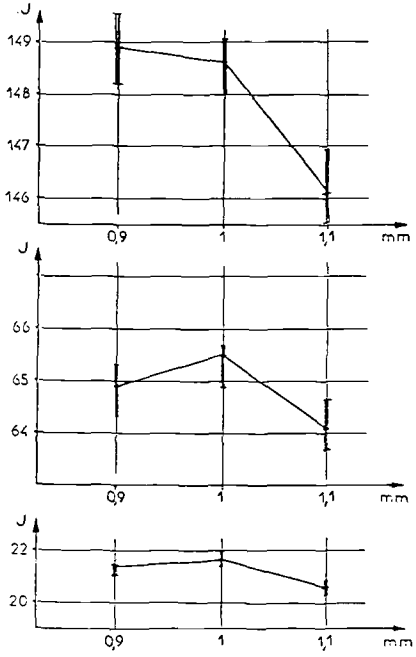

In the aim of having more information on the influence of this parameter, measurements of strain and displacement were made for each test. The maximal effort and deformation has been measured. The averages are shown table VII.

Table VII

Thickness of the sample (mm)	R = 0,9 mm		R = 1,0 mm		R = 1,1 mm	
	F maxi (kN)	d (mm)	F maxi (kN)	d (mm)	F maxi (kN)	d (mm)
3	0,90	21,0	0,95	20,8	0,92	22,4
5	3,0	23,1	2,95	23,2	2,85	23,9
7	6,47	22,6	6,50	22,9	6,29	23,0

The observed differences are more important between radius 1.0 and 1.1 mm than between radius 0.9 and 1.0 mm. However those differences are not negligeable and, when there are compared to the reference values, shows the important role of the radius of anvils in the measured energy.

Since the anvils are opposing the pendulum action, the mark on the sample increases with increasing the anvil reaction and decreasing anvil radius. As the print of the anvil is kept on the test sample, it is possible to look for damage of the anvil. The shape of the sample is measured with a profilometer. The exemple on figure 8 confirms that these phenomena are more important for the sample with the highest bending energy.

figure 8 Print of the anvil on the sample

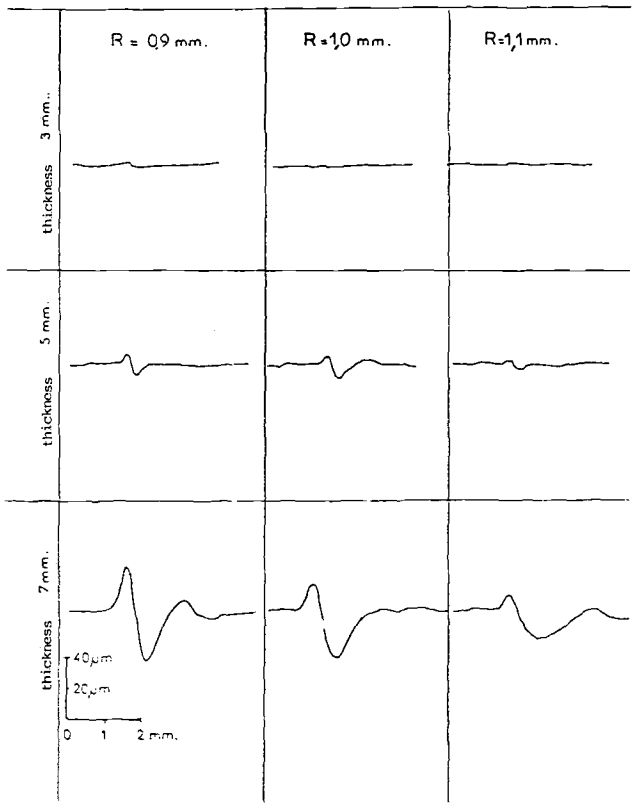

F - Influence of the position of the plan of the anvils

Due to the real difficulty of the evaluation of the position of the vertical plane of the anvils and the very severe specification in the French standard on this point, we have carried out investigations to evaluate the influence of this parameter.

We used anvils with dimensions generaly equivalent to those normally used, but with the planes P_1' and P_1'' identical and making on angle θ with the plane which contains the rotation axis. The tangent is successively equal to 5/1 000, and 10/1 000
(θ_1 = 0° 17' 11" , θ_1 = 0° 34' 22'').

figure 9

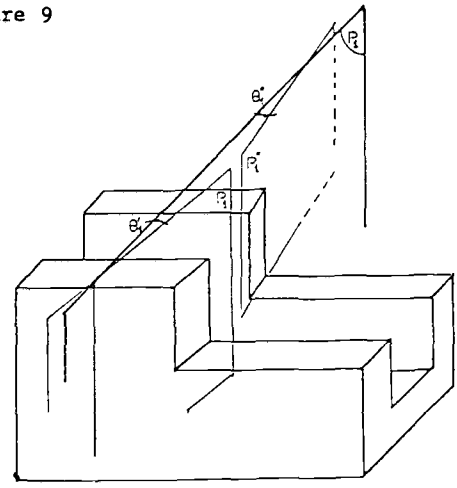

The results of the tests are shown on table VIII.

Due to the difficulty in evaluating this parameter and of its influence on the result of the test, we recommand taking 2.5/1 000 for (tan θ).

In the case when P_1' and P_1'' are parallele, the distance between these two planes must be such as the plane on which the sample rests makes an angle θ_1 with the vertical plane so that its tangent is less than 2.5/1 000. A simple calculation gives a distance less or equal to .118 mm. The tolerance of + .1 mm seems to be acceptable. - 0 mm

G - Influence of the position of the plane of the support

The same questions which arise about the anvils, have been set up about the position of the plane of the support of the sample.

Figure 10.

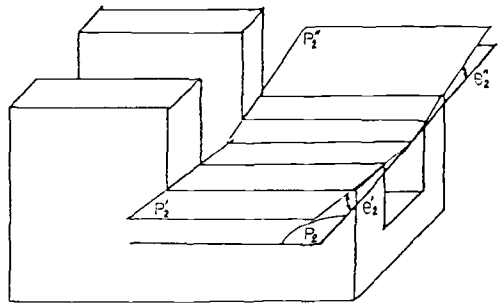

Different supports has been successively mounted with the same anvils. Their planes P_2' and P_2'' are identical, and make with the horizontal plane P_2 (which contain the rotation axis), an angle θ_2 which tangent was set successively 5/1 000, then 10/1 000 (θ_2 = 0°17'11", θ_2 = 0°34'22").

Table VIII

Thickness of the bending sample (mm)	tg(P_1' P''_1)=0	tg (P_1' P''_1) = 5/1 000			tg (P_1' P''_1) = 10/1000		
	Average Value (J)	Average Value (J)	Absolute difference (J)	Distance (%)	Average Value (J)	Absolute difference (J)	Distance (%)
3	21,7	21,2	-0,5	-2,3	20,9	-0,8	-3,7
5	65,5	64,2	-1,3	-2,0	63,8	-1,7	-2,6
7	148,6	147,2	-1,2	-0,8	146,6	-2,0	-1,4

If the axis of the knife doesn't hit the sample in a direction perpendicular to its longitudinal axis the sample can be twisted.

If one of the branchs of the sample is in the reference plane, the other one makes a certain angle with this plane, but it is difficult to evaluate this angle.
Table IX.

Table IX

Thickness of the bending sample (mm)	$tg(P'_2 P''_2)=0$	$tg(P'_2 P''_2) = 5/1\,000$			$tg(P'_2 P''_2) = 10/1000$		
	Average Value (J)	Average Value (J)	Absolute difference (J)	Distance (%)	Average Value (J)	Absolute difference (J)	Distance (%)
3	21,7	21,1	-0,6	-2,8	21,0	-0,7	-3,3
5	65,5	64,8	-0,7	-1,1	64,2	-1,3	-2,0
7	148,6	147,9	-0,7	-0,5	146,4	-2,2	-1,5

H - Influence of the position of a bend sample

The position of the sample depends on the technique of specimen placement and is independance of the machine.

The tests were made with an offset equal to 0.5, and 1.0 mm.

Table X

Thickness of the sample (mm)	Offsetting e = 0 mm Energy (J)	Offsetting e = 0,5 mm			Offsetting e = 1,00 mm		
		Energy (J)	Absolute difference (J)	Distance (%)	Energy (J)	Absolute difference (J)	Distance (%)
3	24,4	23,7	-0,7	-2,9	22,7	-1,7	-7,0
5	69,0	68,1	-0,9	-1,3	65,9	-3,1	-4,5
7	156,8	155,8	-1,0	-0,6	152,8	-4,0	-2,6

The results show the very important influence of the position of the sample on the energy value. A defect of centering of 1 mm can be easily avoided by visual inspection but this value is too large. A compromise was set up to 0.5 mm for industrial machines and 0.1 mm for reference machines.

This work on the effect of the geometrical parameters of impact tests machines on the results of the test, is not complete ; however, it gave some results which were included in the subsequent revision of the French standard.

It is still possible, even when all geometrical parameters are within the tolerances, that the calibration of the test machine by the indirect method gives results out of the standard tolerances. This situation can be easily explained : all geometrical differences, even though they are within the tolerance, correspond to energy differences ; the addition of all these energy differences may exced the limits.

Therefore, the calibration by comparison with calibrated specimens is not sufficient. At the same time, it is necessary to give dimensional measurements of the impact area of the machine and to verify that the dimensional differences are all going in the same direction. This procedure is the only one which will permit an answer to the question :

"What can we do when the two methods, direct and indirect, don't lead to the same conclusions ?".

However, because all the work reported here was done with bending specimens, it will have to be carried out with Charpy reference specimens as required by the future ISO and ECISS standards.

Arthur L. Lowe, Jr.

FACTORS INFLUENCING ACCURACY OF CHARPY IMPACT TEST DATA

REFERENCE: Lowe, A. L. Jr., "Factors Influencing Accuracy of Charpy Impact Test Data," Charpy Impact Test: Factors and Variables, ASTM STP 1072, John M. Holt, Editor, American Society for Testing and Materials, Philadelphia, 1990.

ABSTRACT: The Charpy impact test was originally developed as an acceptance test for steel products. However, using the Charpy test to evaluate the integrity of nuclear reactor vessels has caused the test data to be subject to scientific evaluation. The many small errors in parameters affecting the results produced relatively large errors in any analysis of the data. The sources affecting these errors are identified and an effort is made to quantify them. The Charpy impact test is a simple and convenient test but the end result is engineering data. To provide data for scientific evaluations greater control must be placed on all phases of the testing process.

KEYWORDS: Charpy impact test, Charpy data, neutron radiation, error analysis, controlling parameters, transition temperature shift, upper-shelf energy

INTRODUCTION

The Charpy impact test was developed as an acceptance test for steel products. Over time, the test has come to be used for a number of standard acceptance and regulatory requirements that require evaluating the test results based on specific scientific assumptions. However, little has been done to understand the basic test procedure, or to define which test parameters influence the test results. In performing and evaluating the Charpy impact testing of hundreds of unirradiated and irradiated Charpy specimens as part of the Babcock & Wilcox Owners Group (B&WOG) Reactor Vessel Integrity Program [1], a

Mr. Lowe is an Advisory Engineer (Materials) at B&W Nuclear Service Company, Engineering and Plant Services Division, Post Office Box 10935, Lynchburg, Virginia 24506-0935.

great deal has been learned about the sensitivity of results to test parameters and material conditions.

Variations in the test data can be attributed to parameters divided into two categories: test-procedure related, including the test machine itself; and material related. Only after the influence of these parameters, or variables, are understood, or at least their contribution to data variability recognized, can the Charpy impact data be reliably analyzed. This paper describes the variables that influence the Charpy impact data obtained from reactor vessel surveillance programs and demonstrates how certain of these variables influence the accuracy of the analyzed data.

BACKGROUND

Charpy impact data is widely used in the nuclear industry to evaluate the integrity of nuclear reactor pressure vessels. This usage developed from the fact that the early studies of neutron radiation on the properties of reactor vessel materials were performed, in part, using the Charpy impact specimen. The size of the Charpy specimen permitted the inclusion of a greater number of specimens than would be practical using other types of test specimens such as the drop-weight test. Besides, the study of fracture behavior associated with merchant ship failures had established a correlation between Charpy data and fracture toughness as defined by dynamic tearing or drop-weight testing [2,3]. The characteristic response of steels to irradiation as described by the Charpy impact data curve is shown in Figure 1. The Charpy transition temperature (RT_{NDT}) increases with a corresponding decrease in upper-shelf energy (USE) as the result of exposure to neutron radiation. The Charpy specimen was also adopted as the primary fracture toughness specimen for inclusion in reactor vessel surveillance programs [4].

The Charpy test was further established as the primary method for evaluating irradiated material properties by the specification of the tests in nuclear licensing regulatory requirements 10CFR50, Appendix G, "Fracture Toughness Requirements [5]" and Appendix H, "Reactor Vessel Materials Surveillance Program Requirements [6]." Both of these documents reference the use of Charpy test data to establish operating limits for the reactor vessel. In addition, the Nuclear Regulatory Commission (NRC) published Regulatory Guide 1.99, "Radiation Embrittlement of Reactor Vessel Materials [7]," that describes a procedure for estimating neutron radiation induced changes in Charpy properties as applied to various licensing requirements. In the original version, bounding conditions were defined, but the latest version is based on statistical mean values and margins using standard deviations of the data used to develop the mean values.

More recently, the NRC published the regulations concerning pressurized thermal shock containing a screening criterion based on Charpy data [8]. The latter requirement also contains a criterion of Charpy mean values, plus a margin for the uncertainty of the Charpy data, based on the applicability of the supporting data.

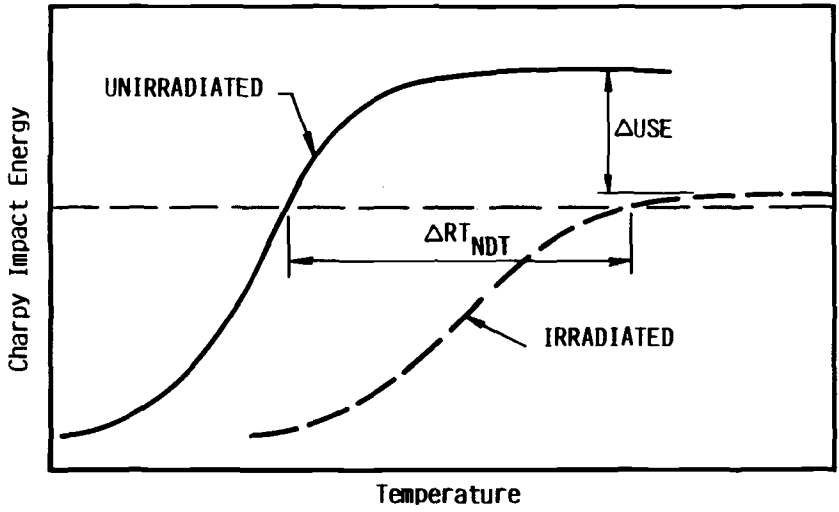

FIGURE 1 -- Characteristic response of a Charpy impact curve to neutron radiation.

Of special interest to the B&WOG Reactor Vessel Integrity Program are the Charpy data related to the Mn-Mo-Ni weld wire/Linde 80 flux submerged-arc weld metals used to fabricate a large number of reactor vessels during the late 1960's and early 1970's. This weld metal exhibits a high sensitivity to neutron radiation, and thus, is the controlling material for licensing purposes for many reactor vessels fabricated during this time period. Also, the margin required to be added to the analysis of these weld metals (per Regulatory Guide 1.99/2 = 28F or 15.6C) represents a significant conservatism compared with the actual data values used in any analytical evaluation. These developments have necessitated a review of the available Charpy test data from reactor vessel surveillance programs in an attempt to identify those parameters that influence the scatter, or uncertainty, in the data. All the Mn-Mo-Ni/Linde 80 submerged-arc data was obtained from appropriate surveillance capsule reports and each data point and related parameter was verified [9]. These data constitute a Charpy data base that is as free from errors and inaccuracies, as is possible. However, this does not mean it is error free, as will be demonstrated. This paper is based on some of the results from this ongoing effort.

Variables Influencing Charpy Data

The materials used in fabricating reactor vessels were reviewed and the role of the many processing and fabrication parameters, or variables, were identified. These parameters are listed with general comments as to the relative importance to influencing the Charpy data from a given piece of steel or weld metal.

Material History

Base metal (plate or forging)

- Product form - large variations are attributable to the differences in product form (i.e. forging or plate).
- Manufacturing process - large variations because process controls cleanliness of the steel which in turn influences Charpy data.
- Fabrication process - large variations because of changes in properties related to working directions. Such as the directional properties resulting from rolling of plate.
- Heat treatment - variations within product form - most important to control sampling requirements to insure uniformity of samples.
- Chemical composition - minor variations within product form but is important to neutron radiation sensitivity of the material.

Weld metal

- Welding process - large variations and must be controlled to provide for good intercomparisons.
- Weld wire chemical composition - minor variations within classification but variations are important to neutron radiation sensitivity.
- Weld flux type - can cause large variations between classification because of its effect on weld cleanliness.
- Weld flux chemical composition - small variations in chemical composition will affect metallurgical characteristics of the deposited weld metal, which can affect Charpy data.
- Welding procedure - variations are primarily a function of heat input, which in turn, is a function of amperage, voltage, and welding travel speed.
- Heat treatment - temperature and time at temperature, plus cooling rate; pre-heat temperature, intermediate stress relief cycles; temperature and time of temperature at the final stress relief - all can have a significant affect on Charpy data.

Specimen Preparation

- Location in material - properties within base metals vary as to location in the final product form; this is not as important a factor for weld metals as for plates or forgings.

- Specimen fabrication - the accuracy of the machined specimen and notch geometry must be maintained within specified dimensions.

- Orientation of notch - orientation of the notch relative to the major axis of the product form must be kept consistent with type data to be obtained.

Service Environment

- Neutron spectrum - importance not defined but it is assumed that the higher the spectrum energy the greater the effect on both transition shift and upper-shelf decrease.

- Neutron flux - importance is not defined but effect believed to be similar to that of spectrum.

- Neutron fluence - the greater the fluence the larger the transition temperature shift and greater the decrease in upper-shelf energy.

- Temperature - the amount of shift, or upper-shelf decrease, is inversely proportional to irradiation temperature.

Testing

- Machine installation - must be installed according to applicable instructions and standards. An improperly installed machine will produce erroneous data.

- Machine calibration - must meet applicable calibration requirements. An uncalibrated machine produces questionable data!

- Operator experience - most important to have an experience operator who understands the test procedure and has developed a smooth and consistent testing technique.

- Operator technique - must demonstrate consistent performance in conducting the actual testing.

Evaluation

- Evaluator experience - experience with the type of material to be evaluated provides for a better interpretation of the data.

- Evaluator technique - an understanding of the principles of statistics is beneficial to interpreting data.

- Manual vs. computer plotting - computer techniques are desirable but must address measured data and not function on idealistic Charpy curve interpretations. Manual plotting has consistently demonstrated better interpretation of data.

Statistical Evaluation Method

The statistical indicators used to evaluate the role of the various parameters that influence the Charpy data are the coefficient of determination and the mean square error, or standard error. The coefficient of determination is a measure of the goodness of fit of the mathematical model to the data with a value of 1.0 being indicative of a perfect fit. The mean square error is a measure of the variation of the data about the regression model. The smaller the standard error of the estimate the smaller the scatter of the observed data to the predicted values produced by the model. A small standard error is desirable.

The coefficient of determination or fit, expresses the proportion of the variance of one variate as given by the other, when the first is expressed as a linear regression of the second. It is a measure of the usefulness of the terms, other than the constant, in the model. For simple linear regression the coefficient of determination measures the proportion of total variation about the mean of the dependent variable explained by the regression. It is the correlation between the observed dependent variable and the predicted values of the dependent variable. A perfect fit of the model to the data would produce a value of 1.0, given no repeated measurements.

The mean square error provides an estimate, based on the degrees of freedom, for the variance about the regression, based on the data set and parameters in the model. If the regression equation were to be estimated from an infinitely large number of observations, the variance about the regression would represent a measure of the error with which any observed value of the dependent variable could be predicted from a given value of the independent variable using the fitted equation.

The formula for the determination of the standard error, or estimate error, from a number of independent contributing factors whose estimates of error are $\sigma_1, \sigma_2 \ldots \sigma_n$ is

$$\sigma = \sqrt{\sigma_1^2 + \sigma_2^2 + \ldots \sigma_n^2}$$

where

σ = Total error from all contributing factors

Review of Variables Influencing Charpy Shift Data

The role of various parameters on Charpy 30 ft-lb transition temperature shift was first observed during the development of new correlations for the Mn-Mo-Ni/Linde 80 weld metal to predict the change resulting from neutron radiation [7]. At the time a number of correlations were being tried that produced different coefficient of fit values. However, for select sets of data the coefficient of fit values remained relatively unchanged but the standard deviation for the fitted curves would vary significantly. Two typical sets of data are presented in Table 1.

These sets of data demonstrate that by carefully defining the selection of data not only was the coefficient of fit changed, but the standard error can be significantly changed. This observation initiated an evaluation as to the role of the various parameters identified in the previous section and their effect on the standard error. Recognizing that a larger number of factors influence the standard error than could be identified, or quantified, a listing was prepared that identified the most probable parameters. A probable error value was assigned to each based on either recognized error values for the data, or an estimate of the probable error was calculated from variations in the parameter. The parameters and their corresponding estimated error are shown in Table 2.

Using the data in Table 2, it is shown that all the estimated errors combined produce a standard error of approximately 20.9F (11.6C) which approximates the larger values shown in Table 1. A lower standard error value of 10.7F (5.9C) is calculated using items 1, 3 and 4 in Table 2 and not including items 2 and 5. This lower value closely approximates the lower values given in Table 1. The exclusion of the two items (Items 2 and 5) is possible because all the fluence analyses were performed using the same procedure and the data interpretation was performed by the same person. Therefore, it is assumed that these errors are constants and did not contribute to the standard errors. This is not to imply that there is no error from these parameters but in the analysis of this selected data base they probably contribute a similar error to each data analysis. The reason that the values for Trials A-1 and B-1 cannot be reduced is that the early fluence analysis was performed using an out-dated procedure which probably had a standard error significantly larger than the one listed in Table 1.

Another group of Charpy data analysis results is presented in Table 3. Two important observations can be made from these data. First, in weld wires A and B, the correlations based on the irradiated 30 ft-lb data produce lower standard errors than those correlations based on 30 ft-lb shift data. This difference implies that errors in the initial values influence the correlation error. This trend appears true whether two or four laboratories (test sites) provided the irradiated data.

Weld wire C poses a different relationship between the test sites when weld metal test results are separated into sub-groupings. When the same test site produced both the initial data and test data, good coefficients of fit and small standard errors were obtained. However, when the same weld metal tested by two sites was evaluated the coefficient of fit was reduced and the standard error increased. This implies the enclusion of a larger error which in this case may be related to the different testing techniques of the two test sites. The inclusion of three test sites expanded the standard error and produced mixed results as to coefficient of fit. This evaluation further demonstrates the interactions of both test procedure parameters and test laboratories.

TABLE 1 -- Selected Charpy transition shift correlation data showing variations in coefficient of fit and standard error of the estimate (Mn-Mo-Ni/Linde 80 weld metal).

Trial Number	Welds Selected	Fluence Range	R^2[a]	Syx[b], F(C)
A-1	B&W	All	0.86	23.9(13.3)
2	B&W	>3E18 n/cm^2	0.90	12.8(7.1)
3	Non-B&W	All	0.83	19.3(10.7)
4	Non-B&W	>3E18 n/cm^2	0.83	21.6(12.0)
B-1	B&W	All	0.86	22.0(12.2)
2	B&W	>3E18 n/cm^2	0.96	10.9(2.8)
3	Non-B&W	All	0.70	22.1(12.3)
4	Non-B&W	>3E18 n/cm^2	0.81	19.8(11.0)

[a]Coefficient of fit.

[b]Standard error of the estimate.

TABLE 2 -- Estimated error values for parameters affecting the accuracy of Mn-Mo-Ni/Linde 80 weld metal Charpy 30 ft-lb transition temperature data.

Item	Parameter	Estimated Error, F(C)	Comments
1	Charpy test temperature*	± 5(3)	Assumes oil baths and minimum transfer time
2	Neutron fluence	±15(8)	Normal accepted error for calculations
3	Irradiation temperature	± 5(3)	Assumes steady-state operations, no transitions in power
4	Chemical composition	± 8(4)	Calculated value based on normal variations in compositions
5	Charpy data interpretation	±10(5)	Assumes no experience with materials data

*Includes the machine error.

Review of Variables Affecting Charpy Upper-Shelf Energy

An effort was made to evaluate Charpy upper-shelf energy data in the same way that the Charpy transition temperature shift data was evaluated. This study did not produce any clearly defined effects of the various parameters with the exception of chemical composition. This effect has been recognized from the earliest studies. However, an interesting observation can be made from a plot of data from a group of weld metals fabricated from the same heat of weld wire. The unirradiated and irradiated data is shown in Figure 2. These data exhibit a variation in responses to testing at various laboratories. Certain of the data sets follow the expected trend while others exhibit sharp changes. While it is difficult to assess the cause of these variations, they are probably the result of either inadequate testing procedures, or related to the installation of the impact test machine. The variations in the data vary between 5 to 10 ft-lbs, not only between different testing laboratories, but between different data sets tested by the same laboratory. Unfortunately, there are no standard test specimens for calibrating impact testers on the Charpy upper-shelf energy region such as are available for the Charpy transition region. Standards would provide a means for cross referencing upper-shelf energy test results.

The interaction of the initial upper-shelf energy on the interpretation of irradiated data is demonstrated by comparing the decrease in Charpy upper-shelf energy to the irradiated Charpy upper-shelf energy for a group of weld metal. Figure 3 shows the effects of irradiation on the upper-shelf as a percent of the initial, or unirradiated, value plotted as a function of the fluence. Based on the power reactor data, the coefficient of fit is 0.47 and the standard error is 3.4%, or approximately 10 percent of the mean decrease value. The same data is shown in Figure 4 as the irradiated Charpy upper-shelf energy as a function of fluence. Again, based on the power reactor data, the coefficient of fit is 0.90 and the standard error is 1.3 ft-lbs, or approximately 2.5 percent of the mean irradiated value. This comparison implies that the error of the initial upper-shelf energy values may be significantly larger than the irradiated values. This evaluation of upper-shelf energy change illustrates a case of basing the evaluation of well characterized data on data that is not of equal quality and thereby producing less than desirable results.

Recommendations to Minimize Errors

The review of Charpy data presented demonstrates that relative small standard errors can be achieved in Charpy data by closely adhering to an established testing procedure. However, to achieve the ultimate in Charpy evaluation error, all the parameters identified as affecting the data must be controlled as close as practical. In the case of surveillance program testing, controlling the final test parameters will not reduce the errors introduced in the initial data set. Since, the final evaluations are often based on the

TABLE 3 -- Evaluation of several Mn-Mo-Ni/Linde 80 weld metals showing influence of test site and inherent properties of weld metal on Charpy 30 ft-lb transition temperature data.

Weld Wire	Number Weld Metals	Number Sites Testing: Initial Data	Number Sites Testing: Test Data	Data Evaluated	R^2[a]	Syx[b] F(C)
A	2	2	2	30 ft-lb shift	0.73	21.4(11.8)
		N/A	2	Irrad. 30 ft-lb	0.88	19.2(10.7)
B	2	2	4	30 ft-lb shift	0.81	26.8(14.9)
		N/A	4	Irrad. 30 ft-lb	0.87	18.9(10.5)
C	2	2	3	30 ft-lb shift	0.44	39.5(21.9)
		N/A	3	Irrad. 30 ft-lb	0.35	39.5(21.9)
C-1	1	1	1	30 ft-lb shift	0.96	14.1(7.8)
		N/A	1	Irrad. 30 ft-lb	0.94	14.9(8.3)
C-2	1	1	2	30 ft-lb shift	0.53	29.0(16.1)
		N/A	2	Irrad. 30 ft-lb	0.51	26.1(14.5)
C-3	1	2	3	30 ft-lb shift	0.87	41.7(23.2)
		N/A	3	Irrad. 30 ft-lb	0.44	42.3(23.5)

[a]Coefficient of fit.

[b]Standard error of the estimate.

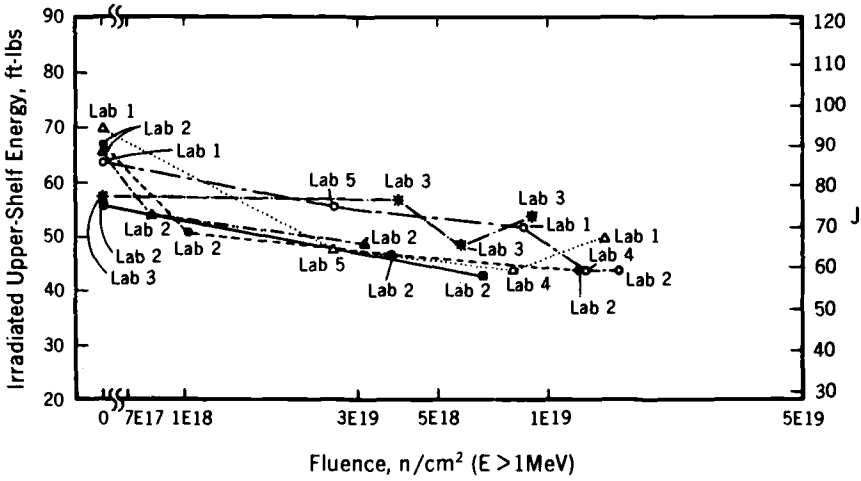

FIGURE 2 -- Irradiated Charpy upper-shelf energy as a function of fluence.

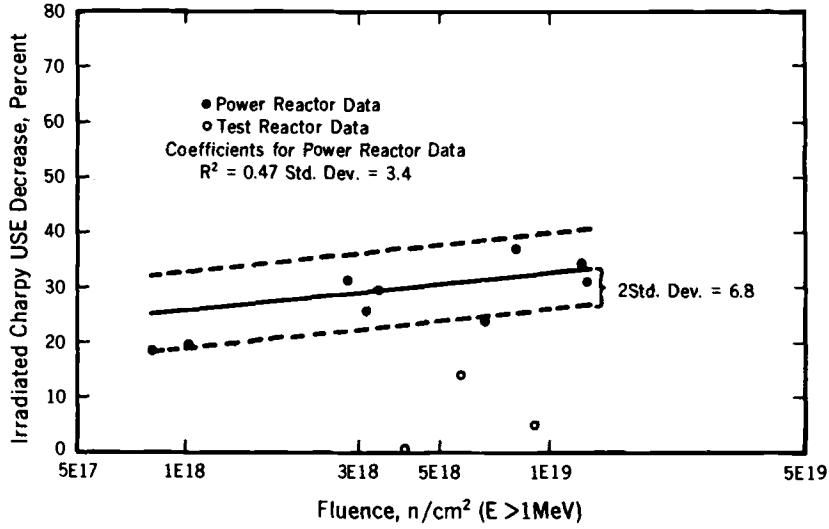

FIGURE 3 -- Irradiated Charpy upper-shelf energy decrease as a function of fluence.

analysis of two sets of data obtained at different times and by different laboratories, the best results (minimum errors) can only be obtained by both testing laboratories closely controlling all testing parameters that can affect data.

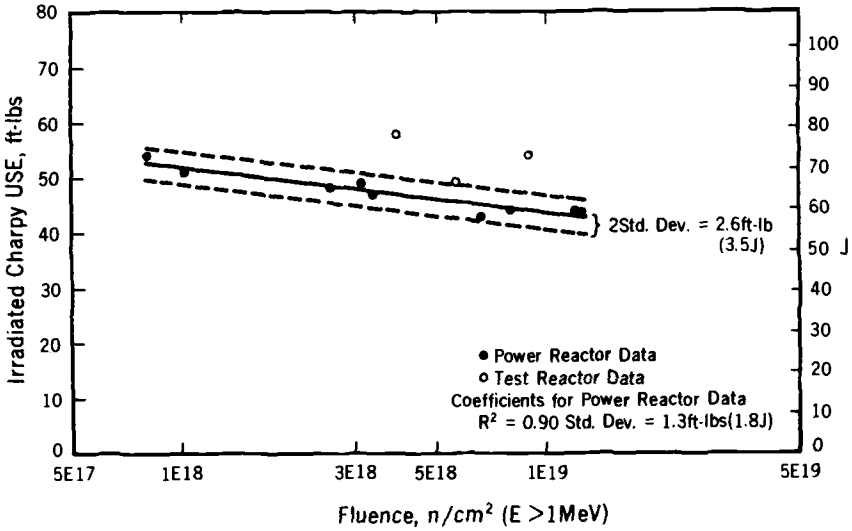

FIGURE 4 -- Irradiated Charpy upper-shelf energy as a function of fluence.

ACKNOWLEDGEMENTS

This paper reports work done in support of the Babcock & Wilcox Owners Group Reactor Vessel Integrity Program. The author acknowledges and expresses appreciation for their support and their permission to report program results. The support of J. W. Pegram in providing the statistical analysis is acknowledged with appreciation.

REFERENCES

[1] Lowe, A. L., Jr., Moore, K. E., and Aadland, J. D., "Integrated Reactor Vessel Materials Surveillance Program for Babcock & Wilcox 177-FA Plants," Effects of Radiation on Materials: Twelfth International Symposium, ASTM STP 870, F. A. Garner and J. S. Perrin, Editors, American Society for Testing and Materials, Philadelphia, 1985, pp. 931-950.

[2] Stout, Robert D., and W. D'Orville Doty, Weldability of Steels, Welding Research Council, New York, 1953.

[3] Control of Steel Construction to Avoid Brittle Failure, M. E. Shank, Editor, Welding Research Council, New York, 1957.

[4] American Society for Testing and Material, Standard Practice for Conducting Surveillance Tests for Light-Water Cooled Nuclear Power Reactor Vessels, E185-82, July 1982.

[5] Code of Federal Regulation, Title 10, Part 50, Fracture Toughness Requirements for Light-Water Nuclear Power Reactors, Appendix G, Fracture Toughness Requirements.

[6] Code of Federal Regulation, Title 10, Part 50, Fracture Toughness Requirements for Light-Water Nuclear Power Reactors, Appendix H, Reactor Vessel Material Surveillance Program Requirements.

[7] U.S. Nuclear Regulatory Commission, Radiation Damage to Reactor Vessel Material, Regulatory Guide 1.99, Revision 2, May 1988.

[8] Code of Federal Regulations, Title 10, Part 50.61, Fracture Toughness Requirements for Protection Against Pressurized Thermal Shock Events.

[9] Lowe, A. L., Jr., and Pegram, J. W., "Improved Correlations for Predicting the Effects of Neutron Radiation on Linde 80 Submerged-Arc Weld Metals," Effects of Radiation on Materials: 14th International Symposium, ASTM STP 1046, Volume II, N. H. Packen, R. E. Stoller and A. S. Kumar, Editors, American Society for Testing and Materials, Philadelphia, 1989.

Toshio Naniwa, Masayuki Shibaike, Megumu Tanaka, Hiroshi Tani, Kenichiro Shiota, Namio Hanawa, and Toshiaki Shiraishi

EFFECTS OF THE STRIKING EDGE RADIUS ON THE CHARPY IMPACT TEST

REFERENCE: Naniwa, T., Shibaike, M., Tanaka, M., Tani, H., Shiota, K., Hanawa, N., and Shiraishi, T., **"Effects of the Striking Edge Radius on the Charpy Impact Test,"** Charpy Impact Test: Factors and Variables, ASTM STP 1072, John M. Holt, Ed., American Society for Testing and Materials, Philadelphia,. 1990.

ABSTRACT: Effects of the striking edge radius of the Charpy impact test on the absorbed energy and the abrasion of the striker were investigated. The absorbed energy of the 8mmR was higher than that of the 2mmR when the absorbed energy was above 200N-m. The cause of this difference is that the bending deformation of the test specimen and the friction between the anvil and the test specimen are large in case of the 8mmR. The abrasion of the 8mmR striker was extremely large and it is too difficult to maintain the radius dimension according to ASTM E 23.

KEYWORDS: Charpy impact test, Charpy apparatus, pendulum striking edge, absorbed energy, abrasion

INTRODUCTION

The Mechanical Testing Subcommittee found the difference in the absorbed energy of the Charpy impact test between the 8mmR and the 2mmR striker[1]. The absorbed energy of the 8mmR striker was higher than that of the 2mmR in case of 400 N/mm^2 class steel. This relation was reversed in case of 800N/mm^2 class steel.

The purpose of this paper is to investigate effects of the striking edge radius on the absorbed energy and the abrasion of the striking edge in addition to our previous investigation.

T. Naniwa and M. Shibaike are with Nippon Steel Corp., M. Tanaka is with NKK Corp., H. Tani is with Sumitomo Metal Industries, Ltd., K. Shiota is with Kobe Steel, Ltd., N. Hanawa and T. Shiraishi are with Kawasaki Steel Corp., All the members belong to The Mechanical Testing Subcommittee, The Joint Research Society of The Iron and Steel Institute of Japan, 9-4, Otemachi-1-Chome, Chiyoda-ku, Tokyo, Japan.

EXPERIMENTAL

Material

Grade and class: Carbon and low-alloyed steel. Values of the tensile strength were from 400 to 600 N/mm^2.

Absorbed energy: From 100 to 500 N-m

Test specimen: ASTM E23 Type A

Instrumentation

ASTM type Charpy impact testing machines (The striking edge radius is 8mm) and JIS type Charpy impact testing machines (The striking edge radius is 2mm) were used.

Dynamic load-time measuring method during the Charpy impact test: Two strain gages were glued on both sides of the striking edge. It was possible to record load during the Charpy impact test. The schematic diagram is shown in Fig. 1.

Static bending device: We made the same devices as strikers and anvils of the Charpy impact test for the static bending test. Devices are shown in Fig. 2. The static bending tests were performed by these devices and the compression testing machine. The load and the displacement of the striker were measured by the compression testing machine and recorded on the X-Y recorder.

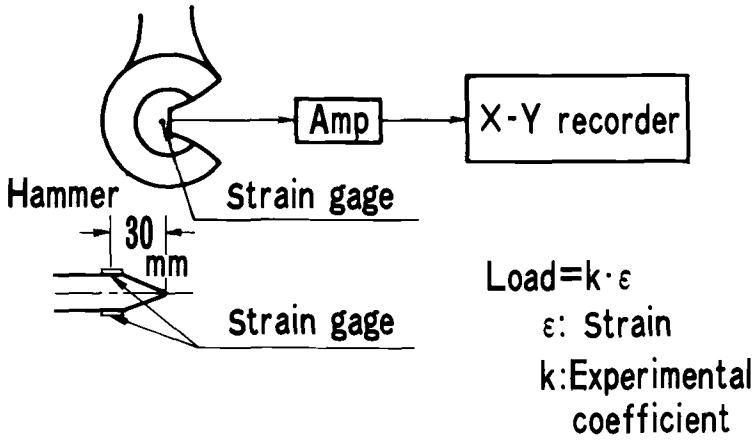

Fig. 1 Dynamic load measuring method for the Charpy impact test.

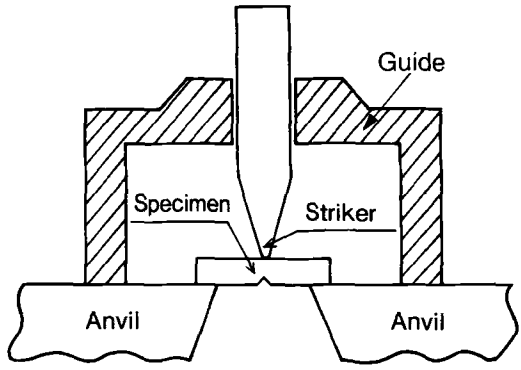

Fig. 2 Devices for the static bending test.

RESULTS

Comparison of Charpy Impact Test Results between the 8mmR and the 2mmR Striker

Charpy impact test results are shown in Fig. $3^{(a)-(d)}$. No difference was recognized in the absorbed energy between the 8mmR and the 2mmR less than 200N-m energy. However, the absorbed energy of the 8mmR was higher than that of the 2mmR above 200N-m energy. The higher the absorbed energy was, the larger the difference of absorbed energies between the 8mmR and the 2mmR was. No difference was recognized in shear fracture, lateral expansion, and transition temperature.

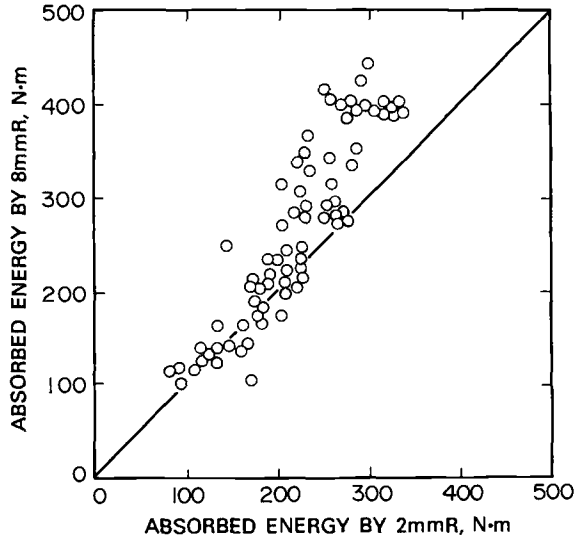

Fig. 3-(a) Comparison of the absorbed energy between the 8mmR and the 2mmR

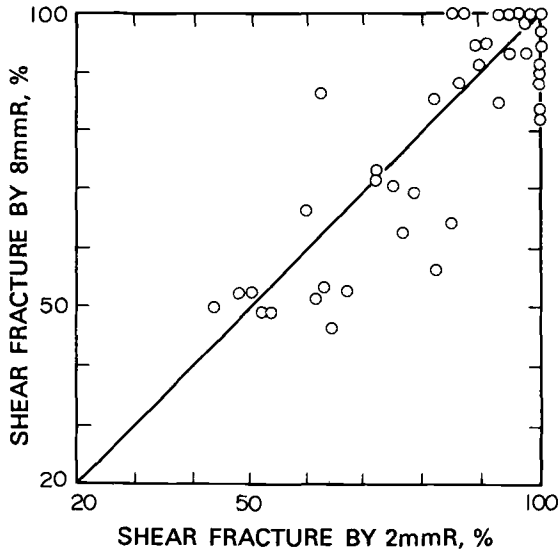

Fig. 3-(b) Comparison of the shear fracture between the 8mmR and the 2mmR.

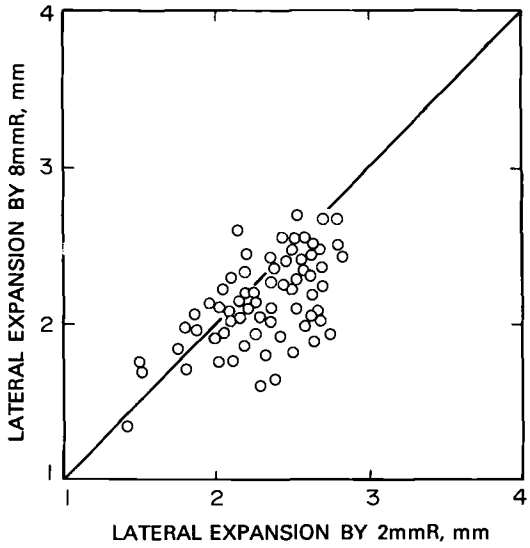

Fig. 3-(c) Comparison of the lateral expansion between the 8mmR and the 2mmR.

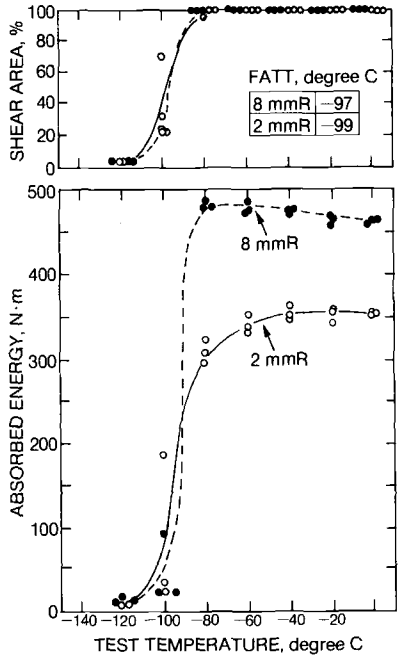

Fig. 3-(d) Comparison of the transition curve between the 8mmR and the 2mmR.

Measurement of Fracture Process

An example of dynamic load-time curves during the Charpy impact test is shown in Fig. 4, and an example of load-displacement curves during the static bending test is shown in Fig. 5. A comparison of Figures 4 and 5 indicates the following.

(1) Load-time curves and load-displacement curves in same test conditions resemble each other.

(2) Shapes of test specimens after test resemble each other, too.

If the static bending energy is defined as the area surrounded by load curve and displacement-axis, it is expressed by the following equation.

$$E_S = \int_o^a f(x) \cdot dx \qquad (1)$$

where

E_S = static bending energy
x = displacement
$f(x)$ = load at displacement(x), function of x
o = displacement at start point
a = displacement at end point

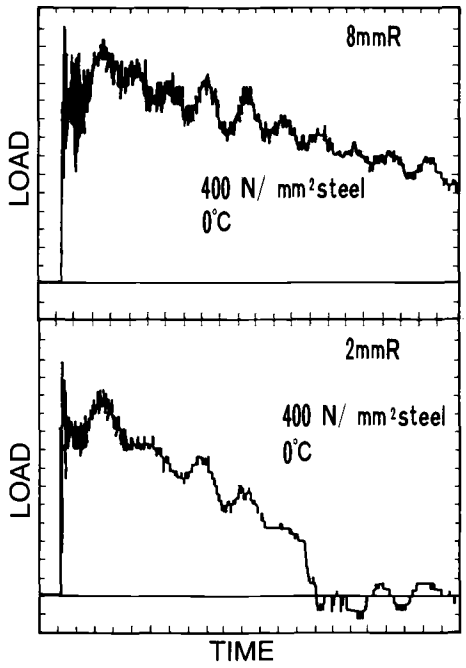

Fig. 4 Examples of the dynamic load vs. time curve obtained by the Charpy impact test.

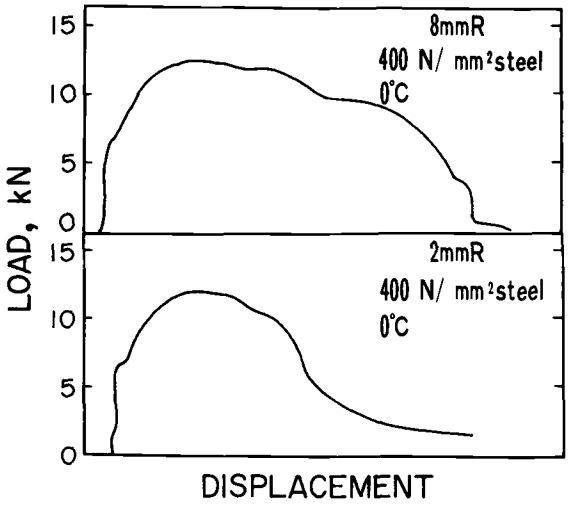

Fig. 5 Examples of the load vs. displacement curve obtained by the static bending test.

Comparison between the Charpy absorbed energy and the static bending energy is shown in Fig. 6. Both energies were strongly correlated. From facts described above, we may conclude that results of the static bending test are applied to explain fracture process of the Charpy impact test.

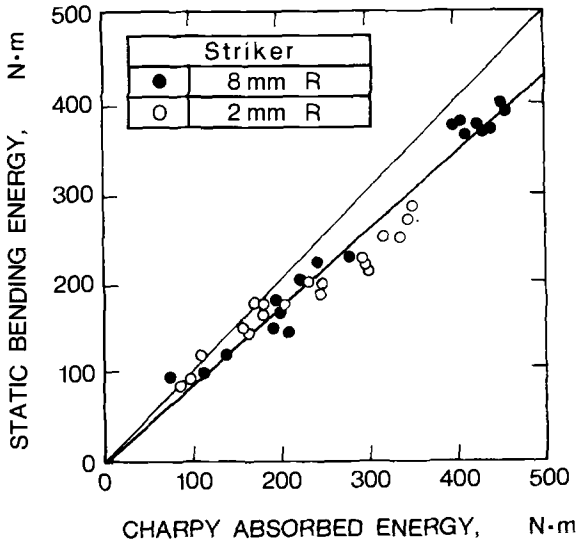

Fig. 6 The relation between the Charpy absorbed energy and the static bending energy.

Results of the static bending test are shown in Fig. 7 and Photo. 1. Results may be summarized as follows.

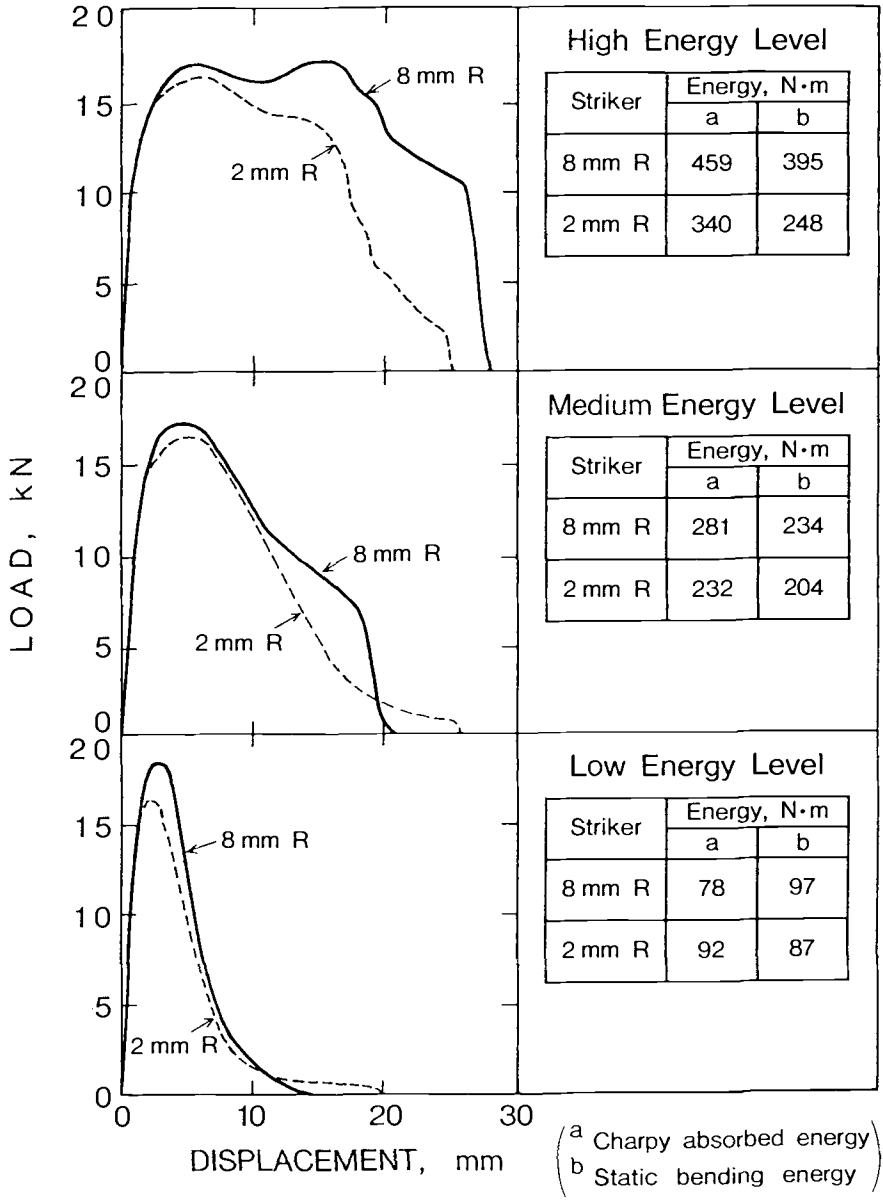

Fig. 7 Load vs. displacement curves by the static bending test.

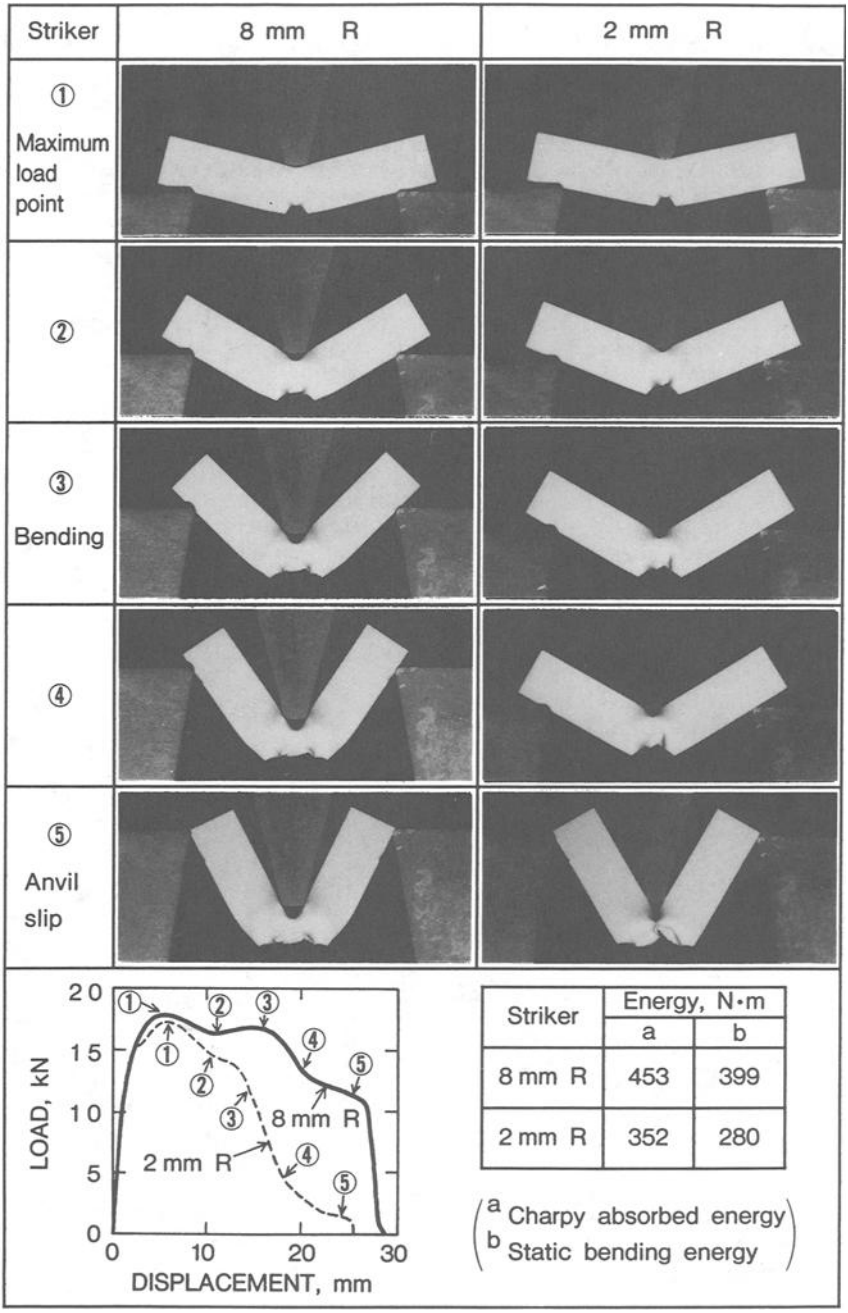

Photo 1. Observation of bending stages in static bending test (High Absorbed Energy Steel).

Low absorbed energy steel:
(1) Load-displacement curves of the 8mmR and the 2mmR were similar.

(2) The maximum load of the 8mmR was higher than that of the 2mmR. The difference in loads was about 1 kN.

High absorbed energy steel:
(1) Load-displacement curves changed into complex ones. The second load peak appeared at the point of about 15mm displacement in medium energy steel in case of the 8mmR. The second and the third peak appeared in high energy steel. The third peak appeared at the point of about 25mm displacement.

(2) The second and the third peak load of the 8mmR were higher than those of the 2mmR. The second peak load of the 8mmR was about 1.5 times that of the 2mmR. The third peak load of the 8mmR was about 4 times that of the 2mmR.

The Abrasion of the Striker

Changes of the striking edge dimensions with tests are shown in Fig. 8. Sections of the plaster molds out of the strikers are shown in Photo. 2. There was a contrast between the 8mmR and the 2mmR. The radius of the 8mmR markedly diminished. If we observe ASTM E 23 strictly that the dimensional tolerance is within ±0.05mm, we must exchange the 8mmR striker within 1,000 tests. On the contrary the 2mmR striker was little worn after 30,000 tests.

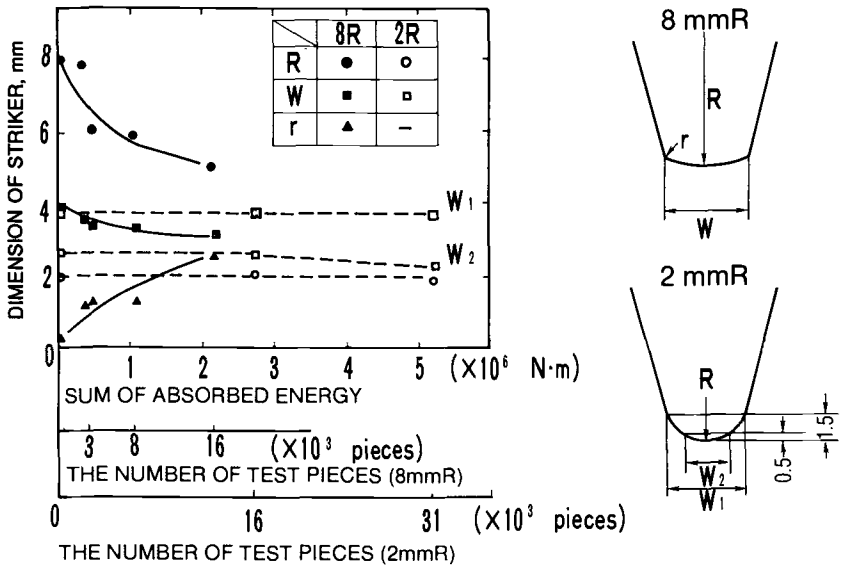

Fig. 8 Change of striking edge dimensions with tests.

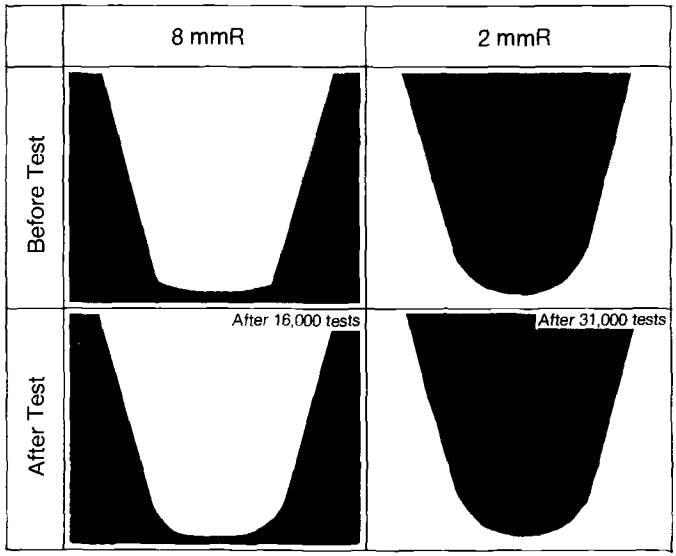

Photo. 2 Cross sections of striking edges.

DISCUSSION

The Difference in the Absorbed Energy

We would like to discuss the cause why the absorbed energy of the 8mmR was higher than that of the 2mmR in high absorbed energy steel. Load-displacement curves had three peaks in case of high energy steel. A typical load-displacement curve is shown in Fig. 9.

The first peak: It is assumed that this peak corresponds to the initiation of the crack at the bottom of the notch. It showed the maximum load. That of the 8mmR was slightly higher than that of the 2mmR. Owing to the fact that the contact length of the 8mmR between the striking edge and the specimen was longer than the 2mmR, we proved it by using elastic dynamics(1).

The second peak: From results of the static bending test, it is assumed the second peak corresponds to the bending deformation occurred near the shoulders of the specimen near the notch. Please refer to Photo 1. The deformation of the 8mmR specimen was larger than that of the 2mmR. For your information, the relation between the striking edge radius and the plastic deformation of the specimen is shown in

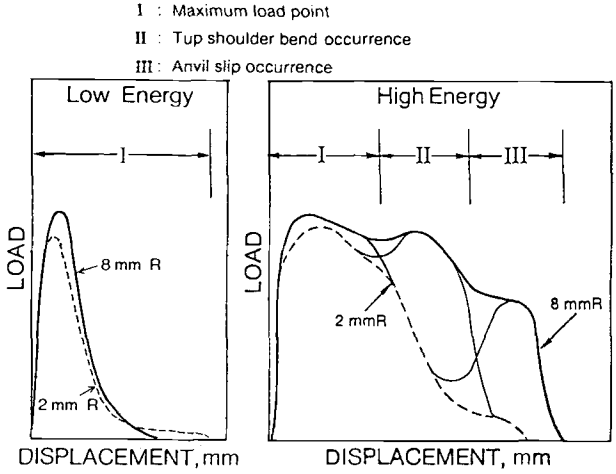

Fig. 9 Three energy regions of the load vs. displacement curve in energy.

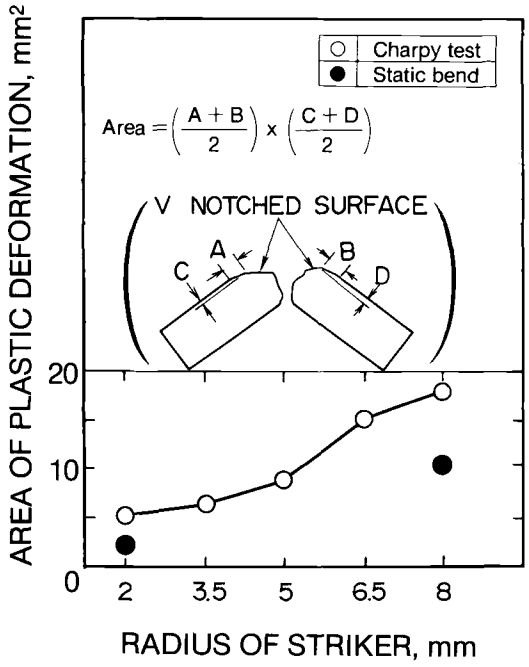

Fig. 10 The relation between the striking edge radius and the deformation of the specimen.

Fig. 10(1). The second peak enlarged in proportion to the absorbed energy of the specimen, too.

The third peak: It is assumed that the third peak is due to the friction between anvils and the test specimen. The friction did not occur in case of low absorbed energy steel. The friction occurred in case of high absorbed energy steel. And the friction of the 8mmR was larger than that of the 2mmR.

The Abrasion of the Striker

As shown in Fig. 8 and Photo. 2, the abrasion of the 8mmR striker was larger than that of the 2mmR. It is considered that the 8mmR striker was worn more than the 2mmR because of more bending deformation and more friction of the specimen.

The Radius Size of the Striking Edge

As mentioned above, it is possible to say that the load-displacement curve having only the first peak corresponds to energy about the initiation and the propagation of the crack. The first peak is the most important peak for the Charpy impact test. On the other hand the second and the third peak are caused by the deformation and the friction respectively. These energies should not be included in the Charpy impact test. The absorbed energy of the 8mmR includes more extra energy than that of the 2mmR.

The abrasion of the 8mmR striker is very large. Since the dimensional tolerances change faster, the striker must be changed more frequently.

From the above experimental results, it is concluded that the 8mmR striker is not as desirable for the Charpy impact test.

CONCLUSIONS

We investigated effects of the striking edge radius on the absorbed energy and the abrasion of the striker. The summary is as follows.

(1) The absorbed energy of the 8mmR striker was higher than that of the 2mmR when the absorbed energy was above 200N-m. No difference was recognized in the shear fracture, the lateral expansion, and the transition temperature.

(2) The difference in the absorbed energy between the 8mmR and the 2mmR is caused by the bending deformation of the test specimen and the friction between the anvil and the test specimen.

(3) The Abrasion of the 8mmR striker was larger than that of the 2mmR. We must exchange the 8mmR striker within 1,000 tests in order to satisfy the dimensional tolerance of striker radius. On the contrary the 2mmR striker was little worn after 30,000 tests.

ACKNOWLEDGMENTS

The authors would like to acknowledge the cooperation and the assistance of the others in The Mechanical Testing Subcommittee, The Joint Research Society of The Iron and Steel Institute of Japan.

REFERENCE

[1] M. Etoh et al., "Investigation of the Effects on Charpy Impact Characteristics by Shape of Pendulum Striking Edge," ASTM A01,13 Subcommittee on testing (seminar), Louisvill K.Y. May 10, 1983.

The Specimen: Notches

Robert D. Koester and Steven E. Barcus

EVALUATION OF FABRICATION METHOD FOR MAKING NOTCHES FOR CHARPY V-NOTCH IMPACT SPECIMENS

REFERENCE: Koester, R. D., and Barcus, S. E. "Evaluation of Fabrication Methods for Making Notches for Charpy V-Notch Impact Specimens," Charpy Impact Test: Factors and Variables: ASTM STP 1072, John M. Holt, American Society for Testing and Materials, Philadelphia, 1990.

ABSTRACT: The effect of preparing the notches for Charpy V-Notch impact specimens is evaluated. Two methods of preparation are used for this evaluation. They are grinding and broaching. Impact specimens with two energy levels were used: low energy, 15 J (11 ft•lbf) and high energy, 94 J (69 ft•lbf). Twenty-four specimens of each level were made with ground notches and with broached notches. Each was tested with a calibrated impact tester. The material used for the specimens was AISI-4340 alloy steel. The notch characteristics were documented by the following methods: notch angles, notch radii, surface conditions, and near-surface microstructure. Other parameters documented for this study were the ligament thickness, specimen width, and specimen length. In addition, test conditions and results are provided as follows: test temperature, absorbed energy, and lateral expansion. Besides tabular data, photographs give views of the notch surface. Evaluation of the results indicated both types of notches gave equally consistent values, but the ground and broached values differed in their averages. Possible causes for this variation were differences in ligament sizes and bottom of notch radii, surface tears and shallow microstructural deformation in the case of the broached notches.

Mr. Koester is an engineering manager for Southwestern Laboratories, Post Office Box 8768, Houston, TX 77249; and Mr. Barcus is president of Sure Tool & Engineering, 302 East Pleasant Street, Churnbusco, IN 46723.

KEYWORDS: Charpy V-notch, impact test, notch machining, AISI-4340 alloy steel, lateral expansion and toughness.

BACKGROUND

The key part of fabricating a Charpy V-notch impact specimen is the method of producing its notch. The other parts of the fabrication cycle must be capable of producing consistent dimensions, squareness, and reasonable surface finish; but the aspect of the machining that can have the most telling effect on the results is the notch itself. For this reason, it was determined that a study aimed at identifying any differences from specimens produced by different notching methods would be a worthwhile endeavor. Of the three most common ways to produce the notch, broaching, grinding, and milling, the former two were chosen for this comparison.

Since the results of this nature are governed by statistics, the use of 24 specimens for each condition being evaluated was felt necessary. This number of samples permits a statistical analysis to be performed that gives validity to any differences that are observed. The results were measured in the English system and converted to the International System of Units.

Previous studies [1] have shown that impact results are reproducible. This study clearly indicates that consistent test specimens and calibrated test machines give this reproducibility. Other studies [2] have addressed the aspect of notch depth and notch radii.

EXPERIMENTAL METHOD

Material

The material was modified AISI-4340 that was processed at the same time that a lot of standard specimens being made for impact machine calibration purposes was processed. The material is, therefore, the same except for the notching that is purchased from the Army Materials Technology Laboratory. This source of material ensured that no variables from the material or heat treating aspects of processing would enter this evaluation.

Machining

The specimens were fabricated, i.e. sawed, milled, and ground, with a lot of standard specimens being made for impact machining calibration purposes. The finished Charpy specimens are, therefore, the same except

for the notching that is purchased from the Army Materials Technology Laboratory. This fabrication approach also ensured that no variables from the fabrication methods used would enter this evaluation.

Notching

The specimens were notched with the following equipment. The ground notches were made using a Mitsui, Model 6-12 Grinder equipped with an Engis Diaform Wheel Dresser. The grinding wheels were Norton No. 38A60K8VBE, and they were 17.8 cm (7") x 0.64 cm (1/4") x 3.18 cm (1-1/4") in size. Grinding is done in a normal plunging style to the appropriate depth. The number of wheel dressings will vary; however, the wheel is dressed just prior to grinding the last 0.076 mm (0.003") of notch depth. The grinding operation is done with the specimen flooded in coolant.

The broaching was accomplished on a Blacks Equipment, Type CNB14 Broacher. It is a motorized broach. The broach cutter is No. NBT-VT .010 that has 56 teeth. The notch is cut with one pass of the broach cutter while adding a liberal amount of cutting oil to the broach cutter prior to the cut. The broach used for the notching had been used previously to notch about 1000 specimens.

Testing

The Charpy specimens were tested on a Tinius Olsen Impact Machine, Model No. 64. This machine has as its capacity 358 J (264 ft•lbf). The machine had been calibrated using standard Charpy specimens in accordance with **ASTM E 23** [3] procedures on January 27, 1989. The results of that calibration showed that all aspects of the testing procedure and equipment met the requirements of **ASTM E 23**. The results compared to the standard values given by Army Materials Technology Laboratory appear in **Table 1**. It can be seen that this machine is within the calibration requirements of **ASTM E 23**. It may be noted that it is on the low side of the nominal value established by the Army Materials Technology Laboratory.

The Charpy tests conducted for this evaluation were performed on March 4, 1989, which was a short time after the calibration described above. The tests were performed per **ASTM E 23** procedures at -40°C (-40°F). The specimens met all of the above dimensional requirements for an **ASTM E 23** Type A specimen. The cross sections were 10.0 mm (0.394") x 10.0 mm (0.394"). The ligament sizes were 7.98 mm (0.314") to 8.03 mm (0.316"). The ground notches typically had ligament sizes of 7.98 mm (0.314") while the broached notches, 8.03 mm (0.316"). The notches had angles of 46° with the **ASTM E 23** required bottom radii of 0.25 mm

(0.0107") being 0.229 mm (0.009") for the broached notch and 0.259 mm (0.010") for the ground notches. The surface finish on the notched face and the face opposite from the notch was observed to be within the requirement of two microns (63 micro-in) per **ASTM E 23**. Comparison on an optical compartor of the ground and broached notches to a certified outline of the Charpy V-notch requirements of **ASTM E 23** indicated that both notches met all requirements.

TABLE 1–Calibration of Tinius Olsen impact testing machine

Source of Value	Low-Energy Charpy Specimens Absorbed Energy J (ft•lbf)	High-Energy Charpy Specimens Absorbed Energy J (ft•lbf)
Measured on standard AMTL specimens by SwL	15.7 (11.6)	99.0 (73.0)
Published as nominal energy value by AMTL	16.7 (12.3)	101.1 (74.6)
Allowable range of values to meet **ASTM E 23** requirements	15.3 (11.3) to 18.0 (13.3)	96.1 (70.9) to 106.2 (78.3)

Test Results

Tables 2 and 3 show the absorbed-energy values and lateral-expansion results of the two energy levels of Charpy specimens that were tested. The low-energy specimen results appear on Table 2 and the high-energy level on Table 3.

TABLE 2–Impact results on low-energy Charpy impact specimens with broached or ground notches.

Absorbed Energy		Lateral Expansion	
Value J (ft•lbf)	No. of Specimens	Value mm (mils)	No. of Specimens
	Ground Notches		
13.6 (10.0)	9	0 (0)	20
14.2 (10.5)	10	0.02 (1)	1
14.9 (11.0)	3	0.05 (2)	3
15.6 (11.5)	2		
	Broached Notches		
13.6 (10.0)	5	0 (0)	21
14.2 (10.5)	1	0.02 (1)	3
14.9 (11.0)	10		
15.6 (11.5)	5		
16.3 (12.0)	3		

TABLE 3–Impact results on high-energy Charpy impact specimens with broached or ground notches.

Absorbed Energy		Lateral Expansion	
Value J (ft•lbf)	No. of Specimens	Value mm (mils)	No. of Specimens
	Ground Notches		
88.1 (65)	1	0.89 (35)	2
89.5 (66)	3	0.91 (36)	1
90.8 (67)	1	0.94 (37)	3
92.2 (68)	4	0.97 (38)	8
93.6 (69)	5	0.99 (39)	5
94.9 (70)	6	1.02 (40)	1
96.3 (71)	1	1.04 (41)	4
97.6 (72)	0		
99.0 (73)	3		
	Broached Notches		
85.4 (63)	1	0.84 (33)	1
86.8 (64)	1	0.86 (34)	3
88.1 (65)	3	0.89 (35)	3
89.5 (66)	5	0.91 (36)	5
90.8 (67)	2	0.94 (37)	4
92.2 (68)	4	0.97 (38)	5
93.6 (69)	3	0.99 (39)	3
94.9 (70)	4		
96.3 (71)	1		

A statistical analysis of these results was performed in order to define any difference. The results of this analysis are shown as Tables 4, 5, and 6 for the low-energy absorbed-energy values, the high-energy absorbed-energy values and the high-energy lateral-expansion values, respectively. The low-energy lateral-expansion values were not included in the evaluation since they were, by and large, zero values.

TABLE 4–Statistical analysis of absorbed-energy values from low-energy Charpy impact specimens with broached or ground notches.

Parameter	Ground Notches	Broached Notches
Number of specimens, n	24	24
Average of n specimens, $\bar{x}$ J (ft•lbf)	14.2 (10.5)	14.9 (11.0)
Standard deviation for n specimens, σ_n J (ft•lbf)	0.7 (0.5)	0.8 (0.6)
Percent variation from average, $\sigma_n/\bar{x} \cdot 100$	4.8	5.5

The average for the low-energy absorbed-energy value is 0.7 J (0.5 ft•lbf) higher for the broach notched specimens than for the ground notched specimens. The standard deviation for the low-energy absorbed-energy values is 0.1 J (0.1 ft•lbf) higher for the broach-notched specimens than for the ground-notched specimens **(see Table 4)**. This difference reversed itself for the high-energy absorbed energy values. The average for the high-energy absorbed-energy value is 2.4 J (1.7 ft•lbf) lower for the broach-notched specimens than for the ground-notched specimens. The standard deviation is the same for both the ground- and broach-notched specimens in this case **(see Table 5)**. Comparison of the lateral-expansion results for the high-energy level specimens indicates the same situation as for the average absorbed-energy values for this range. The average for the broach-notched specimens is 0.04 mm (1.8 mils) lower than the average for the ground-notched specimens. The standard deviations are again the same **(see Table 6)**.

TABLE 5–Statistical analysis of absorbed energy values from high-energy Charpy impact specimens with broached or ground notches.

Parameter	Ground Notches	Broached Notches
Number of specimens, n	24	24
Average of n specimens, $\bar{x}$ J (ft•lbf)	93.6 (69.0)	91.2 (67.3)
Standard deviation for n specimens, σ_n J (ft•lbf)	2.8 (2.2)	2.8 (2.2)
Percent variation from average, $\sigma_n/\bar{x} \times 100$	3.2	3.2

TABLE 6–Statistical analysis of lateral-expansion results from high-energy Charpy impact specimens with broached or ground notches.

Parameter	Ground Notches	Broached Notches
Number of specimens, n	24	24
Average of n specimens, $\bar{x}$ mm (mils)	0.97 (38.3)	0.93 (36.5)
Standard deviation for n specimens, σ_n mm (mils)	0.04 (1.7)	0.04 (1.7)
Percent variation from average, $\sigma_n/\bar{x} \cdot 100$	4.4	4.7

In order to characterize the condition of the notches, the samples were examined by stereomicroscopy. **Figures 1 and 2** show the bottoms of the notches. These views show continuous score marks in the bottom of the ground notch and the presence of surface checks in the bottom of the broached notch. In an effort to show any microstructural effect of the two methods of notching, a metallographic specimen was prepared through each notch on specimens that were not impact tested. This view was prepared transverse to the notch direction. The specimens were prepared by the standard methods of **ASTM E 3** [4] and **E 407** [5].

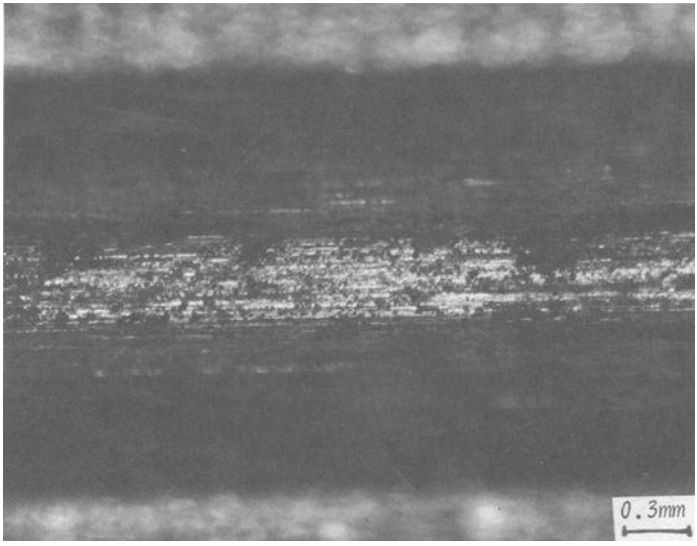

FIG. 1–Visual appearance of notch bottom for ground-notch Charpy specimen.

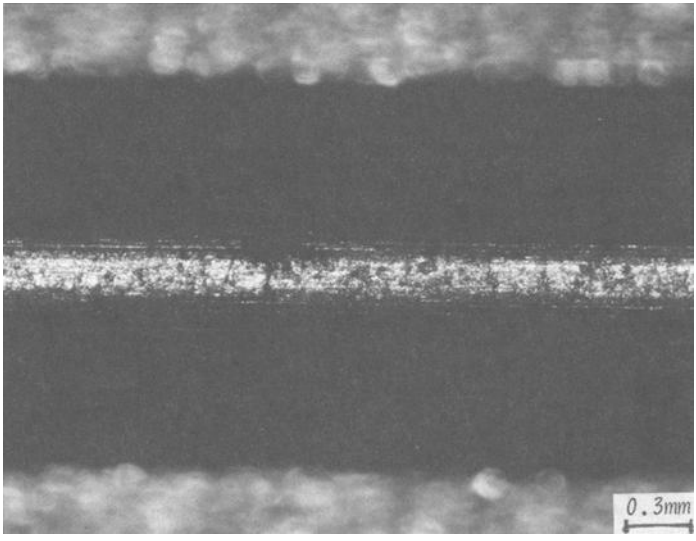

FIG. 2–Visual appearance of notch bottom for broached-notch Charpy specimen.

Prior to metallographic preparation, the specimens were nickel plated in order to improve edge retention during these operations. Views of these cross sections are shown in **Figures 3 and 4**. These views give additional information on the shapes of the notches made by grinding and broaching, respectively.

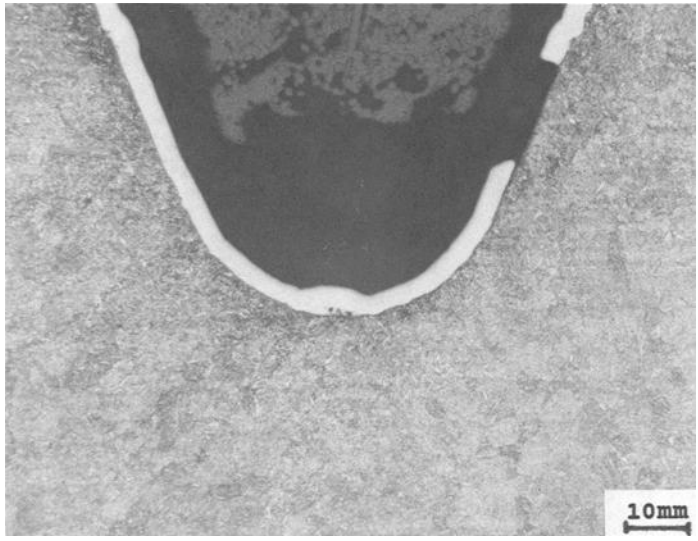

FIG. 3–Cross sectional view of ground notch with nickel plating added for edge retention.

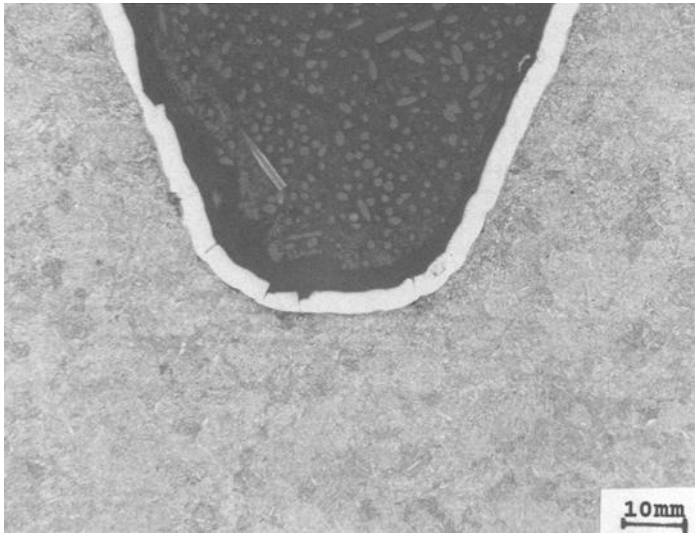

FIG. 4-Cross sectional view of broached notch with nickel plating added for edge retention.

While the ground notch has a uniformly rounded bottom, the broached notch has a slight flattening apparent. The results are shown as the photomicrographs in **Figures 5 and 6** for the ground and broached specimens. The microstructure for the ground specimen showed no evidence of disturbed metal at the bottom of the notch. In the case of the broached notch, a shallow effect was observed. The depth of this effect was measured as 6.4 microns (250 micro-in) at the notch bottom.

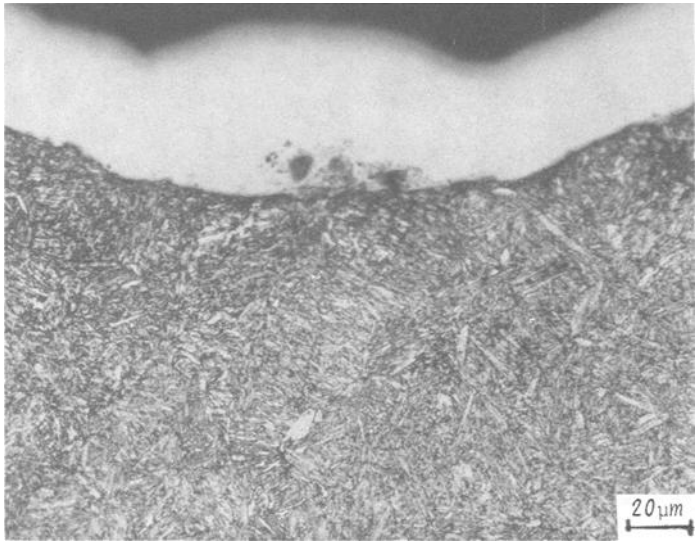

FIG. 5–Etched (2% nital) microstructure at notched edge of ground-notched Charpy specimen. (The white nickel plating at top field of view is for edge retention.)

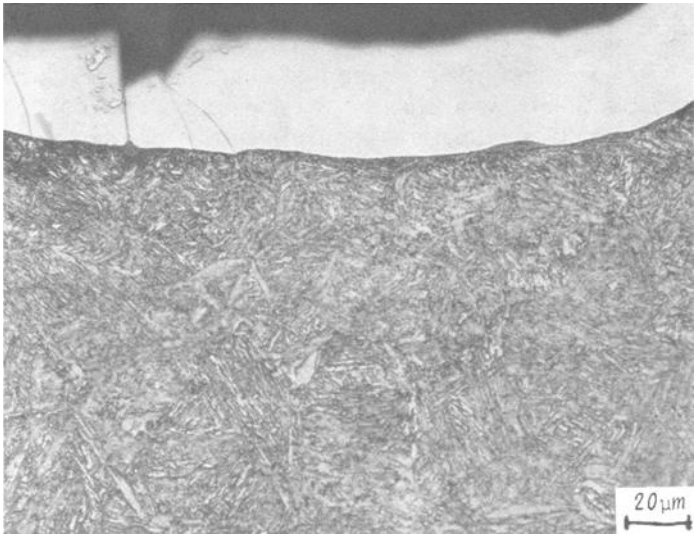

FIG. 6–Etched (2% nital) microstructure at notched edge of broach-notched Charpy specimen. (The white nickel plating at top field of view is for edge retention.)

A higher magnification view of this same effect on the side wall of the broached notch is shown in **Figure 7.** Its depth on the side was 15.9 microns (626 micro-in).

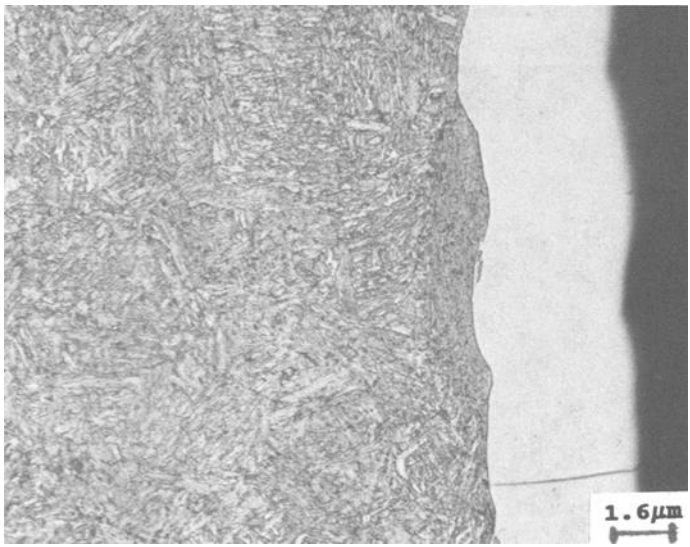

FIG. 7-Etched (2% nital) microstructure at notch surface of broach-notched Charpy specimen. (The white nickel plating at the right side of the field of view is for edge retention).

Discussion of Results

This evaluation has indicated that both grinding and broaching yield acceptable Charpy V-notches. The grinding method of notch fabrication has an advantage in that the grinding wheel is dressed prior to the final notch pass of 0.076 mm (0.003"). The broached notch produced for this study had surface checks (tears) that ran transverse to the notch direction. A slight indication of this effect was also apparent in the microstructure immediately adjacent to the notched surface. This effect is assumed to be deformation in the microstructure caused by the broach. It was also observed on the cross section for the microstructural examination that the ground notch had a uniformly-rounded bottom while the broached notch had a slightly flattened bottom. Dimensionally, the ground notches had smaller ligament sizes and sharper bottom of notch radii than the broached notches. The statistical comparison of the 24 values for each method of notching indicated nearly identical consistency, i.e. in standard deviations.

Conclusion

Notches acceptable for **ASTM E 23** Charpy V-notch impact testing can be made either by broaching or grinding. Possible causes for the minor variations observed were the following factors: ligament sizes were different; radii at bottom of notches were different; the broached notch had a slight flattening at its bottom; the broached notch had surface checks (tears) and a shallow amount of microstructural damage at the bottom of the notch.

ACKNOWLEDGMENTS

The authors wish to thank Messrs. W.M. Buffaloe, S.H. Nguyen, R.C. French and W. Bodenhamer of Southwestern Laboratories for their assistance in performing the test work, and Mr. D. Burns of Spraymetal, Inc., Houston, TX, for the nickel plating. We also thank Ms. Pat Koester for help in the preparation of this paper.

REFERENCES

[1] D.E. Driscoll, "Reproducibility of Charpy Impact Test," Symposium on Impact Testing, ASTM STP 176, American Society of Testing and Materials, 1955, p. 170.

[2] N.H. Fahey, "Effects of Variables in Charpy Impact Testing," Materials Research & Standards, Vol. 1, No. 11, November 1961, page 872.

[3] **ASTM Standard E 23**, "Standard Methods for Notched Bar Impact Testing of Metallic Materials," **1988 Annual Book of ASTM Standards**, Vol. 03.01, Metals-Mechanical Testing; Elevated and Low-Temperature Tests; Metallography, by **American Society for Testing and Materials**, Philadelphia, 1988, p. 191.

[4] **ASTM Standard E 3-80** (Reapproved 1986), "Standard Methods of Preparation of Metallographic Specimens," ibid. p. 74.

[5] **ASTM Standard E 407-70** (Reapproved 1982), "Standard Methods for Microetching Metals and Alloys," ibid. p. 505.

David A. Fink

QUANTITATIVE COMPARISON AND EVALUATION OF VARIOUS NOTCH MACHINING METHODS AND HOW THEY AFFECT ASTM E23 AND ISO R442 TESTING EQUIPMENT RESULTS

REFERENCE: Fink, D. A., "Quantitative Comparison and Evaluation of Various Notch Machining Methods and How They Affect ASTM E23 and ISO R442 Testing Equipment Results", Charpy Impact Test: Factors and Variables, ASTM STP 1072, John M. Holt, American Society for Testing and Materials, Philadelphia, 1990.

ABSTRACT: The differences obtained when conducting Charpy impact tests using an ASTM method E23 specification, versus the ISO type impact tester have been reported with little agreement upon the comparisons. There has also been historically much controversy as far as the proper method of machining the notch into the Charpy specimen. This paper compares the effects of the two different types of impact testing equipment and evaluates machining of the notch by the methods of grinding, broaching and milling with a single toothed fly cutter.

It was determined that results obtained with the ISO type impact machine were elevated by approximately 4%. It was also determined that a slightly lower impact value was obtained with broached specimens. Photomicrographs of typical notch profiles were also obtained.

KEYWORDS: Charpy impact testing, notching, machining methods, impact testing

Mr. David Fink is a Project Engineer for The Lincoln Electric Company, 22801 St. Clair Avenue, Cleveland, Ohio 44117-1199. Mr. Fink is a member of the AWS A5 Filler Metal Committee, and is Chairman of the AWS A5O and A5P Subcommittees on Consumables for gas metal arc, electroslag and electrogas welding.

INTRODUCTION

Charpy impact testing is used for many purposes in industry today. It is used as a design tool to allow a relatively quick and inexpensive measure of a steel or a weldment's fracture toughness. These results are then correlated with successful applications and service life histories which have been used previously. Charpy impact testing is also used as a procurement and quality control test to verify minimum acceptance levels in specifications. It is this application which is most often controversial.

The two sources for the basic specifications covering Charpy impact testing today are ASTM and ISO. ASTM (American Society for Testing and Materials) is an organization made up largely of volunteers which prepares consensus specifications on a multitude of topics. ISO (International Standards Organization) is made up of member countries and prepares specifications for international application.

In view of the international nature of today's economy, it is not unusual to evaluate Charpy testing done in several locations worldwide. The problem this presents is the fact that the results reported generally are not comparable due to the different nature of the impact machines being used, and the lack of a recognized proof testing program for ISO machines.

This state of affairs often leads to much controversy, especially when the results of the test may show an out-of-specification or out-of-conformance condition on one type of machine and not necessarily on the other. For this reason, it is becoming increasingly important to understand the differences between the ASTM and ISO type impact testers [1,2].

The method of the machining of the notch has received some attention previously [3], but it is often overlooked in the study of the effects in Charpy testing [4,5]. The use of grinding to machine the notch is often regarded as the referee method; however, it is slow and expensive. The use of a broach to produce the notch is much faster and less expensive, but experience has shown that it can often lead to poor notch profiles if the broach is not properly maintained or replaced at sufficient intervals. An alternate method which is thought to be a compromise in speed and cost is the use of milling by means of a single toothed fly cutter. All three of these methods will be examined.

The U.S. Army Materials Technology Laboratory has for many years maintained a program of verification testing and qualification of impact machines [2]. The author is unaware of any equivalent program for ISO machines. Verification of the ISO type machine is based on physical measurements of dimensions and of velocities of the hammer and weights of the various components.

DESCRIPTION OF EQUIPMENT

The two machines used for this test program were both Tinius Olsen Universal Impact machines. The machine used for the ASTM testing has been used for this purpose for a number of years. It has been subjected to annual verification testing based on U.S. Army Materials Laboratory standards and has been recertified annually based on those specimens. It is also subjected to monthly calibration checks with standardized specimens to ensure its continuous conformance.

The impact machine used for the ISO testing was originally configured for ASTM testing. Replacement parts were purchased from Tinius Olsen and retrofitted to the machine to bring it into conformance with ISO Standard R442. This machine was then calibrated and inspected by a representative of TUV America, Inc. (a subsidiary of TUV Bayern). Their report concluded that, "The evaluation confirms full compliance with ISO standard R442-1963(E) and the production of acceptable energy values at high and low energy levels. The impact machine is in good condition." This machine was used for all of the ISO testing. For simplicity's sake, the resulting values were recorded in terms of ft-lbs. from the dial, rather than Joules. (It should be noted that the high and low values referred to the MTL specimens as shown in Table 1.)

The difference between the ASTM E23 specification and the ISO R442 standard is primarily the difference of the striker tip on the hammer. The ASTM specification has a much blunter striker profile with nominally an 8 mm radius, while the ISO striker profile specifies a 2 to 2.5 mm radius as shown in Figure 1. The ASTM specification also requires annual verification testing using standard specimens obtained from the Army Materials Technology Laboratory.

As part of the initial calibration check of the ISO machine by TUV America, two sets of Army MTL standard specimens were broken after verification of the machine had been completed. These low and high energy standards gave values within the allowable variation for proof testing. This confirmed the fact that this ISO designed machine could meet the proof testing requirements of ASTM. The results of the proof testing are shown in Table 1.

EXPERIMENTAL PROCEDURE

A large number of un-notched impact blanks were purchased from the manufacturing facility which provides them to the U.S. Army Materials Testing Laboratory. These were of the low energy level and high energy level type, finish machined, with the exception of the notch being absent. These specimen blanks were prepared from SAE 4340 steel, specially heat treated to give specific notch toughness levels at -40°F in a reproducible fashion. These impact specimen blanks were then notched by the following methods:

1. Grinding conducted by the contractor for U.S. Army Materials Testing Lab (data identified as "Standard

Ground" or "Ground #1"), and also a duplicate set by another machining concern (data identified as "Ground" or "Ground #2").

2. Broaching.

3. Milling with a single toothed fly cutter.

One half of each group of specimens were broken on each of the ASTM and ISO machines after examination of the representative notch profiles and inspection of all specimens for proper depth under the notch. These specimens were all broken at -40°F.

In addition, samples of both ASTM A537 steel and HY-80 type steel were used to prepare specimens which were notched by the method of milling with the single toothed fly cutter. These specimens were used to compare the ASTM and ISO machines in addition to the previous mentioned specimens. These specimens were broken at various temperatures as reported.

RESULTS

Results obtained by testing the standardized impact specimens are shown in Table 2. This shows the values obtained when testing the various notching methods on both ASTM and ISO machines at two different impact levels. These results are shown graphically in Figures 2 and 3, which show the comparisons for each method or source of notching. The results obtained by breaking impact specimens machined from steel plate are shown in Table 3, for both ASTM A537 and HY-80 base material. The results for ASTM A537 are shown graphically in Figure 4.

Notched profiles for the various methods were studied using a scanning electron microscope. Representative photographs of the profiles obtained with each method are shown in Figures 5 thru 8.

Figure 9 shows the contour obtained with a broach which was not replaced soon enough.

DISCUSSION

The overall correlation of results from all tests including several other smaller tests not related to this study are shown in Figures 10 and 11. These graphs show that in almost every case, the results obtained with the ISO machine fall above the 1:1 correlation line. The best fit regression line was determined to be:

$$(ISO) = 1.0420\ (ASTM) + .5160$$

There is an excellent agreement with the regression line, with a Coefficient of Determination (r^2) of .9987, and a standard error of estimate of 1.36.

This would indicate the ISO results are approximately 4% higher than ASTM values. This is supported also in reviewing specific notching results shown in Figures 2 and 3, where in each case the ISO results showed a noticeably higher value.

It is also apparent that the method of grinding the notch gives the smoothest and most consistent profile. The broached notches give a lower impact value, which may be related to the roughness of the surface and the microscopic tears observed in the surface as a result of the machining. The milling using the single toothed fly cutter produces results very similar to those of the ground method. Although in several cases the milling results are elevated slightly, they still fall well within the normal acceptable tolerances, as generally required by the MTL program (Table 1).

ACKNOWLEDGEMENTS

The author acknowledges with appreciation the help of numerous members of the staff of both The Lincoln Electric Company, Cleveland, Ohio, U.S.A., and Lincoln Electric (Europe) S.A. (Rouen, France); in particular, for their assistance in the preparation and testing of specimens; Mr. Charles Hayes and Mr. John Baker of the U.S.A.; and Mr. Leon Keromnes and G. Bordenave of France; and for the preparation of the presentation, Susan Powell and Beverly Young of the U.S.A.

REFERENCES

1. "ISO Recommendation R442," Verification of Pendulum Impact Testing Machines for Testing Steels, ISO/R442-1965(E), First Edition, July 1965.

2. ASTM E23-88 "Standard Test Methods for Notched Bar Impact Testing of Metallic Materials," 1989 Annual Book of ASTM Standards, Vol. 03.01, ASTM, Philadelphia, PA pp. 198-213.

3. Towers, O.L. "Charpy V-Notch Tests: Influences of Striker Geometry and of Specimen Thickness," Report 7709.01/83/354.2, The Welding Institute, Abington Hall, Cambridge, England, March 1983.

4. Fahey, Robert N. "Effects of Variables in Charpy Impact Testing," Technical Report WAL TR112.5/2, Watertown Arsenal Laboratories, Watertown, Mass. March 1962.

5. Cuthbert, Alan "Impact Properties," Australian Welding Journal, Vol. 28, No. 4, Summer 1983, pp 26-27.

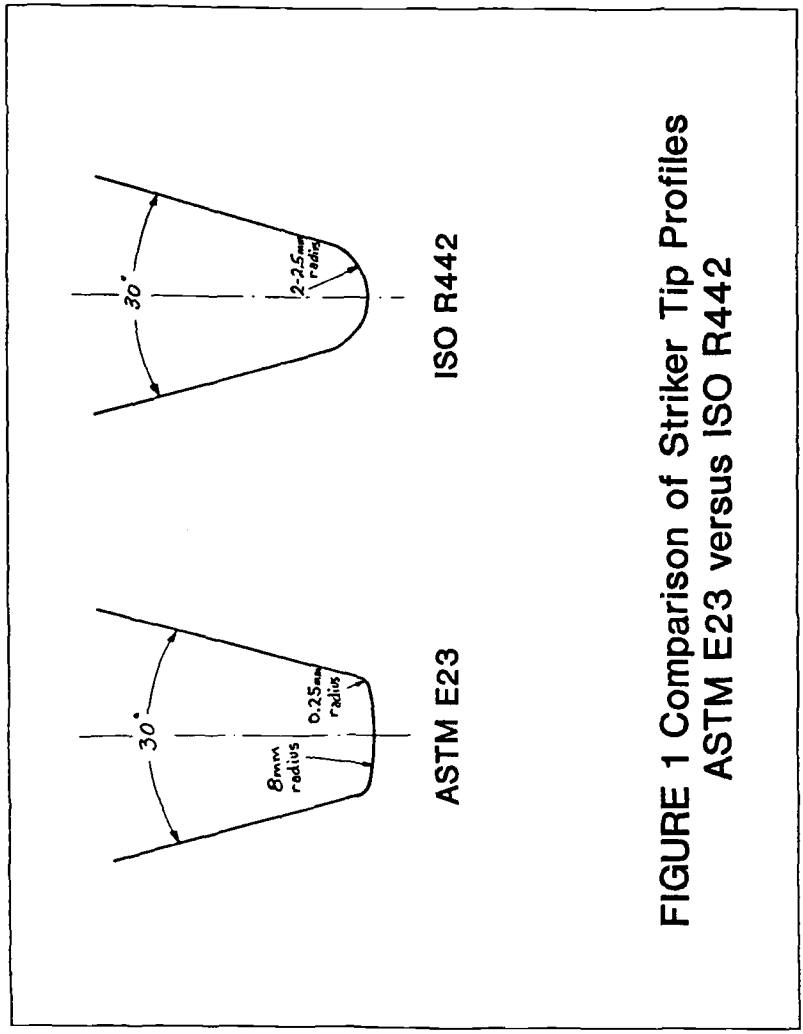

FIGURE 1 Comparison of Striker Tip Profiles ASTM E23 versus ISO R442

TABLE 1 -- Testing of ISO Impact Tester using U.S. Army Materials Testing Lab Specimen

	LOW SET	HIGH SET
	12.5	73.0
	11.5	73.0
	12.5	75.0
	12.0	75.0
	14.0	75.0
Average (ft-lbs)	12.5	74.2
MTL Reported Average (ft-lbs)	11.8	72.7
Allowable Variation per MTL	± 1.0 ft-lb.	± 5.0%
Actual Variation	+ 0.7 ft-lbs.	+ 2.1%

TABLE 2 -- Results of Testing Standardized Specimens

Notching Method	Standard Ground	Standard Ground	Ground	Ground	Broached	Broached	Flycut	Flycut
Batch	HH	HH	HH	HH	HH	HH	HH	HH
Testing Machine	ASTM	ISO	ASTM	ISO	ASTM	ISO	ASTM	ISO
	73	72	69	76	65	69	69	74
	74	75	69	73	69	72	73	75
	69	75	71	71	68	73	71	79
	70	74	71	73	69	73	71	74
	72	75	72	72	69	74	74	76
	76	74	69	79	69	75	73	76
	73	79	71	73	73	74	74	71
	68	78	71	73	69	74	70	73
	69	73	70	74	67	76	73	77
	70	75	75	76	70	75	73	75
	66	74	70	77	67	73	...	...
	73	72	73	71	69	71	...	...
	68	79	69	75	68	71	...	...
	71	71	69	71	71	71	...	...
	71	78	73	76	66	72	...	...
Mean	70.9	74.9	70.8	74.0	68.6	72.9	72.1	75.0
Std.Dev.	2.58	2.46	1.76	2.34	1.89	1.82	1.64	2.10

All values in ft-lbs.

TABLE 2 -- Results of Testing Standardized Specimens (Continued)

Notching Method	Standard Ground	Standard Ground	Ground	Ground	Broached	Broached	Flycut	Flycut
Batch	LL	LL	LL	LL	LL	LL	LL	LL
Testing Machine	ASTM	ISO	ASTM	ISO	ASTM	ISO	ASTM	ISO
	11	11.5	11.5	12	10.5	13	12.5	12.5
	12	12.5	11.5	12.5	11.5	11	12.5	12.5
	12	12.5	12	12.5	10.5	12	12.5	11.5
	12	11.5	12	12.5	11	12	12	12.5
	12	12.5	11	12.5	10.5	12.5	12.5	13
	12.5	12.5	12	12.5	10.5	11	11.5	13
	12.5	12	12.5	13	10.5	10.5	12.5	12.5
	11	12	12	13	11	11.5	11.5	11.5
	11.5	12.5	12.5	11.5	10.5	12	12	12.5
	11	13	10	12	11	11.5	12	13
	11.5	12	11.5	13	11	12	...	...
	12	12	12	11.5	12	10.5	...	...
	11	12.5	11	12.5	11.5	12	...	...
	11	12.5	12.5	13.5	11.5	11	...	...
	11.5	12	12.5	13	11	12	...	...
Mean	11.6	12.2	11.8	12.5	11.0	11.6	12.2	12.5
Std.Dev.	0.53	0.40	0.68	0.55	0.46	0.69	0.39	0.52

All values in ft-lbs.

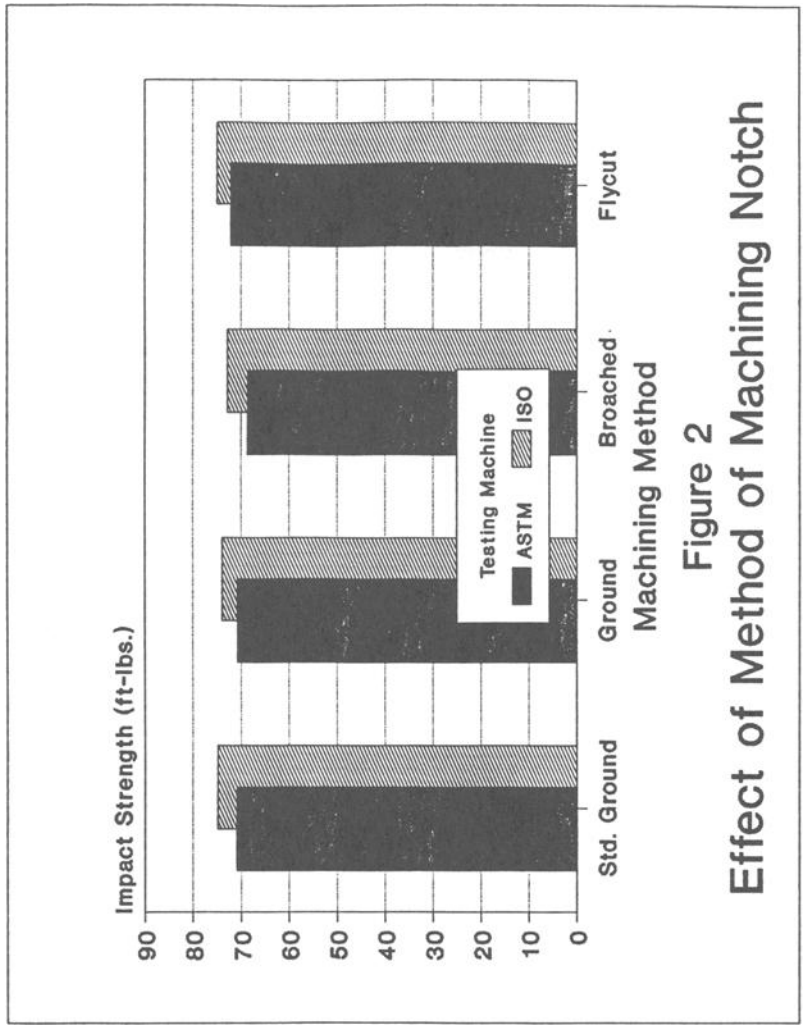

Figure 2
Effect of Method of Machining Notch

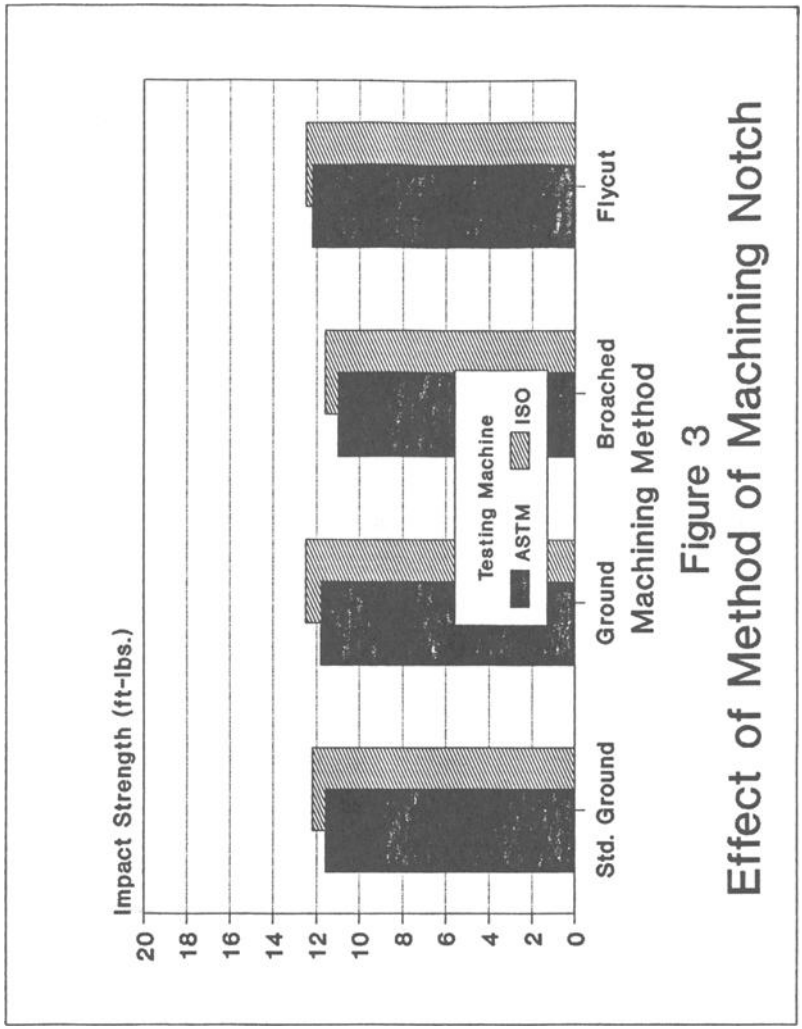

Figure 3
Effect of Method of Machining Notch

TABLE 3 -- Testing Machine Comparison Using Steel Plate Specimens (Fly Cut Samples)

A537 STEEL			A537 STEEL			HY80 STEEL		
Test Temperature (F)	ASTM	ISO	Test Temperature (F)	ASTM	ISO	Test Temperature (F)	ASTM	ISO
70	44	47	-20	31	28	-40	145	118
	45	44		31	28		147	154
	40	44		29	34		150	140
	46	45		30	34		147	143
	43	42		28	32		147	146
	43.6 Avg.	44.4 Avg.		26	31		116	139
				29	37		136	149
				27	35		124	162
				28.9 Avg.	32.4 Avg.		141	153
							146	152
32	43	45	-40	22	26		139.9 Avg.	145.6 Avg
	45	44		21	25			
	46	48		23	24			
	49	45		26	24			
	43	45		25	23			
	43	48		20	23			
	40	50		21	23			
	42	45		21	22			
	43.9 Avg.	46.2 Avg.		22.4 Avg.	23.8 Avg.			
0	30	39	-60	21	16			
	31	44		20	18			
	34	41		19	17			
	39	38		18	19			
	40	38		17	17			
	32	43		19	22			
	34	38		19	20			
	36	43		17	18			
	34.5 Avg.	40.5 Avg.		18.8 Avg.	18.4 Avg.		All values in ft-lbs.	

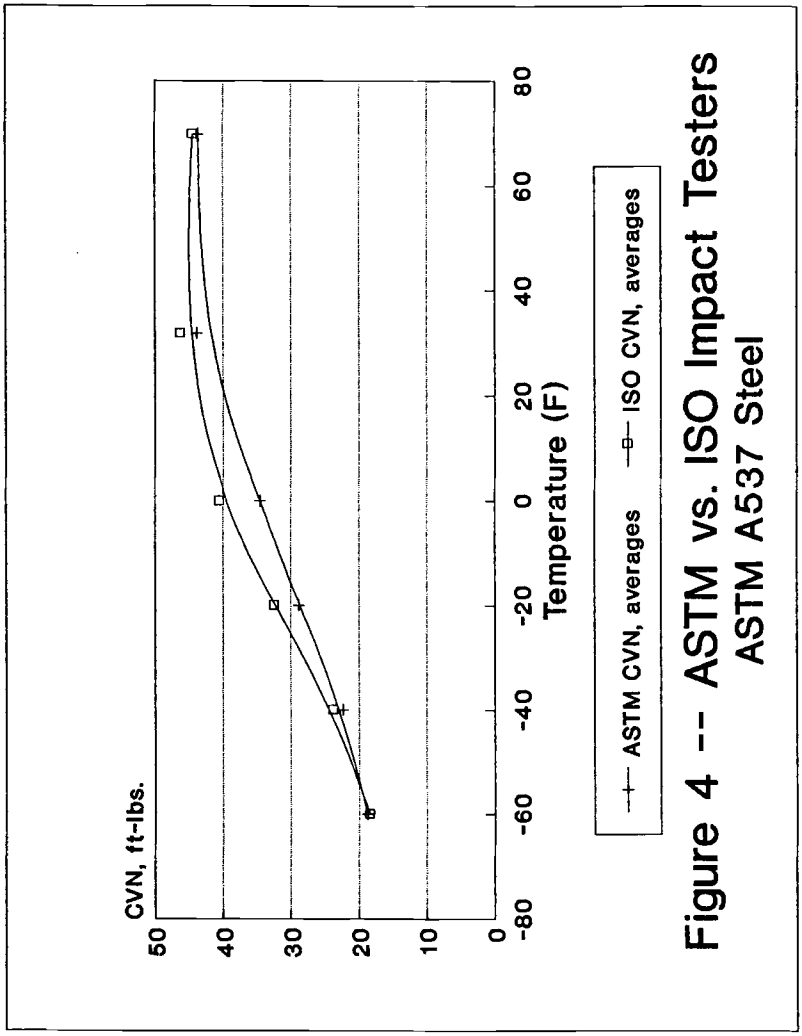

Figure 4 -- ASTM vs. ISO Impact Testers
ASTM A537 Steel

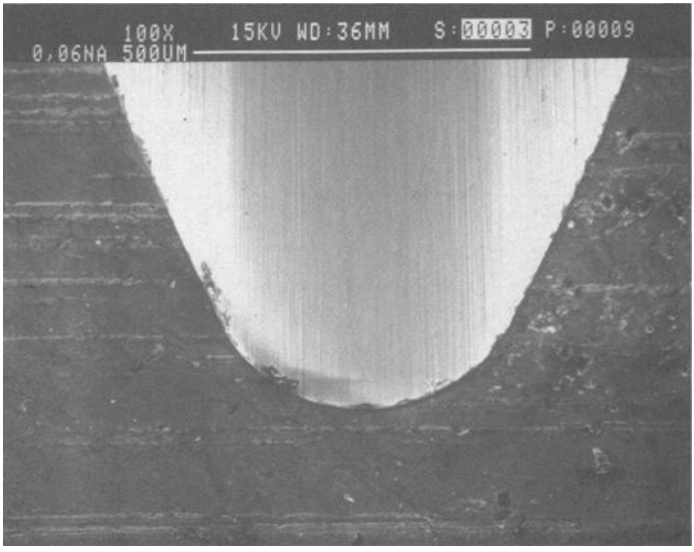

Figure 5a -- Ground Notch (#1) - Entry Side

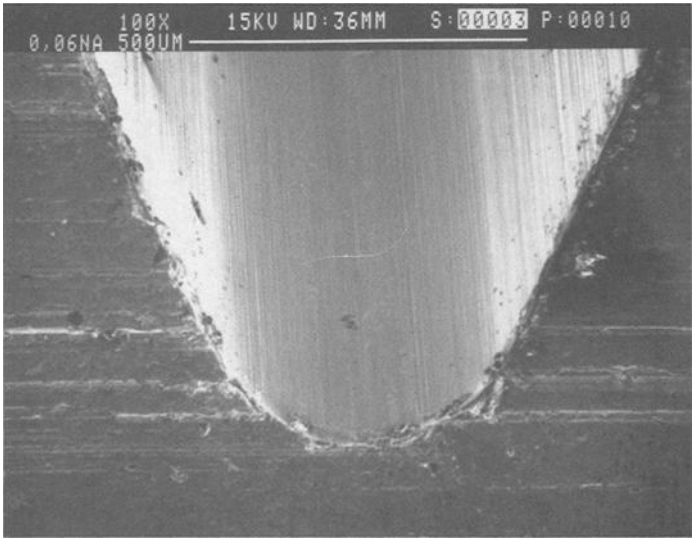

Figure 5b -- Ground Notch (#1) - Exit Side

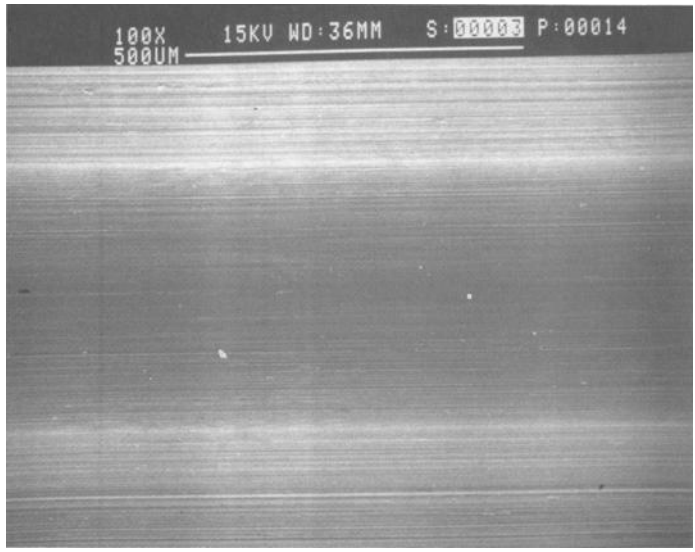

Figure 5c -- Ground Notch (#1) - Root of Notch

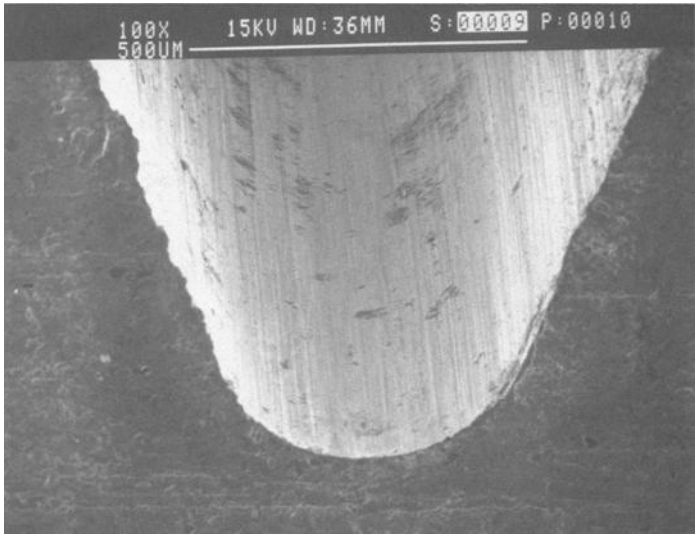

Figure 6a -- Ground Notch (#2) - Entry Side

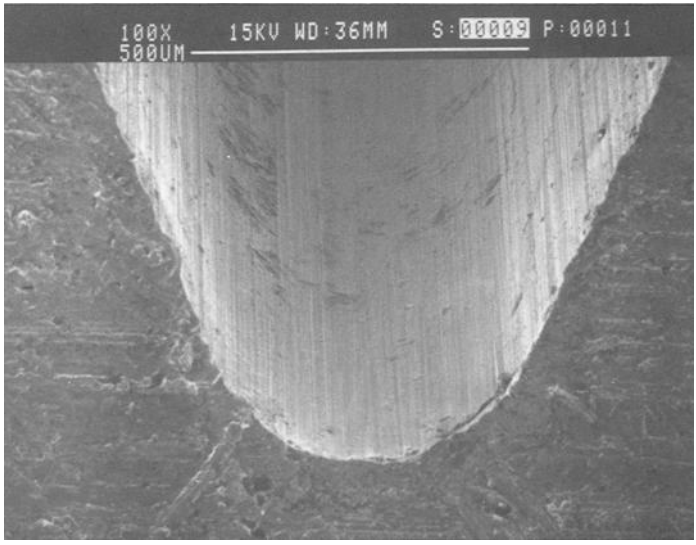

Figure 6b -- Ground Notch (#2) - Exit Side

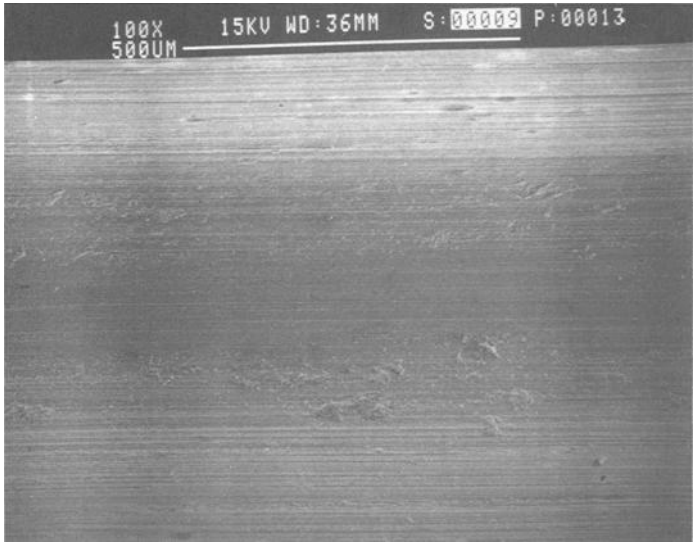

Figure 6c -- Ground Notch (#2) - Root of Notch

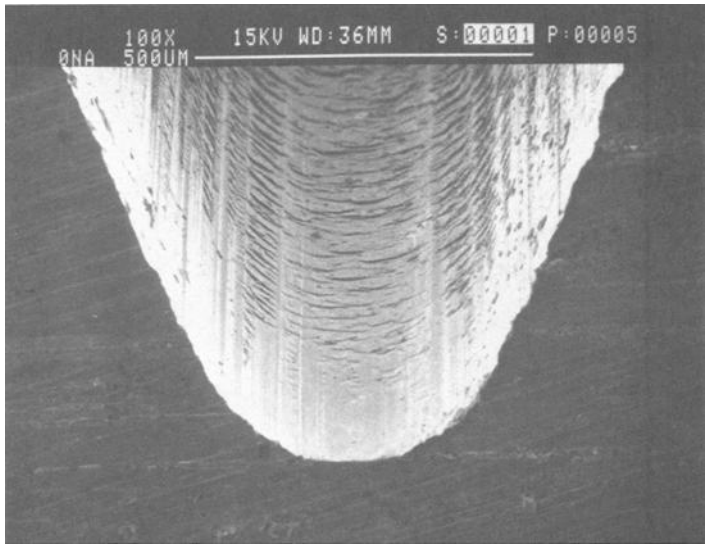

Figure 7a -- Broached Notch - Entry Side

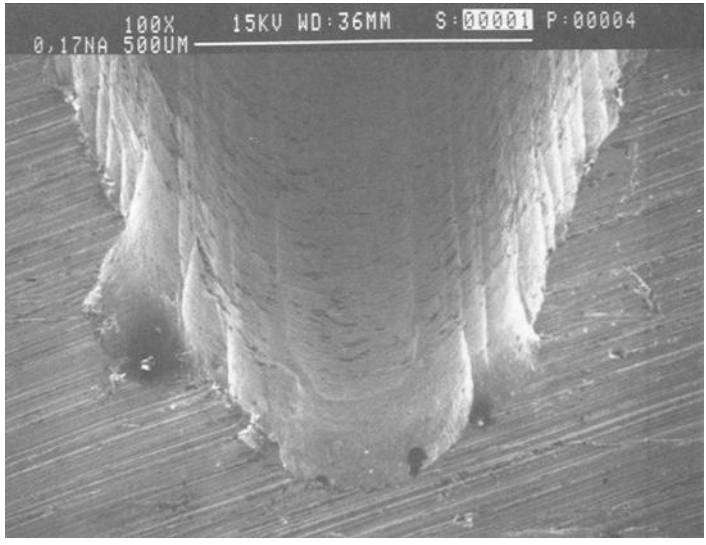

Figure 7b -- Broached Notch - Exit Side

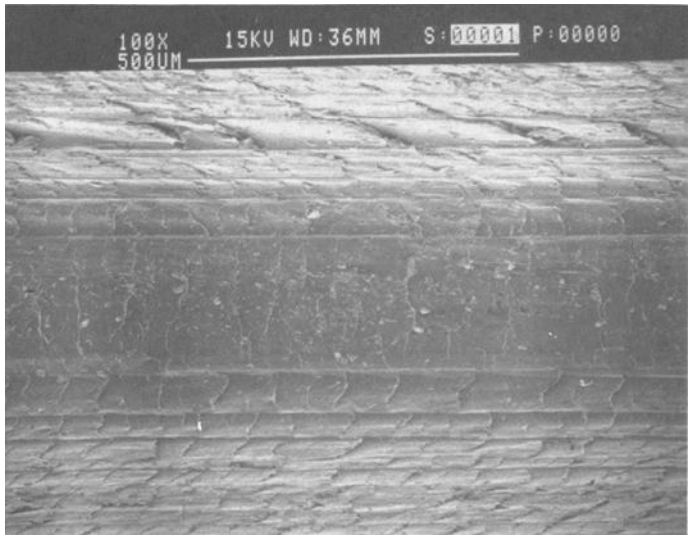

Figure 7c -- Broached Notch - Root of Notch

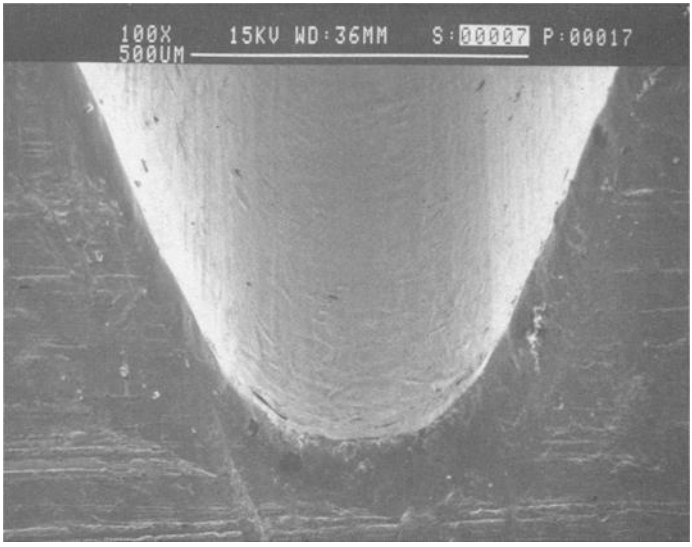

Figure 8a -- Milled (Flycut) Notch - Entry Side

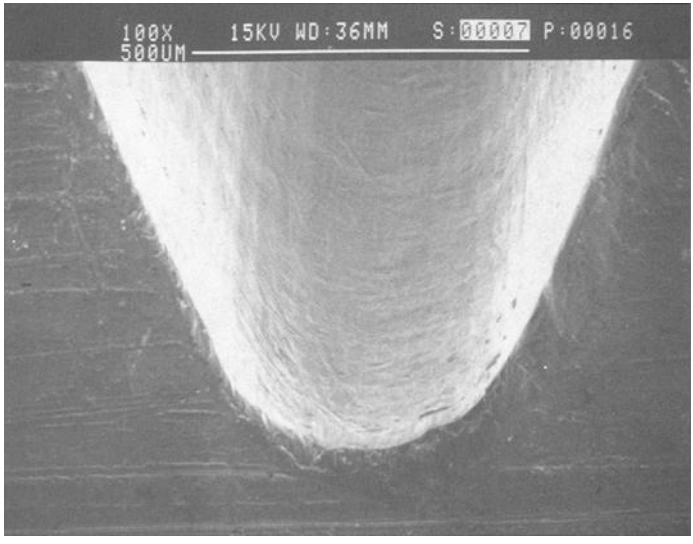

Figure 8b -- Milled (Flycut) Notch - Exit Side

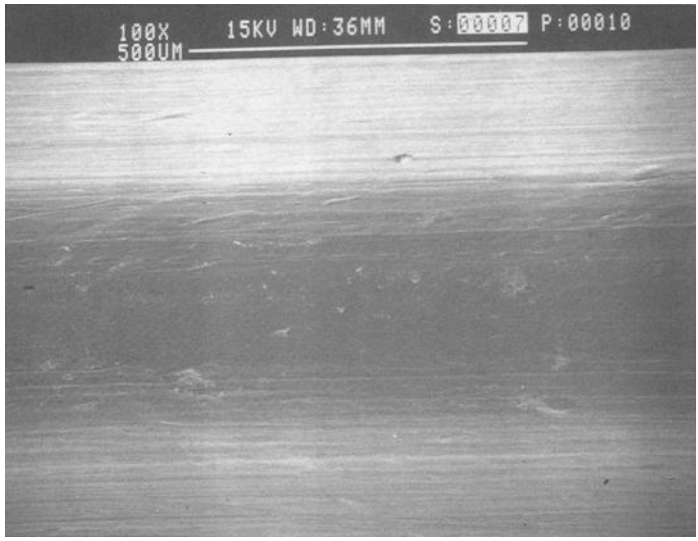

Figure 8c -- Milled (Flycut) Notch - Root of Notch

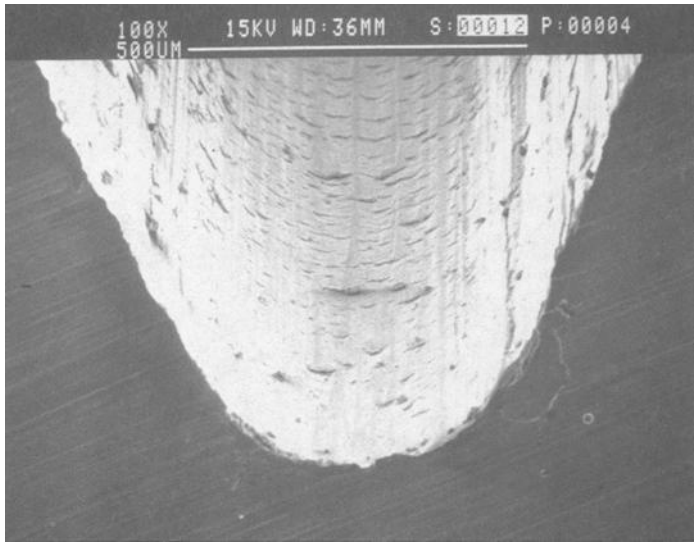

Figure 9a -- Notch Produced with Worn Broach - Entry Side

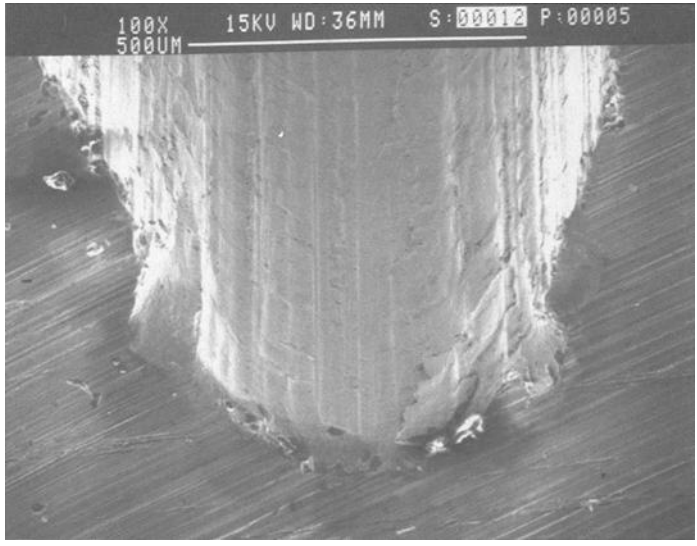

Figure 9b -- Notch Produced with Worn Broach - Exit Side

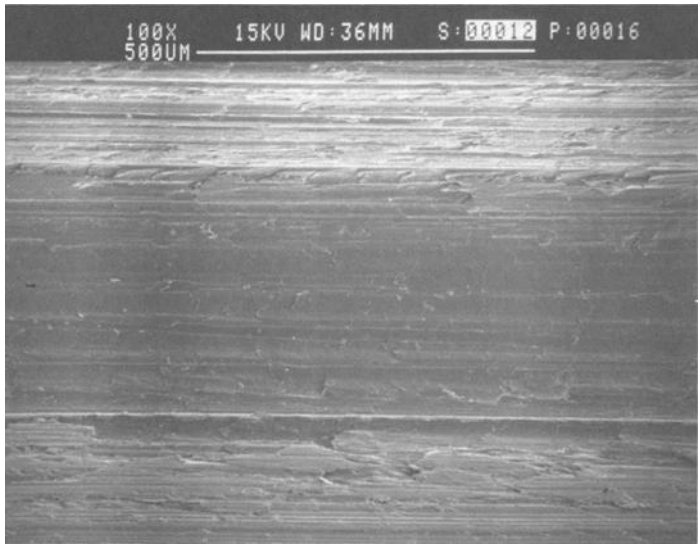

Figure 9c -- Notch Produced with Worn Broach - Root of Notch

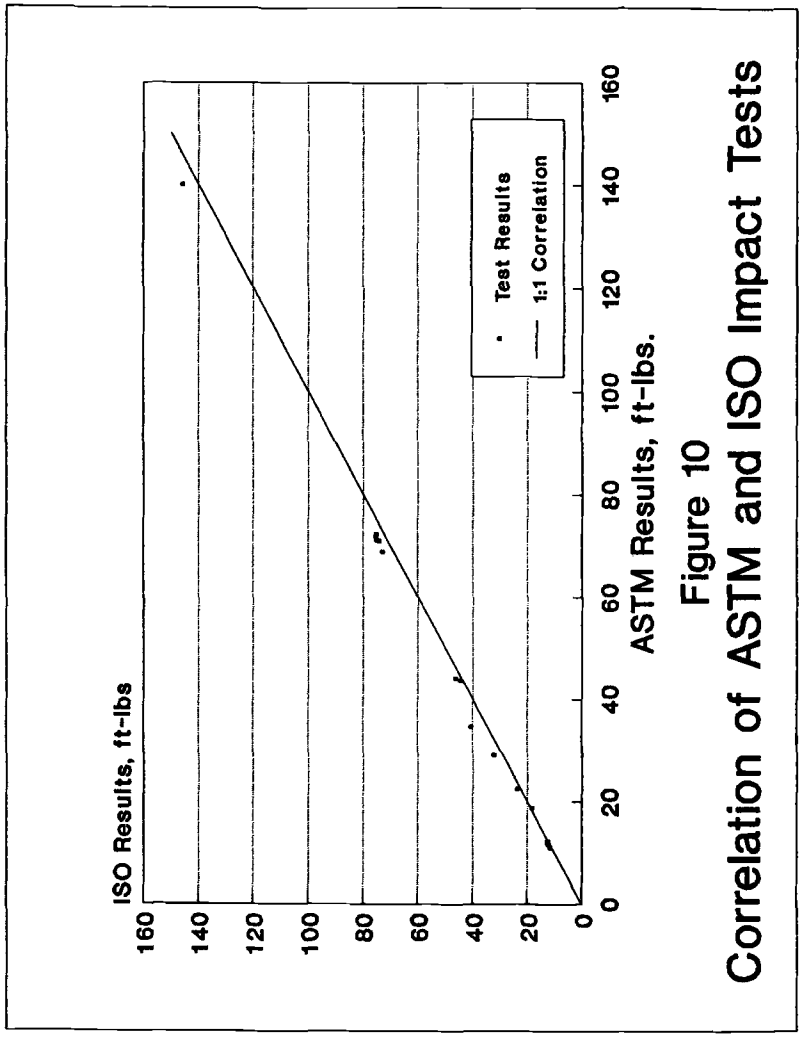

Figure 10
Correlation of ASTM and ISO Impact Tests

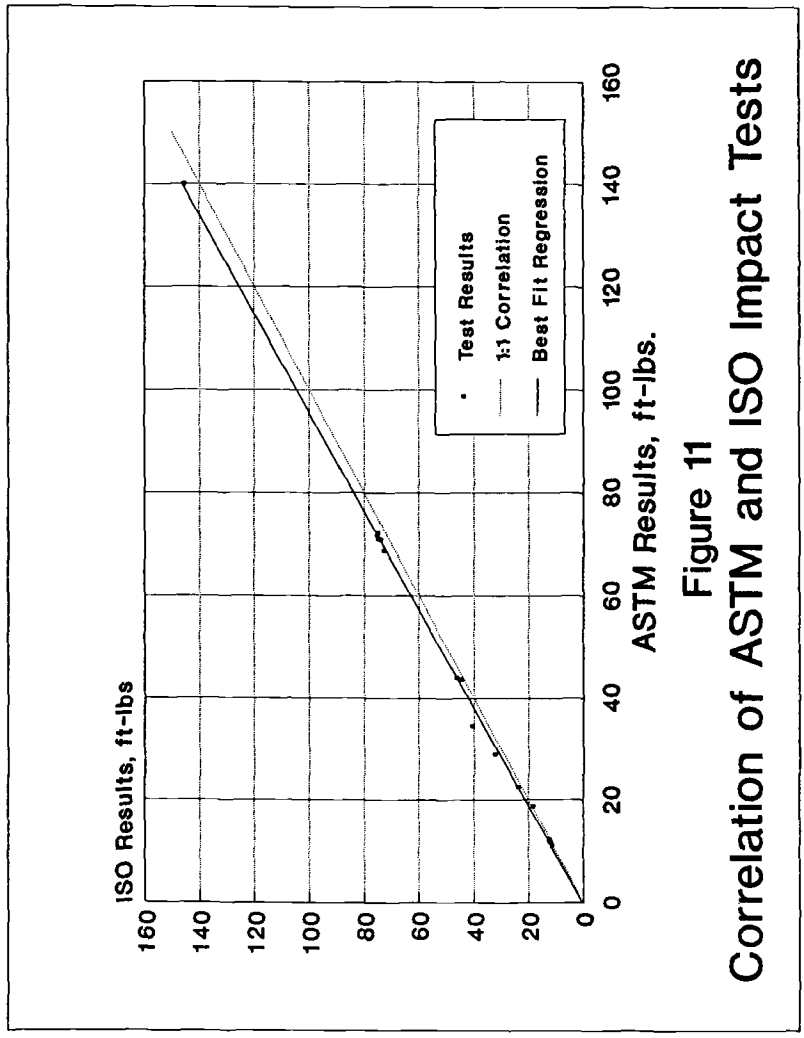

Figure 11
Correlation of ASTM and ISO Impact Tests

B. Anne Fields, Samuel R. Low, III, and James G. Early

THE EFFECT OF FATIGUE PRE-CRACKING VERSUS V-NOTCHING ON IMPACT TESTING OF CHARPY SPECIMENS

REFERENCE: Fields, B. A., Low, S. R., and Early, J.G., "The Effect of Fatigue Pre-Cracking Versus V-Notching on Impact Testing of Charpy Specimens," Symposium on Charpy Impact Test: Factors and Variables, ASTM STP 1072, John M. Holt, Editor, American Society for Testing and Materials, Philadelphia, 1990.

ABSTRACT: Charpy impact testing was carried out on both V-notch and fatigue pre-cracked specimens of two steels: AAR M128, and ASTM A212-65. Values of total energy absorbed, lateral expansion and shear fracture appearance were found for both types of specimen. The total energies absorbed by the fatigue pre-cracked specimens were markedly less than those by V-notch samples.
Transition temperature ranges were found for both the V-notch and pre-cracked specimens. The energy absorption results show a small increase in transition temperatures for the pre-cracked specimens. The lateral expansion results are the same in both types of specimen for the AAR M128 steel and show only a small change in the ASTM A212-65 steel. Also for the A212 steel the shear fracture appearance results can be represented by a single curve for V-notch and pre-cracked specimens. However, for the M128 steel these curves occur at lower temperatures for the pre-cracked specimens.

KEY WORDS: AAR M128 steel, ASTM A212 steel, Charpy test, fatigue pre-crack, instrumented impact test, transition temperature.

When a standard V-notch Charpy specimen is tested under impact loading the energy absorbed includes both the energy needed for the initiation of a moving crack and that for its propagation. The former may be considerably greater than the latter due to the large amount of energy required to generate a crack at a notch. Using only the total energy absorbed by a standard V-notch test can mask the fact that in a

Dr. Fields is a guest scientist in the Metallurgy Division, National Institute of Standards and Technology (NIST), Gaithersburg, MD 20899; Mr. Low is a mechanical engineer in the Metallurgy Division at NIST; Dr. Early is a metallurgist and a scientific advisor to the director of the Institute for Materials Science and Engineering at NIST.

given material the energy required to reinitiate a sharp crack already present in the material may be quite low. Thus, when using a fatigue pre-cracked specimen, the initiation energy may be a much smaller part of the total energy. This means that a pre-cracked Charpy test can more closely simulate the conditions under which an existing sharp crack extends.

However, if pre-cracked specimens are to be more commonly used, it is necessary to consider whether the standard transition temperatures for energy absorbed, shear fracture appearance and lateral expansion, as evaluated for V-notch tests, are still relevant or whether new specifications need to be introduced. This report contains results pertinent to such considerations.

EXPERIMENTAL DETAILS

Materials

All the samples were extracted from the head plates of three railroad tank cars, two of which were fabricated from Association of American Railroads (AAR) M128-69 steel [1] and are given the notations of G and U. The third plate used was ASTM A212-65 Grade B steel and will be referred to as plate S. The compositions of the two steels are given in Tables 1 and 2. The head plates from which these samples were taken are presumed to be in the hot-rolled, hot-formed and stress-relieved condition. Details concerning the exact thermomechanical condition of the three plates were not reported to NIST. The tensile properties of the 'as received' steels from the three plates are given in Table 3.

Specimens

Both standard V-notch specimens and specimens with an additional fatigue crack were tested [2,3,4]. The nominal dimensions were those given in ASTM E 23-72 (Notched Bar Impact Testing of Metallic Materials - Fig. 4, Charpy type A). These are 10 mm thick by 10 mm deep by 55 mm long. For pre-cracked specimens the machined notch was extended about 2.5 mm by fatigue cycling such that the total depth of the notch plus the crack was between 4.5 mm and 5.5 mm. The fatigue cracking was carried out following the procedure given in ASTM E 399-74.

Two orientations of specimens were used. In one, the longitudinal specimen axis was aligned parallel to the principal rolling direction and the plane of notching was in the long transverse direction. In the other the longitudinal axis was transverse to the rolling direction, while the notch plane was in the rolling direction. These two orientations are given the standard notations of LT and TL respectively.

Test Method

Standard Charpy V-notch tests were carried out in accordance with ASTM E 23-69. The values of total energies absorbed were obtained from the dial energies recorded. The pre-cracked specimens were tested using a standard Charpy machine modified for the acquisition of load-time data. Strain gauges placed on the striking tup were used to sense the load

TABLE 1 -- Chemical Compositions of Plates G and U (percent by weight)

Element	Specification AAR M128-69 Ladle Analysis		Tank Car GATX 93412 Check Analysis	Tank Car UTLX 38498 Check Analysis
	Grade A	Grade B	Plate "G"	Plate "U"
Carbon	0.25 max		0.23	0.24
Manganese	1.35 max		1.15	1.24
Phosphorus	0.04 max		0.01	0.01
Sulfur	0.05 max		0.017	0.014
Silicon	0.30 max		0.19	0.28
Copper	(a)	0.35 max	0.02	0.06
Nickel	(a)	0.25 max	0.20	0.15
Chromium	(a)	0.25 max	0.09	0.06
Molybdenum	(a)	0.07 max	0.05	0.01
Vanadium	0.02 min	(a)	0.026	0.01
Aluminum	(a)		0.02	0.025

(a) Element not specified, fine grain practice is required.

TABLE 2 -- Chemical Composition of Plate S (percent by weight)

Element	Specification ASTM A212-65-B Ladle Analysis	Plate "S" Check Analysis
Carbon	0.31 max	0.24
Manganese	0.90 max	0.73
Phosphorus	0.04 max	<0.005
Sulfur	0.05 max	0.026
Silicon	0.13/0.33	0.26
Copper	(a)	<0.05
Nickel	(a)	<0.05
Chromiun	(a)	0.07
Molybdenum	(a)	<0.05
Vanadium	(a)	<0.01
Aluminum	(a)	<0.01

(a) Element not specified, either fine- or coarse-grain practice allowed.

TABLE 3 -- Tensile Properties of AAR M128 and ASTM A212 Steels

Material Sample Code and Orientation	Ultimate Tensile Strength MPa(1)	Yield Strength 0.2% Offset MPa(1)	Elongation in 25.4 mm %	Reduction in Area %
M128 G TL	621	389	26.9	57.4
M128 G LT	582	380	31.7	63.2
M128 U TL	608	364	33.9	61.0
M128 U LT	610	403	31.4	61.0
A212 S TL	466	222	35.8	57.2
A212 S LT	468	227	37.4	61.4

(1) To convert stresses from MPa to ksi multiply by 0.145.

variation with time. An idealized load-time plot is shown in Figure 1. P_{GY} is the load at general yield and P_M is the maximum load. The energy absorbed, E, can be calculated at time t as discussed by Server [5]:

$$E = V_o \int_o^t P \, dt \qquad (1)$$

where V_o is the initial impact velocity and P is the load. This equation assumes that the velocity is nearly constant throughout the impact time, ie. that the kinetic energy of the hammer is much greater than the energy absorbed by the specimen. This assumption is valid since the mass of the hammer is large and E is small. The energy absorbed at maximum load, E_M, can be determined from equation 1 when $t=t_M$, where t_M is the time at which P_M is reached. E_M is the energy at crack initiation. Propagation energy is calculated by subtracting E_M from total energy.

Additional requirements for acceptable frequency response, initial oscillation damping, velocity reduction and electronic curve fitting as discussed by Server [5] are summarized in Appendix A of reference [4]. Details of the calculation of the true energy absorbed at maximum load are also described in reference [4].

When comparing energies absorbed in standard Charpy V-notch specimens and pre-cracked specimens it should be noted that the ligament area, B(W-a) (where B is the specimen thickness, W is the depth ,and a is the length of the notch plus the crack), will be smaller in the latter case because of the extension of the notch by fatigue cracking. Thus, it is not accurate to directly compare energies for the two types of specimens. A solution is to normalize the energy values by dividing by the fracture ligament area. This was done for all subsequent results.

RESULTS AND DISCUSSION

The normalized energies absorbed during standard Charpy V-notch tests for the plates G, U, and S are shown in Figures 2-7. Also included in these figures are the normalized total and initiation energies obtained for the pre-cracked specimens. These results, along with the calculated propagation energies for the pre-cracked specimens are all tabulated in previous reports [2,3,4]. Figures 8, 10, 12 show the

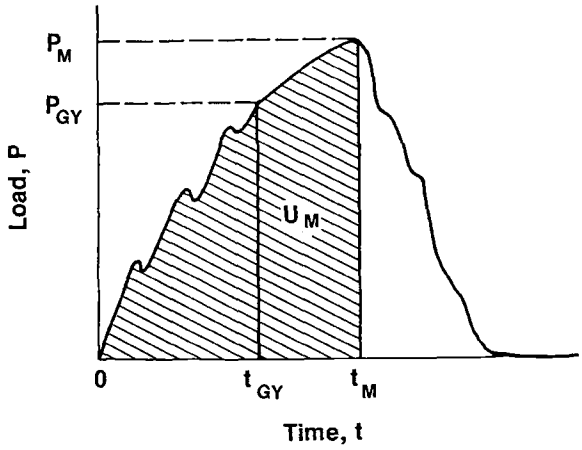

FIG. 1 -- Idealized load-time record for impact loading of a three point bend specimen.

lateral expansion measurements for the TL orientation of both the V-notch and pre-cracked specimens of plates G, U, and S. Similarly Figures 9, 11, 13 give the results of percentage shear fracture appearance for the TL specimens. Transition temperatures for the three plates and for three criteria are given in Table 4: the 270 KJ/m^2 energy absorption (equivalent to the 15 ft-lb energy in V-notch specimens), the 50% shear fracture appearance and the 0.38 mm (15 mils) lateral expansion. For the initiation energy results the critical temperature is given as that found at the midpoint of the transition range. Also included are the nil ductility temperatures previously reported [2,3].

There are some slight variations (≤7C) between some of the transition temperature values given here for the V-notch specimens as compared to the results listed in reference 4. These are due to differences in fitting the curves for the transition temperature ranges, but are not felt to be significant considering the amount of scatter among the individual data points.

As was stated in the introduction, the energy required to reinitiate a sharp crack already present in a pre-cracked specimen may be quite low. This can be seen to be true in Figures 2 to 7, where the lowest curve in each case is the energy absorbed during initiation. For the lower shelf, when cracking is cleavage, the energy required for initiation is close to zero. On the upper shelf the initiation energy is of the order of 125 KJ/m^2; or approximately one quarter of the total energy absorbed.

Absorbed Energy Transition Temperatures

Figures 2 to 7 also show that for any given temperature the total energy absorbed by a pre-cracked specimen is markedly less than that

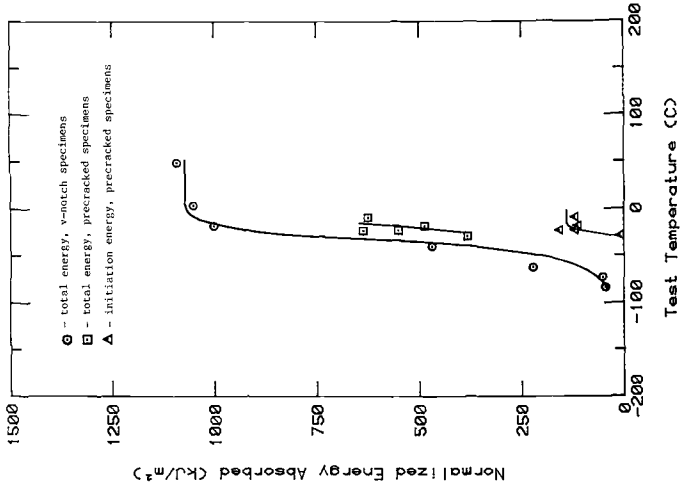

FIG. 3 -- Normalized energy absorbed for V-notch and pre-cracked LT specimens of plate G.

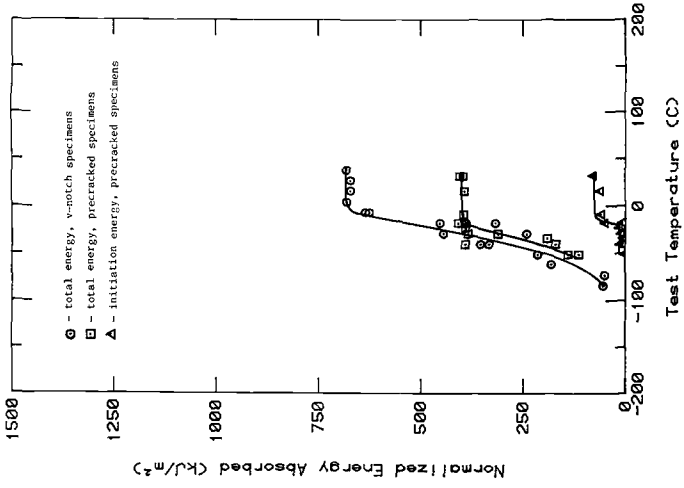

FIG. 2 -- Normalized energy absorbed for V-notch and pre-cracked TL specimens of plate G.

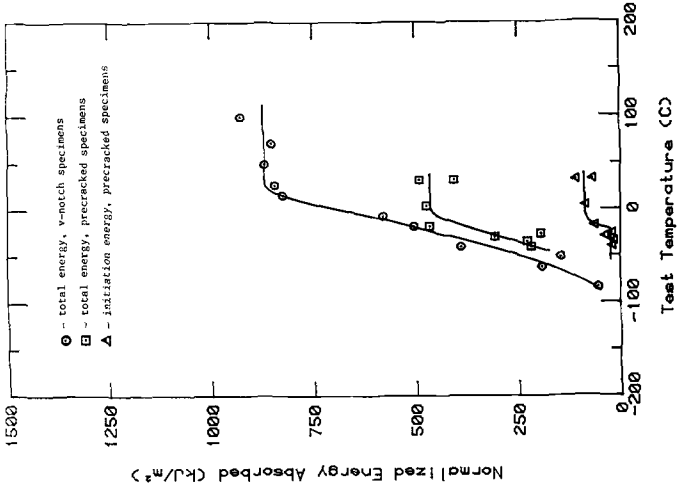

FIG. 5 -- Normalized energy absorbed for V-notch and pre-cracked LT specimens of plate U.

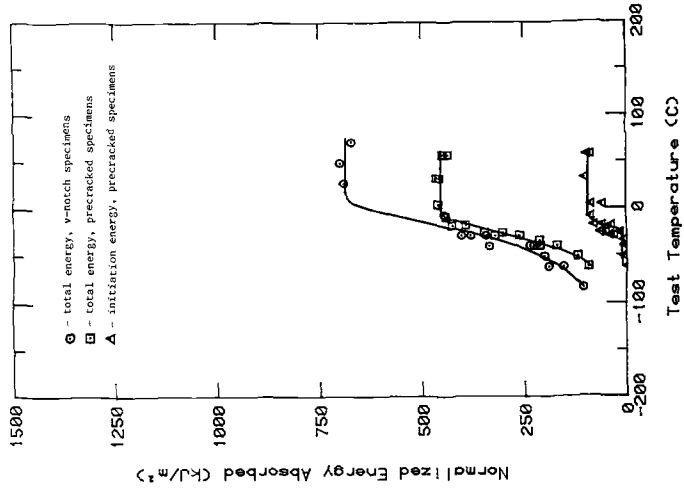

FIG. 4 -- Normalized energy absorbed for V-notch and pre-cracked TL specimens of plate U.

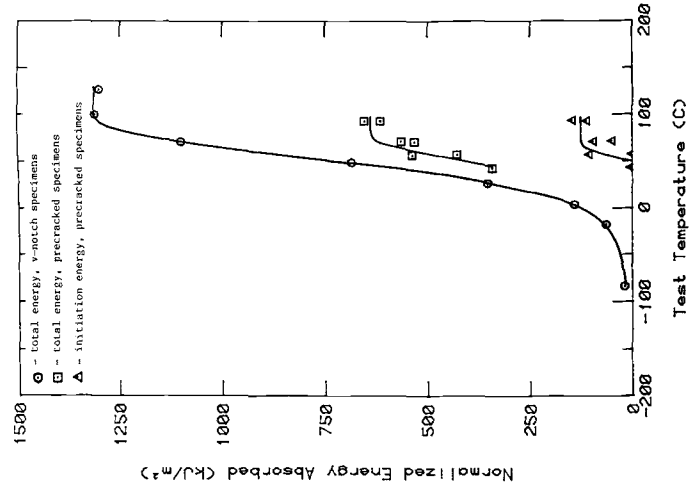

FIG. 7 -- Normalized energy absorbed for V-notch and pre-cracked LT specimens of plate S.

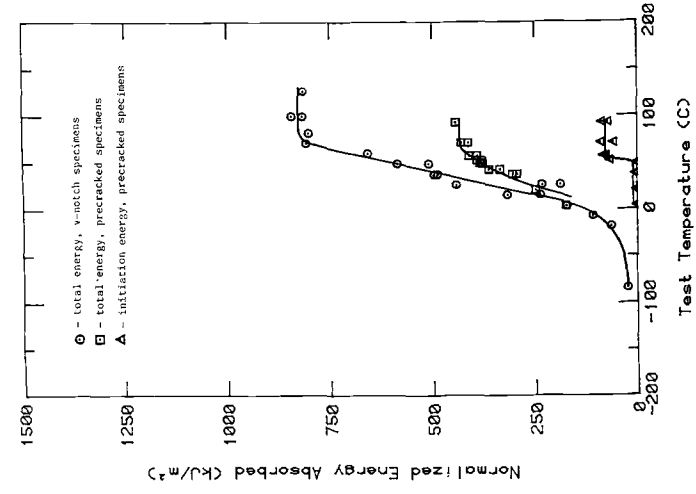

FIG. 6 -- Normalized energy absorbed for V-notch and pre-cracked TL specimens of plate S.

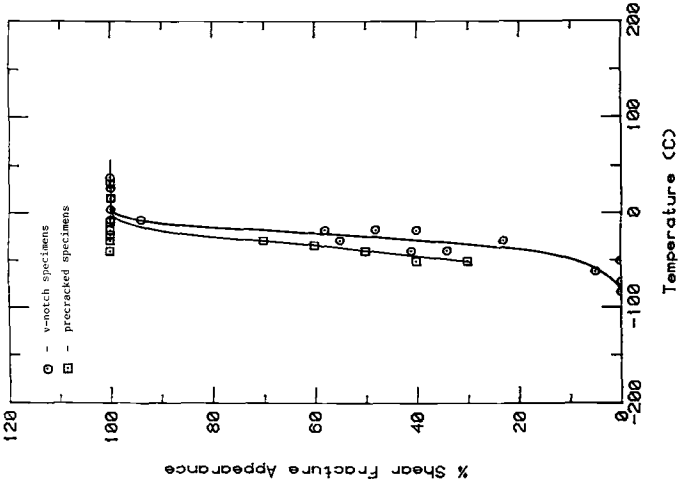

FIG. 9 -- Shear fracture appearance results for V-notch and pre-cracked TL specimens of plate G.

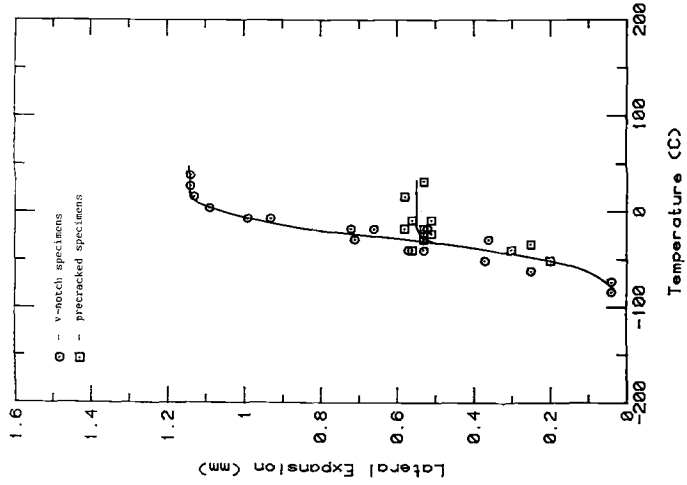

FIG. 8 -- Lateral expansion results for V-notch and pre-cracked TL specimens of plate G.

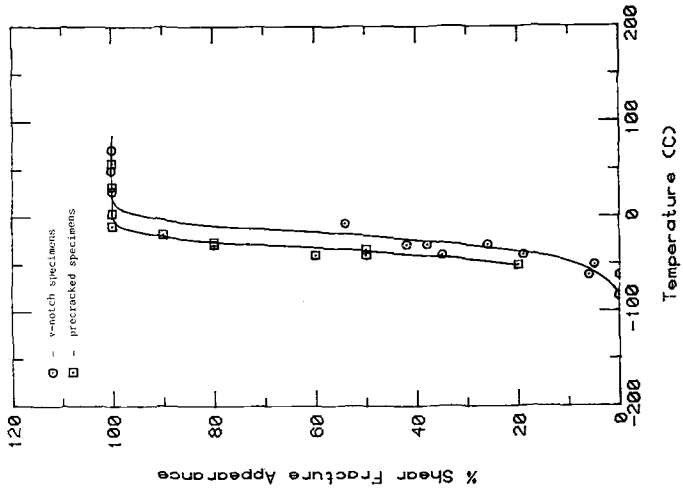

FIG. 11 -- Shear fracture appearance results for V-notch and pre-cracked TL specimens of plate U.

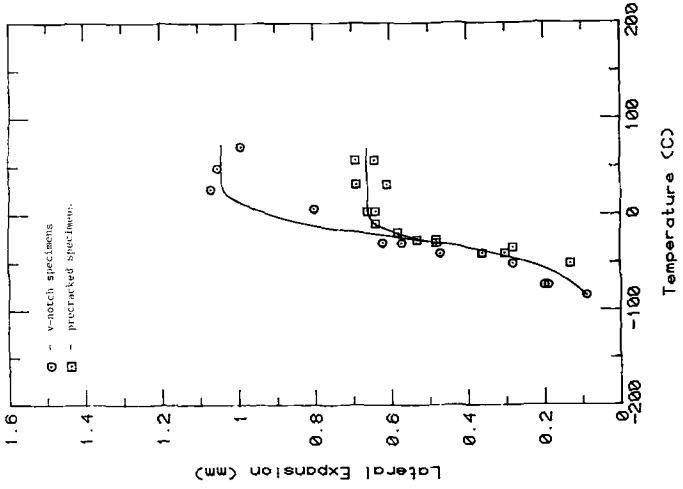

FIG. 10 -- Lateral expansion results for V-notch and pre-cracked TL specimens of plate U.

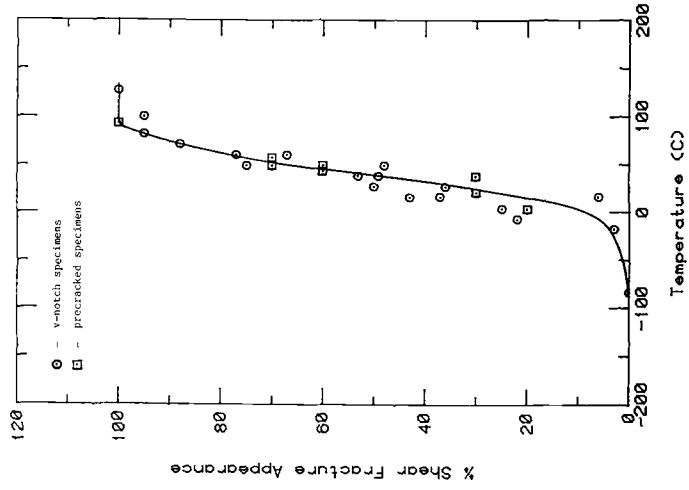

FIG. 13 -- Shear fracture appearance results for V-notch and up pre-cracked TL specimens of plate S.

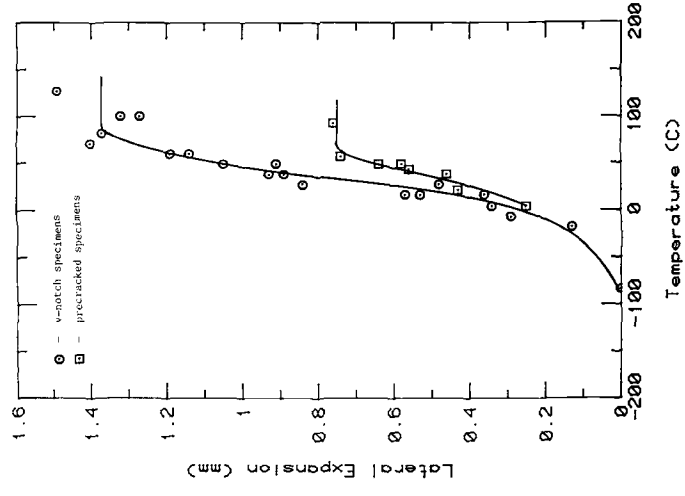

FIG. 12 -- Lateral expansion results for V-notch and pre-cracked TL specimens of plate S.

TABLE 4 -- Transition Temperatures for Plates G, U and S

Plate	Specimen Orientation	270 KJ/m^2 (a) Energy Absorption Charpy C	PC Total C	50% Shelf Energy PC Init C	50% Shear Fracture Charpy C	PC C	0.38 mm (b) Lateral Expansion Charpy C	PC C	Nil Ductility Temp. (c) C
G	TL	-41 (-43)	-35	-13	-25 (-27)	-40	-39 (-46)	-39	(-29)
	LT	-51 (-50)	-36(d)	-27	... (-34)	...	... (-53)	...	
U	TL	-40 (-41)	-31	-19	-20 (-16)	-37	-36 (-43)	-36	(-40)
	LT	-44 (-44)	-27	-21	... (-22)	...	... (-43)	...	
S	TL	17 (19)	28	52	39 (38)	39	14 (7)	23	(-1)
	LT	19 (19)	38(d)	57	... (44)	...	...(10)	...	

( ) Data Taken from reference [4].
(a) Equivalent to 15 ft-lbs in Charpy V-notch tests.
(b) Equivalent to 15 mils in Charpy V-notch tests.
(c) Determined by ASTM E 208, "Drop-Weight Test to Determine Nil-Ductility Transition Temperature of Ferritic Steels", using specimen size P-3.
(d) Values were obtained by extrapolation.

absorbed by a V-notch specimen. This is due to the large amount of energy required to generate a crack at the notch. This difference is greatest at the upper shelf level where the deformation is entirely plastic. At lower temperatures where fracture is partly cleavage the difference is not so large. One point to be noted is that at temperatures where the initiation energy for the pre-cracked specimens is close to zero, i.e. for cleavage, there is still a difference between the total energies absorbed by the V-notch and pre-cracked specimens. This means that there is still a significant energy required to initiate a crack at the V-notch even when this energy is close to zero for the pre-cracked specimens.

It should be noted that because the pre-cracked specimens show a lower total absorbed energy at all temperatures, the 270 KJ/m^2 energy absorption temperatures (15 ft-lb energy in V-notch tests) are necessarily higher than those for the V-notch tests. This can easily be seen in Figures 2 to 7. However these differences are not large, less than 20 degrees C for each of the tests.

Lateral Expansion Results

The results of the lateral expansion measurements for the TL orientation specimens of the G, U, and S plates are shown in Figures 8, 10 and 12 respectively. For the G and U plates the results can be represented by a single curve up to the upper shelf for the pre-cracked tests. This means that the temperature for which there is a lateral expansion of 0.38 mm (15 mils) is the same for both plates. For plate S the curves, while separate, are not greatly different and the 0.38 mm temperatures are only 9 degrees apart. This is not large when the scatter in the data is considered. Therefore the 0.38 mm lateral expansion temperature appears, from the present results, to be a temperature common to both V-notch and pre-cracked tests.

Shear Fracture Appearance Results

Shear fracture appearance results for the TL orientations of plates G, U, and S are shown in Figures 9, 11 and 13. For plates G and U it can be seen that this transition temperature range is actually lower for the pre-cracked specimens. These tests are the only ones of those carried out here where this was observed. The differences obtained for the 50% shear fracture appearance are 15 and 17 degrees C respectively. In spite of the scatter in the data this appears to be a real effect, although the reason for the difference is not known. For plate S the results for both types of specimen can be represented by a single curve.

CONCLUSIONS

1. The energy required to reinitiate cracking in a previously pre-cracked specimen is close to zero for cleavage and only of the order of 125 KJ/m^2 for ductile fracture.

2. The total energy absorbed by the pre-cracked specimens is markedly less than that for the V-notch specimens. This is due to the large

amount of energy needed to generate a crack at a blunt notch. This effect is greatest at the upper shelf where fracture is 100% shear.

3. The energy absorption transition temperature range is slightly higher for the pre-cracked specimens. For the 270 KJ/m^2 (15 ft-lb) energy absorption temperatures this difference is less than 20 degrees for all tests.

4. The temperatures at which there is a lateral expansion of 0.38 mm (15 mils) are the same for both types of specimen from M128 steel. For A 212 steel the pre-cracked specimens show an increase of 9 degrees over the V-notch tests.

5. The transition temperature results for shear fracture appearance in both types of specimen from A212 steel can be represented by a single curve. For M128 steel the results for the pre-cracked specimens give lower transition temperatures than for the V-notch specimens. This is not understood at this time.

6. Present results indicate that for pre-cracked specimens of M128 steel the best correlation with standard Charpy V-notch transition temperatures is found using values of lateral expansion, while for A212 steel the best correlation is found using shear fracture appearance.

ACKNOWLEDGEMENTS

The authors wish to express thanks to Mr. D. E. Harne for his contributions to the mechanical testing involved in this project and to the Federal Railroad Administration for support under Interagency Agreement A R-40008 and for valuable comments and advice.

REFERENCES

[1] AAR M128 Specification for High Strength Carbon Manganese Steel Plates for Tank Cars, Manual of Standards and Recommended Practices, Section C - Part III, Specifiaction M-1002, pp M-7, M-8, The Association of American Railroads, 50 F St., N.W., Washington, D.C. 20001, 1985.

[2] Early, J.G., "A Metallurgical Analysis of an ASTM A212-B Tank Car Head Plate", Report No. 9, NBSIR-78-1582, National Bureau of Standards, Sept. 1978.

[3] Early, J.G. and Interrante, C.G., "A Metallurgical Evaluation of Two AAR M128 Steel Tank Car Head Plates Used in Switchyard Impact Tests", Report No. 10, NBSIR-80-2039, National Bureau of Standards, May 1980.

[4] Early, J.G., Interrante, C.G., Low, S.R., and Fields, B.A., "Dynamic Mechanical Properties of Two AAR M128 and One ASTM A212-B Steel Tank Car Head Plates", Report No. 14, NBSIR-88-3690, National Bureau of Standards, June 1988.

[5] Server, W.L., "Impact Three-Point Bend Testing for Notched and Precracked Specimens", Journal of Testing and Evaluation, JTEVA, Vol. 6, No. 1, Jan. 1978, pp. 29-34.

Stephanie Mikalac, Michael G. Vassilaros, and Harold C. Rogers

PRECRACKING AND STRAIN RATE EFFECTS ON HSLA-100 STEEL CHARPY SPECIMENS

REFERENCE: Mikalac, S., Vassilaros, M.G., and Rogers, H.C., "Precracking and Strain Rate Effects on HSLA-100 Steel Charpy Specimens," Charpy Impact Test: Factors and Variables, ASTM STP 1072, J. M. Holt, Ed., American Society for Testing and Materials, Philadelphia, 1990.

ABSTRACT: Improved predictions of the ductile-to-brittle transition behavior of structures are possible using Charpy specimens that have increased constraint. This report contains the results of an investigation into the combined effects of a change in notch acuity and a change in loading rate on the transition curve of a high-strength, low alloy (HSLA) steel. Specifically, the changes in absorbed energy and ductile-to-brittle transition temperature were noted. Standard Charpy V-notch specimens were fatigue precracked to a total crack depth (notch and precrack) of approximately 0.280 cm. The specimens were subsequently tested using an impact loading rate of 5.1 m/sec over a wide range of temperatures to fully develop the transition temperature curve. The transition temperature was determined using the 50% Fracture Appearance Transition Temperature (FATT). As expected, the level of absorbed energy was lower for precracked specimens as compared to standard specimens. The transition temperature of the precracked specimens was shifted upward by approximately 40°C. Both standard V-notch specimens and fatigue precracked specimens were tested at a slower loading rate of 0.0025 cm/sec to determine the combined effects of the sharper crack tip and the change in loading rate on both the energy absorbed and the transition temperature. At the slow loading rate the absorbed energy was lower for precracked specimens while the transition temperature was shifted upward by approximately 20°C. The results were also compared with those from 1.6-cm thick dynamic tear (DT) tests. It was found that the transition curve developed through fracture appearance for the DT test was identical to that of the precracked CVN tested at the impact loading rate.

KEYWORDS: ductile-to-brittle transition, Charpy, notch acuity, loading rate, transition temperature, dynamic tear, energy absorption, precracking, impact testing

S. Mikalac and M.G. Vassilaros are research engineers at David Taylor Research Center, Code 2814, Annapolis, MD 21402; Professor Rogers is head of the Materials Engineering Department, Drexel University, Philadelphia, PA, 19104.

BACKGROUND

Since its introduction in the early 1900's [1], the Charpy V-notch (CVN) impact test has been the one most commonly used to characterize the notched impact behavior of structural metals. It is especially useful for characterizing the transition from ductile to brittle fracture behavior in steel under varying conditions of temperature and loading rate. Ductile fracture is the dominant mode in the plastic regime, that is, the upper shelf region of the transition curve. General yielding occurs in this region usually accompanied by the development of shear lips oriented at 45 degrees to the direction of the applied stress. In the lower shelf region of the transition curve, brittle fracture occurs under elastic stresses. In this case, fracture is normal to the direction of the principal stress with little or no shear lip development. Within the transition portion of the curve, sometimes known as the elastic-plastic region, CVN specimens show a mixed mode of fracture.

The CVN test has many advantages over the more complex methods for analyzing material toughness. The sample size is small, the test itself is quick and easy to conduct, and it is relatively inexpensive. However, there are some significant disadvantages. First, because of the small sample size, the constraint developed in the specimen may be very limited. This may lead to non-conservative predictions of the toughness and transition behavior of the material. Second, the test cannot differentiate between energy consumed in crack initiation and that absorbed during crack propagation. Finally, the Charpy impact test does not provide results that can be utilized directly in structural design as can K_{Ic}, the fracture toughness level of a material.

There have been countless reports deriving empirical relationships between CVN energy values and fracture toughness. Any correlations that have been developed between fracture toughness measured by standard procedure, *i.e.*, ASTM E399, and CVN test results may not be applicable when the materials or operating conditions change. Although it is doubtful that a single correlation between Charpy test results and fracture toughness that is valid for all materials and conditions may be obtained, there is a possiblity that a modified Charpy test could replace other toughness testing that requires larger specimens such as the dynamic tear test [2,3].

Fatigue precracking is one method of increasing the constraint under which the Charpy specimen deforms. The sharper crack tip increases the level of tensile stress below the notch. It also reduces the energy required to initiate crack propagation. Precracking generally results in a lowering of the upper shelf energy of the material and shifts its transition temperature upward. [2-7].

Variations in the strain rate will also change the constraint by

changing the yield stress of the steel. For a given geometry, an increase in flow strength (which occurs when the strain rate is increased) will drive the specimen behavior toward linear-elastic plane strain behavior. This would be manifested by a drop in energy absorption. In addition, at standard impact loading rates, the transition temperature will usually be shifted upward as the strain rate is increased. [5,7,8].

INTRODUCTION

The objective of this study was to understand the separate and combined effects of notch acuity and loading rate on the ductile-to-brittle fracture behavior of HSLA-100 steel. The effects of precracking standard Charpy V-notch specimens on both the energy absorption and the transition temperature were investigated. The effects of a change in loading rate on CVN behavior were also examined with respect to the absorbed energy and transition temperature shift. Results were used to establish the change in constraint in the specimen measured through energy absorption and fracture appearance.

The chemical composition, heat treatment and mechanical properties of the steel are shown in Table 1:

TABLE 1 -- HSLA-100 3-cm thick plate chemistry (weight percent)
Lukens Steel Company
Austenitized at 900°C for 75 minutes, water quenched
Aged at 640°C for 75 minutes, water quenched

C	Mn	Si	Cu	Ni	Cr	Mo	Al	Cb
0.04	0.86	0.27	1.58	3.55	0.57	0.60	0.032	0.030

Transverse tensile properties:
0.2% Yield strength: 758 MPa
Tensile strength: 807 MPa
Elongation: 25%
Reduction in area: 76%

PROCEDURE

Charpy V-notch (CVN) specimens (type A, ASTM E23) were cut from a 3-cm plate and tested in the transverse-longitudinal (T-L) direction. Testing was performed over a wide range of temperatures in order to fully develop the temperature transition curve of the steel. Specimens were tested at temperatures of -120°C, -90°C, -30°C, 0°C, and at room temperature. The total energy absorption and fracture appearance were recorded.

Precracked specimens were prepared by loading the specimen in three point bend and subjecting them to an oscillating load guided by ASTM E812.

Standard V-notch and fatigue precracked CVN specimens were tested according to ASTM E23. The impact velocity generated by the testing machine was 5.1 m/sec. Standard and precracked CVN specimens were also tested at a loading rate of 0.0025 cm/second using anvils and tup from a standard Charpy testing machine. The absorbed energy was measured as the area under the recorded load versus cross-head displacement curve corrected for machine compliance. Measured energy absorption values were normalized with respect to the remaining ligament below the V-notch or fatigue precrack.

Transition temperatures were developed using the 50% Fracture Appearance Transition Temperature (FATT) method; this is defined as the temperature at which the surface of the Charpy specimen exhibits equal amounts of cleavage and ductile (shear) fracture.

Dynamic Tear (DT) specimens (ASTM E604) were also cut from the same plate and tested in the transverse-longitudinal direction over a wide range of temperatures in order to fully develop the transition curve. Fracture appearance as a function of testing temperature was recorded.

RESULTS AND DISCUSSION

Figure 1 shows the transition curves of the two different notch configurations for CVN specimens tested at the impact loading rate of 5.1 m/sec. The normalized values of energy absorbed by the steel was lower in precracked specimens at all temperatures. The results agree with those of [3,4,6]. The transition from mostly ductile fracture to mostly cleavage (50% FATT) occurred at -90^{o}C (+/- 3^{o}C) as shown in figure 1(b) in the standard V-notch CVN specimens. The precracked Charpy specimens had a much higher 50% FATT of -50^{o}C. Clearly, the sharp crack tip of these specimens caused the transition temperature to shift upward significantly, consistent with [3-7]. By reducing the notch tip radius in a CVN specimen, the stress concentration at the tip of the crack is increased. This also causes an increase in the effective strain rate and also increases the concentration of strain at the crack tip. The end result is an increase in the tensile stress level below the notch [9,10]. Brittle fracture is thus promoted with the sharper crack tip; this is seen in an increase of the 50% FATT and a decrease in normalized energy absorption.

The transition curves for the two different notch configurations for CVN specimens tested at a loading rate of 0.0025 cm/sec are shown in figure 2. As in the tests performed at the impact loading rate, the normalized absorbed energy was lower with precracked specimens at all temperatures. The decrease in absorbed energy at the slow loading

rate, however, was not as large as when the tests are performed at the impact loading rate. Also, with the reduction in strain rate, the notch effect on the transition temperature was smaller. Although there was substantial scatter in the transition region at this loading rate, the transition temperature appeared to increase for the precracked specimens by about 20°C, from -75°C to -55°C. The smaller change in energy absorption and in transition temperature with precracking at the slower rate may be the result of opposing constraint changes. At the slower loading rate, the effective yield strength of the material is lower [7], thus reducing the constraint developed. Therefore, the changes in the transition temperature curves, when testing is carried out at the slower loading rates, would be expected to be smaller than those at the impact loading rate because the increased constraint caused by fatigue precracking is geometrical, independent of the rate of testing.

The transition curves of the standard V-notched specimens tested at the two different loading rates are shown in figure 3. At the slower strain rate there was a decrease in normalized energy absorption at all temperatures. In terms of fracture appearance, the upper and lower shelves were quite similar. There appeared to be an increase in the 50% FATT on the order of 15°C with the slow loading rate. This behavior cannot be explained using the strain rate effect model discussed earlier in the background section.

The transition curves of the fatigue precracked specimens tested at the two loading rates are seen in figure 4. The upper shelf energy (USE) at the two loading rates was similar. In the transition region, however, the energy absorption at the slow loading rate was higher than at the impact loading rate. These results corroborate with those observed by [8]. The transition temperature was approximately -50°C (+/- 3°C) for the impact loading rate. The transition temperature at the slower loading rate was approximately -55°C. As seen in figure 4(b) the values of percent shear as a function of temperature measured for fatigue precracked CVN specimens tested at the impact loading rate appeared to provide a lower bound for the results obtained at the slower rate. The increased flow strength caused by the increase in strain rate appears to change the transition characteristics of the steel, particularly in terms of normalized energy absorption.

It is expected that in front of a sharp crack (such as the fatigue precracked CVN specimens), the plastic zone size is smaller than that found in a blunt notch (such as the V-notch CVN specimen). Also the maximum stress developed is higher and located closer to the crack tip [11,12]. Thus the microstructural features that control fracture (thus controlling energy absorption and transition temperature) in the fatigue precracked specimens are not necessarily identical to those controlling fracture in the standard V-notch specimens [5]. The end result is that the models [2,3,8,9], which appear to work well for the sharp notch configuration when describing loading rate effects cannot always be used successfully when considering blunt notches [12]. Loading rate changes did not affect the standard V-notch specimens in

the same manner as they did the fatigue precracked specimens. For example, the upper shelf energies of the V-notched specimens were dramatically changed with changes in loading rate while the precracked specimens had similar upper shelf energies despite the difference in loading rate. This may be the result of a difference in the microstructural factors controlling fracture in the two specimen types as discussed by others [5,12].

The following table summarizes the major findings of this study of the separate and combined effects of a change in notch acuity and loading rate on the energy absorption and 50% FATT of HSLA-100 steel Charpy specimens.

TABLE 2 -- Summary of Charpy Test Results

Standard V-notch	Precracked V-notch
Impact Loading Rate:	
USE = 3.06 J/mm^2	USE = 2.19 J/mm^2
50% FATT = -90°C	50% FATT = -50°C
Slow Loading Rate:	
USE = 2.43 J/mm^2	USE = 1.97 J/mm^2
50% FATT = -75°C	50% FATT = -55°C

Figure 5 shows the transition temperature curve developed from 1.6-cm dynamic tear specimens made of the same HSLA-100 steel. The 50% FATT is approximately -50°C. Comparing the precracked CVN curve tested at the impact loading rate with the DT transition curve, one can see the results: the transition temperature curves were almost identical. Through-thickness stresses increase as the thickness of the specimen is increased. These increasing stresses cause greater plastic constraint at the notch root [13]. As discussed earlier in the background section, precracking increases the constraint under which the Charpy specimen deforms by increasing the level of tensile stress below the notch. The constraint developed in the 10-mm precracked Charpy V-notch specimen, as measured through fracture appearance, was increased enough to mimic the constraint developed in the thicker 1.6-cm DT tests. Similar results were reported by [2,3].

CONCLUSIONS

Fatigue precracking of Charpy V-notch specimens of HSLA-100 steel caused the energy absorption to drop and the 50% Fracture Appearance Transition Temperature to shift upward by approximately 40°C when tested at an impact loading rate of 5.1 m/sec.

At a slower loading rate of 0.0025 cm/sec, fatigue precracking still resulted in a decrease in energy absorption at all temperatures although the change was not as large as observed at the impact loading rate. There was a smaller increase in the 50% FATT of approximately 20°C when the V-notch was fatigue precracked.

With a blunt notch, the slower loading rate decreased the energy absorption at all temperatures. At the slower loading rate there was a shift upward of approximately 15°C in the 50% FATT.

With the sharper crack tip, there was a slight increase in energy absorption at the slower loading rate in the lower transition region. The 50% Fracture Appearance Transition Temperature changed only slightly with loading rate; however, at temperatures below the transition temperature, the standard rate appeared to provide a lower-bound estimate of the transition curve.

Precracked Charpy V-notch specimens were found to provide a more conservative measure of a material's notch toughness and were less rate sensitive than the blunt V-notch specimen. The constraint developed in a fatigue precracked Charpy V-notch specimen tested at an impact loading rate appeared to be similar to that of a dynamic tear specimen made of the same HSLA-100 steel. Both specimen types had a 50% FATT of approximately -50°C.

ACKNOWLEDGMENTS

The authors acknowledge Dr. A.K. Vasudevan from the Office of Naval Research for his support. Thanks also go to E. Tees, J. Sanders, C. Fraser, E. Czyryca, E. Hackett, R. Link, and P. Joyce.

REFERENCES

[1] McAdam, D.J. and R.W. Clyne, "The Theory of Impact Testing: Influence of Temperature, Velocity of Deformation, and Form and Size of Specimen on Work of Deformation," Symposium on Impact Testing, American Society for Testing and Materials, 1938, pp. 112-134.

[2] Sharkey, R.L. and D.H. Stone, "A comparison of Charpy V-notch, dynamic tear, and precracked Charpy impact transition-temperature curves for AAR grades of cast steel," Transactions of the ASME, May 1976, pp. 446-452.

[3] Diesburg, D.E., "Transition temperature characterized by precracked Charpy specimens," Toughness Characterization and Specifications for HSLA and Structural Steels, ed. P.L. Mangonon, Jr., AIME: 1979, pp. 19-36.

[4] Louden, et al., "The influence of specimen size on Charpy impact testing of unirradiated HT-9," Journal of Nuclear Materials, 155-157, pp. 662-667, (1988).

[5] Tvergaard, V. and A. Needleman, "An analysis of the temperature and rate dependence of Charpy V-notch energies for a high nitrogen steel," International Journal of Fracture, Vol. 37, pp. 197-215, (1988).

[6] McKinney, K.E. et al., "An evaluation of the toughness of ductile iron vs cast steel using modified Charpy test specimens," AFS Transactions, 84-122, pp. 239-250.

[7] Wullaert, R.A., "Applications of the Instrumented Charpy Impact Test," Impact Testing of Metals, ASTM STP 466, American Society for Testing and Materials, 1970, pp. 148-164.

[8] Barsom, J.M. and S.T. Rolfe, "Correlations between K_{Ic} and Charpy V-notch test results in the transition-temperature range," Impact Testing of Metals, ASTM STP 466, American Society for Testing and Materials, 1970, pp. 281-302.

[9] Dieter, Jr., G.E., Mechanical Metallurgy, McGraw-Hill Book Company, Inc., New York, NY, 1961.

[10] Wullaert, R.A., Ireland, D.R., and Tetelman, A.S., "Radiation Effects on the Metallurgical Fracture Parameters and Fracture Toughness of Pressure Vessel Steels," Irradiation Effects on Structural Alloys for Nuclear Reactor Applications, ASTM STP 484, American Society for Testing and Materials, 1970, pp. 20-41.

[11] Veistinen, M.K. and K. Wallin, "Cleavage Fracture in 26Cr-1Mo Ferritic Stainless Steel," Materials Science Technology, July 1986, pp. 666-670.

[12] Lin, T. and R.O. Ritchie, "On the Effect of Sampling Volume on the Microscopic Cleavage Fracture Stress," Engineering Fracture Mechanics, Vol. 29, No. 6, pp. 697-703, 1988.

[13] Hertzberg, R.W., Deformation an Fracture Mechanics of Engineering Materials, 2nd ed., John Wiley & Sons, New York, NY, 1983.

ERRATUM FOR ASTM STP 1072

The publisher regrets that five pages of figures to the pap "Precracking and Strain Rate Effects on HSLA-100 Steel Char Specimens," by Stephanie Mikalac, Michael G. Vassilaros, an Harold C. Rogers (pp. 134-141), were inadvertently omitted.

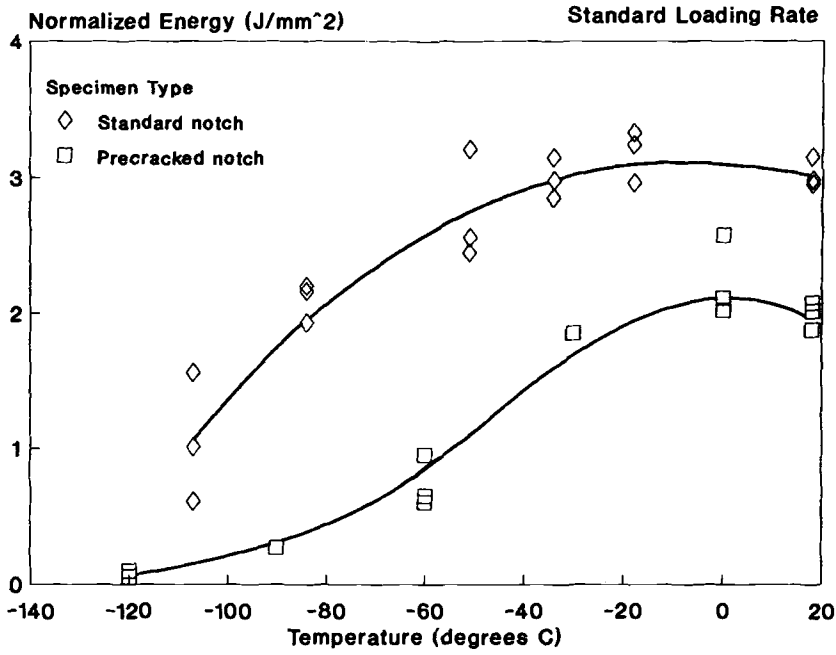

Figure 1(a): Normalized Charpy V-notch Energy versus Temperature; Standard Loading Rate; for HSLA-100 Steel

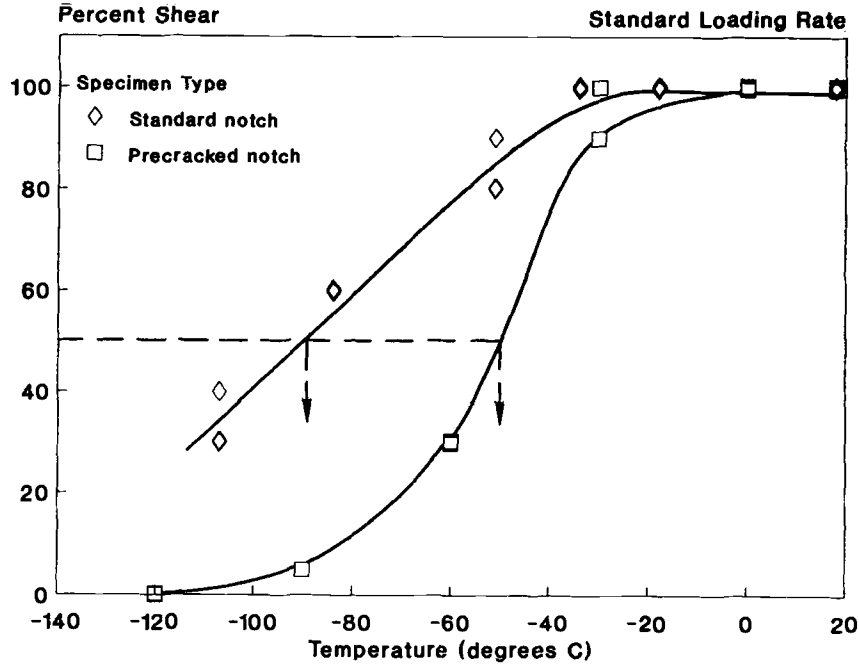

Figure 1(b): Percent Shear in Charpy V-notch Specimens versus Temperature; Standard Loading Rate; for HSLA-100 Steel

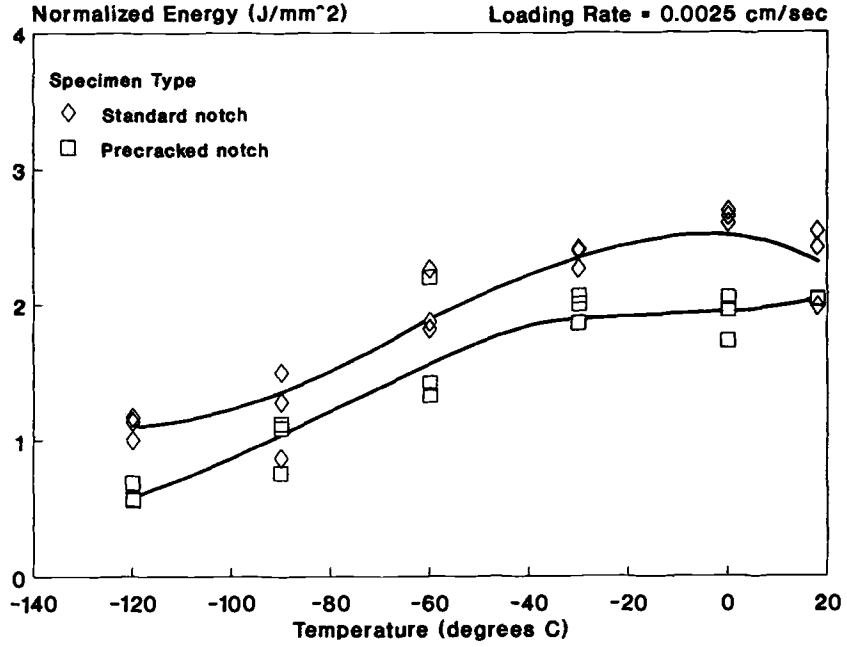

Figure 2(a): Normalized Charpy V-notch Energy versus Temperature; Loading Rate = 0.001"/sec; for HSLA-100 Steel

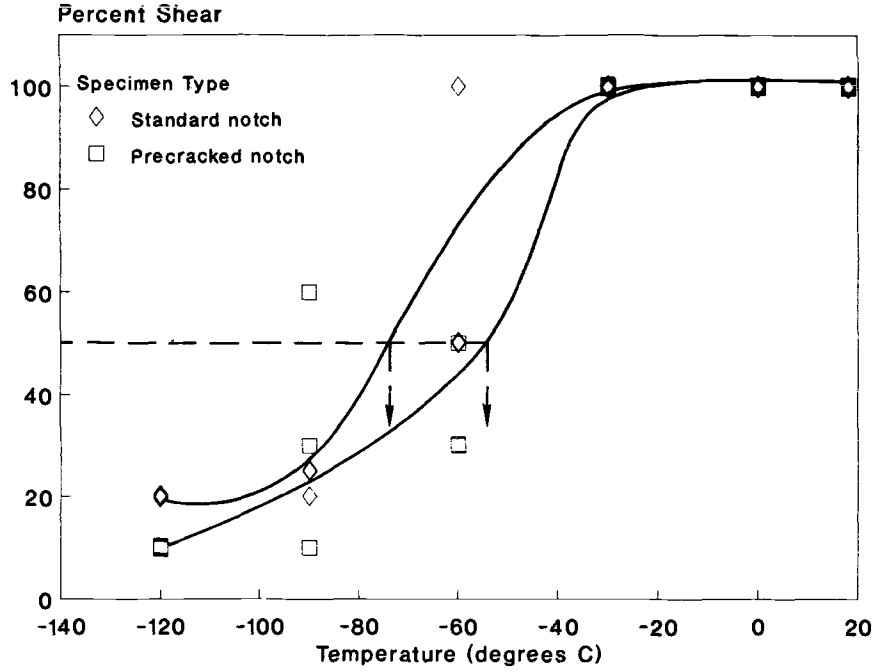

Figure 2(b): Percent Shear in Charpy V-notch Specimens versus Temperature; Loading Rate = 0.001"/sec; for HSLA-100 Steel

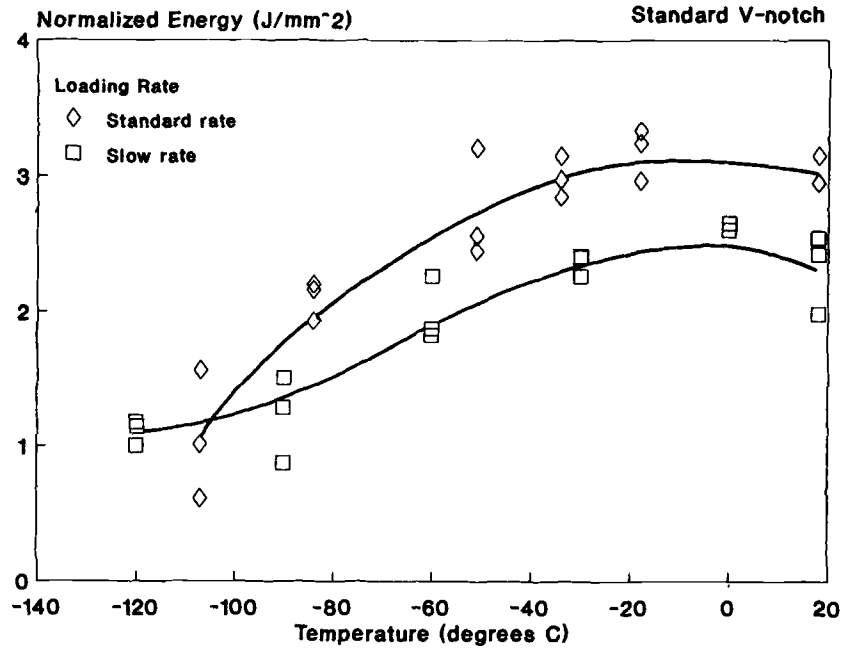

Figure 3(a): Normalized Charpy V-notch Energy versus Temperature; Standard V-notch; for HSLA-100 Steel

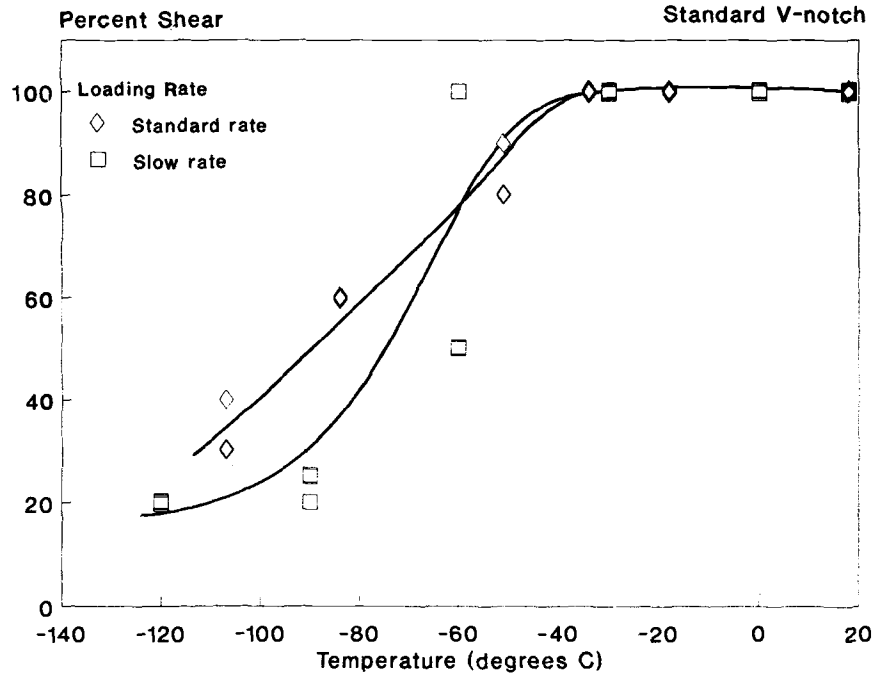

Figure 3(b): Percent Shear in Charpy V-notch Specimens versus Temperature; Standard V-notch; for HSLA-100 Steel

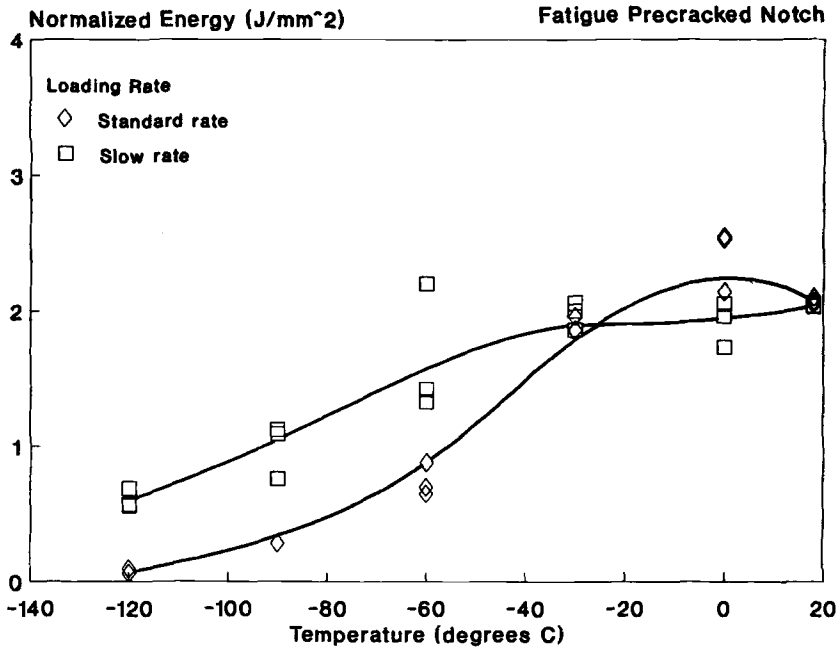

Figure 4(a): Normalized Charpy V-notch Energy versus Temperature; Fatigue Precracked Notch; for HSLA-100 Steel

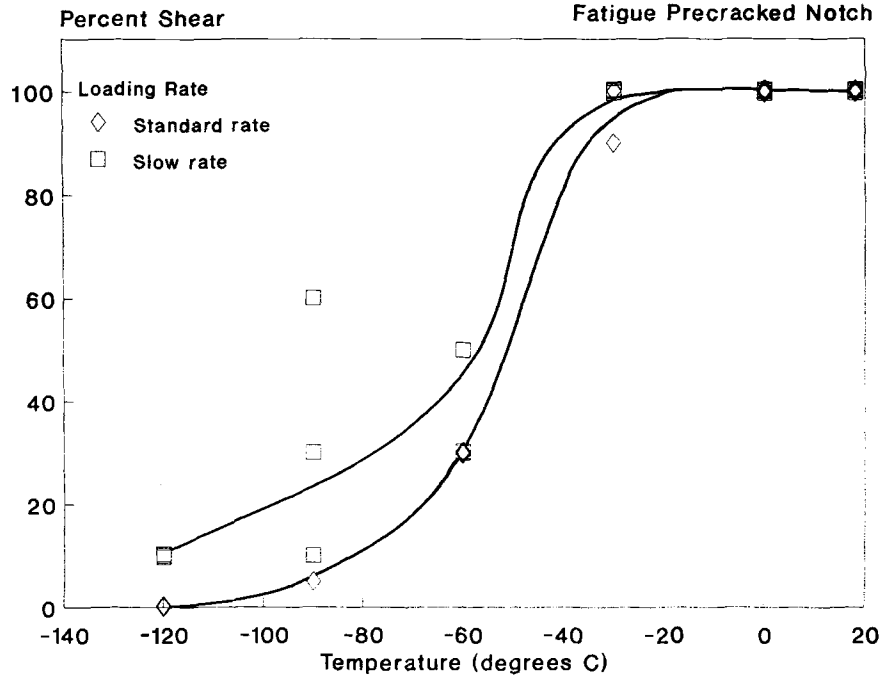

Figure 4(b): Percent Shear in Charpy V-notch Specimens versus Temperature; Fatigue Precracked Notch; for HSLA-100 Steel

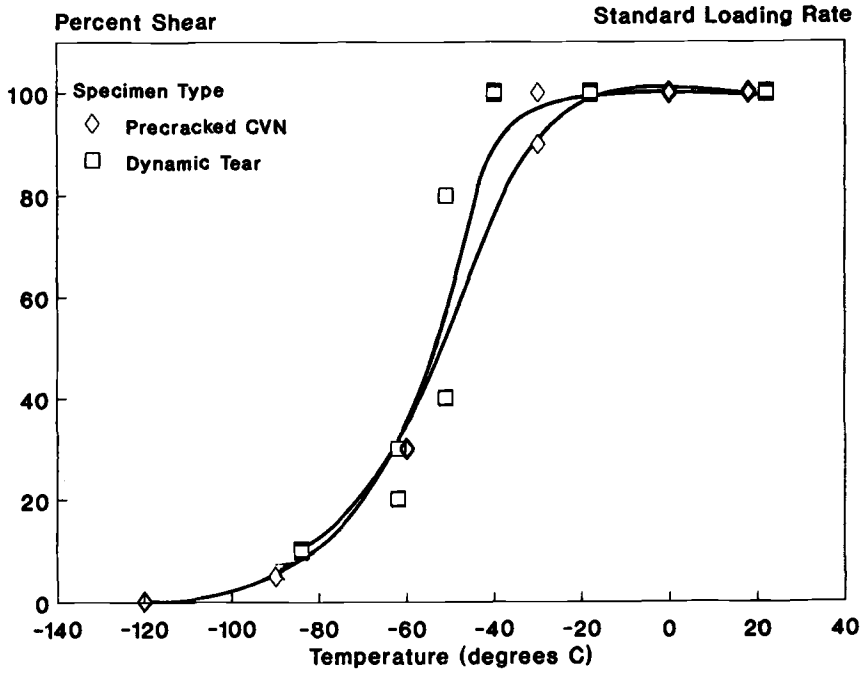

Figure 5: Percent Shear in Precracked Charpy V-notch and Dynamic Tear Specimens versus Temperature; Standard Loading Rate; for HSLA-100 Steel

Charles G. Interrante and James J. Filliben

SIGNIFICANCE OF PRECRACKING VARIABLES FOR SLOW-BEND CHARPY TESTS

REFERENCE: Interrante, C. G. and Filliben, J. J., "Significance of Precracking Variables for Slow-Bend Charpy Tests," Charpy Impact Test: Factors and Variables, ASTM STP 1072, John M. Holt, editor, American Society for Testing Materials, Philadelphia, 1990.

ABSTRACT: The significance of four variables in the technique used to precrack Charpy specimens of metallic materials is determined by analyses of seven responses computed from results of slow-bend tests. The variables include crack size, stress-intensity factor at the start of precracking, notch preparation prior to precracking, and material. All four variables are shown here to be significant for more than one of the computed responses. Seven response parameters, each representing alternative methods for evaluations of fracture toughness, were evaluated for each test. Responses are based either on a single value of load or energy absorbed in the test. The results indicate that (1) all seven computed responses are linearly related to crack length and the sensitivity to crack length is a function of both response parameter and material, and (2) precracking at either very high or very low levels of stress-intensity factor, K_f, are to be avoided. This work is the result of a study conducted by ASTM Task Group E-24.03.03 and members of eight participating laboratories.

KEYWORDS: aluminum; Charpy; crack size; fatigue precracking; fracture toughness; K_f maximum; Kruskal-Wallis test; linear regression; notch preparation; precracking; statistical tests; steel; stress-intensity factor; titanium

List of Symbols

A - Area of uncracked ligament at start of test: $A=B(W-\bar{a})$

A, Aluminum - Aluminum alloy 2419-T851 in the aged condition.

Dr. Interrante is currently a Senior Metallurgist with the U.S. Nuclear Regulatory Commission, Washington, DC 20555 and Dr. Filliben is a Statistician in the Mathematical Analysis Division at the National Institute of Standards and Technology, Gaithersburg, MD 20899, where this paper was produced.

a_{25} - Crack length at one quarter-thickness location
a_{50} - Crack length measured at mid-thickness location
a_{75} - Crack length measured at the other quarter-thickness location
$\bar{a}$ - $(a_{25} + a_{50} + a_{75})/3$ = crack-size factor
$\bar{a}/W$ - Normalized crack size
B - Specimen thickness = 10 mm (0.394 in)
β - A coefficient that is a result of a regression analysis
CVN - Charpy V-notch (test specimen)
CPS - Cumulative probability statistic
C(T) - Compact specimen loaded in tension
C - Experimental determination of total elastic compliance of specimen (=D1/P1)
C_m - Machine compliance
C_s - Theoretical, elastic specimen compliance
D1 - Displacement to an arbitrary point "1" in the elastic region
δ - Displacement
E - Young's modulus
E_c - Energy correction based on specimen compliance and crack length
EDM - Electric discharge machining
E_M - Energy to maximum load, under the load-displacement trace
E_T - Total energy under the load-displacement trace
E_T/A - Total energy divided by area of uncracked ligament
E'_M - Corrected energy to maximum load EM = E'_M - E_c
K - Stress-intensity factor
K^*_d - A response, computed from P* and Y*, termed lower-bound or equivalent energy (EE)
K_f - Stress-intensity factor in fatigue precracking
K_f maximum - K_f at the start of precracking in a constant-deflection apparatus
K_f ratio - K_f maximum/K smallest
K smallest - The smallest value of K computed from equations 1, 2, and 3 of this report
K_{Ic} - Reference values of fracture toughness obtained from CTS tests, whether valid (E 399) K_{Ic} or invalid K_Q
K_J - A response computed from energy to maximum load
K'_J - Response K_J corrected for machine compliance of specimen
K_Q - A response computed using P_Q as in ASTM Method E 399
K_{Q-PM} - A response computed as for K_Q except P_M is used in place of P_Q
K'_Q - A response computed from total energy absorbed in fracture
μ - Poisson's ratio
N - The number of observations
ν - Residual degrees of freedom
MLR - Multiple linear regression
NP - Notch preparation
N/A - Not applicable
%RD of K - Percent relative deviation = $(K - K_{Ic}) \times 100/K_{Ic}$
%RD of R_{sb} Percent relative deviation = $(R_{sb} - R_{sb}) \times 100/R_{sb}$

Pl	-	Load to an arbitrary point "l" in the elastic region
P_M	-	Maximum load
P_Q	-	Load at the 5-percent secant intercept
P*	-	A value of load used to compute equivalent energy
RSD	-	Residual Standard Deviation
R_{sb}	-	Specimen strength ratio in slow-bend testing
$\bar{R}_{sb}$	-	Mean R_{sb} for each material
S, Steel	-	Steel alloy AL MAR (200) in the maraged condition
S_y	-	Significant differences based on magnitude of test responses
S_s	-	Significant differences based on reproducibility of test responses.
s	-	Standard deviation for replicate responses
s_p	-	Standard deviation pooled for all responses of a material
σ_U	-	Ultimate tensile strength
σ_Y	-	Yield strength
σ_{Y1}	-	σ_Y at the precracking temperature
σ_{Y2}	-	σ_Y at the Charpy test temperature
T, Titanium	-	Titanium alloy Ti-6Al-4V in the annealed condition
W	-	Specimen width = 10.0 mm (0.394 in)
$\bar{Y}$	-	Mean response
Y*	-	A function of a/W used to compute K_d^*
y_i	-	An individual test response

1. Background

A proposal for standardization of a precracked Charpy impact test was made by the Executive Committee of ASTM Committee E24, in January of 1971. Task Group E24.03.03 was formed to deal with this problem. The task group drafted a preliminary document titled "Proposed Method for Precrack Charpy Impact and Slow-Bend Testing of Metallic Materials," which required experimental work to determine the significance of variables in the fatigue precracking procedures prescribed in the proposed method. The "best procedures" for fatigue precracking had to be established. Further, the expected variability of test results had to be determined for a multiplicity of laboratories using a prescribed best method.

At the request of the Chairman of Task Group E24.03.03, the authors, from the National Institute of Standards and Technology (NIST), formerly the National Bureau of Standards (NBS), furnished a proposed statistically designed experiment for determining the significance of four precracking variables on results of tests conducted with fatigue precracked Charpy specimens. This proposal included three levels for each of the four variables (here called factors). The factors and their levels were later modified at meetings of the Task Group before test specimens were prepared. In addition, the proposal specified two methods of testing, slow-bend and impact; together, these proposed tests comprised what the Task Group called Phase I of their testing program.

This is an analysis of the results of the slow-bend tests conducted for Phase I. At the time that this work was being planned, a report published by the National Materials Advisory Board [1] recommended... "that the fatigue-precracked Charpy-size specimen,

tested in slow bending to measure the ratio of specimen strength to either the yield strength or the ultimate tensile strength of the material (ASTM E 399) be utilized, when applicable, for establishing correlation with plane-strain fracture toughness and minimum acceptance standards in quality-control programs. To foster implementation of this recommendation, the Committee urges that the test method be standardized as soon as practicable..." The Phase I test program was distinguished from other extensive research programs [2,3][1] that have used precracked Charpy specimens, as the objective of this program was to establish the effects of precracking variables. The proposed Phase II effort was to be conducted by many laboratories to establish a lab-to-lab variability for precracked Charpy test results.

Charpy test specimens used in this program differ from the standard ASTM E 23 type A, V-notch Charpy specimen: (1) Charpy specimens for this program contain a fatigue precrack; in this respect they are similar to valid plane-strain fracture toughness specimens (ASTM E 399), while the standard Charpy specimen is not precracked; and (2) the standard V-notch root-radius of 0.25 mm (0.010 in) is here modified in various ways, as shown below, to facilitate crack initiation under fatigue loading.

TABLE 1 -- Three Notch Preparation Used Before Precracking

Machined Root Radius (mm)	(in)	Notch Preparation Code	Special Preparation	Final Root Radius
.250	.010	1	razor scratch	~ .05 mm (.002 in)
.125	.005	2	none	.125 mm (.005 in)
.250	.010	3	EDM with razor electrode	~ .05 mm (.002 in)

2. Test Matrix

In the proposed Phase I program, each of three materials are designated to be tested after being precracked in the various ways specified in the proposed test matrix. These specified precracking variables are notch preparation (NP), stress-intensity factor at the start of precracking (K_f maximum), and crack size ($\bar{a}$). Each precracking variable is controlled at three levels, which are coded 1, 2, and 3 in the proposed matrix. Thus, there are a total of four factors and three levels per factor in the experimental design. In addition, replicate specimens were specified for each test condition in the proposed text matrix. The actual numbers of specimens tested at each condition, given in Table 2 to be discussed later, differ slightly from the proposed 2 replicate tests per condition.

2.1 Materials

Three materials included in the Phase I program are an aluminum

[1]Figures in brackets indicate the literature references at the end of this paper.

TABLE 2 -- Actual Numbers of Tests Conducted for Each Level of the Factors and for Each Material.

K_f* code	NP code	$\bar{a}$ code = 1			$\bar{a}$ code = 2			$\bar{a}$ code = 3			Sum for all $\bar{a}$ levels			
		0.097"<$\bar{a}$<0.140			0.140<$\bar{a}$<0.180			0.180<$\bar{a}$<0.242			All	Ti**		
		Al	Ti	Steel	Al	Ti	Steel	Al	Ti	Steel	Al	Ti**	RTL	Steel
1	1	1	0	1	1	2	2	0	1	3	2	3	3	6
	2	1	2	2	0	1	2	1	1	2	2	4	4	6
	3	1	1	2	2	2	2	0	0	2	3	3	3	6
2	1	2	2	2	2	2	1	2	2	3	6	6	6	6
	2	2	2	1	2	2	1	2	2	2	6	6	6	4
	3	2	3	2	1	1	2	3	2	2	6	6	6	6
3	1	2	2	1	2	1	3	2	1	1	6	4	0	5
	2	2	3	2	2	2	2	2	1	2	6	6	0	6
	3	2	4	2	1	0	2	3	2	2	6	6	0	6
								TOTALS			43	44	28	51

* See Table 7 for codes used in computer analysis.

**Data used in the analyses for Titanium include R, T, and L specimens and exclude all Charpy specimens prepared from a CTS specimen that was designated W. See Table 3 for definitions of R, T, L, and W.

alloy (2419-T851) in the aged condition [4], a titanium alloy (Ti-6Al-4V) in the annealed condition, and an 18 NiCoMo steel [AL MAR 18 (200)] in the maraged condition. These materials are referred to here as aluminum, titanium, and steel, and they are coded 4, 5, and 6, respectively, for purposes of computer sorting and analysis and for presentations made in the Appendices. They are also coded A, T, and S in some data plots. Some mechanical properties of the materials are given in Table 3. Properties listed in Table 3 are those used for calculations made in the preparation of this report, after the completion of all slow-bend tests.

Reference values of fracture toughness for these materials were furnished from tests conducted with the Compact Specimen loaded in tension, C(T). The results of these tests, given in Table 3, indicate that not all test results meet the validity requirements of E 399. The tests were conducted in accordance with ASTM Method E 399-74 [5]; and according to the Method, the results are either valid and are referred to as K_{Ic} plane-strain fracture toughness, or they are not valid and are referred to as K_Q. Table 3 gives the particular requirement that was not met for each test that failed the E 399 validity requirements. For simplicity in this writing, these reference values of K will be referred to as K_{Ic} values, even though some of the results are actually termed K_Q test results by Method E 399. In this report, these reference values are used to assess the accuracy of the various responses (K values) computed from results of Charpy tests.

Specimens used for the reference values of K_{Ic} were used for machining of the Charpy specimens tested under this program, except for the aluminum Charpy specimens, which were taken from the same cast as the plate used to prepare the compact specimens [6]. For aluminum, the two reference K_{Ic} values given in Table 3 for the C(T) tests are averaged to obtain a single reference for all aluminum Charpy specimens. For titanium, the C(T) test results represent two specimen orientations, longitudinal (LT) with values of 77.9 and 80.2 ksi $(in)^{\frac{1}{2}}$, which are designated R and L respectively (see Table 3), and transverse (TL) with values of 77.4 and 85.5, which are designated W and T respectively. In the analyses presented here, the reference for each Charpy specimen of titanium is the K_{Ic} result of its parent C(T), i.e., the specimen from which the Charpy specimens were machined. For steel, three C(T) test results are averaged to obtain a single reference value of 120.5 ksi $(in)^{\frac{1}{2}}$ for steel Charpy specimens.

2.2 Laboratory Variabilities

Various task were undertaken by each of eight laboratories that participated in the Phase I program [6]. One objective of this program was to conduct the Charpy tests as though only a single laboratory had done the work. In keeping with this objective, only one laboratory can be involved for each step of the procedures of preparation and testing of specimens, and analysis of the data, except for those steps for which ASTM prescribed methods are applicable. In practice, this objective was largely met even though some discrepancies did arise [6] as described in Section 2.4. Other procedures with potential for giving rise to undesirable lab-to-lab procedural effects were generally controlled closely enough so that

TABLE 3 -- Mechanical Properties and Results of Tests of Compact Tension Specimens C(T) Tested by Method ASTM E 399

Material and Orientation	σ_Y (ksi)	σ_U (ksi)	Plot characters	CTS Fracture Toughness K_{Ic} or K_Q (ksi(in)$^{1/2}$)	CTS Thickness (in)	$2.5(K_{Ic}/\sigma_Y)^2$ E-399 Minimum Thickness Requirement	Handbook Properties Elastic Mod. E x10^6 (psi)	Handbook Properties Poisson's Ratio
4 Al, aged----------			A					
Al-2419-T851						1.43		
Longitudinal	52	67		39.3[a], 38.4[b]	1.500	1.36	10.5	.33
Ti, annealed----------			T					
Ti-6Al-4V								
Longitudinal	112	125	R≡77.9 L≡80.2		1.375	1.28	16.2	.30
Transverse	120	128	W≡77.4[c] T≡85.5		1.375	1.26	16.2	.30
S, maraged----------			S					
AL MAR 18 (200)								
Transverse	203	223		120.5[d] ave. of 3 tests	0.750[d]	.875	30.0	.33

*Fails: E-399 requires $P_M/P_Q < 1.1$.
Departures from E-399 Requirements: (a) $P_M/P_Q = 1.12$.* (b) $P_M/P_Q = 1.14$.* (c) $P_M/P_Q = 1.54$* (These specimens were eliminated from this analysis).
(d) Fails thickness requirement -- computed K from Charpy specimens of this material were generally greater than K_{Ic} indicated by this test result.

they are considered to have had no significant effects on the test results.

2.3 Notch-Preparation Factor

The notch-preparation (NP) factor in the experimental design has three levels, as shown in Table 1, which are coded 1, 2, and 3 for purposes of computer sorting and analysis of the data.

2.4 Stress-Intensity Factor at Start of Precracking

The stress-intensity factor at the start of precracking (K_f maximum) was controlled at three levels for each material in the proposed test matrix. The three levels are dependent upon properties of the materials, as described below. To compute the proposed levels, first a stress-intensity-factor parameter here called "K smallest" is computed by using three formulae:

$$K_{(1)} = (\sigma_{Y1}/\sigma_{Y2}) \times K_{Ic} \text{ (ksi (in)}^{\frac{1}{2}}\text{)} \quad (1)$$

$$K_{(2)} = 0.002 \times E \text{ (ksi (in)}^{\frac{1}{2}}\text{)} \quad (2)$$

and

$$K_{(3)} = 0.57\ \sigma_{Y1} \text{ (ksi (in)}^{\frac{1}{2}}\text{)}, \quad (3)$$

where σ_{Y1} and σ_{Y2}, which are equal in this case, are static yield stress in ksi at the precracking temperature and at the Charpy slow-bend test temperature, respectively, and E is the elastic modulus in psi. The smallest of these calculated K values is called K smallest. Then, loads at the start of precracking are computed to give the following proposed values of K_f maximum (the value at the start of precracking in a constant-deflection machine): K smallest, (2/3)K smallest, and (1/3)K smallest. These K_f maximum values are coded 3, 2, and 1, respectively, for purposes of computer sorting and analysis of data within each material. This is shown in Table 4 which gives the fatigue precracking levels, and their codes used for sorting and analysis of data within a material. While three levels (coded 3, 2, and 1) are indicated (in the table) for analyses within each material, a total of 4 levels are indicated for combined materials: aluminum and steel have levels 3, 2, and 1, and titanium has levels 2, 1, and 0. This coding became necessary for combined results because the actual K_f maximum levels used for titanium are different from (lower than) the proposed K_f maximum levels. The highest actual level for titanium is 20 ksi(in)$^{\frac{1}{2}}$, which is nearly equal to (2/3)K smallest, the proposed code 2; the next actual level for titanium is nearly equal to (1/3)K smallest, which is the proposed code 1; and the lowest actual level for titanium is much lower than any other levels used in these tests. Thus, for combined materials, the analysis requires four levels, coded 3, 2, 1, and 0.

Further, as noted in Table 4, for steel each of the three actual levels covers a range that is, in general, slightly higher than the proposed level. In addition, for steel specimens, K_f maximum was measured at the finish of precracking, whereas levels of K_f maximum for aluminum and titanium were measured at the start of precracking.

TABLE 4 -- Fatigue Precracking Levels, and Their Codes for Purposes of Data Analysis

Material Code	Calculated	Proposed		Actual		Codes for Computer	
	$K_{smallest}$[1] (ksi $(in)^{1/2}$)	K_f maximum (ksi $(in)^{1/2}$)	K_f Ratio[2]	K_f maximum (ksi $(in)^{1/2}$)	K_f Ratio[2]	Within a material	For combined materials
Aluminum, 4	20						
Level 3		20.0	1.00	20.0	1.0	3	3
Level 2		13.3	0.67	13.3	0.67	2	2
Level 1		6.67	0.33	6.7	0.33	1	1
Titanium, 5	33						
Level 3		33.0	1.00	20.0	0.61	3	2
Level 2		22.0	0.67	13.3	0.40	2	1
Level 1		11.0	0.33	6.7	0.20	1	0
Steel, 6	60						
Level 3		60.0	1.00	(>55 to 77)*	(>0.91-1.3)**	3	3
Level 2		40.0	0.67	(>35 to 55)	(>0.58-0.91)**	2	2
Level 1		20.0	0.33	(20 to 55	(0.33-0.58)**	1	1

[1]See Eq. 1, 2, 3.

[2]$K_f \text{ Ratio} = \frac{K_f \text{ maximum}}{K_{smallest}}$.

*This means that "actual K_f maximum" values in the range from greater than 55 to 70 are included in level 3.

**These represent values at the finish of precracking. K_f at the start would be slightly greater.

In the precracking machines used for this Phase I program, K decreases slightly as crack length increases, so that K_f at the finish of precracking is slightly lower than that at the start. Thus, for a short crack length, K_f at the start of precracking would be slightly greater than K_f "maximum" tabulated for the steel; and for longer cracks, K_f maximum at the start of precracking is greater still. Thus, actual K_f maximum levels for each material represent different fractions of the K smallest computed for the proposed levels. These fractions are called the K_f ratio and they are greatest for the steel specimens and least for the titanium specimens, and they are grouped into 3 levels for each material and into 4 levels for combined materials.

2.5 Crack-Size Factor

The test matrix gives three levels for the crack-size factor ($\bar{a}$) used in calculations. These levels of $\bar{a}$ are coded as follows:

Code 1: $\bar{a}$ = 2.5 to 3.6 mm (0.097 to 0.140 in)
Code 2: $\bar{a}$ = 3.6 to 4.6 mm (0.1405 to 0.180 in)
Code 3: $\bar{a}$ = 4.6 to 6.1 mm (0.1805 to 0.242 in)

The lower bound for Code 1 was established as follows. After testing had been completed, it was observed that a crack was never initiated in some specimens fatigue cycled at the lowest level of K_f maximum; further, during a preliminary screening of the data, results for specimens with $\bar{a}$ less than 2.48 mm (0.097 in) were found to be more highly variable and in this respect inconsistent with the data for specimens with $\bar{a}$ between 2.48 and 6.15 mm (0.097 and 0.242 in). Data for specimens below this limit are not included here. No upper limit was warranted for $\bar{a}$ values to be included in this analysis.

2.6 Actual Number of Tests Conducted

The actual number of tests conducted for each test condition is given in Table 2. Difficulties encountered in the process of precracking at the lowest levels of the stress-intensity factor, K_f, are responsible for the differences between the proposed and actual number of test specimens tested. Deficiencies in the numbers of tests for each of these materials are mainly in the K_f code 1 level, and the analysis of the results for K_f code 1 are adversely affected by these deficiencies.

3. Test Procedures

Precracked Charpy specimens were tested in three-point bend tests, using a bend test fixture with the geometry and dimensions recommended in ASTM Designation E 23-72 for Charpy impact testing. No movable support pins are used in this fixture, which uses two anvil blocks to provide support at a fixed span. The cross-head speed was 2.5 mm/min (0.10 in/min). Load and displacement were measured and plotted. The load was taken from the load cell of the test machine and the displacement was measured using a transducer (LVDT) placed between the top and bottom plates of the bend test fixture. Load P, displacement δ, and energy absorption E (area under the P-δ plot) were measured using a digitizer to trace along the P-δ plot of

the test record. From the raw data, various fracture-toughness test responses were computed. These responses are here designated K'_Q, K_{Q-PM}, K_Q, K'_J, K_J, K^*_d, and R_{sb}, and are computed by methods described here, in section 4. As is shown in Figure 1, each response is based on one of three principal measurements, total energy (E_T), energy to maximum load (E_M or E'_M) or a single value of load (P_M or P_Q).

To compute the response K'_Q, the total energy E_T (Fig. 1A) is measured. To compute the responses K_J, K'_J, and K^*_d (Fig. 1B), several measurements were taken: maximum load P_M, compliance D1/P1, and energy to maximum load, E_M. The responses R_{sb}, KQ_{-PM}, and K_Q (Fig. 1C) require measurement of either the load P_M, or the load P_Q measured by the 5-percent-secant method, as described in Method E 399.

For all aluminum and titanium specimens, and for most steel specimens, the load-displacement plots were observed to be of the type (general shape) shown in Figure 1A, in which there is no indication of a cleavage initiation event. For some steel specimens the plots were bimodal, indicating a cleavage fracture with rapid machine unloading. During the unloading of the first mode of the bimodal type, the energy of the test machine is released to the specimen and it was not recorded on the test record. Thus, while the area under each of the two modes is included in the measurement of E_T, this energy of unloading, which contributes to the fracture process, is not included in this measured value. The bimodal load-displacement plot is observed only for steel specimens with crack size less than 3.56 mm (0.140 in), i.e. small crack lengths. The E_T values used in this analysis were not corrected to take machine unloading into account; as the analysis had been nearly completed when this was discovered, time constraints precluded this correction.

4. Calculation of Response from Charpy Test Results

Raw data taken in precracked slow-bend Charpy tests are not directly used to assess material properties. Rather, data are converted to responses of fracture toughness, designated by the symbol K, or specimen strength ratio, R_{sb}. These responses are calculated by various methods given below. The computed K and R_{sb} results for all specimens included in this analysis are given elsewhere [6].

Relationships used to compute responses of K are as follow:

$$K_Q = (P_Q S/B\ W^{3/2})\ f(a/W), \qquad (4)$$

where S = 1.574 and

$$f(a/W) = \frac{3(a/W)^{\frac{1}{2}}\ [1.99-(\bar{a}/W)(1-\bar{a}/W(2.15-3.93\ \bar{a}/W\ 2.7\ \bar{a}^2/W^2)]}{2(1+2\bar{a}/W)(1-\bar{a}/W)^{3/2}}$$

after ASTM Method E 399 [5].

$$K_{Q-PM} = (P_M S/B\ w3/2)\ f(a/W), \qquad (5)$$

which is the same as the equation for K but maximum load P_M, rather than P_Q, is used;

$$K'_Q = [0.5\ E\ E_T/A\ (I-\mu^2)]^{\frac{1}{2}}, \text{ after Ronald [7]}, \quad (6)$$

$$K_J = [2\ E\ E_M/A\ (1-\mu_2)]^{\frac{1}{2}} \text{ after Rice [8]}, \quad (7)$$

$$K'_J = [2\ E\ E'_M\ /A(1-\mu^2)]^{\frac{1}{2}}, \text{ after Rice [8]}, \quad (8)$$

Figure 1A

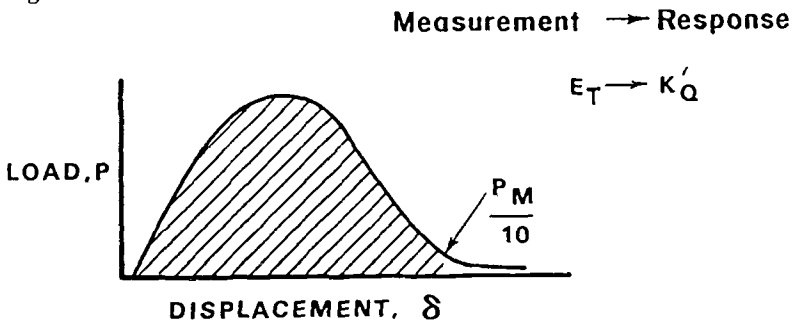

Figure 1B

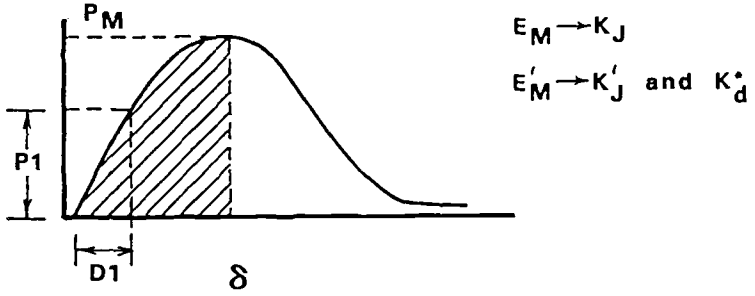

Figure 1C

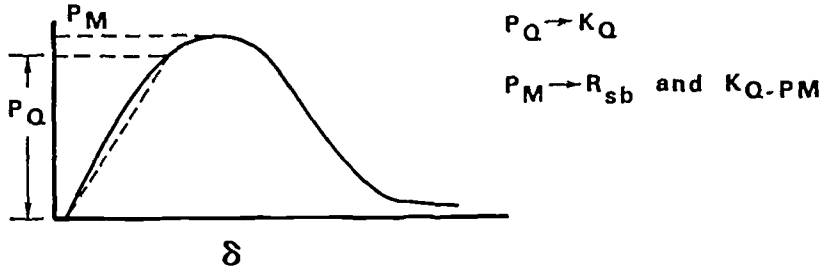

Figure 1. Fracture toughness responses and the principal measurements used to compute them.

where E'_M is E_M corrected for the compliance of the test machine: $E'_M = E_M - P_M^2 C_m/2$; where C_m is machine compliance, after EPRI procedures [9,10]; $C_m = C - C_s$. The C and C_s, respectively, representing experimental and specimen (theoretical) compliance values. Measured values of C are given as D1/P1 elsewhere [6].

$$K_d^* = \frac{6\ Y^*\ (a)^{\frac{1}{2}}\ P^*}{B\ W}, \tag{9}$$

where

$$Y^* = 1.93-3.07(\bar{a}/W) + 14.53(\bar{a}/W)^2 - 25(a/W)^3 + 25.8(a/W)^4$$

$$P^* = [2\ E'_M\ /C_s]^{\frac{1}{2}}.$$

It is noted that K_d^* can also be computed using P* in place of P_Q in Equation 4. The lower-bound (or equivalent-energy) procedure (K_d^*) arises from concepts developed by Witt [11].

Responses of strength ratio in slow-bend testing, R_{sb} were computed using the equation

$$R_{sb} = 6\ P_M\ W\ /B\ (W-\bar{a})^2\sigma_Y, \tag{10}$$

after Method E 399 [5].

5. Statistical Tests

Responses computed using equations (4) through (10) are used here to determine statistically whether or not the level for each of the four factors significantly affects the test result. The accuracy of a Charpy test response is assessed, as described in Section 5.1.3 for each of the various fracture toughness measures of having the symbol K. This is done using an appropriate reference value of K_{Ic} for each material. The reproducibility is assessed, as described in Section 5.1.2, using replicate responses.

The controlled variables, called factors in this analysis, are notch preparation (NP), fatigue-load at the start of precracking (K_f maximum), and original crack size ($\bar{a}$) and material. The goals of this experiment do not include between material differences. Material-to-material differences are known to exist and in this analysis this variable is not considered as a factor in the analysis. In the proposed test matrix, each factor is tested at three levels only; however, for the factors $\bar{a}$ and K_f maximum, many more than three levels were actually tested. A variety of analytical methods are used here to determine whether or not statistically significant difference exists among the levels of a factor. These include (1) the Kruskal-Wallis (KW) test, (2) multiple linear regression (MLR) analysis, and (3) graphical analysis of variance. The results of both the KW test and the MLR analysis is a Cumulative Probability Value (CPV) which corresponds to a percent point of the null distribution. The two tests are not identical and were run because they are sensitive to different aspects of the same problem [6]. To determine whether a

factor is significant, the MLR analysis is conducted using the individual responses. The KW test used ranks of these responses and each factor is subdivided into three levels to test whether the levels are significant. These differences are expected to give rise to differences in the CPV results for the two tests. In this analysis, when either of these tests indicates a factor or its levels to be significant, then graphical analysis is used to further describe the effect.

5.1 Kruskal-Wallis Test

One procedure used here to carry out the test of significance is based on the Kruskal-Wallis [12] test statistic, H. Calculated values of H which fall out in the extreme regions of the null distribution are deemed to be indicative of a false null hypothesis--thus, the levels within a factor are concluded to be significantly different. Associated with any given value of the Kruskal-Wallis test statistic, H, is a cumulative probability value (CPV). If the null hypothesis H_o is true, one would expect CPVs generally between 0.0 and 0.90. If H_o is false, one would hope to obtain CPVs larger than 0.90. In the present analysis, all cases with CPV > 0.90 will be discussed and the values are expressed in percentage points (i.e., 90 percent rather than 0.90). This CPV is reported here as the result of a test for the equality of the levels within a factor. The CPV is rather simply related to the probability of erroneously concluding that the difference between levels is significant.

5.1.1 Significance -- For each factor, it is of interest to test whether the various levels of that factor give the same result or a significantly different result. If the different levels do not (within random error) give the same value, the factor is said to be statistically significant. In this report, a test of significance is applied independently to data sets representing each of the materials tested and to data representing all materials (of Phase I) combined into a single set. The result of the test of significance is a determination of whether the levels of a factor are significantly different.

The parameters used to conduct the KW statistical test are the standard deviation for replicate responses, s, the individual test responses, y_i, and the mean response, Y. Responses derived from these three parameters are the specimen strength ratio R_{sb} and the percent relative deviation (%RD) which is computed relative to the reference K_{Ic} value given for each material, as described below. The %RD values are given for each of several measures of fracture toughness (Section 4) designated K'_Q, K_{Q-PM}, K_Q, K'_J, K_J, and K^*_d.

When the test of significance indicates that significant differences exist among the responses for the various levels of a factor, the question becomes which level is best. For the responses given above, low values of s and |%RD| indicate, respectively, better reproducibility and more accuracy. Thus, they are considered better than high values of s and |%RD|; therefore, the best level can be determined for computed responses of K by selection of the level with the lowest values of either s or |%RD|. However, for the computed values of specimen strength ratio, R_{sb}, the best level can be

determined only from the reproducibility parameter s, because no reference values of R_{sb} (from which to make a determination of accuracy) are available for this analysis. Hence, for R_{sb} responses, the parameters y_i and Y are used only to determine of the significance of differences (in the R_{sb} responses) among the levels of each factor, and the question as to which level is most accurate cannot be addressed without reference values of R_{sb}.

5.1.2 Reproducibility -- Reproducibility of the test results is estimated from replicate responses. Let y_i denote the individual response for a group of replicate specimens. A mean response, Y, and a standard deviation, s, are computed for each set of replicates in accordance with the following formulae:

$$\bar{Y} = \sum_{1}^{N} (y_i)/N, \tag{11}$$

and

$$s = [\sum_{1}^{N} (y_i - \bar{Y})^2/(N-1)]^{\frac{1}{2}} \tag{12}$$

where N = the number of responses in the group (see Table 2). For the test of significance, a CPV is computed from a data set for each factor. The set includes the standard deviation, s, responses and their corresponding levels for one of the factors.

In this way, reproducibility evaluations are made for each material and for data combined for more than one material. The response parameter in each case is the value of s, converted to rank within a material. For combined data, this same rank (of s within a material) is the response parameter. The variance of data for each material to be combined is different, i.e. the pooled s for all responses of a material differ for the various materials evaluated. In the test of significance, each s response is assigned a rank that depends performance within one of the materials, so that the effects of differences among the variances of the three materials are effectively eliminated, when the CPV is computed.

5.1.3 Accuracy -- The test of significance is an estimate of the accuracy of the responses for each level of a factor whenever the CPV is obtained from computed estimates of K for which reference K_{Ic} values are available. The estimator of accuracy used here is called the percent relative deviation (%RD). This estimator of accuracy is based upon the difference between a value of fracture toughness, K, computed by one of the described methods (Section 4) used for precracked Charpy specimens, and the reference value (K_{Ic}) computed in accordance with ASTM Method E 399 [5] for large compact tension specimens. The %RD is this difference expressed as a percentage of K_{Ic}, or (as was noted earlier) of K_Q that is here called K_{Ic} for simplicity. The %RD has an advantage in studies of this type. It can sometimes be used as a measure of the accuracy of the response. The formula for relative deviation is

$$\%RD = \frac{(K - K_{Ic})}{K_{Ic}} \times 100. \tag{13}$$

The test of significance is conducted independently for each of two response parameters: y_i, the individual response, and Y, the mean response for replicates. This was done so as to assure that the conclusions of the analysis were not dependent on a single approach. This follows a general principle of data analysis which states that perturbations in the analysis should be introduced whenever possible so as to assess the sensitivity of the conclusion to various facets of the analysis.

The accuracy of responses for combined materials is given a test of significance in a manner similar to that described earlier for the reproducibility responses, except that both replicated and nonreplicated responses are included in the data set and two tests of significance are made. The response for one test is the rank of y_i within a material and the response for the other is the rank of Y within a material.

5.2 Multiple Linear Regression

A procedure based on linear regression is used to complement the Kruskal-Wallis analysis. It is important to carry out alternative analyses (such as the regression procedure discussed in this section and the graphical procedure to be discussed in the following section) so as to assure that conclusions are not approach-dependent. Conclusions which do not hold up over all three different approaches would lead one to suspect their validity; alternatively, a consistency of conclusions over the three separate approaches is highly supportive of their validity.

The first step in the regression approach consisted of fitting the response versus $\bar{a}$ as described by the model:

$$y = \beta_0 + \beta_1 \bar{a}. \tag{14}$$

Due to results from the Kruskall-Wallis test, $\bar{a}$ was chosen as the first factor of interest. After this linear fit was performed, the residual standard deviation was computed and noted. A simplest such test is to note whether the slope β_1 is significantly nonzero. A second test is to compare the 1-factor residual standard deviation with the residual standard deviation gotten by fitting the model:

$$y = \beta_0 + e. \tag{15}$$

If a significant reduction has occurred, then $\bar{a}$ is interpreted as being significant. The next step was to augment the 1-factor model to a 2-factor model as follows:

$$y = \beta_0 + \beta_1 \bar{a} + \beta_2 K_f. \tag{16}$$

The K_f factor was chosen again from Kruskall-Wallis test results. The residual standard deviation for this 2-factor model was computed. The appropriate test of significance was then carried out to determine if a significant reduction occurred in the residual standard deviation in going from the 1-factor model to the 2-factor model. Such a significant reduction would be interpreted as the second factor (K_f) being significant. Likewise a final step was to similarly augment the

2-factor model to a 3-factor model:

$$y = \beta_0 + \beta_1 \bar{a} + \beta_2 K_f + \beta_3 NP. \quad (17)$$

As before, the residual standard deviation was computed and compared to the 2-factor residual standard deviation. A significant reduction would imply the significance of the notch preparation factor.

5.3 Graphical Analysis

The graphical approach is a valuable complement to the Kruskall-Wallis and regression procedures. The rationale behind the graphics approach is multifold [6], but one obvious advantage of the graphical approach is that of communication: Whereas the use of the Kruskall-Wallis and regression procedures of the analysis may not be fully understood by some researchers, a properly constructed plot to emphasize the significance of a factor is easily understood by all.

6. Results

The results indicate the following: (1) All seven computed responses are linearly related to crack size and the sensitivity to crack size varies with the choice of response parameter and with material. (2) Precracking at either very high or very low levels of stress-intensity factor, K_f, are to be avoided. (3) For the three methods of notch preparation used in this study, no significant effects (of notch preparation) on the responses were observed, except for razor-scratched steel specimens. This presentation describes results for R_{s_b} in detail and results for various responses of K more succinctly. Results are presented for each of the factors: crack size, K_f maximum, and notch preparation. Finally, the sensitivity to crack size is discussed for the responses. More detailed discussions are available [6].

6.1 Anomalies in the Data

A preliminary analysis of the data indicated that responses computed for test specimens with crack size less than 2.46 mm (0.097 in) should be excluded from the analysis because their variability was greater than that for specimens with larger crack sizes. As the depth of the machined notch is about 2.0 mm, and cut-off establishes a crack-extension of 0.5 mm as a limit below which variability of the response increased greatly.

Anomalies in the data set [6] required that selected specimens be omitted from the analysis, e.g. (1) responses computed using total energy to fracture for steel specimens with the smallest crack-size factor ($\bar{a}$ code 1), (2) the titanium code W specimens, which K_f Code 3 (highest level) were excluded.

While the original experimental design proposed three discreet K_f ratios, a wide range of actual K_f ratios (K_f maximum/K smallest) were used in this test program. This range is illustrated elsewhere [6]. For the steel specimens the three proposed "discreet" levels of the factor K_f maximum at the "start" of precracking--which were used for the aluminum and titanium specimens--were not used; rather, the finish

of precracking was varied over a wide range of ratios from 0.33 to a level of 1.3, which is well above the proposed Code 3 level of 1.0. Thus, the range of stress-intensity ratios used in precracking the three materials was varied (inadvertently) from less than 0.20 to more than 1.3, and the levels for only two of the materials are discrete and are measured at the start of precracking.

6.2 Results of KW Test of Significance for R_{sb} Responses

The CPV results of the KW tests of significance conducted for the R_{sb} responses are presented in Table 5 and described here. Included are the results for aluminum, "all" titanium (including the Code W specimens), titanium (including only the R, T, and L specimens), and steel. In addition, results for the combined materials, aluminum, titanium (R,T,W,&L), and steel are presented. The results related to crack-size factor are discussed later. In summary, these cumulative probability results indicate that the three levels of the factor NP are not significantly different from one another on the basis of either the level of the response, y_i or Y, or the reproducibility of the response, s. Thus it is concluded, on the basis of a distribution-free analysis of variance, that the levels of the factor NP do not significantly affect the R_{sb} response for the materials tested.

The level of the factor K_f maximum is significant for steel and possibly significant for titanium. This conclusion is supported with the CPV (Table 5). For steel, the response parameters y_i and Y are, respectively, 98% and 96%, indicating that the effect on the response R_{sb} is significant at the 5% confidence level. The CPV for the reproducibility parameter s is only 25%; thus, reproducibility of R_{sb} responses for steel is considered to be not affected significantly by the level of the factor K_f maximum.

For titanium, the y_i and Y results clearly indicate that the response is not affected significantly by the level of the factor K_f maximum, but the value of 90% for s is marginal, and required clarification from a more thorough analysis [6]. The results for "all titanium" data, which include W specimens, contradict these conclusions for titanium and this points up the impropriety of the use of the Code W data. Code W data for titanium were excluded from the analyses and findings of this report of the Phase I program.

6.3 Results of KW Test of Significance for All Responses

The results of the KW tests conducted for each of the responses R_{sb}, K_Q', $K_{Q\text{-}PM}$, K_Q, K_J', K_J, and K_d^* are presented in Appendices I to III given for factor K_f maximum, notch preparation factor, and crack-size factor, respectively. Included are data for each of the materials and for the combined materials.

In general, the results of the KW tests of significance for all responses indicate the following:

(1) The level of the crack-size factor (a) is significant for all three materials and for almost every computed response. This is evident from the results of both the individual response parameter y_i

and from the mean response parameter Y.

(2) The level of the stress-intensity factor used in precracking (K_f maximum) is significant for one or more responses for each material, but the significance levels are generally not as high as for the crack-size factor.

(3) The level of the notch preparation factor (NP) is not significant.

(4) For selected cases, the reproducibility parameter (s) is significant for the factors ($\bar{a}$) and K_f maximum, in support (1) and (2) above.

TABLE 5 -- Kruskal-Wallis Test of Significance and Cumulative Probability Values for Response R_{sb}.

Type of Statistic	Response Parameter	N	Matl.	Cumulative Probability NP	Cumulative Probability K_f	Values for a
Single Material						
Individual Responses	y_i	43	Al	68.9	56.9	>99.9
Mean Responses	Y	24	Al	61.2	52.8	99.4
Reproducibility	s	17	Al	51.3	70.7	96.8
Individual Responses	y_i	44	Ti, all	22.5	100.0**	93.4
Mean Responses	Y	24	Ti, all	7.3	>99.9	41.9
Reproducibility	s	16	Ti, all	57.2	94.3	69.8
Individual Responses	y_i	28	T RTL only	57.2	49.89	96.9
Mean Responses	Y	16	T RTL only	25.0	20.9	95.1
Reproducibility	s	11	T RTL only	40.9	89.8	37.2
Individual Responses	y_i	51	S	63.5	98.5	99.9
Mean Responses	Y	27	S	35.5	96.0	99.6
Reproducibility	s	21	S	77.8	25.5	75.5
Combined Materials	Rank* of					
Individual Responses	y_i	122	A,T(all),S	61.3	99.3	100.0**
Mean Responses	Y	67	A,T(all),S	92.7	99.2	>99.9
Reproducibility	s	48	A,T(all),S	53.5	3.5	99.5

$R_{sb} = 6P_mW/B(W-\bar{a})_2\sigma_Y$

*Rank is assigned within the responses for a material.
**>99.9995

Fig. 2A

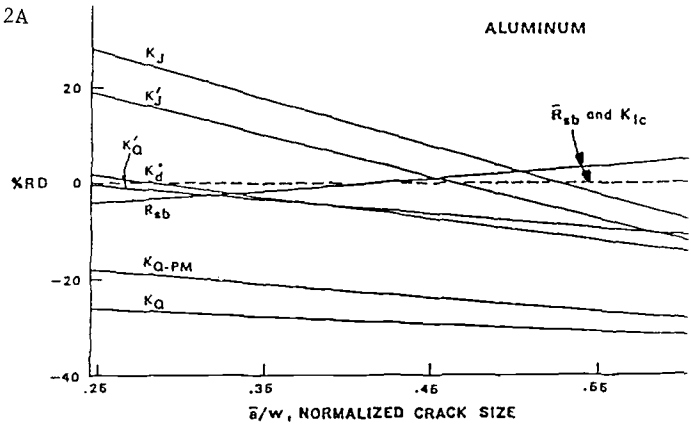

Fig. 2B

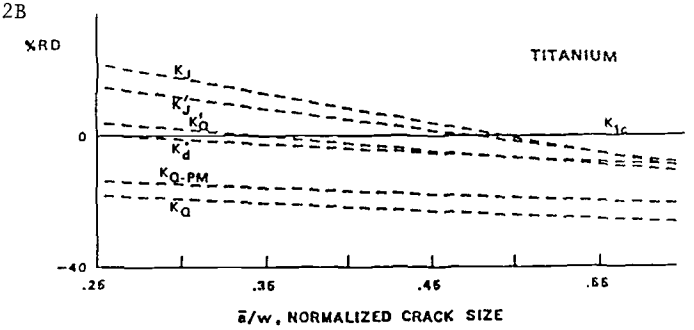

Fig. 2C

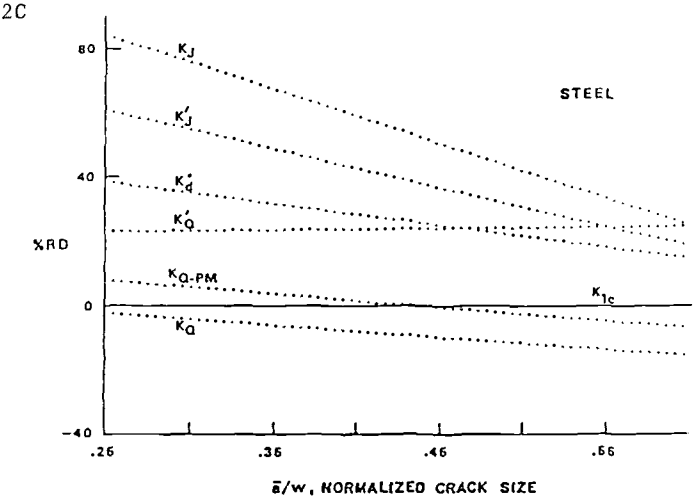

Figure 2. Results of seven regression analyses for aluminum (Fig. 2A), titanium (Fig. 2B), and steel (Fig. 2C) data showing the relationship between percent relative deviation (RD) and normalized crack size ($\bar{a}/W$).

6.4 Effects of Crack Size and Material

Responses are shown to be linearly related to crack size. With increases in normalized crack size, responses of R_{sb} increase and responses of K decrease. The relationship between response and crack size depends on the choice of response parameter and on the material.

The CPV values of the KW test of significance highlight the effect of crack-size factor, $\bar{a}$. For each material, both y_i and Y are significant at the 5-percent level. The predominant effect of crack size on the test responses is illustrated by selected plots presented as Figures 2 and 3. In general, the responses of K (or %RD of K) decrease roughly linearly with increases in normalized crack size and response R_{sb} increases in normalized crack size. The plots and the results of regression analyses [6] both support the conclusion that the slopes and the magnitudes of the responses are functions of the response parameter. In the figures, R_{sb} is the only response with a positive slope. Further, the magnitudes of the responses of K are shown to decrease roughly in the order K_J, K'_J, K^*_d, K'_Q, $K_{Q\text{-}PM}$, and K_Q, but the magnitude and the order are dependent on the material and the crack size. The sensitivity of the response to crack size is a function of both the residual standard deviation (RSD) and the slope (β_1) of these plots and it is discussed elsewhere [6]. Sensitivity of the response to crack size is shown [6] to be a function of the choice of response parameter and of the material with the steel being most sensitive to crack size and the aluminum least sensitive to crack size. In addition, on the basis of the residual standard deviation aluminum is least variable; for six of the seven responses, RSD is smaller for aluminum than for either of the other two materials. The effect of the material is further illustrated in Figure 2 and in Appendix Tables IV and V. From the regression results, given in the figures and in the tables, it is seen that, at any crack length the magnitude of the expected response (%RD of K or R_{sb}) is much greater (and less "accurate" by this measure) for steel than for aluminum or titanium, and this effect is especially marked for all of the K responses. This result opens to question the validity of the reference value of K_{Ic} used for this steel. As was shown earlier among the C(T) results used to obtain K_{Ic} reference values (Table 4), the steel failed to meet the thickness requirement, whereas the aluminum and the titanium both passed this requirement. Hence, this K_{Ic} for steel is unique among the K_{Ic} reference values used in this analysis. Further, Figure 3, shows that the K'_Q data, which are based on total energy, are inaccurate (as discussed earlier) for the code-1 crack sizes. Thus, they were omitted from the calculations.

6.5 Effect of K_f maximum

The results indicate that precracking at levels of K_f maximum outside the range of 0.4 to 0.9 times K smallest is to be avoided, as either the magnitude or the variability of computed responses of K or R_{sb} may be greater than that for responses for specimens precracked within this range. These observed effects of the level of K_f maximum are somewhat dependent on the response parameter and are generally dependent on crack-size factor. While conclusions of this analysis are presumed to be generally applicable to all materials tested, this presumption could not be completely tested for K_f maximum using the

available data. The implications of these findings should be explored for their applicability to recommended precracking procedures for fracture testing, e.g. in Methods E-399 and E-812.

A summary of significant results, for all seven responses and for the three materials, is given in Table 6. A CPV is shown for the F test of the relevant MLR analysis and for each of the relevant parameters (y_i, Y and s) of the KW test. The CPV is given for each significant result and for a few others, included for comparison. In addition, some symbols are presented in this table, to represent the significance. The symbols S_y and S_s represent those cases in which the K_f ratio significantly affects the magnitude and reproducibility, respectively, of the response. The symbol "?" is used in selected cases to indicate a questionably significant result; for each of these results graphical analysis was conducted to further establish, illustrate, and describe the effect. The combined results of these methods of analysis gives a final result indicated in Column B (for the effect of K_f on the magnitude of the response) or in Column D (for that of the reproducibility).

The conclusion that precracking at levels below a K_f ratio of about 0.4 is to be avoided comes from results for tests of aluminum and titanium that indicate either the magnitude or the variability of the response may be increased at lower values of this ratio. Indications that precracking very high K_f ratios above 0.9 are to be avoided come from results for steel specimens, for which the magnitude of the responses increase with an increase in the K_f ratio over the range of ratios of from 0.33 to 1.3.

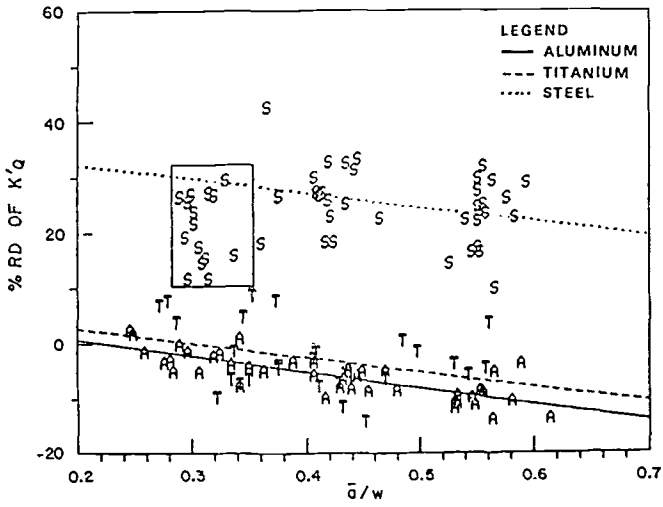

Figure 3. Plot of data and regression results for response %RD of K'_Q as a function of normalized crack size, ā/W, for three materials. This plot shows the necessity for omission of K'_Q data for steel specimens of crack size code 1 (ā/W < 0.356).

TABLE 6 -- Summary of Results for the Factor K_t Maximum.

Symbol	Meaning
NC	Not computed.
?	Significance of K_t maximum is open to question.
S_s	K_t maximum has a significant effect on the reproducibility s of the response.
-	K_t maximum does not have a significant effect.
S_y	K_t maximum is significant for response magnitude.
()	Not significant (included for comparions).

		CPV from KW Test			CPV from MLR		Test for Significant Differences in the Magnitude of Test Response		Test for Significant Differences in the Reproducibility of Test Responses	
							Column A	Column B	Column C	Column D
Material	Response	N	y_i	Y	F test	ν	Combined Results of KW Test and MLR Analysis	Combined Results of Column A and Graphical Analysis	Significant CPV for reproducibility parameter s of the KW test	Result of Column C plus graphical analysis
4	R_{sb}	43	-	-	-	40	-	-	-	-
Aluminum	K'_Q	43	-	-	-	40	-	-	-	-
	K_{Q-PM}	43	98	95	(71)	40	?	S_y	-	-
	K_Q	43	(84)	(64)	(86)	40	?	?	-	-
	K_J	43	96	88	91	40	S_y	S_y	-	-
	K_J	43	95	88	95	40	S_y	S_y	-	-
	K^*_d	43	96	85	(86)	40	?	S_y	-	-
5	R_{sb}	28	-	-	-	25	-	-	90	S_s
Titanium	K_Q	28	-	-	-	25	-	-	90	?
	K_{Q-PM}	28	--	-	-	25	-	-	96	S_s
	K_Q	28	96	92	>99	25	S_y	S_y	(85)	S_s
	K'_J	28	-	-	-	25	-	-	96	S_s
	K_J	28	-	-	-	25	-	-	99	S_s
	K^*_d	28	-	-	-	25	-	-	96	S_s
6	R_{sb}	51	99	96	>99	48	S_y	S_y	-	S_s
Steel	K'_Q	36	NC	NC	94	33	S_y	S_y	NC	-
	K_{Q-PM}	51	95	(70)	>99	48	S_y	S_y	-	-
	K_Q	51	97	(70)	98	48	S_y	S_y	-	-
	K'_J	51	(54)	(32)	94	48	?	S_y	-	-
	K_J	51	(38)		91	48	?	S_y	91	-
	K^*_d	51	(51)	(51)	94	48	?	S_y	-	-

6.5.1 Aluminum (material code 4)-- Results for aluminum specimens indicate that for $\bar{a}$ codes 1 and 2, at a K_f ratio less than 0.4 the magnitude of the response is greater than at higher K_f ratios. As is indicated in Table 6, column B, the magnitudes for all responses, except R_{sb}, K_Q, and K'_Q, are significant. This effect of a low K_f ratio is illustrated in a plot given as Figure 4 for %RD of K'_J, with plot characters representing coded crack length. For specimens precracked at a ratio of 0.33 the magnitude of the response increases for $\bar{a}$ codes 1 and 2. This plot typifies and represents four of the five significant responses for aluminum specimens; these are $K_{Q\text{-}PM}$, K'_J, K_J, and K^*_d. For aluminum specimens, K_Q responses were unique among the seven responses, while the other significant responses behaved similarly to that shown in Figure 4 for K'_J.

6.5.2 Titanium (material code 5)-- Results for titanium specimens indicate that the factor K_f maximum is significant for all seven responses (see Table 6 columns C and D); it is concluded that responses for specimens precracked at a very low K_f ratio of 0.20 may have greater variability than the variability for specimens precracked at a ratio of 0.40. For titanium specimens, data is available only for two levels of the K_f ratio and at the lowest level (0.20) the data are sparse for specimens of $\bar{a}$ code 1 and very sparse for those of $\bar{a}$ code 3. Thus, the conclusions are somewhat tentative.

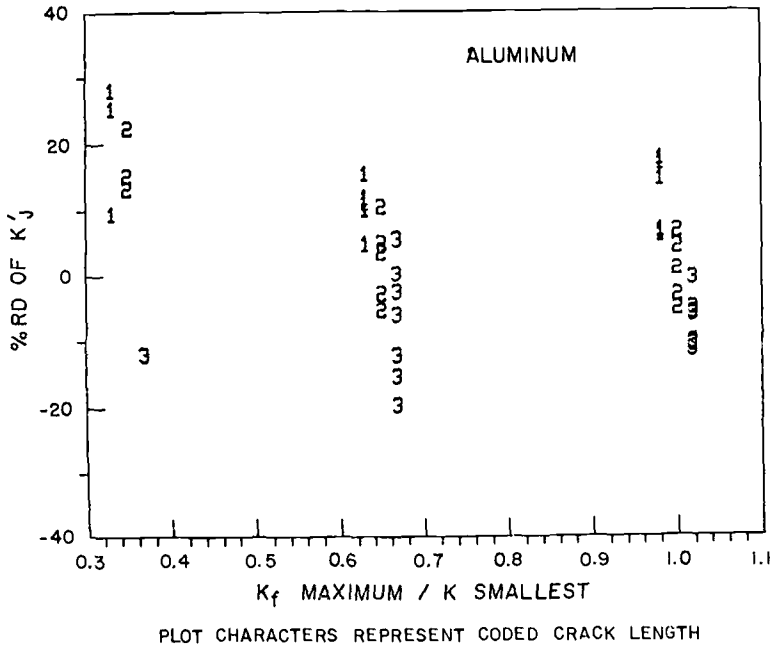

Figure 4. Plot of %RD of K'_J versus the K_f ratio, K_f maximum/K smallest, for aluminum specimens.

The unique behavior observed for the response parameter K_Q for both the aluminum and the titanium specimens, as discussed in this section, give the authors pause and we note that in a previous work [15], the parameter K_Q (based on the same 5%-secant intercept used in the present work) was found to be an inappropriate parameter for evaluations of fracture toughness in subsized specimens of a heat of 4340 steel at a yield strength of 180 ksi. **It is concluded that K_Q may be an inappropriate parameter for evaluations of the fracture toughness using Charpy tests conducted under conditions used in this study, i.e. conditions that give a load-displacement trace of the type in which there is no indication of a cleavage initiation event.**

6.5.3 Steel (material code 6)-- Only a limited number of steel specimens were precracked at a ratio of less than 0.4, so the results for steel are used here for conclusions concerning the general trends for ratios above 0.4. In general, the data for steel indicate that the magnitude of each of the seven responses tends to increase with increases in the K_f ratio. This effect is most marked for steel specimens of $\bar{a}$ code 2 and it indicates that precracking at K_f ratios above 0.9 is to be avoided. In addition, for R_{sb}, variability of responses may increase at either high or low levels of the K_f ratio.

The general tendency for increases in the response with increases in the K_f ratio has been illustrated [6]. Table 6 (column B) indicates the magnitude of the response is significant for all response parameters. Although the reproducibility parameter in the KW test (column C) does not indicate a significant effect, it is apparent from a plot of R_{sb} data [6] that for $\bar{a}$ codes 2 and 3, variability is decidedly smaller at intermediate levels of the K_f ratio. Thus, it is concluded that both the magnitude and the variability of response R_{sb} may be significantly affected by the level of K_f ratio for steel specimens. The marked effect of K_f ratio on the responses of %RD of K observed for $\bar{a}$ code 2
specimens is also illustrated for response $K_{Q\text{-}PM}$ [6]. Significance tests (Table 6) indicate S_y (K_f maximum has a significant effect on the response magnitude) for both the KW tests and the MLR analyses, except for responses based on energy to maximum load (K_J, K_J', and K_d^*), for which only the MLR analyses lead to a significant effect of K_f maximum. Graphical analyses for these three responses indicate a significant behavior only for $\bar{a}$ codes 1 and 2. **Thus, it is concluded that the magnitude of each of the seven responses tends to increase with increases in the K_f ratio for steel specimens. This effect is most marked for steel specimens of intermediate crack size ($\bar{a}$ code 2) and it is an indication that precracking at K_f ratios above 0.9 is to be avoided. In addition, it was shown that for response R_{sb}, variability of the response may increase at either high or low levels of the K_f ratio, and this is another indication that these extreme K_f levels are to be avoided.**

6.6 Effects of Notch Preparation

Significant effects of the level of notch preparation (NP) on the responses were observed only for steel specimens, for three responses R_{sb}, $K_{Q\text{-}PM}$ and K_Q'. These effects were supported by results of MLR and graphical analyses, but they went largely undetected by the KW test for significant differences among coded levels of the factor NP. The

results indicate that for a hard material, such as the maraging steel used in the Phase I program, razor scratching before precracking may lead to increases in either the variability or the magnitude of the response. Figure 5 is a plot of K_{Q-PM} data that illustrates an effect observed in plots for each of three responses R_{sb}, K_{Q-PM} and K'_Q: Variability of responses for NP code 1 is greater than that for codes 2 or 3.

Figure 5 also illustrates two effects observed only for responses R_{sb} and K_{Q-PM}: (1) the mean and median responses for NP code 1 are greater than those for codes 2 or 3, and (2) there exists along the top of the trend band (of each plot) a set of NP code 1 data, with no data there for the other NP codes.

These effects of NP were not observed for the softer materials, aluminum and titanium. Our interpretation of these findings is that some steel specimens of NP code 1 (razor scratched) were somehow improperly prepared for the precracking process. The net result of this improper preparation is that something (perhaps an uneven crack front or perhaps cold work) occurred in the test specimen during precracking. As a result of this, (1) responses that are a function of maximum load (R_{sb} and K_{Q-PM}) sometimes have greater than expected magnitude, (2) the response that is a function of total energy absorbed (K'_Q) sometimes has smaller magnitude, and (3) those that are a function of either P_Q or energy to maximum load do not appear to be affected by NP.

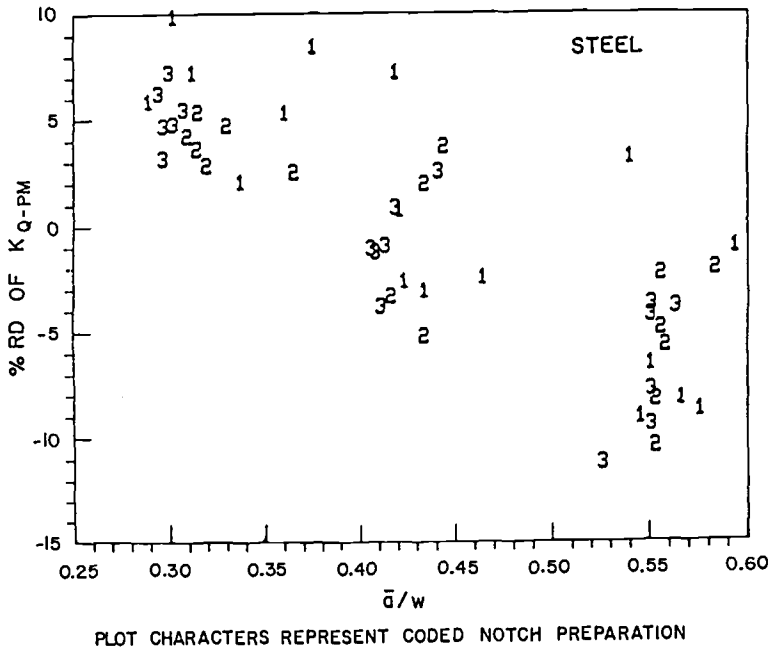

Figure 5. Plot of %RD of K_{Q-PM} versus normalized crack size for steel specimens.

7. Conclusions and Recommendations

7.1 From a preliminary analysis of the data it was concluded that a minimum crack extension equal to 0.5 mm may be required. This is consistent with (but only half the value of) the requirement (of E-399 and E-812) for a minimum crack extension of 1 mm.

7.2 Computed responses are linearly related to crack size. With an increase in crack size, the response of R_{sb} increases and the K responses decrease.

7.3 The accuracy of the response varies significantly as functions of the crack size and the computed response parameter. Thus, correlations with K_{Ic}, which are commonly made using slow-bend test results [16], would be expected to vary accordingly.

7.4 The sensitivity of the response to crack size is a function of both the response parameter and of the material.

7.5 Precracking at levels of K_f maximum outside the range of from 0.4 to 0.9 times K smallest is to be avoided, as either the magnitude or the variability of computed responses of K or R_{sb} may be greater than that for responses for specimens precracked within this range.

7.6 Among the three levels of notch preparation tested, significant effects of the level of NP on the response were not observed, except for steel specimens. The results indicate that for materials similar to those used in the Phase I program, similar responses are to be expected from a standard notch that is either razor scratched or EDM sharpened or from a sharply (non-standard) machined notch. However, the results indicate that for a hard material, such as the maraging steel used in the Phase I program, razor scratching before precracking may lead to increases in either the variability or the magnitude of the response.

7.7 The results indicate that the response K_Q based on a 5-percent-secant intercept may be inappropriate for characterization of fracture toughness using precracked Charpy tests conducted under conditions used in this study.

7.8 While the above conclusions are generally supportive of the presently recommended precracking practices of E-399 and E-812, it is recommended that these conclusions, especially those of 7.1 and 7.5, should be carefully explored by members of Committee E24, so as to establish whether any modifications of the precracking requirements of these methods is warranted.

ACKNOWLEDGMENTS

The authors would like to thank two NIST (formerly NBS) workers, Mr. David E. Schwab for extensive computations and programming assistance in the computations of the Kruskal-Wallis Test of Significance and Mr. Sam R. Low for making numerous plots and tablets needed for this analysis. In addition, this analysis was made possible through the ASTM Task Group E24.03.03, its chairman Dr. C. Hartbower and the work of participating members, M. W. Brennecke, A. Burnett, C. Curll, R. E.

Davies, S. Fisher, and the extensive works of members, T. Ronald and W. Server. As a result of a study conducted by G. E. Hicho (NIST) for Subcommittee E24.02 on Fractography for Fracture Testing, an error in the data set used for this study was discovered and corrected.

REFERENCES

[1] NMAB Committee on Rapid Inexpensive Tests for Determining Fracture Toughness, Washington, DC: National Materials Advisory Board, Commission of Sociotechnical Systems, National Research Council, National Academy of Science; 1976.

[2] Schwabe, J., et al., "Report of Working Group on Instrumented Precrack Charpy Test for Medium Strength Nuclear Pressure Vessel Steels (Parts 1 and 2), IIPC-PVRC Joint Task Group on Fracture Toughness Properties of Materials for Nuclear Components -- Final Report," Library of Congress No. 77-88087, 1977.

[3] Wullaert, R. A. Olefield, W. and Server, W. L., "Fracture Toughness Data for Ferritic Nuclear Pressure Vessels -- Final Report of Research Project 232-1," Vol. I, II and III, Electric Power Research Institute, NP-121, 1976 April.

[4] Aluminum Standards and Data, New York, Publications Dept., Aluminum Association, Inc. 750 Third Ave. New York, NY 10017; 1976.

[5] ASTM Designation E399-74; Standard Method of Test for Plane-Strain Fracture Toughness of Metallic Materials, in Part 10, Annual book of ASTM standards. Philadelphia: American Society for Testing and Materials; 1976.

[6] Interrante, C. G. and Filliben, J. J., "Factors Significant to Precracking of Fracture Specimens," NISTIR-89-89-4214, U.S. Department of Commerce, National Institute of Standards and Technology, October 1989.

[7] Ronald, T., Hall, J. A. and Pierce, C. M., " Usefulness of Precracked Charpy Specimens for Fracture Toughness Screening Tests of Titanium Alloys," Metallurgical Transactions 3:1-6; 1972 April.

[8] Rice, J. R. Paris, P. C. and Merkle, J. G., "Some Further Results of J-integral Analysis and Estimates," ASTM STP 536; 1973 July. 231 p.

[9] Ireland, D. R. Server, W. L. and Wullaert, R. A., Procedures for Testing and Data Analysis: "Task A Topical Report," Effects Technologies Inc., Technical Report 75-43, 1975 October.

[10] Server, W. L., "Impact Three-point Bend Testing for Notched and Precracked Specimens," ASTM Journal of Testing and Evaluation, 1978 January.

[11] Witt, F. J., "Equivalent Energy Procedures for Predicting Gross Plastic Fractures," Oak Ridge Nat. Lab., U.S. AEC Report ORNL-TM-0172,: 1972.

[12] Kruskal, W. H. and Wallis, W. A., "Use of Ranks in One-Criterion Variance Analysis," JASA, 47(260): 583-618; 1952 December.

[13] Draper, N. and Smith, H., Applied Regression Analysis, New York, Wiley and Sons, 1956.

[14] J. J. Filiben, "Dataplot, An Interactive System for Graphics, Fortran Function Evaluation, and Linear/Nonlinear Fitting," Proceedings of the Statistical Computing Section of the American Statistical Association, 1978.

[15] Jones, M. H. and Brown, W. F., Jr., "The Influence of Crack Length and Thickness in Plane Strain Fracture Toughness Tests," Review of Developments in Plane Strain Fracture Toughness Testing, ASTM STP 463, Philadelphia: American Society for Testing and Materials; 1970; 81 p.

[16] Succop, George and Brown, W.F., Jr., "Estimation of K_{I_c} from Slow Bend Precracked Charpy Specimen Strength Ratios," Developments in Fracture Mechanics Test Methods Standardization, ASTM STP 632, W.F. Brown, Jr., and J.G. Kaufman, Eds., American Society for Testing and Materials, 1977, pp. 179-192

APPENDIX TABLE I

Results of Kruskal-Wallis Test of Significance, Cumulative Probability Values, for the Factor K_f maximum.

Aluminum	N	R_{sb}	K_Q'	K_{Q-PM}	K_Q	K_J'	K_J	K_J^*
Accuracy (based upon y_i)	43	56.9	79.5	98.2	83.9	96.0	94.8	95.5
(based upon Y)	24	52.8	78.0	94.7	63.7	88.3	88.2	84.9
Reproducibility (based on s)	17	70.7	38.1	72.4	43.6	60.4	87.5	53.7
Titanium R, T, & L data)								
Accuracy (y_i)	28	49.8	22.6	3.8	96.1	76.9	80.5	83.6
(Y)	16	20.9	36.6	44.0	91.9	84.7	73.4	89.9
Reproducibility (s)	11	89.8	89.8	95.9	84.7	95.9	98.6	95.9
Steel								
Accuracy (y_i)	51	98.5	52.0	95.4	96.8	52.9	37.6	68.8
(Y)	27	96.0	49.5	70.4	69.6	32.0	13.0	51.7
Reproducibility (s)	21	25.5[2] N = 20	43.4	81.2	40.7	85.1	90.8	74.5
Combined[1]								
Accuracy (y_i)	122	99.3	84.1	98.0	99.9	56.8	50.9	62.3
(Y)	67	92.7	39.6	66.7	98.1	16.1	11.9	31.8
Reproducibility (s)	49	3.5[3] M = 48	31.8	1.1	59.5	20.4	10.7	40.5

[1] Includes specimens listed above for all three materials.
[2] N = 20 for R_{sb} only.
[3] N = 48 for R_{sb} only.

APPENDIX TABLE II

Results of Kruskal-Wallis Test of Significance, Cumulative Probability Values, for the Factor Notch Preparation, NP.

Aluminum	N	R_{sb}	K'_Q	K_{Q-PM}	K_Q	K'_J	K_J	K^*_d
Accuracy (based upon y_i)	43	68.9	36.3	68.4	0.0	41.0	50.8	62.5
(based upon Y)	24	61.2	36.7	67.8	4.6	56.9	60.0	66.1
Reproducibility (based on s)	17	51.3	86.1	67.2	83.6	8.2	56.2	18.4
Titanium R, T, & L data)								
Accuracy (y_i)	28	57.5	91.6	37.8	49.2	28.8	25.5	57.5
(Y)	16	25.0	80.1	16.7	2.5	23.9	17.6	50.7
Reproducibility (s)	11	40.9	47.7	52.8	6.9	16.0	38.2	2.6
Steel								
Accuracy (y_i)	51	63.5	79.8	15.3	22.6	7.7	7.6	21.7
(Y)	27	35.3	72.1	13.0	23.4	8.3	0.7	26.0
Reproducibility (s)	21	77.8[2] N = 20	36.9	94.1	58.2	58.2	74.4	77.6
Combined[1]								
Accuracy (y_i)	122	61.3	33.3	61.4	26.8	50.6	47.5	72.1
(Y)	67	59.1	22.6	43.3	21.9	52.7	40.7	73.9
Reproducibility (s)	49	53.3[3] M = 48	40.2	48.0	38.2	43.6	26.1	57.6

[1] Includes specimens listed above for all three materials.
[2] N = 20 for R_{sb} only.
[3] N = 48 for R_{sb} only.

APPENDIX TABLE III

Results of Kruskal-Wallis Test of Significance,
Cumulative Probability Values, for Factor Crack-Size, $\bar{a}$.

Aluminum	N	R_{sb}	K'_Q	K_{Q-PM}	K_Q	K'_J	K_J	K^*_J
Accuracy (based upon y_i)	43	>99.9	100.0	>99.9	99.4	100.0	100.0	>99.9
(based upon Y)	24	99.9	>99.9	99.9	95.7	>99.9	>99.9	99.9
Reproducibility (based on s)	17	96.8	76.9	69.7	57.8	94.6	69.0	96.8
Titanium R, T, & L data)								
Accuracy (y_i)	28	96.9	69.3	94.9	98.5	96.8	99.7	69.4
(Y)	16	95.1	76.0	94.1	92.7	96.2	97.8	83.8
Reproducibility (s)	11	37.2	2.6	8.7	79.2	6.9	34.6	36.0
Steel								
Accuracy (y_i)	51	99.9	98.0	100.0	100.0	100.0	100.0	100.0
(Y)	27	99.6	88.7	>99.9	99.9	>99.9	>99.9	>99.9
Reproducibility (s)	21	75.5[2] N = 20	86.9	78.2	42.0	60.3	8.2	59.5
Combined[1]								
Accuracy (y_i)	122	100.0	98.6	100.0	100.0	100.0	100.0	100.0
(Y)	67	99.9	94.9	100.0	>99.9	100.0	100.0	100.0
Reproducibility (s)	49	99.547[3] N = 48	95.4	90.0	0.0	94.6	42.1	96.3

[1]Includes specimens listed above for all three materials.
[2]N = 20 for R_{sb} calculation
[3]N = 48 for R_{sb} calculation
*>99.9995

APPENDIX TABLE IV

Residual-Standard-Deviation from Multiple Linear Regression Analyses for Seven Responses and Three Materials.

Material	Response[1]	N	$\bar{a}$ (Eq.14) res. S.D.	ν	$\bar{a}+K_f$ (Eq. 16) res. S.D.	ν	$\bar{a}$ K_f+NP (Eq. 17) res. S.D.	ν
4	R_{sb}	43	0.077	41	0.076	40	0.073	39
5	R_{sb}	28	0.118	26	0.119	25	0.105	24
6	R_{sb}	51	0.072	49	0.060**	48	0.059	47
4	K_Q'	43	2.39	41	2.41	40	2.44	39
5	K_Q'	28	5.94	26	6.06	25	6.03	24
6	K_Q'	51	6.56	49	6.49	48	6.46	47
6	K_Q[2]	36	6.14	34	5.65*	33	5.42	32
4	K_{Q-PM}	43	3.03	41	3.02	40	2.97	39
5	K_{Q-PM}	28	4.70	26	4.77	25	3.18	24
6	K_{Q-PM}	51	3.07	49	2.52**	48	2.38	47
4	K_Q	43	3.95	41	3.83	40	3.87	39
5	K_Q	28	4.95	26	3.70**	25	3.67	24
6	K_Q	51	4.09	49	3.72**	48	3.76	47
4	K_J'	43	6.23	41	5.94*	40	6.00	39
5	K_J'	28	8.67	26	8.64	25	8.64	24
6	K_J'	51	7.08	49	6.72*	48	6.62	47
4	K_J	43	5.28	41	4.92**	40	4.98	39
5	K_J	28	8.15	26	8.14	25	8.13	24
6	K_J	51	6.91	49	6.65*	48	6.65	47
4	K_d^*	43	5.82	41	5.64	40	5.70	39
5	K_d^*	28	7.60	26	7.57	25	7.49	24
6	K_d^*	51	6.10	49	5.77**	48	5.65	47

[1]For the R_{sb} responses, for which reference values of the response are not available, the residual standard deviation is computed from the response R_{sb}. For each of the K responses the computation is made using the % RD of K and the magnitude of the residual S.D. will reflect this.

[2]Includes results for only specimens with $\bar{a} > 140$ mils.
* Significant at the 10 percent level
**Significant at the 5 percent level

APPENDIX V -- Results of Regression Analyses Conducted for Each of Three Materials and for all Computed Responses.

Material 4 = Aluminum 5 = Titanium 6 = Steel			Observed Responses[1] Min.	Max.	$Y = \beta_1 \bar{a} + \beta$ Slope β_1	Y-Int. β_o	$\bar{a}$ at K_{Ic} (mils)	Standard Deviation Pooled	Residual	Deg. of Freedom ν
4		RSB	1.83	2.20	0.0013	1.77	-1400.18	0.24	0.08	41
5		RSB	1.83	2.39	0.0011	1.86	-1625.20	0.15	0.12	26
6		RSB	1.96	2.35	0.0011	1.89	-1658.58	0.05	0.07	49
4	% RD of	RSB	-7.35	11.47	0.0638	-10.64	166.74	-	3.87	41
5	% RD of	RSB	-18.65	16.42	0.0560	-9.05	161.79	-	5.77	26
6	% RD of	RSB	-6.09	20.32	0.0586	-10.02	171.08	-	3.67	49
4	% RD of	KQ'	-13.65	2.47	-0.0739	6.46	87.35	2.73	2.39	41
5	% RD of	KQ'	-14.09	8.73	-0.0665	7.93	119.28	5.78	5.94	26
6	% RD of	KQ'>140[2]	9.86	42.47	-0.0660	37.62	-570.00	-	6.14	34
4	% RD of	KQ-PM	-32.37	-14.42	-0.0730	-11.06	-151.57	3.14	3.03	41
5	% RD of	KQ-PM	-27.75	-2.13	-0.0911	1.02	11.24	5.39	4.70	26
6	% RD of	KQ-PM	-11.10	9.90	-0.1145	19.14	167.26	2.62	3.07	49
4	% RD of	KQ	-37.81	-19.68	-0.0400	-22.43	-561.17	3.60	3.95	41
5	% RD of	KQ	-33.51	-10.87	-0.0963	-3.99	-41.47	2.76	4.95	26
6	% RD of	KQ	-21.99	0.34	-0.1021	7.69	75.33	3.06	4.09	49
4	% RD of	KJ'	-19.63	28.19	-0.2191	40.06	182.78	6.23	6.23	41
5	% RD of	KJ'	-10.48	31.89	-0.2026	41.06	202.65	9.89	8.67	26
6	% RD of	KJ'	15.65	67.33	-0.3111	91.26	293.32	6.08	7.08	49
4	% RD of	KJ'	-10.79	38.85	-0.2505	52.04	207.75	6.02	5.28	41
5	% RD of	KJ'	-8.53	35.43	-0.2472	50.69	205.06	9.42	8.15	26
6	% RD of	KJ'	24.82	89.83	-0.4343	127.05	292.51	5.96	6.91	49
4	% RD of	Kd*	-23.92	13.33	-0.1124	12.32	109.59	5.73	5.82	41
5	% RD of	Kd*	-15.51	16.70	-0.0982	15.45	157.37	8.28	7.60	26
6	% RD of	Kd*	9.33	45.04	-0.1774	55.82	314.65	5.31	6.10	49

[1]Given as an R_{sb} response or as a % RD response.

[2]Only specimens with $\bar{a}$ > 140 mils are included in the analysis.

The Specimen: Size

David J. Alexander and Ronald L. Klueh

SPECIMEN SIZE EFFECTS IN CHARPY IMPACT TESTING

REFERENCE: Alexander, D. J., and Klueh, R. L., "Specimen Size Effects in Charpy Impact Testing," Charpy Impact Test: Factors and Variables, ASTM STP 1072, John M. Holt, Editor, American Society for Testing and Materials, Philadelphia, 1990.

ABSTRACT: Full-size, half-size, and third-size specimens from several different steels have been tested as part of an ongoing alloy development program. The smaller specimens permit more specimens to be made from small trial heats and are much more efficient for irradiation experiments. The results of several comparisons between the different specimen sizes have shown that the smaller specimens show qualitatively similar behavior to large specimens, although the upper-shelf energy level and ductile-to-brittle transition temperature are reduced. The upper-shelf energy levels from different specimen sizes can be compared by using a simple volume normalization method. The effect of specimen size and geometry on the ductile-to-brittle transition temperature is more difficult to predict, although the available data suggest a simple shift in the transition temperature due to specimen size changes. The relatively shallower notch used in smaller specimens alters the deformation pattern, and permits yielding to spread back to the notched surface as well as through to the back. This reduces the constraint and the peak stresses, and thus the initiation of cleavage is more difficult. A better understanding of the stress and strain distributions is needed.

KEYWORDS: Charpy, fracture, size effects, constraint, cleavage, critical tensile stress, ductile-to-brittle transition temperature, upper-shelf energy, slip-line field theory, finite-element analysis.

Dr. Alexander and Dr. Klueh are in the Metals and Ceramics Division of Oak Ridge National Laboratory, P.O. Box 2008, Oak Ridge, Tennessee, 37831-6151.

INTRODUCTION

The Charpy test is widely used for the study of ferritic materials. It is a rapid, inexpensive, and simple test which provides a qualitative measure of toughness. The large body of data and experience gained with the use of this test over many years gives added confidence to interpretation of test results, whether the test is used for alloy development or for monitoring the effects of irradiation on the mechanical properties of nuclear pressure vessel steels.

These two areas of research have created an impetus for a reduction in size of the Charpy specimen. Smaller specimens permit the measurement of mechanical properties during alloy development when only limited material is available, yet retain the advantages of simplicity and convenience of the traditional Charpy specimen. However, the major reason for considering smaller specimens is the fact that many more specimens can be irradiated in the space available in radiation facilities. Approximately eight half-size specimens or eighteen third-size specimens can be located in the same space that a conventional full-size specimen would require. This provides a tremendous advantage for irradiation effects studies.

The use of smaller specimens raises a number of important issues. It is well established that these smaller specimens show behavior which is qualitatively similar to the full-size specimens [1-4]. At higher temperatures ductile modes of fracture occur and the energy absorbed tends toward an upper-shelf level. As the temperature is reduced, a brittle mode of fracture occurs with a concomitant decrease in the energy absorbed. Thus these specimens show a ductile-to-brittle transition similar to that observed for full-size specimens. However, due to the reduction in size of the specimens, the stresses and strains which develop in the specimens differ with specimen size, and so the transition in fracture mode will occur at different temperatures for different specimen geometries. In addition, the energy absorbed will obviously vary with specimen size. Therefore, it is not clear how data generated with various specimen geometries can be compared and related. The subsize specimen geometries have not been standardized, with different researchers using different notch geometries for specimens having the same nominal dimensions. These slight differences may have significant effects on the stresses and strains, and thus the fracture process. Finally, it may be possible to analyze these impact tests to determine the values of material properties such as dynamic yield stress (σ_{yd}) or the critical tensile stress required for cleavage fracture, the cleavage fracture stress (σ_{fc}) [4,5]. This requires an accurate knowledge of the stress and strain distributions in these specimens, which will certainly vary with specimen size and geometry.

The aim of this research is to compare a large number of data sets which have been generated with different specimen sizes to see if the data can be normalized or adjusted to allow different specimen sizes to be compared directly. Most of the data given below have been generated at Oak Ridge National Laboratory (ORNL) through alloy development programs sponsored by the Fusion Energy Program. These efforts have been aimed at designing steels with improved resistance to irradiation, both through a reduction in radiation-induced embrittlement and an increase in the rate of decay of radiation-induced radioactivity. Different models proposed in the literature for

normalizing the upper-shelf energy (USE) will be compared. The shift in the ductile-to-brittle transition temperature (ΔDBTT) as a function of specimen size and other material parameters will also be considered.

RESULTS

The subsize specimens were tested on a semiautomated Charpy impact machine modified for testing small specimens [2,6]. The full-size specimens were 10 × 10 × 55 mm with a 45° notch 2 mm deep, notch radius 0.25 mm. The half-size specimens were 5 × 5 × 25.4 mm with a 30° notch 0.76 mm deep, notch radius 0.075 mm, and the third-size specimens were 3.33 × 3.33 × 25.4 mm with a 30° notch 0.51 mm deep, notch radius 0.075 mm. Note that the subsize specimens are not geometrically similar to the full-size specimens, since the notch is relatively shallower (notch depth/thickness = a/W = 0.15 for the subsize specimens, while a/W = 0.2 for the full-size specimen) but sharper (30° for the subsize vs 45° for the full-size specimen).

The impact data were fitted to a hyperbolic tangent function which allowed the upper-shelf energy level and the transition temperature to be determined. The transition temperature was taken at the midpoint between the upper- and lower-shelf energy levels. Some investigators [2] have used half of the upper-shelf energy as the transition point: the difference between these definitions is very small, since the lower-shelf energies are very low.

The results of the tests are shown in Tables 1 and 2, which compare full-size specimens to half-size and third-size specimens, respectively [7-12]. Mechanical property data are included. Similar data from the literature which compare half-size and third-size specimens to full-size specimens are given in Table 3 [3,13]. These investigations employed subsize specimens with notch geometries identical to those described above. Some additional data [5] from subsize specimens have been included, although that investigation used third-size specimens with notches which were wider (45°) and deeper (a/W = 0.2) than those of the ORNL specimen (30° and a/W = 0.15). In addition, the span was reduced from 20 to 13.3 mm [4]. The values given in Table 3 were read from the figures [5].

DISCUSSION

The effect of specimen size on the USE can be considered by normalizing the energy by some factor related to the specimen dimensions. Various researchers have used different normalization factors [2,3,4] and a "volume" approximation in which the energy is divided by the nominal volume of the deformed zone beneath the notch has been shown to give the best results [2,3]. The nominal volume is given by $(Bb)^{3/2}$ where B is the specimen width and b is the remaining ligament thickness beneath the notch. This procedure gives better results than using Bb^2 as the nominal volume [4] or using an area normalization (Bb) [2-4].

The results of using this volume normalization are shown in Fig. 1, which compares the normalized data for subsize specimens to the full-size specimens. The solid lines in Fig. 1 indicate a 1:1 correspondence between the subsize and the full-size specimen data,

Table 1. ORNL data for full-size vs half-size specimens [2,7-12]

Alloy	Nominal composition (wt %)	Strength[a] (MPa)		Total elongation[a] (%)	Specimen size	Transition temperature (°C)	ΔDBTT (°C)	Upper-shelf energy (J)	Normalized USE (mJ/mm^3)
		Yield	Ultimate						
3590	9Cr-1Mo-V-Nb	541	656	10	F	-15	15	266	372
					1/2	-30		50.0	512
3591	9Cr-1Mo-V-Nb-2Ni	734	851	8	F	-45	35	177	247
					1/2	-80		28.2	289
3593	9Cr-1Mo-V-Nb-2Ni (adjusted)	817	927	8	F	-15	15	142	198
					1/2	-30		21.6	221
30176	9Cr-1Mo-V-Nb	539	630	13	F	-32	4	262	366
					1/2	-36		34.0	348
		b	b	b	F	-13	15	200	280
					1/2	-28		28.3	290
3587	12Cr-1Mo-V-W	553	759	10	F	0	15	137	191
					1/2	-15		21.1	216
3588	12Cr-1Mo-V-W-1Ni	576	800	11	F	-20	10	131	183
					1/2	-30		21.2	217
3589	12Cr-1Mo-V-W-2Ni	719	899	8	F	-30	10	106	148
					1/2	-40		17.8	182
3592	12Cr-1Mo-V-W-2Ni (adjusted)	769	938	8	F	10	0	101	141
					1/2	10		16.5	169
91353	12Cr-1Mo-V-W	549	716	10	F	10	25	149	208
					1/2	-15		20.2	207
9607-R2	12Cr-1Mo-V-W	556	738	14	F	0	19	115	161
					1/2	-19		20.8	213

[a]Room temperature properties.

[b]Not measured.

Table 2. ORNL data for full-size vs third-size specimens [2,7-12]

Alloy	Nominal composition (wt %)	Strength[a] (MPa)		Total elongation[a] (%)	Specimen size	Transition temperature (°C)	ΔDBTT (°C)	Upper-shelf energy (J)	Normalized USE (mJ/mm³)
		Yield	Ultimate						
3785	2.25Cr-V	674	742	8	F	87	51	245	342
					1/3	36		9.4	328
3786	2.25Cr-1W-V	727	773	6	F	54	58	224	313
					1/3	-4		9.7	340
3787	2.25Cr-2W	594	677	10	F	25	73	278	389
					1/3	-48		9.6	335
3788	2.25Cr-2W-V	649	729	6	F	33	33	272	380
					1/3	0		9.7	339
3789	5Cr-2W-V	577	712	10	F	-48	32	245	342
					1/3	-80		10.0	349
3790	9Cr-2W-V	597	735	9	F	-22	48	216	302
					1/3	-70		9.4	328
3791	9Cr-2W-V-Ta	645	784	8	F	-55	23	255	356
					1/3	-78		9.7	339
30176	9Cr-1Mo-V-Nb	539	630	13	F	-32	26	262	366
					1/3	-58		9.7	339
		b	b	b	F	-13	44	200	280
					1/3	-57		8.8	307
3792	12Cr-2W-V	606	767	9	F	10	60	192	268
					1/3	-50		9.0	314
9607-R2	12Cr-1Mo-V-W	556	738	14	F	0	46	115	161
					1/3	-46		5.9	206

[a]Room temperature properties.

[b]Not measured.

Table 3. Literature data for subsize specimens [3,5,13]

Alloy	Nominal composition (wt %)	Specimen size	Transition temperature (°C)	ΔDBTT (°C)	Upper-shelf energy (J)	Normalized USE (mJ/m^3)
		Half-size specimens				
2W	9Cr-2W	F	-57	33	245	342
		1/2	-90		34.3	351
9607-R2	12Cr-1Mo-V-W	F	-2	45	129	180
		1/2	-47		19	195
		Third-size specimens				
1W	9Cr-1W	F	-66	47	259	362
		1/3	-113		10.8	377
2W	9Cr-2W	F	-57	56	245	342
		1/3	-113		9.8	342
4W	9Cr-4W	F	-24	74	221	309
		1/3	-98		8.8	307
9607-R2	12Cr-1Mo-V-W	F	-2	62	129	180
		1/3	-64		6	210
A 302-B	1.5Mn-0.2C	F	6	63	64	89
		1/3	-57		3.8	131
A 508-B	0.6Mn-0.6Ni-0.6Mo-0.2C	F	-14	25	123	172
		1/3	-39		6.7	235
A 508-B reaustenitized	0.6Mn-0.6Ni-0.6Mo-0.2C	F	91	50	74	103
		1/3	41		4.1	142
A 710 as-received	1Ni-0.7Cr-1.2Cu-0.04C	F	-37	51	161	224
		1/3	-88		7.4	256
A 710 underaged	1Ni-0.7Cr-1.2Cu-0.04C	F	-52	29	188	262
		1/3	-81		7.7	268
A 710 overaged	1Ni-0.07Cr-1.2Cu-0.04C	F	-55	54	177	247
		1/3	-109		8.3	289
A 710 peak aged	1Ni-0.07Cr-1.2Cu-0.04C	F	-16	54	161	224
		1/3	-70		7.7	270

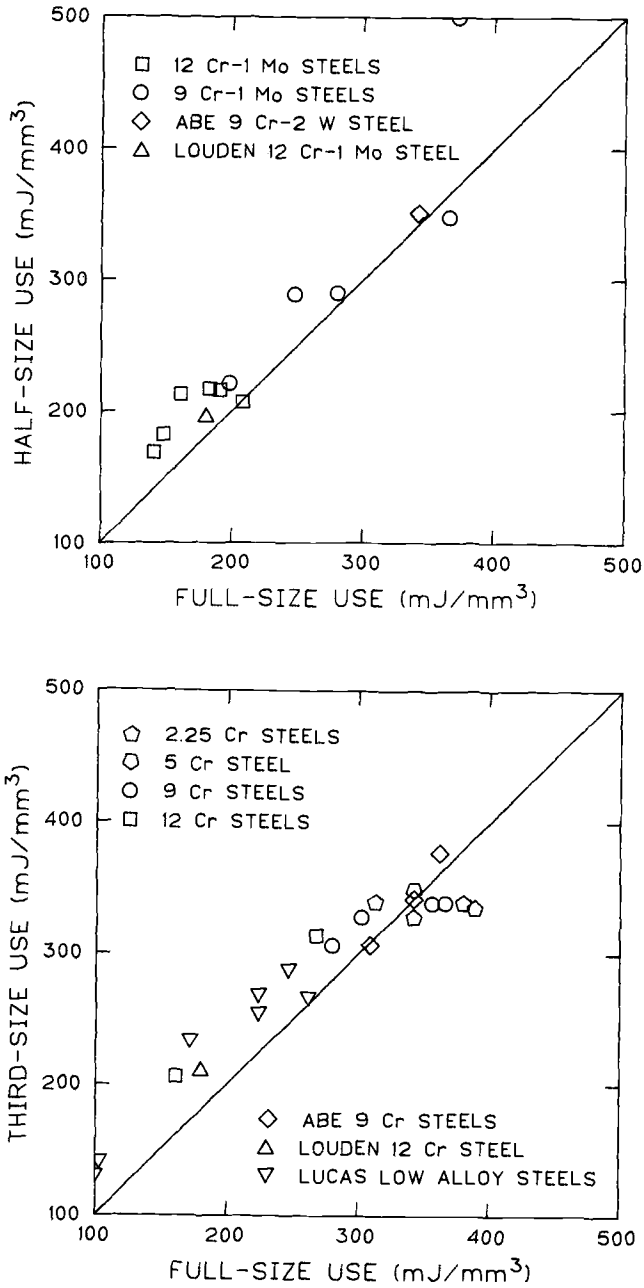

Fig. 1. Normalized upper-shelf energies for subsize specimens vs full-size specimens. Top: half-size specimens. Bottom: third-size specimens. The solid line indicates a 1:1 correlation rather than a fit to the data.

rather than a fit to the data. As the figures show, this simple normalization process provides a good means for comparing the data from different specimen sizes for several different steels.

Other methods have been proposed for accounting for the specimen sizes. Louden et al. [13] have developed a model which normalizes the USE by a factor which incorporates the specimen width, ligament thickness, and span, as well as an elastic stress concentration factor which will depend on the notch depth, angle, and root radius. Thus, all of the specimen dimensions are included. However, the use of an elastic stress concentration factor for the upper-shelf regime, where fracture is occurring only after extensive plastic deformation, and by a mechanism which is more likely strain controlled than stress controlled, is difficult to justify. The results of their normalization [13] give a correspondence similar to the much simpler volume normalization used here.

Kumar et al. [14] have developed a model to predict the USE of full-size specimens by using both notched and fatigue precracked subsize specimens. This allows the energy for crack initiation and crack propagation to be separated. Good agreement for a ferritic 12Cr-1Mo-V-W steel (HT-9) was observed. This procedure imposes the added complexity of testing precracked specimens. Although further testing is needed, the model is expected to be useful for a wide range of alloys and the study of irradiation effects also.

A possible problem due to the smaller specimen dimensions may arise when testing tough materials with high USE levels. At higher temperatures extensive deformation may occur without fracture intervening. If the material is sufficiently tough, the specimen will bend to such an extent that it will be squeezed out between the anvils rather than fracturing. This behavior has been observed when testing stainless steel specimens. The shallow notch and reduced thickness of the subsize specimens increases the likelihood of this behavior, while the deeper notch and greater thickness of the full-size specimen favor the occurrence of fracture. This may affect the correlation of USE data, if these different behaviors are present. In addition, some investigators [3,13] use specimens which are shorter than that described above, i.e., 23.6 vs 25.4 mm. If the same span (20 mm) is used in both cases, the shorter specimens may be squeezed through the anvils more readily than the longer specimens, and thus give a lower USE. The width and radius of the tup may also play a role, as well as the span length. Despite these differences, the data from Lucas et al. [5] can be normalized quite well, as Fig. 1(a) shows.

The effect of specimen size on the DBTT is more difficult to account for. There is no obvious effect of material parameters such as the yield strength on the ΔDBTT caused by a change in specimen size, as Fig. 2 shows. Abe et al. [3] have noted a qualitative trend that brittle alloys show larger size effects, although considerable scatter was observed. In Fig. 3 the subsize specimen transition temperature is plotted as a function of the full-size specimen transition temperature. The data suggest that the subsize specimen transition temperature is related to the full-size specimen transition temperature. The solid lines in Fig. 3 have been drawn with a slope of 1, and are not fits to the data. However, these lines do suggest a reasonable correlation. If the slope is 1, then one can write:

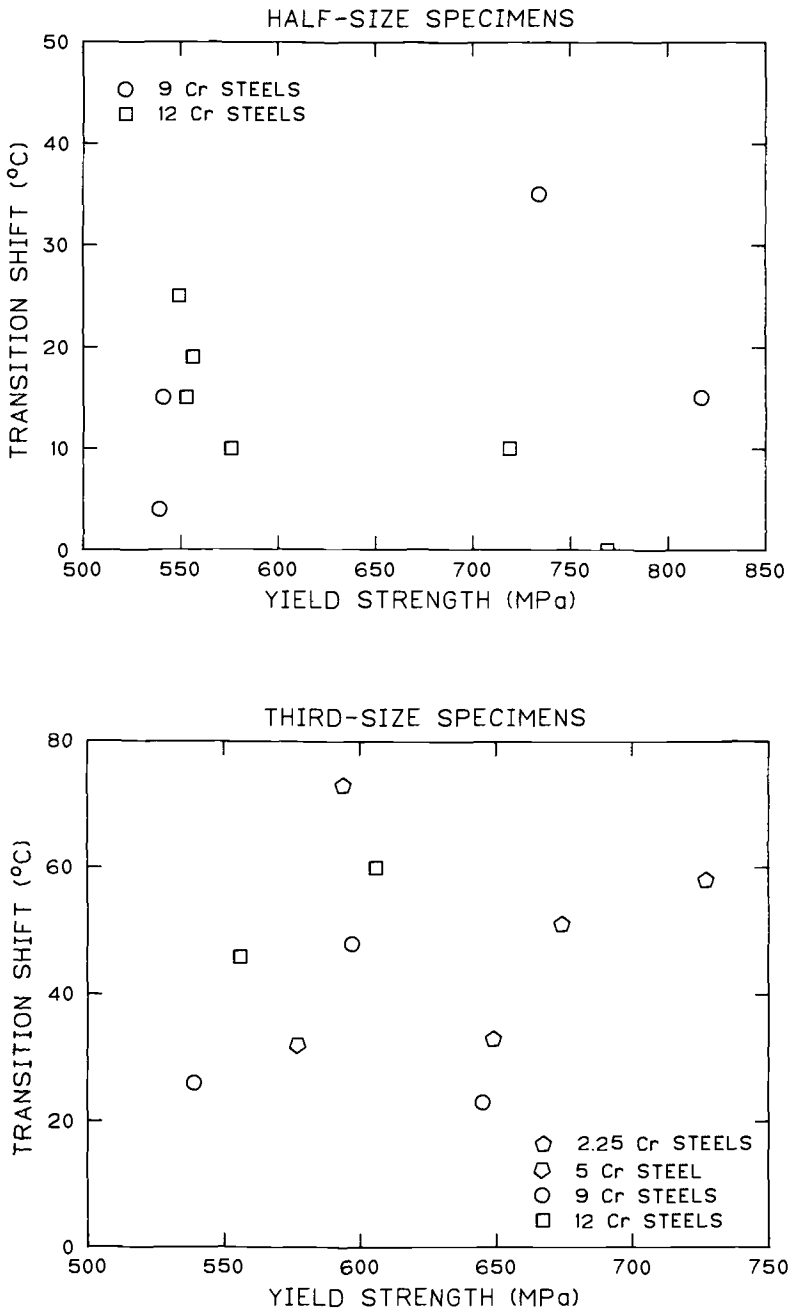

Fig. 2. Shift in ductile-to-brittle transition temperature as a function of yield strength. Top: half-size specimens. Bottom: third-size specimens.

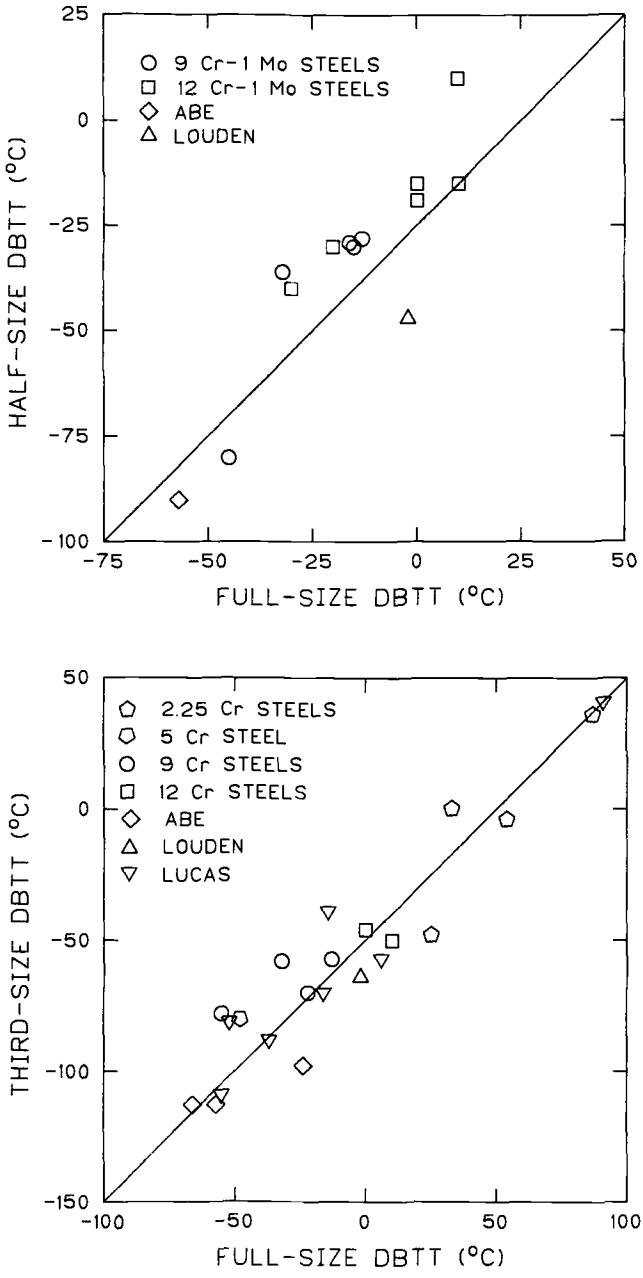

Fig. 3. Transition temperature of subsize specimens vs transition temperature of full-size specimens. Top: half-size specimens. Bottom: third-size specimens. The solid line has a slope of 1, and is not a fit to the data.

$$DBTT_{1/2} = DBTT_F + C_1 , \quad (1)$$

or

$$DBTT_{1/3} = DBTT_F + C_2 , \quad (2)$$

where $DBTT_F$, $DBTT_{1/2}$, and $DBTT_{1/3}$ are the ductile-to-brittle transition temperatures for full-, half-, and third-size specimens, respectively, and C_1 and C_2 are constants. This relationship is very similar to that suggested by Louden et al. [13] but differs in that the transition temperatures have not been normalized.

It follows from this formulation that ΔDBTT will be a constant for any fixed change of specimen geometry. The existing data suggest that the shift in transition temperature is roughly 15°C for full- to half-size specimens, and 50°C for full- to third-size specimens. However, it must be emphasized that this approach is strictly empirical. In addition, irradiation or alloying effects may result in different shifts rather than merely changing the specimen size. Although the fit shown in Fig. 3 is encouraging, more testing and analysis is necessary to examine the validity of this simple relationship. A more rigorous model of size effects will require a better understanding of the cleavage process in subsize specimens.

It is generally agreed that cleavage fracture will occur when the peak tensile stress beneath the notch exceeds the cleavage fracture stress σ_{fc} [4,5,13]. The peak stress will be located some distance beneath the notch root surface, as analysis of notched bars has shown [15,16]. Abe et al. [3] have presented convincing fractographic evidence that fracture initiates at particles some distance beneath the surface in full-, half- and third-size specimens. Thus, the smaller specimens still show fracture at a critical stress level σ_{fc}. However, how σ_{fc} might be determined is unclear. A complete understanding of the stress and strain distributions in these small specimens is essential to determine the plastic stress concentration factor. At present, empirical results are used [4,5,13]. However, these procedures are based on slip-line field theory, which assumes elastic-perfectly plastic flow behavior, and plane strain conditions. In addition, general yielding is assumed to occur at the first deviation from linearity in the load-displacement trace as the specimen is loaded. Full-size specimens of materials which exhibit pronounced Luders deformation on yielding may approach these conditions [17] which may justify this approach, but this will clearly not be satisfactory for smaller specimens of smoothly yielding materials. Analysis of these specimens requires a better understanding of the constraint and stress distributions. Full three-dimensional finite-element calculations are required for these subsize specimens. Such calculations are being performed at ORNL, and the results will be reported separately.

The need for this type of calculation is emphasized by recent slip-line field analyses of three-point bend specimens with shallow notches [18]. These results indicate that deformation from the notch will spread back toward the notched surface, which relieves the constraint and thus reduces the peak stresses beneath the notch root. The critical notch depth for three-point bend specimens for fully constrained yielding through the specimen to the back face rather than to the notched surface has been shown to be $a/W = 0.18$ [19]. Note that the full-size specimen exceeds this critical depth, while the subsize

specimens do not. Thus, the deformation patterns will be much more complicated than for the deeper notch. The edge effects for the smaller specimens will only increase the difference between the actual behavior and that predicted by slip-line field theory. Therefore, three-dimensional finite element analyses are needed.

CONCLUSIONS

Subsize Charpy specimens offer important advantages for alloy development and irradiation effects studies through their reduction in size. However, this size reduction raises concerns about the analysis of test data. Upper-shelf energies from different specimen sizes can be compared quite well by using a simple volume normalization of the energy absorbed during fracture. Understanding the shift in the ductile-to-brittle transition temperature as a function of specimen size requires a better understanding of the stresses and strains in these specimens, which may be provided by finite element analyses.

ACKNOWLEDGMENTS

The authors would like to thank R. K. Nanstad for helpful discussions, W. R. Corwin and M. L. Grossbeck for reviewing the manuscript, and J. L. Bishop for preparation of the manuscript.

This research is sponsored by the Office of Fusion Energy, U.S. Department of Energy, under contract DE-AC05-840R21400 with Martin Marietta Energy Systems, Inc.

REFERENCES

[1] Grounes, M., in *Effects of Radiation on Structural Materials, ASTM STP 426*, American Society for Testing and Materials, Philadelphia, 1967, pp. 224-59.

[2] Corwin, W. R., and Hougland, A. M., in *The Use of Small-Scale Specimens for Testing Irradiated Material, ASTM STP 888*, W. R. Corwin and G. E. Lucas, Eds., American Society for Testing and Materials, Philadelphia, 1986, pp. 325-38.

[3] Abe, F., Noda, T., Araki, H., Okada, M., Narui, M., and Kayano, H., *Journal of Nuclear Materials*, Vol. 150, 1987, pp. 292-301.

[4] Lucas, G. E., Odette, G. R., Sheckherd, J. W., McConnell, P., and Perrin, J., in *The Use of Small-Scale Specimens for Testing Irradiated Materials, ASTM STP 888*, W. R. Corwin and G. E. Lucas, Eds., American Society for Testing and Materials, Philadelphia, 1986, pp. 305-24.

[5] Lucas, G. E., Odette, G. R., Sheckherd, J. W., and Krishnadev, M. R., *Fusion Technology*, Vol. 10, 1986, pp. 728-33.

[6] Alexander, D. J., Nanstad, R. K., Corwin, W. R., and Hutton, J. T., in *Applications of Automation Technology to Fatigue and Fracture Testing, ASTM STP* (to be published).

[7] Klueh, R. L., Vitek, J. M., and Grossbeck, M. L., *Journal of Nuclear Materials*, Vol. 103-104, 1981, pp. 887-92.

[8] Klueh, R. L., Vitek, J. M., and Grossbeck, M. L., in *Effects of Radiation on Materials: Eleventh Conference, ASTM STP 782*, H. R. Brager and J. S. Perrin, Eds., American Society for Testing and Materials, 1982, pp. 648-64.

[9] Klueh, R. L., *Metallurgical Transactions A*, Vol. 20A, 1989, pp. 463-70.

[10] Corwin, W. R., Klueh, R. L., and Vitek, J. M., *Journal of Nuclear Materials*, Vol. 122-123, 1984, pp. 343-48.

[11] Klueh, R. L., and Corwin, W. R., *Journal of Materials Engineering*, Vol. 11, 1989, pp. 169-75.

[12] Klueh, R. L., and Alexander, D. J., *Journal of Nuclear Materials* (to be published).

[13] Louden, B. S., Kumar, A. S., Garner, F. A., Hamilton, M. L., and Hu, W. L., *Journal of Nuclear Materials*, Vol. 155-57, 1988, pp. 662-67.

[14] Kumar, A. S., Garner, F. A., and Hamilton, M. L., in *Effects of Radiation on Materials: Fourteenth International Symposium, (Vol. II), ASTM STP 1046*, N. H. Packan, R. E. Stoller, and A. S. Kumar, Eds., American Society for Testing and Materials, Philadelphia, 1990, p. 487-95.

[15] Griffiths, J. R., and Owen, D. R. J., *Journal of the Mechanics and Physics of Solids*, Vol. 19, 1971, pp. 419-31.

[16] Norris, Jr., D. M., *Engineering Fracture Mechanics*, Vol. 11, 1979, pp. 261-74.

[17] Alexander, D. J., Lewandowski, J. J., Sisak, W. J., and Thompson, A. W., *Journal of the Mechanics and Physics of Solids*, Vol. 34, 1986, pp. 433-54.

[18] Wu, S.-X., Cotterell, B., and Mai, Y.-W., *International Journal of Fracture*, Vol. 37, 1988, pp. 13-29.

[19] Knott, J. F., *Fundamentals of Fracture Mechanics*, Wiley, New York, 1973, p. 41.

The Test Technique

Randy K. Nanstad, Ronald L. Swain, and Reynold G. Berggren

INFLUENCE OF THERMAL CONDITIONING MEDIA ON CHARPY SPECIMEN TEST TEMPERATURE

REFERENCE: Nanstad, R. K., Swain, R. L., and Berggren, R. G., "Influence of Thermal Conditioning Media on Charpy Specimen Test Temperature," Charpy Impact Test: Factors and Variables, ASTM STP 1072, John M. Holt, Editor, American Society for Testing and Materials, Philadelphia, 1990.

ABSTRACT: The Charpy V-notch (CVN) impact test is used extensively for determining the toughness of structural materials. Research programs in many technologies concerned with structural integrity perform such testing to obtain Charpy energy vs temperature curves. American Society for Testing and Materials Method E 23 includes rather strict requirements regarding determination and control of specimen test temperature. It specifies minimum soaking times dependent on the use of liquids or gases as the medium for thermally conditioning the specimen. The method also requires that impact of the specimen occur within 5 s of removal from the conditioning medium. It does not, however, provide guidance regarding choice of conditioning media. This investigation was primarily conducted to investigate the changes in specimen temperature which occur when water is used for thermal conditioning. A standard CVN impact specimen of low-alloy steel was instrumented with surface-mounted and embedded thermocouples. Dependent on the media used, the specimen was heated or cooled to selected temperatures in the range -100 to 100°C using cold nitrogen gas, heated air, acetone and dry ice, methanol and dry ice, heated oil, or heated water. After temperature stabilization, the specimen was removed from the conditioning medium while the temperatures were recorded four times per second from all thermocouples using a data acquisition system and a computer. The results show that evaporative cooling causes significant changes in the specimen temperatures when water is used for conditioning. Conditioning in the other media did not result in such significant changes. The results demonstrate that, even within the guidelines of E 23, significant test temperature changes can occur which may substantially affect the Charpy impact test results if water is used for temperature conditioning.

Dr. Nanstad and Mr. Swain are in the Metals and Ceramics Division of Oak Ridge National Laboratory, P.O. Box 2008, Oak Ridge, Tennessee, 37831-6151; Mr. Berggren is a consultant, retired from Oak Ridge National Laboratory.

KEYWORDS: acetone, air, Charpy V-notch, cooling rate, evaporation, methanol, nitrogen gas, oil, thermal conditioning, water.

INTRODUCTION

The Charpy V-notch (CVN) impact test is used extensively for determining the toughness of structural materials. For example, it is required by the *American Society of Mechanical Engineers Boiler and Pressure Vessel Code* [1] for both nuclear and nonnuclear applications; by *Title 10, Part 50 of the Code of Federal Regulations* [2] for nuclear plants; by the American Association of Highway and Transportation Officers [3] standard for bridges; and by similar international codes and standards. In the case of commercial light-water nuclear reactor pressure vessels, CVN specimens are tested prior to operation to verify acceptable as-fabricated toughness and during operation to monitor changes in toughness due to neutron irradiation. For both the preirradiated and postirradiated testing, full Charpy impact energy vs temperature curves are obtained and used to determine the effects of irradiation on fracture toughness of the reactor vessel. Research programs in many technologies concerned with structural integrity perform similar experimental studies.

The American Society for Testing and Materials (ASTM) Method E 23-88, "Standard Methods for Notched Bar Impact Testing of Metallic Materials," includes rather strict requirements regarding determination and control of specimen test temperature. It specifies minimum soaking times dependent on the use of liquids or gases as the medium used to thermally condition the specimen. For liquids, the specimen is required to remain in the bath at the desired temperature within ±1°C for at least 5 min. For gases, the soaking time is 30 min. Whatever method is used for heating or cooling the specimen, E 23 requires that impact of the specimen occur within 5 s after removal from the medium. The method does not, however, provide guidance regarding choice of conditioning media, except to note that temperatures up to 260°C may be obtained with certain oils. Commonly used media within the testing community include air, nitrogen gas, acetone, oil, and water. The primary objective of this experimental study was to compare the effects of these different conditioning media on the temperature of the test specimen between the time of removal from the medium and impact. A second objective was the comparison of test results of the same heat of steel from two laboratories which showed consistent differences in reported energy values, especially in the ductile-to-brittle transition region, one laboratory using heated air and the other using heated water.

Figures 1(a) and 1(b) are photographs of the computer-automated test system used for testing standard and subsize CVN specimens. The system includes a conditioning chamber where the test specimen is heated with hot air from a controlled heat gun, or cooled with cold nitrogen gas from a pressurized liquid nitrogen supply. More detailed descriptions of the testing system are provided in refs. 4 and 5. Another objective for this study was the overall characterization of the testing system performance regarding the use of heated air and cold nitrogen gas.

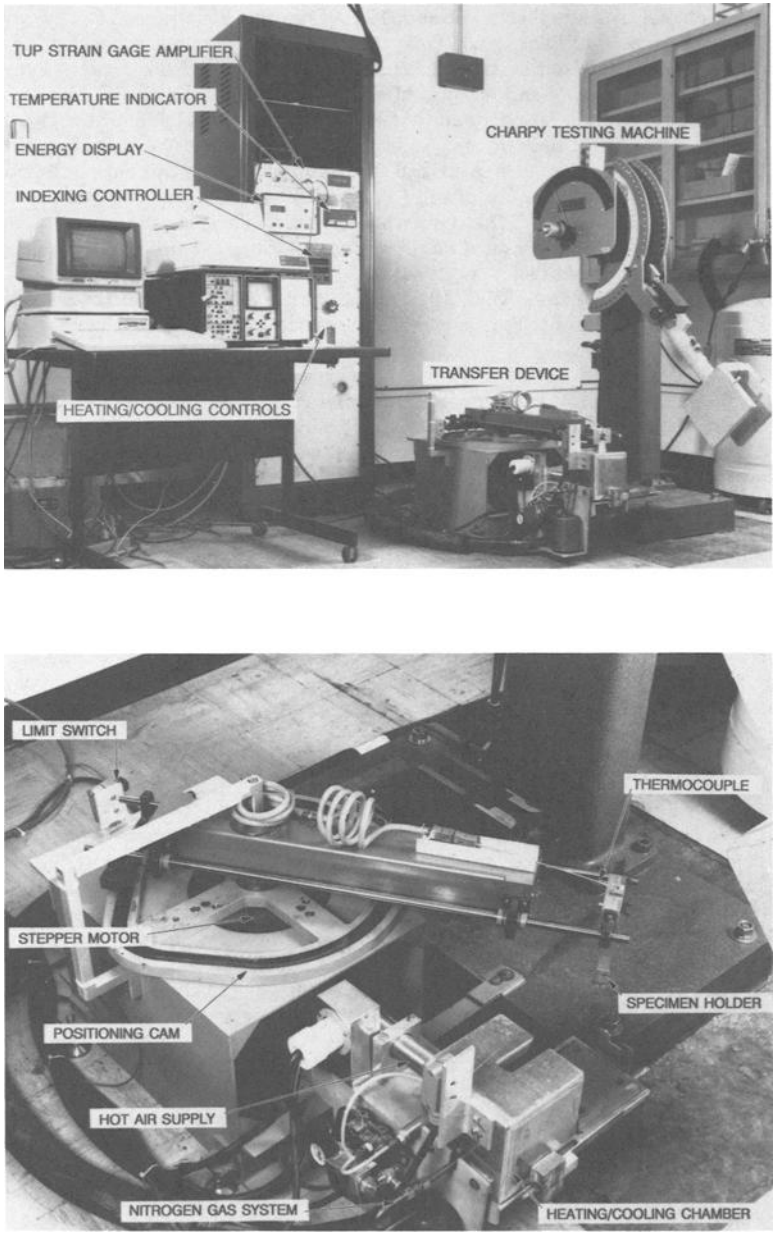

Fig. 1. Photographs of (a) Computer interactive Charpy impact test system and (b) Charpy transfer device, conditioning chamber for heating and cooling test specimens, and temperature control system.

PROCEDURES

A standard CVN impact specimen of a low-alloy steel was instrumented with five chromel-alumel thermocouples. Figure 2 schematically shows the locations of one surface and four "buried" thermocouples. The buried thermocouples were located approximately symmetrically relative to the notch, at mid-width, and along the longitudinal axis of the specimen. The thermocouple ends were beaded (welded), then welded onto the bottoms of 4.76-mm-deep drilled holes 4.76 mm in diameter; ceramic cement was used to fill the holes and allowed to harden. The surface thermocouple was tack-welded to the surface directly opposite the notch and at mid-thickness (Fig. 2). The thermocouples were connected to a Hewlett-Packard Model 3497 Data Acquisition/Control Unit, containing a 5 1/2-digit integrating voltmeter, which was connected to a Hewlett-Packard Series 200/300 computer. The maximum error of temperature measurement for a given thermocouple reading is estimated to be about 0.5°C.

For all the conditioning media investigated, comparisons were made of the temperature changes in the specimen after removal from the medium into laboratory air, and after removal from the medium directly to the anvil of the Charpy machine. For the tests in heated air and cold nitrogen gas, the instrumented CVN specimen was placed in the conditioning chamber of the testing system. For the tests in liquids, the instrumented specimen was placed in the liquid bath already stabilized at the target temperature. In all cases, temperatures were monitored during conditioning, and withdrawal did not take place until all five thermocouples had stabilized at the target temperature. The system was programmed to read all thermocouples at an interval of 0.25 s and provide a hard copy of the results. The thermocouples were read sequentially, and the acquisition rate resulted in about a 0.05-s time difference between readings.

RESULTS AND DISCUSSION

Figure 3 shows the results of conditioning the specimen with heated air from room temperature to 100°C. The spread in temperature readings from the five thermocouples does not change appreciably over the 8-min heating cycle, indicating that, for the heating rate used, the surface thermocouple reading is a reasonable representation of the temperature in the interior of the specimen. Figure 4 shows similar results of cooling with cold nitrogen gas to -100°C, although the spread in temperature readings increased somewhat throughout the cooling cycle of about 4 min. During CVN impact testing with this system, the specimen is kept at the target test temperature for 1 to 2 min to allow for complete stabilization. To track temperature changes following removal from the conditioning media, thermocouple 2 was chosen because it is one of the buried thermocouples located near the region of the specimen where fracture occurs.

Figure 5(a) shows the results of heating with air to target temperatures from 52 to 102°C followed by removal of the specimen from the chamber and immediate placement on the anvil of the machine. The start time for temperature recording ($t = 0$ s) was upon removal from the chamber. The vertical dashed line at 5 s represents the maximum allowable time specified in E 23 for impact of the specimen following

LEGEND:

1. TACK-WELDED SURFACE THERMOCOUPLE LOCATED CENTER OF SPECIMEN, BEHIND NOTCH.
2 BURIED THERMOCOUPLE (3/16" DEEP (TYP.)), 7/8" FROM LEFT END OF SPECIMEN.
3 BURIED THERMOCOUPLE, 3/4" FROM RIGHT END OF SPECIMEN.
4. BURIED THERMOCUPLE, 5/16" FROM LEFT END OF SPECIMEN.
5. BURIED THERMOCOUPLE, 1/4" FROM RIGHT END OF SPECIMEN.

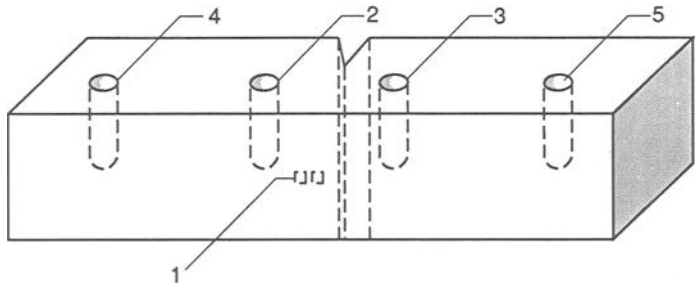

Fig. 2. Schematic drawing showing thermocouple locations on Charpy specimen used for influence of thermal conditioning media studies.

removal from the conditioning medium. Very little change is apparent even over a 10-s period. Figure 5(b) provides a plot of the temperature change (cooling) vs time for that experiment. After 5 s the greatest change is about 1°C. The accuracy of the thermocouples is estimated to be about 0.5°C and, thus, the ordering of the temperature changes relative to the target temperatures are likely obscured by the fact that the measured changes are of the same order as the measurement accuracy. Figures 6(a) and 6(b) show similar plots for cooling with cold nitrogen gas to temperatures from 0 to -101°C. After 5 s, the greatest rise in temperature is about 1.5°C from a target temperature of -101°C.

The results of heating with oil are shown in Fig. 7. The greatest decrease in temperature after 5 s is about 1°C from a target temperature of 204°C. Similar results were obtained for cooling to temperatures from 0 to -75°C in mixtures of methanol and dry ice, and acetone and dry ice, respectively. After 5 s, the temperature changes were less than 1°C. A heated bath of acetone at a target temperature of 50°C was also investigated and Fig. 8 shows the temperature changes for the experiments conducted in acetone. For target temperatures from 0 to -75°C, temperature decreases initially occur after removal from the bath; the same result was observed for the methanol and dry ice. This is the result of evaporation of the liquids and the resultant evaporative cooling of the specimen. At 50°C the same phenomenon occurs but with greater changes in specimen temperature, although still less than 2°C after 5 s. At 50°C, the acetone is near its boiling point and evaporation occurs rapidly. At the cold target temperatures, the evaporative cooling effect reaches a maximum at about 5 s.

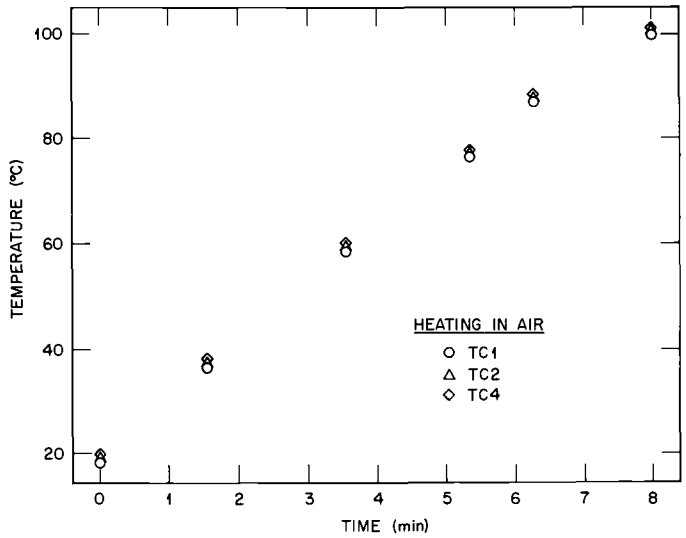

Fig. 3. Plot of temperature vs elapsed time for all five thermocouples during heating of the specimen with air in the conditioning chamber. The measurements indicate that exterior and interior temperatures of the Charpy specimen are essentially the same during heating to 100°C in 8 min.

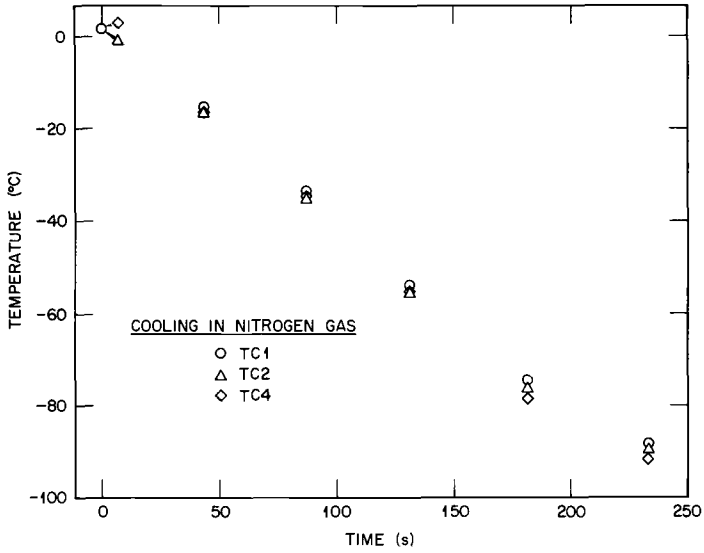

Fig. 4. Plot of temperature vs elapsed time for all five thermocouples during cooling of the specimen with nitrogen gas in the conditioning chamber. The measurements indicate that exterior and interior temperatures of the Charpy specimen are essentially the same during cooling to -100°C in 6 min.

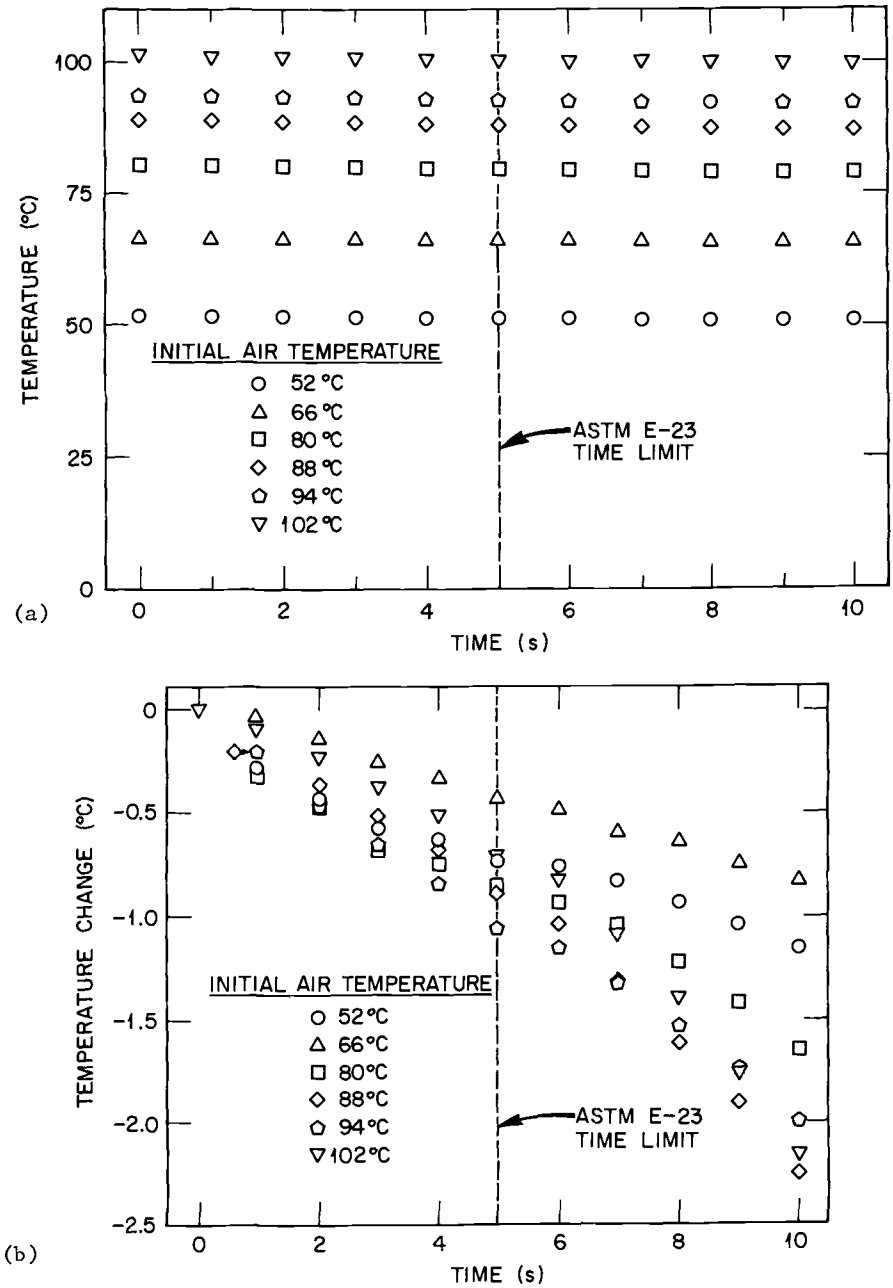

Fig. 5. Plots of (a) temperature, and (b) temperature change, from buried thermocouple 2, vs elapsed time following removal of the specimen from the heated air environment to the anvil of the Charpy machine for conditioning temperatures from 52 to 102°C. As shown in (b), the temperature decrease is about 1°C or less after 5 s.

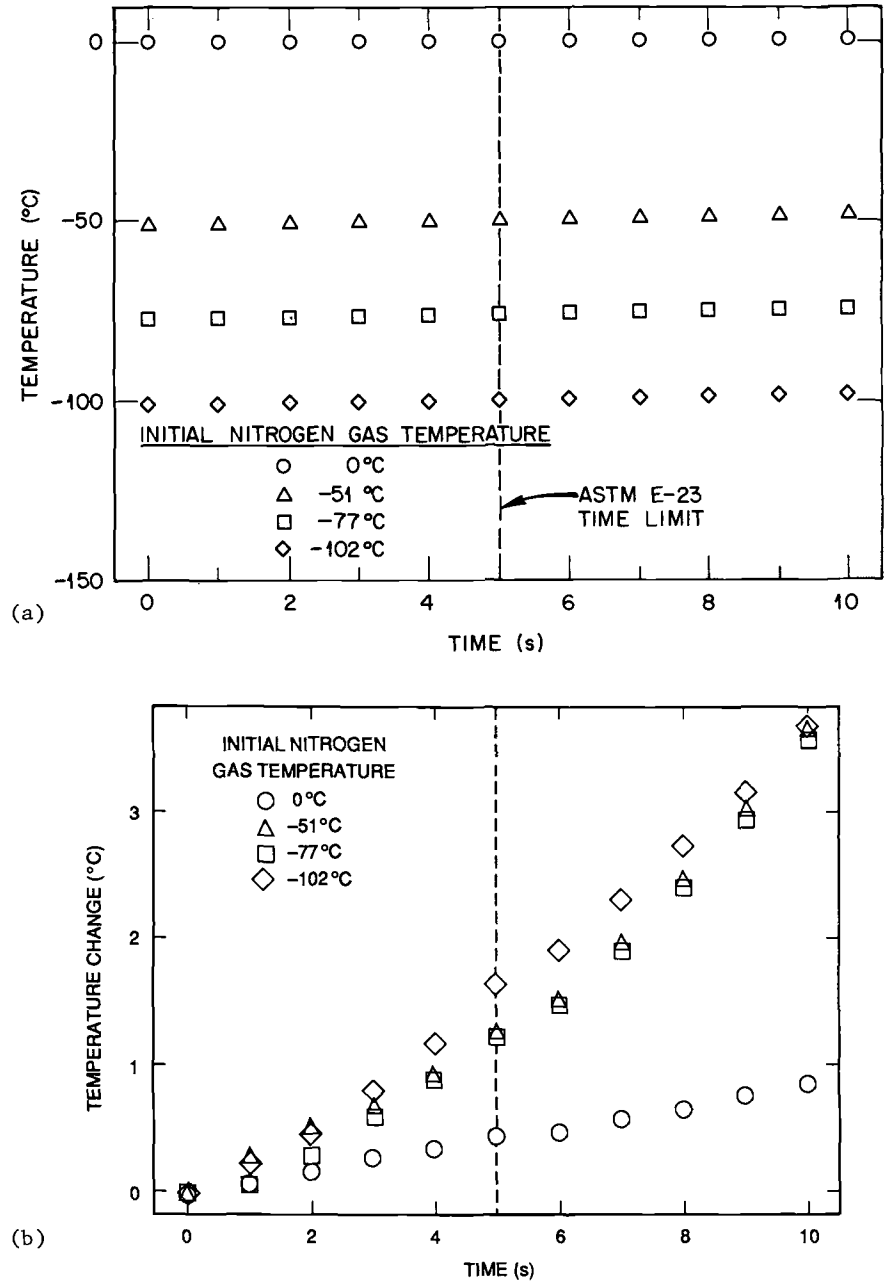

Fig. 6. Plots of (a) temperature, and (b) temperature change, from buried thermocouple 2, vs elapsed time following removal of the specimen from the cold nitrogen gas environment to the anvil of the Charpy machine for conditioning temperatures from 0 to -102°C. As shown in (b), the temperature increase is about 1.5°C or less after 5 s.

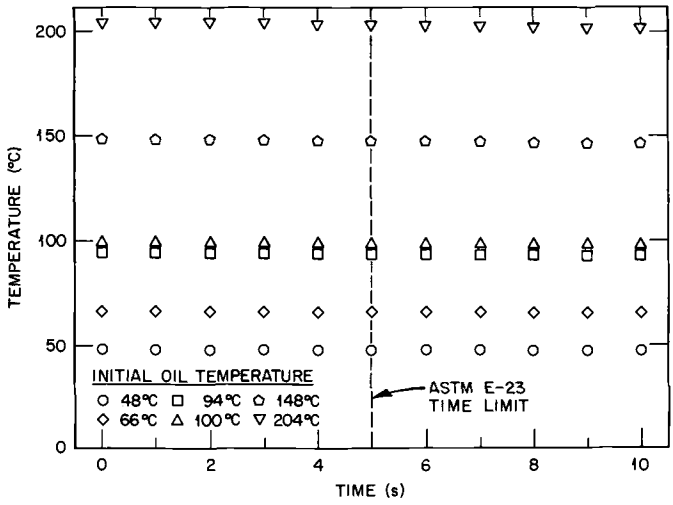

Fig. 7. Plot of temperature, from buried thermocouple 2, vs elapsed time following removal of the specimen from the heated oil bath to the anvil of the Charpy machine for conditioning temperatures from 48 to 204°C. Virtually no cooling takes place after 5 s.

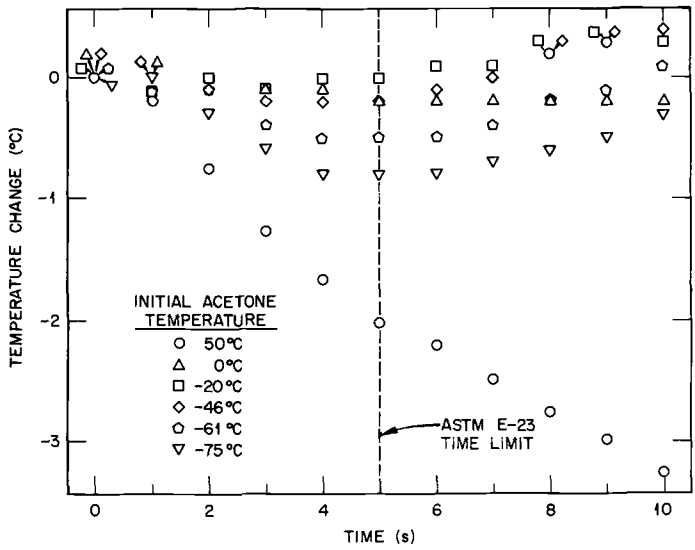

Fig. 8. Plot of temperature change, from buried thermocouple 2, vs elapsed time following removal of the specimen from a heated acetone bath and a cold bath of acetone and dry ice to the anvil of the Charpy machine. For conditioning temperatures from 0 to -75°C, the temperature changes are less than 1°C after 5 s; for a temperature of 50°C, the temperature change is about 2°C after 5 s. Evaporative cooling of the specimen takes place for both the hot and cold conditions.

The experiments with water as the conditioning medium were conducted at six target temperatures from 52 to 100°C. Figure 9(a) shows the temperature profiles for each of the six temperatures. It is obvious that the temperature changes are greater as the target temperature approaches 100°C. Figure 9(b) shows the temperature changes vs time and amplifies that observation. At the two lowest target temperatures, the cooling is only about 1°C after 5 s. At the higher target temperatures, however, the cooling effects become significant. At 100°C, the temperature decrease is over 9°C after 5 s, and about 19°C after 10 s. The change from 5 to 10 s is noted to amplify the observation that significant changes in temperature can occur in very little time at those temperatures when water is used as the conditioning medium.

Figures 10(a) and 10(b) show the temperature changes which occur at the various locations in the specimen from a target temperature of 100°C. Thermocouples 4 and 5, near the specimen ends, show greater changes in temperature than do thermocouples 2 and 3, located near the notch region. It is likely that greater cooling takes place near the ends because cooling occurs through the ends as well as the side surfaces. The fact that the specimen rests on the room temperature anvil near the ends of the specimen likely has some effect on that observation; however, an experiment was performed in which the specimen was removed from the 100°C water and left in still air, that is, not placed on the anvil, and the cooling rates were about the same as for those moved directly to the anvil. Thus, the cooling mechanism appears to be primarily due to evaporation of the water.

It should be noted that, even given the sequential nature of the thermocouple readings, a 10°C change in 5 s would result in a maximum difference of about 0.1°C between the first and last thermocouple readings during the 0.25-s cycle. Thus, the sequential procedure used to read the temperatures does not have a significant bearing on the observations. The average temperature change for the two buried thermocouples in the central region of the specimen is about 10°C after 5 s. A simple heat transfer analysis was performed to compare with the experimental results [6]. Heat losses during the experiment occur as the result of evaporation, natural convection, and radiation. To obtain accurate (±5%) results, a much more sophisticated analysis would be required because the problem is basically three-dimensional and transient. A correlation developed by Langhaar [7] was identified as an appropriate simplified model that combines heat transfer by all three aforementioned mechanisms. Prior to use of that model, however, a simple calculation was performed to check the film thickness of water required on the specimen to result in a temperature drop of 15°C by evaporation alone. A film thickness of 0.056 mm (0.0022 in) was calculated and, without considering surface tension and wettability, that result seems reasonable as a possible film thickness. Then, using the Langhaar model with the assumptions of the surrounding air at 22°C, a wind velocity (walking) of 0.894 m/s (2.93 ft/s), and a uniform rate of cooling, the average time (average for specimen temperatures of 100 and 85°C) the model predicts to dissipate the 297 J (heat loss required for a 15°C temperature drop) from the surface area of the Charpy specimen is about 18 s, or about 1°C/s. That compares with the observed cooling rate of about 2°C/s. Considering that a very simplified model was used for this application, the model calculation demonstrates that the experimental observations are credible. Regarding the postulated dominance of

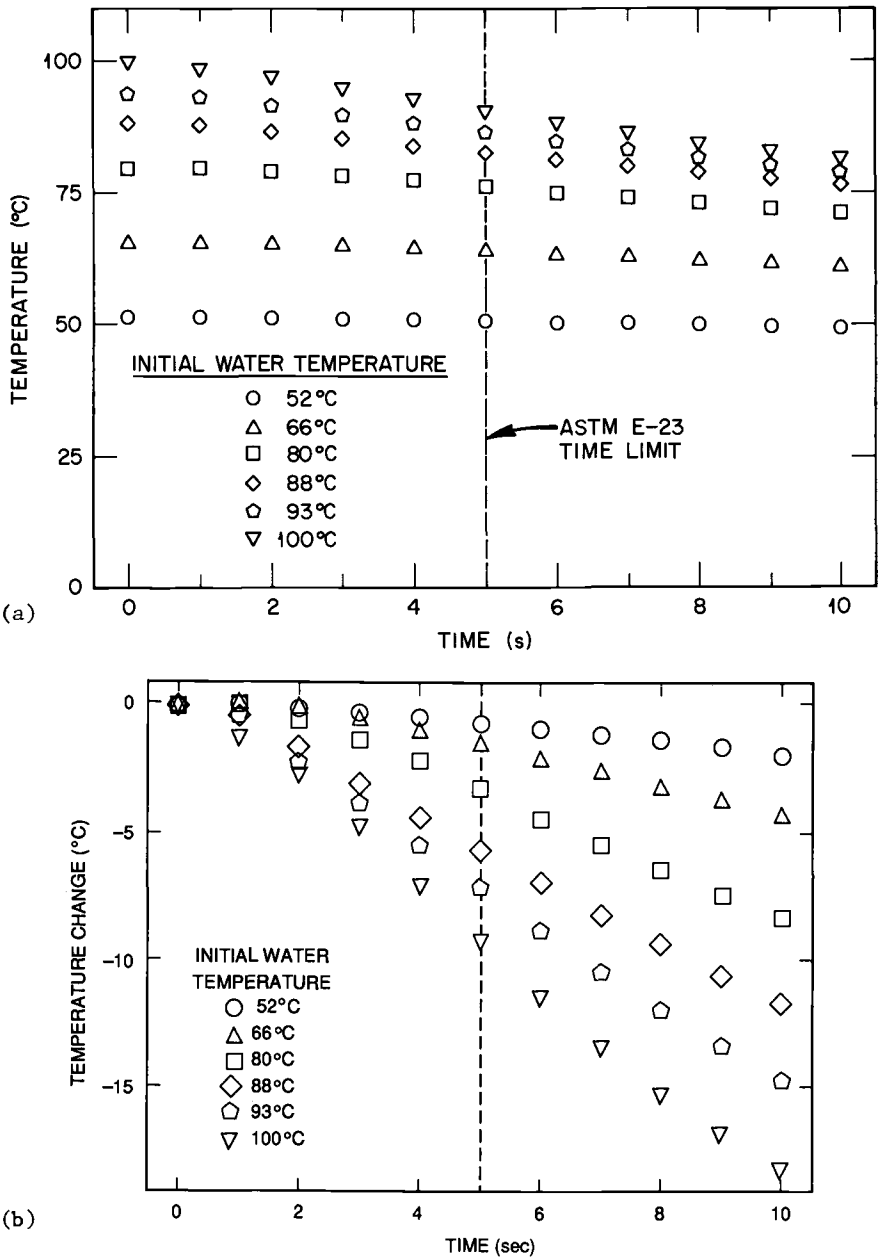

Fig. 9. Plots of (a) temperature, and (b) temperature change, from buried thermocouple 2, vs elapsed time following removal of the specimen from the heated water bath to the anvil of the Charpy machine for conditioning temperatures from 52 to 100°C. As shown in (b), the evaporative cooling effects increase as the conditioning temperature approaches 100°C, resulting in a decrease of about 10°C in the interior temperature of the specimen.

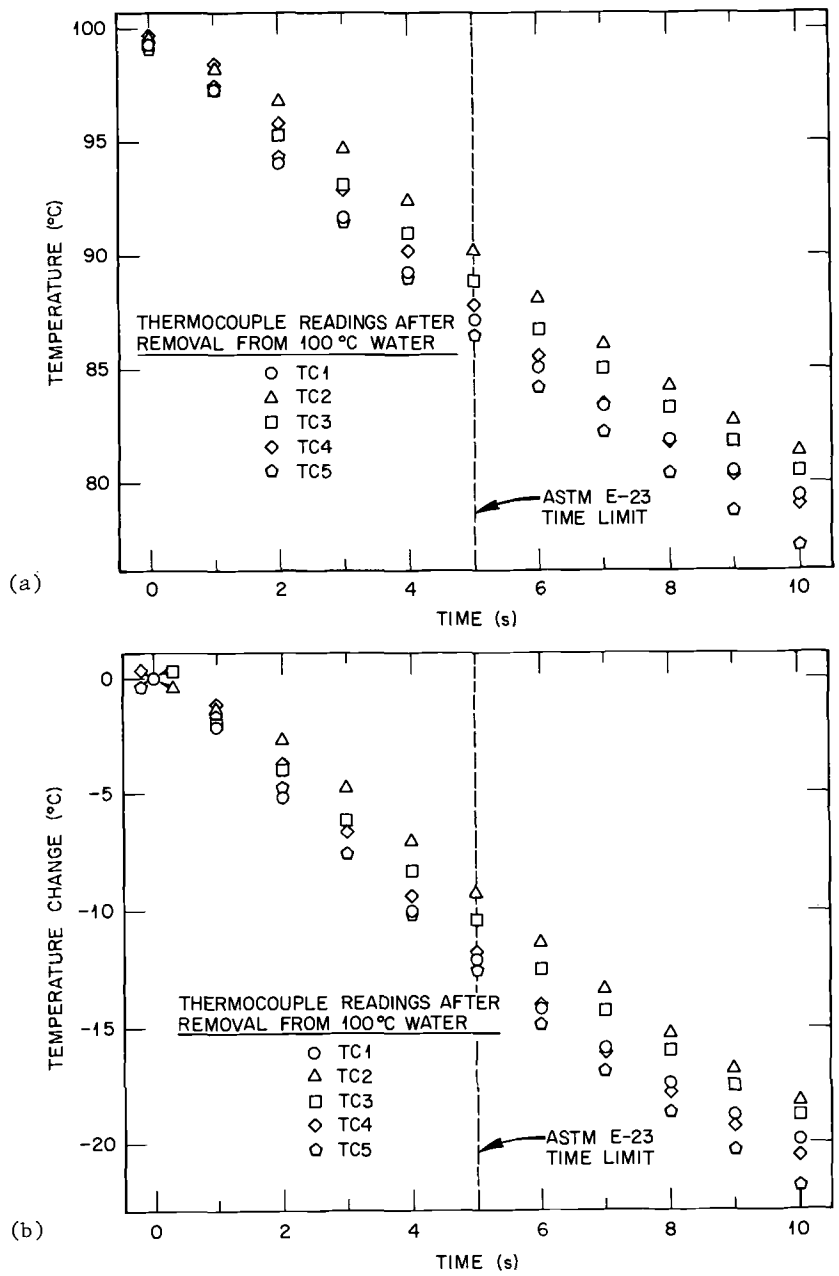

Fig. 10. Plots of (a) temperature, and (b) temperature change, from all five thermocouples, vs elapsed time following removal of the specimen from the heated water bath to the anvil of the Charpy machine for a conditioning temperature of 100°C. Thermocouples 4 and 5, near the ends of the specimen, experience greater cooling rates due to heat loss from the ends as well as the sides of the specimen.

evaporative cooling, a simple calculation was performed using a lump model for purely natural convection in air (using an average heat transfer coefficient of 8.5 $W/m^2/°C$ for all surfaces). That calculation indicated a cooling rate of 0.080°C/s, more than ten times less than that indicated by the Langhaar model and twenty times less than the experimental results. The Langhaar model calculations showed, in fact, that only about 10% of the heat flux from the water on the specimen surface comes from convection. Thus, the comparison demonstrates that evaporation of water from the specimen is the primary cooling mechanism.

These experiments show that evaporative cooling can cause significant changes in the specimen temperature when water is used for conditioning. Figure 11 shows a plot of the temperature decrease at 5 s after removal from the water bath vs the water bath temperature. The magnitude of the changes increase and the rate of change increases rapidly as the test temperature approaches 100°C. At 100°C, the temperature change in 5 s is about 10°C, while it is less than 1°C at a test temperature of 50°C. The effects of the evaporative cooling at the 5-s limit become increasingly significant at temperatures above about 65°C. The changes at 7 and 10 s following removal from the bath are also plotted in the figure and show the same trend. As shown earlier, the cooling changes which occur when heated air is used as the conditioning medium are minimal. The temperature changes which occur when using heated air will become significant at temperatures well above 100°C; however, this investigation was conducted to compare various conditioning media with heated water and, therefore, was limited to 100°C. Within the range studied for the other conditioning media, -100 to 50°C, temperature

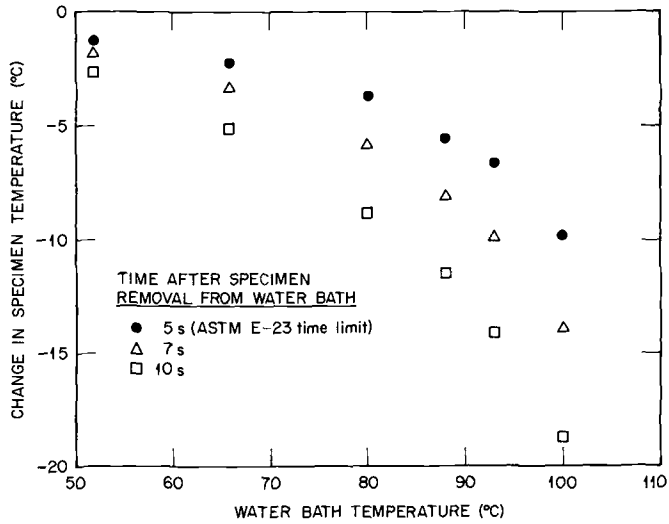

Fig. 11. Plot of temperature decrease at various elapsed times vs bath temperature following removal of the specimen from the heated water bath to the anvil of the Charpy machine. For water bath temperatures ranging from about 52 to 100°C, evaporative cooling decreases the interior specimen temperature from 2 to 10°C after 5 s, respectively.

changes at 5 s after removal from the environment were also small, 1°C or less. Two exceptions are heated acetone (not recommended) at 50°C and nitrogen gas at -100°C, both of which cooled the specimen about 2°C after 5 s.

The potential effects of these temperature changes on impact properties is highly dependent on the material being investigated. For a typical low-alloy pressure vessel steel tested in the mid-transition region, a decrease of 10°C in test temperature would cause a decrease in absorbed energy of about 12 J (8.8 ft-lb). In the determination of the reference NDT temperature, RT_{NDT}, for nuclear reactor vessel steels, the attainment of 68 J (50 ft-lb) at 33°C (60°F) above the NDT temperature is required for the RT_{NDT} to be equal to the drop-weight NDT. If the 50-ft-lb criterion is not met, testing must be performed at higher temperatures until 50 ft-lb is obtained (specific requirements for number of specimens, retests, etc. are delineated in Subsection NB, Section III of the ASME Code[1]). Thus, the Charpy impact toughness of steels which have a ductile-to-brittle transition in the 50 to 100°C range could be affected by the evaporative cooling effect; an artificially high RT_{NDT} could be determined. The degree to which this cooling affects such determinations is dependent on the specific material. In the same way, the testing of irradiated surveillance specimens from commercial nuclear power plants may result in an artificially high irradiation-induced transition temperature shift which can influence the operation of the reactor vessel. Finally, in the certification of materials where impact toughness requirements are specified, the impact energy obtained at the target test temperature would be artificially low. There are, of course, many factors in these and other examples which complicate the simplified scenarios described; however, the significant effects of evaporative cooling on the test specimen temperature are certain.

Regarding the heating of specimens with air and the cooling of specimens with nitrogen gas, the results showed that the interior regions of the Charpy specimen achieve the target temperature at about the same rate as the specimen surface. The need for soaking the specimen at the test temperature for 30 min seems unnecessarily restrictive. Many investigators have the equipment (use of buried thermocouples, etc.) to demonstrate that the target temperature is achieved throughout the specimen in less time than specified by ASTM Method E 23. It is recommended that a provision be considered for inclusion in the method that would allow such users to take advantage of those capabilities in the conduct of Charpy impact testing.

CONCLUSIONS

A study was performed to investigate the effects of various thermal conditioning media on temperature changes in the standard Charpy impact specimen during the time between removal from the environment and impact. The conclusions are:

1. Conditioning in heated water between 50 and 100°C results in significant evaporative cooling of the specimen at 5 s after removal from the water bath; the effects are increasingly greater approaching 100°C where the temperature decrease was 10°C.

2. The use of heated air up to 100°C results in temperature changes less than 1°C at 5 s after removal from the chamber.

3. The use of oil up to 100°C results in temperature changes less than 1°C at 5 s after removal from the bath.

4. The use of mixtures of acetone or methanol with dry ice from 0 to -75°C resulted in temperature changes less than 1°C at 5 s after removal from the bath.

5. The use of cold nitrogen gas from 0 to -100°C resulted in temperature changes less than 2°C at 5 s after removal from the chamber.

6. The use of heated water for specimens tested in the ductile-to-brittle transition region can have a significant effect on the test temperature, with the magnitude of the effects on the Charpy impact toughness dependent on the specific material.

7. A warning to users of ASTM Method E 23 should be considered for inclusion in the method regarding the potential effects of using heated water baths for thermal conditioning.

8. A provision should be considered for inclusion in the method which would give flexibility in the soaking time requirement for gas environments when the user can demonstrate that the target temperature of the specimen is achieved in less time than specified.

ACKNOWLEDGMENTS

This research is sponsored by the Office of Nuclear Regulatory Research, U.S. Nuclear Regulatory Commission, under Interagency Agreement DOE 1886-8109-8L with the U.S. Department of Energy under contract DE-AC05-84OR21400 with Martin Marietta Energy Systems, Inc.

The submitted manuscript has been authored by a contractor of the U.S. Government under contract DE-AC05-84OR21400. Accordingly, the U.S. Government retains a nonexclusive, royalty-free license to publish or reproduce the published form of the contribution, or allow others to do so, for U.S. Government purposes.

The authors gratefully acknowledge I. L. Simon-Tov for heat transfer analyses, F. M. Haggag, D. J. Alexander, and R. E. Pawel for their reviews of the manuscript and helpful comments, and J. L. Bishop for preparation.

REFERENCES

[1] *ASME Boiler and Pressure Vessel Code, an American National Standard*, American Society of Mechanical Engineers, New York, 1986.

[2] *Title 10, Code of Federal Regulations*, Part 50, U.S. Government Printing Office, Washington, D.C., January 1987.

[3] *American Association of Highway Transportation Officials - Material Specifications*, Association General Offices, Washington, D.C., 1974.

[4] Corwin, W. R., and Hougland, A. M., "Effect of Specimen Size and Material Condition on the Charpy Impact Properties of 9Cr-1Mo-V-Nb Steel," *The Use of Small-Scale Specimens for Testing Irradiated Material, ASTM STP 888*, W. R. Corwin and G. E. Lucas, Eds., American Society for Testing and Materials, Philadelphia, 1986, pp. 325-338.

[5] Alexander, D. J., Nanstad, R. K., Corwin, W. R., and Hutton, J. T., "A Semiautomated Computer-Interactive Dynamic Impact Testing System," *Applications of Automation Technology to Fatigue and Fracture Testing, ASTM STP 1092*, American Society for Testing and Materials, Philadelphia, 1990.

[6] Simon-Tov, I., Oak Ridge National Laboratory, "Transient Temperature Distribution in Charpie (sic) Specimen," Letter Report to R. K. Nanstad, Oak Ridge National Laboratory, November 1, 1989.

[7] Langhaar, J. W., "Cooling Pond May Answer Your Water Cooling Problem," *Chemical Engineering*, 194-98 (August 1953).

Author Index

Subject Index

ISBN 0-8031-1295-5